Metabolic engineering of *Corynebacterium glutamicum* for the production of succinate and 2,3-butanediol

Dušica Radoš

Supervisor: Prof. Helena Santos

Co-supervisor: Dr. Ana Rute Neves

Dissertation presented to obtain the Ph.D. degree in Biochemistry

Instituto de Tecnologia Química e Biológica António Xavier | Universidade Nova de Lisboa

Oeiras, December 2015

From left to right: César Simões da Fonseca, Michael Bott, Dušica Radoš, Maria Helena Dias dos Santos, Rute de Almeida Ferreira de Castro, Isabel Maria Godinho de Sá Nogueira, Hermínia Maria Francisco Roncon Garcez de Lencastre. Oeiras, 7th of December, 2015.

Financial support for this thesis was provided by Fundação para a Ciência e a Tecnologia (FCT), Ph.D. fellowship SFRH/BD/73265/2010.

Cover photo credits: Philipp von Zaluskowski, Stevan Radović and Nuno Borges.

Acknowledgements

The work presented in this dissertation would not have been possible without the help and encouragement of some people to whom I want to express my gratitude.

First of all, I thank Prof. Helena Santos, my supervisor, for having accepted me in her laboratory. For investing extraordinary time and effort into one student's scientific education and for being a truly inspiring guide through the entire Ph.D. path. For teaching me that "*biotechnology is our excuse to do biochemistry*". For caring and for constant effort to provide the best possible conditions to perform the work.

Dr. Ana Rute Neves, my co-supervisor and the person that is responsible for the fact that I arrived to ITQB in the first place. For the help with bench-work, data analysis, and writing manuscript.

Prof. Bernhard Eikmanns, my external co-supervisor, for his warm reception during my visit to University of Ulm. For helping me to learn more about the physiology and genetics of *Corynebacterium glutamicum*.

Prof. David Turner, for being constantly involved in the work and providing help at most critical times. For giving valuable input from a different point of view.

Dr. Bastian Blombach, for being always available for discussion, giving advice on the practical work and constructing important mutant strains.

Dr. Luís Fonseca, for guiding my first steps in isotopic labeling and NMR experiments. For all the patience that he had for me.

Dr. Ana Lúcia Carvalho, for teaching me secrets of molecular biology in a most selfless way possible. For all the care and friendship.

Dr. Nuno Borges, for important guiding and help with all the practical issues, for the friendship, honesty, and support.

Dr. Stefan Wieschalka, for helping me with the work at the University of Ulm.

To Ana Isabel Mingote and Sara Rebelo, for being great help in the lab, and making team work a very positive experience.
To Prof. Teresa Catarino, Dr. Carla Jorge, Dr. Ana Maria Esteves, Dr. Luis Gafeira, Dr. Gonçalo Graça and Dr. Pedro Lamosa for all the useful discussions and for always being there to help. To Cristiana Faria, Joana Sousa and Ana Rita Rosas for the support and group spirit. To Dr. Tiago Pais, Dr. Marta Rodrigues, Inês Torcato, Carla Patricia Almeida and Sónia Neto; also to Dr. Sandra Carvalho, Dr. Laura Paixão, Dr. Paula Gaspar and Dr. Pedro Quintas for the pleasant work atmosphere and friendship.
To Dr. Michal Malecki, Dr. Rajesh Ponnusamy, Dr. Manolis Matzapetakis and Małgorzata Magoch for being my “foreigner support”.
To everyone above mentioned, once again, for being my family abroad during this journey.

Mojoj porodici, za bezuslovnu ljubav i podršku.

This work was supported by Fundação para a Ciência e a Tecnologia, Portugal (FCT), FEDER and projects ERA-IB/BIO/0002/2008 and PTDC/BBB-BEP/2532/2012. I acknowledge FCT for the award of Ph.D. grant SFRH/BD/73265/2010. The NMR spectrometers are part of the National NMR Facility, supported by FCT (RECI/BBB-BQB/0230/2012).

Abstract

The depletion of fossil raw materials and the environmental pollution associated with their processing motivated the development of alternative methods for production of fuels and bulk chemicals. The solution offered by White Biotechnology is to produce these chemicals from biomass, a renewable resource rich in carbohydrates, using microorganisms as biocatalysts. *Corynebacterium glutamicum* is a well-known industrial bacterium employed for decades in the large scale production of L-amino acids. In this work, the potential of *C. glutamicum* as a bio-platform for the production of succinate and 2,3-butanediol was explored.

Wild-type *C. glutamicum* produces lactic, succinic, and acetic acids from glucose under oxygen limitation. In the first part of this work, the effect of CO_2 on the production of organic acids was investigated. For this purpose, a two-stage process was designed: cells were grown aerobically on glucose (1^{st} stage), and subsequently organic acid production by non-growing cells was carried out under anaerobic conditions (2^{nd} stage). The addition of CO_2 caused an up to a 3-fold increase in the succinate yield (1 mol per mol of glucose), and an about 2-fold increase in acetate, at the expense of L-lactate production; in addition, dihydroxyacetone formation was eliminated. The redistribution of carbon fluxes in response to CO_2 was estimated by using ^{13}C-labeled glucose and ^{13}C-NMR analysis of the labeling patterns in end products. The flux analysis showed that 97% of succinate was formed through the reductive part of the tricarboxylic acid cycle, with the low activity of the oxidative branch providing the reducing

equivalents needed for the redox balance. Pentose phosphate pathway flux was low (~5% of total glycolytic flux), regardless of the presence or absence of CO_2. We also observed significant channeling of carbon to storage compounds (glycogen and trehalose), and parallel catabolism of these reserves. Intracellular and extracellular pools of lactate and succinate were quantified non-invasively by *in vivo* ^{13}C-NMR, and the stoichiometry (H^+:organic acid) of the respective exporters was estimated. In brief, we demonstrated that it is feasible to take advantage of natural cellular regulation mechanisms in *C. glutamicum* to obtain high yields of succinate, without genetic manipulation.

In the second part of the work, 2,3-butanediol production was engineered in *C. glutamicum*. This diol is an important bulk chemical with extensive applications in cosmetics, food, medicine, chiral synthesis, transport fuels, cryoprotection, and the polymer industry. 2,3-Butanediol is a fermentation product of many microorganisms, though traditional producers are pathogenic. In the cell, this metabolite is synthesised from pyruvate in a three-step pathway involving α-acetolactate synthase, α-acetolactate decarboxylase, and 2,3-butanediol dehydrogenase. As part of our engineering strategy, a gene cluster encoding the 2,3-butanediol biosynthetic pathway of *Lactococcus lactis* was assembled and expressed in background strains, *C. glutamicum* Δ*ldhA*, *C. glutamicum* Δ*ldhA*Δ*aceE*Δ*pqo*, and *C. glutamicum* Δ*ldhA*Δ*aceE*Δ*pqo*Δ*mdh*, tailored to minimize pyruvate-consuming reactions and prevent carbon loss in organic acids. Production of 2,3-butanediol by the engineered strains was carried

out in a two-stage fermentation process: first, cells were grown aerobically on acetate and subsequently, non-growing cells were used to convert glucose into 2,3-butanediol under oxygen-limiting conditions. Productivity was maximized by manipulating the aeration rate in the production phase. Under optimized conditions, the best producer strain, *C. glutamicum* Δ*ldhA*Δ*aceE*Δ*pqo*Δ*mdh* (pEKEX-2 *alsaldB*P_{tuf}*butA*), accumulated 2,3-butanediol with a 0.66 mol·mol^{-1} yield on glucose, overall productivity of 0.2 g·L^{-1}·h^{-1} and a titer of 6.3 g·L^{-1}, proving that *C. glutamicum* can be developed successfully into a cell factory for 2,3-butanediol production.

In the third part of the work, the stereospecificity of 2,3-butanediol dehydrogenase of *C. glutamicum* was investigated. For this purpose, a 2,3-butanediol forming pathway, consisting of α-acetolactate synthase and α-acetolactate decarboxylase from *Lactococcus lactis,* and the 2,3-butanediol dehydrogenase from *C. glutamicum*, was assembled and transformed into *C. glutamicum* background strains. Surprisingly, engineered strains produced *meso*-2,3-butanediol under oxygen limitation. This finding was difficult to reconcile with the reported absolute stereospecificity of *C. glutamicum* 2,3-butanediol dehydrogenase for (*S*)-acetoin, and the fact that the two enzymes recruited from *L. lactis* produce exclusively the other enantiomer, (*R*)-acetoin. This apparent inconsistency prompted us to purify the recombinant 2,3-butanediol dehydrogenase and characterize its stereospecific properties. As the pure enantiomers of acetoin are not commercially available, NMR was used to monitor online the time courses for utilization of the individual acetoin enantiomers in a

racemic mixture supplied as substrate. The assays carried out in the presence of excess NADH clearly showed that (*R*)-acetoin was used, though at an apparent rate approximately 20 times lower than (*S*)-acetoin. The kinetic parameters for oxidation of different forms of 2,3-butanediol were determined in standard spectrophotometric assays to show that the specificity constant, k_{cat}/K_m, for *meso*-2,3-butanediol is about two-orders of magnitude lower than that for (*2S,3S*)-2,3-butanediol, but still clearly measurable. In conclusion, our results definitely show that the 2,3-butanediol dehydrogenase of *C. glutamicum* can use (*R*)-acetoin *in vivo* as well as *in vitro*.

In summary, a metabolic model was developed for glucose fermentation by wild-type *C. glutamicum* under anaerobic conditions and used to calculate carbon fluxes. The carbon flux analysis highlighted the ability of the cell machinery to respond to environmental perturbations, such as high CO_2, by shifting metabolism towards succinate production. Moreover, genetic engineering strategies were successfully applied to transform *C. glutamicum* into a cell factory for 2,3-butanediol production with a high yield. Finally, the stereospecific properties of 2,3-butanediol dehydrogenase were characterized both *in vitro* and *in vivo*, providing useful guidelines for the development of producers of 2,3-butanediol with high optical purity. This thesis represents a significant contribution to the fields of physiology and metabolic engineering of *C. glutamicum*.

Resumo

O esgotamento previsível das reservas mundiais de matérias-primas fósseis, bem como o pesado impacto ambiental dos processos petroquímicos, impulsionaram o desenvolvimento de métodos alternativos para a produção em larga escala de combustíveis e reagentes para a industria química. A solução proposta pela designada “Biotecnologia Branca” consiste em usar microrganismos para a conversão de biomassa, uma reserva renovável de hidratos de carbono, em produtos químicos tradicionalmente derivados do petróleo. *Corynebacterium glutamicum* é uma bactéria industrial utilizada há décadas para a produção de L-aminoácidos em larga escala. A presente tese teve como objetivo principal investigar a possibilidade de utilizar *C. glutamicum* como uma bioplataforma para a produção de succinato e 2,3-butanodiol, dois compostos químicos com enorme procura no mercado mundial.

A estirpe selvagem de *C. glutamicum*, em condições de limitação de oxigénio, produz ácidos láctico, succínico e acético a partir de glucose. Na primeira parte deste trabalho, descobriu-se que a produção de sucinato aumentava substancialmente quando se fornecia dióxido de carbono durante a fermentação. Com base neste resultado, desenvolveu-se um processo com duas fases: numa primeira fase as células foram cultivadas em condições aeróbias para produção de biomassa; na fase subsequente, fase de produção, esta biomassa foi utilizada em condições anaeróbias para produzir ácidos orgânicos, em particular ácido succínico. O

fornecimento de dióxido de carbono durante a fase de produção levou a um aumento de três vezes no rendimento de sucinato (1 mol de sucinato por mol de glucose), enquanto o rendimento de acetato duplicou à custa da diminuição concomitante na produção de lactato. Além disso, a formação de dihidroxiacetona, um sub-produto da fermentação, foi eliminada. Esta redistribuição dos fluxos metabólicos, induzida pela presença de CO_2, foi caracterizada em detalhe usando glucose isotopicamente marcada com ^{13}C e analisando os perfis de marcação dos produtos finais por técnicas de RMN de carbono 13. A análise de fluxos mostrou que 97% do succinato era formado através do braço redutor do ciclo de Krebs, com uma contribuição pequena do braço oxidante, mesmo assim essencial para prover os equivalentes redutores necessários ao equilíbrio do balanço redox. O fluxo pela via dos fosfatos de pentose era diminuto (~ 5%), independentemente da presença ou ausência de CO_2. Observou-se também uma mobilização considerável de carbono para compostos de armazenamento (glicogénio e trealose) e, em paralelo, o catabolismo destas reservas. Os níveis intracelulares e extracelulares de lactato e succinato foram quantificados diretamente em células vivas, recorrendo a ^{13}C-RMN *in vivo*; deste modo foi possível estimar a estequiometria dos respetivos exportadores (H^+: ácido orgânico). Em suma, demonstrou-se ser possível tirar partido dos mecanismos de regulação celular intrínsecos e obter elevados rendimentos em succinato, sem recorrer a manipulação genética de *C. glutamicum*.

Numa segunda parte do trabalho usaram-se abordagens de engenharia genética para converter *C. glutamicum* num produtor de 2,3-butanodiol. Este diol é um reagente químico com ampla aplicação em cosméticos, industria alimentar, medicina, síntese de compostos quirais, combustíveis líquidos, crioproteção e indústria de polímeros. 2,3-Butanodiol é um produto de fermentação em muitos microrganismos, mas os produtores convencionais são microrganismos patogénicos. Na célula a síntese ocorre a partir de piruvato numa via metabólica com três reações catalisadas pelas seguintes enzimas: sintase do α-acetolactato, descarboxilase do α-acetolactato e desidrogenase do 2,3-butanodiol. A nossa estratégia de engenharia metabólica usou o conjunto de genes que codificam a via de síntese de 2,3-butanodiol em *Lactococcus lactis*, inserindo-os em estirpes de *C. glutamicum* desenhadas para minimizar as reações que consomem piruvato, impedindo assim a perda de carbono sob a forma de ácidos orgânicos. Usaram-se as seguintes estirpes como hospedeiras: *C. glutamicum* ΔldhA, *C. glutamicum* ΔldhAΔaceEΔpqo e *C. glutamicum* ΔldhAΔaceEΔpqoΔmdh. Implementou-se um processo de fermentação em duas fases para a produção de 2,3-butanodiol: na primeira fase as células foram cultivadas em acetato e em condições aeróbias; subsequentemente, esta biomassa foi utilizada como fábrica celular para converter glucose em 2,3-butanodiol, em condições de limitação de oxigénio. A produtividade do processo foi maximizada por manipulação da taxa de arejamento na fase de produção. A melhor estirpe produtora, *C. glutamicum* Δ*ldhA*Δ*aceE*Δ*pqo*Δ*mdh* (pEKEX-2

alsaldB$_{Ptuf}$*butA*), produz 2,3-butanodiol com um rendimento de 0.66 mol por mol de glucose, uma produtividade global de 0.2 $g \cdot L^{-1} \cdot h^{-1}$ e um título de 6,3 $g \cdot L^{-1}$. Estes valores provam o sucesso da estratégia usada.

Estudou-se ainda a estereoespecificidade da desidrogenase de 2,3-butanodiol de *C. glutamicum* e implicações na pureza estereoquímica do produto. Para tal, um plasmídeo contendo uma via biossintética de 2,3-butanodiol, constituída por sintase e descarboxilase de α-acetolactato de *L. lactis* e desidrogenase de 2,3-butanodiol de *C. glutamicum*, foi construído e introduzido em estirpes de *C. glutamicum* com genótipos apropriados. Surpreendentemente, as estirpes transformadas produziam a forma *meso*-2,3-butanodiol, em condições de rarefação de oxigénio. Este resultado é incompatível com a estereospecificidade absoluta da enzima para (*S*)-acetoína descrita na literatura, e com o facto de as duas enzimas recrutadas de *L. lactis* produzirem exclusivamente o outro enantiómero, (*R*)-acetoína. Esta aparente incongruência levou-nos a investir na produção e purificação da desidrogenase do 2,3-butanodiol de *C. glutamicum* com a intenção de reavaliar as propriedades de estereoespecificidade da enzima. Como os enantiómeros de acetoína não estão comercialmente disponíveis na forma opticamente pura, utilizámos RMN de protão para monitorizar os perfis temporais de utilização de cada um dos enantiómeros presentes numa mistura racémica de acetoína, fornecida como substrato. Os ensaios realizados na presença de excesso de NADH mostraram nitidamente que (*R*)-acetoína era utilizada, embora a uma velocidade aproximadamente 20 vezes inferior à da (*S*)-acetoína. Os

parâmetros cinéticos para a oxidação de diversas formas de 2,3-butanodiol foram determinados por espetrofotometria, em ensaios standard, mostrando que a constante de especificidade, k_{cat}/K_m, para *meso*-2,3-butanodiol é cerca de duas ordens de grandeza inferior à obtida para (*2S,3S*)-2,3-butanodiol, mas definitivamente mensurável. Em conclusão, os resultados mostram de modo definitivo que a desidrogenase de 2,3-butanodiol de *C. glutamicum* usa (*R*)-acetoína, quer *in vivo* quer *in vitro*.

Em suma, neste trabalho de tese construiu-se um modelo metabólico para descrever o metabolismo de glucose em condições anaeróbias numa estirpe selvagem de *C. glutamicum*; este modelo permitiu o cálculo dos fluxos metabólicos principais. A análise de fluxos revelou a capacidade da maquinaria celular para responder a perturbações ambientais, tais como aumento da concentração de CO_2, redirecionando o metabolismo para a produção de succinato. Além disso, estratégias de engenharia metabólica foram usadas, com êxito, para converter *C. glutamicum* numa fábrica celular para produzir 2,3-butanodiol com rendimento elevado. Finalmente, caracterizou-se a estereospecificidade da desidrogenase de 2,3-butanodiol de *C. glutamicum in vitro* e *in vivo*, obtendo-se pistas para o desenvolvimento de estirpes produtoras de 2,3-butanodiol com elevada pureza estereoquímica. Este trabalho representa uma contribuição relevante nas áreas de fisiologia e engenharia metabólica de *C. glutamicum*.

Contents

Abbreviations

α-KIV, α-ketoisovalerate

α-KG, α-ketoglutarate

2,3-BD, 2,3-butanediol

Ac, acetate

AceE, E1-subunit of the pyruvate dehydrogenase complex

ADH, alcohol dehydrogenase

AHAS, acetohydroxyacid synthase

AlaT, alanine-glutamate transaminase

ALDC, α-acetolactate decarboxylase

ALS, α-acetolactate synthase

ATP, adenosine 5ˈ-triphosphate

AvtA, alanine-valine transaminase

BDH, butanediol dehydrogenase

CDW, cell dry weight

CR, carbon recovery

DHA, dihydroxyacetone

DHAP, dihydroxyacetone phosphate

E4P, erythrose 4-phosphate

EMP, Embden-Meyerhof Parnas Pathway

F6P, fructose 6-phosphate

FBP, fructose 1,6-biphosphate

G6P, glucose 6-phosphate

GAP, glyceraldehyde 3-phosphate

GAPDH, glyceraldehyde-3-phosphate dehydrogenase

GCR, glucose consumption rate

Glc, glucose

Glyox, glyoxylate

GRAS, Generally Recognized As Safe

HPLC, High Performance Liquid Chromatography

IPTG, isopropyl β-D-1-thiogalactopyranoside

IsoCit, isocitrate

L-Ala, L-alanine

Lac, lactate

Lac_{in}, intracellular lactate

Lac_{out}, extracellular lactate

LDH, lactate dehydrogenase

L-Ile, L-isoleucine

L-Leu, L-leucine

L-Val, L-valine

MDR, medium-chain dehydrogenase/reductase

MES, 2-(N-morpholino)ethanesulfonic acid

MOPS, 3-(N-morpholino)propanesulfonic acid

MQH_2, menaquinone reduced form

NAD^+, nicotinamide adenine dinucleotide

NADH, dihydronicotinamide adenine dinucleotide

$NADP^+$, nicotinamide adenine dinucleotide phosphate

NADPH, dihydronicotinamide adenine dinucleotide phosphate

NMR, Nuclear Magnetic Resonance

OAA, oxaloacetate

PCR, Polymerase Chain Reaction

PCx, pyruvate carboxylase

PDHC, pyruvate dehydrogenase complex

PEP, phosphoenol pyruvate

P_i, inorganic phosphate

PIPES, piperazine-N,N′-bis(2-ethanesulfonic acid)

PPP, pentose phosphate pathway

PQO, pyruvate:quinone oxidoreductase

Pta-Ack, phosphotransacetylase and acetate kinase

PYR, pyruvate

SH7P, sedoheptulose 7-phosphate

SDR, short-chain dehydrogenase/reductase

Suc, succinate

Suc_{in}, intracellular succinate

Suc_{out}, extracellular succinate

TCA cycle, tricarboxylic acid cycle

Tris, 2-amino-2-hydroxymethyl-propane-1,3-diol

Wt, wild-type

CHAPTER 1

General introduction

Contents

Metabolic engineering in industrial biotechnology

The application of microbial biotechnology principles started long before the discovery of bacterial cells or enzymes, and it was associated with bread-making and alcohol-brewing purposes. The establishment of microbiology and biochemistry as scientific disciplines in the 19th century provided the basis for the industrial biotechnology field to develop during the following century. Namely, during World War I, the need for glycerol and solvents, such as acetone and butanol, led to the first application of yeast and Clostridia for large scale production of these chemicals. Some years after, penicillin was discovered, and, owing to the joint effort of UK and US labs in the 1940s, first strains of *Penicillium* spp., able to produce high amounts of penicillin, were isolated. The development of penicillin fermentation marked the true beginning of golden era of industrial biotechnology. Also called white biotechnology, present industrial biotechnology is defined as “the application of modern biotechnology for the industrial production of chemical substances and bioenergy, using living cells and their enzymes, resulting in inherently clean processes with minimum waste generation and energy use” (Royal Belgian Academy Council of Applied Science 2004).

Microorganisms, the most used living cells by the industrial biotechnology, are natural producers of a spectrum of compounds that are of commercial interest. In most cases, their industrial production is not economically feasible due to a variety of factors, such as low product yields, low rate of conversion of substrates into products, fastidious growth requirements or other difficulties in growing the producer strain. The efficiency of substrate

conversion into the product depends on the properties of the microbial producer and the production conditions, and commonly these properties can be optimized in the course of development of a biotechnological process.

One of the most powerful tools used for strain improvement is metabolic engineering, defined as targeted and purposeful alteration of metabolic pathways using genetic engineering techniques in order to enhance production of valuable compounds (Lessard 1996). Metabolic engineering relies on knowledge of chemical engineering, computational sciences, biochemistry, and molecular biology. The (re)design of metabolic pathways, that has a goal of producing the desired compound with maximal yield and productivity, can be done in a natural producer or in a more suitable host that is not necessarily a natural producer (Fig. 1.1). As stated above, being a natural producer does not necessarily mean that the chosen host is the optimal choice. An example is succinate production in yeast: the production of succinate via the most commonly used pathway (reductive tricarboxylic acid cycle), was not straightforward, as the yeast fumarase has higher affinity towards fumarate than towards malate, and cytosolic malate dehydrogenase is degraded in the presence of glucose (Pines et al. 1996, Hung et al. 2004). Thus, the development of successful succinate producing yeast strains required several rounds of non-intuitive and rational optimization steps (van den Tweel 2010, Otero et al. 2013).

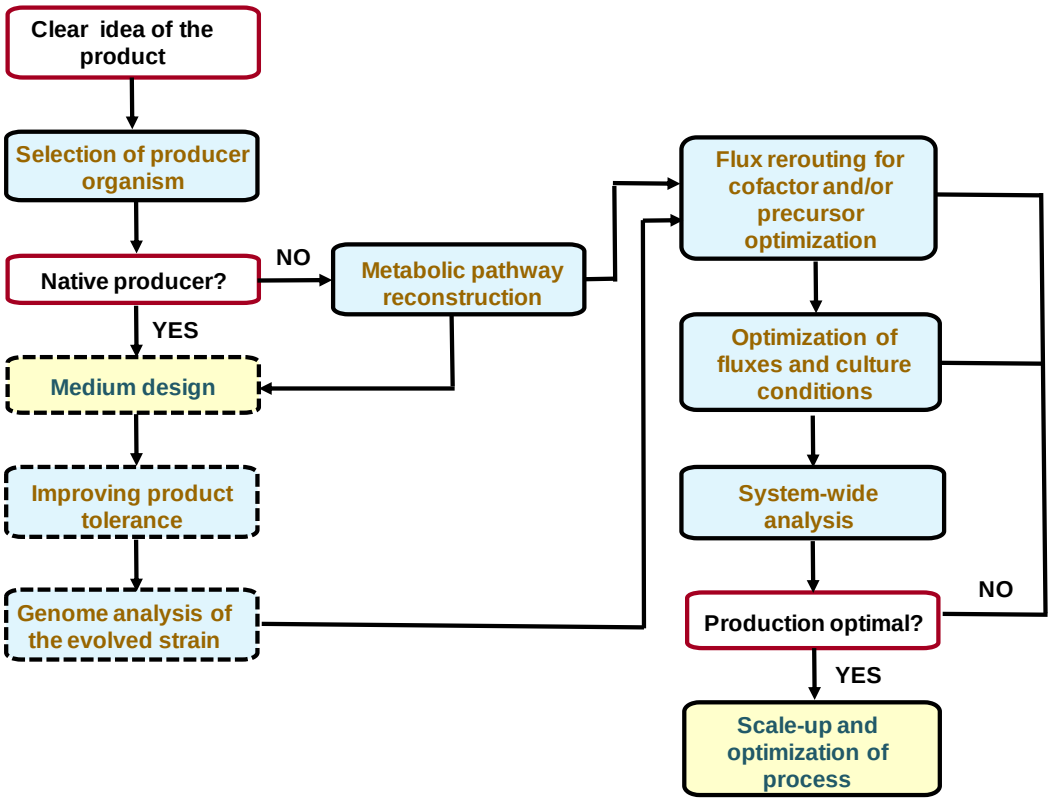

Figure 1.1. A scheme of a metabolic engineering process and approaches which are typically undertaken, not necessarily in the order shown. Blue boxes refer to strain optimization steps, while the yellow boxes indicates the process optimization related steps. Adapted from (Lee and Kim 2015).

When choosing the host, several aspects can be evaluated, among which: utilization of various carbon sources, availability of genetic information, amenability to genetic manipulation, possibility of fermentation in an inexpensive medium, ease of scale-up, requirement for anaerobic versus aerobic conditions and the suitability for cost effective downstream processes (Lee and Kim 2015). *Escherichia coli*, *Saccharomyces*

cerevisiae, *Corynebacterium glutamicum*, are examples of well established industrial strains that are used as hosts for the production of various compounds. However, it is also important to note that, with the recent development of systems biology tools, even the unknown organisms can be characterized and turned into producers relatively fast, as in the case of *Basfia succiniciproducens,* used for industrial production of succinate (Hong et al. 2004, Becker et al. 2013).

If the chosen host organism is not a natural producer, it can be transformed with heterologous pathways that are active in other microorganisms; additionally, artificial *de novo* biosynthetic pathways can be assembled and introduced into hosts, in the case of products that are non-native to microorganisms, or non-native to living organisms (Fisher et al. 2014, Lee and Kim 2015). Relatively low cost of DNA synthesis makes artificial pathway assembly easier; other optimization techniques, such as gene expression optimization, codon optimization, are also useful. In itaconate producing *C. glutamicum*, exchange of the ATG start codon to GTG or TTG reduced isocitrate dehydrogenase activity and resulted in maximal itaconate titers (Otten et al. 2015).

Increasing tolerance of the host organism to the product is an important step in strain optimization. The most common approach for developing product-tolerant strains is serial culturing of cells with increasing concentrations of product or analogs, with or without mutagen treatment, and subsequent identification of cells that outgrow. Tolerance level is gradually increased as the process is repeated. Using this method, yeast

was created with increased tolerance to n-butanol, a solvent that is highly toxic for microorganisms (González-Ramos et al. 2013, Ghiaci et al. 2013).

When the product synthesis is assured, it is often necessary to optimize the availability of cofactors and precursor metabolites by redistributing the metabolic fluxes. This is most commonly done by gene knockout or knockdown approaches. At this stage, it is necessary to estimate the effect of the elimination of a certain gene on growth and physiology, a task for which systems approach can be useful (Lee et al. 2012, Lee and Kim 2015). In *E. coli* NZ111, an attempt to channel carbon and cofactors towards succinate production was performed by inactivating lactate dehydrogenase and pyruvate:formate lyase (Stols and Donnelly 1997). However, this strain grew poorly under anaerobic conditions and growth was restored only after the inactivation of the glucose PTS system, due to the enhanced availability of PEP for the carboxylation reactions (Vemuri et al. 2002).

An important instrument in systems approach to metabolic engineering is metabolic flux analysis (MFA), which aims at the determination of fluxes of metabolites under certain conditions. Experimentally measured metabolite concentrations are included in the stoichiometric model that consists of all the reactions in the network and allows determining the unknown fluxes. By analyzing concentrations and labeling patterns of metabolites derived from ^{13}C-labeled substrates, it is possible to gather even more information about the operating pathways. ^{13}C-MFA became a standard methodology to identify bottleneck (rate-limiting) reactions and consequences of genetic

manipulations; thus it is very useful for providing information necessary for further improvement of microbial producers (Zamboni et al. 2009). Another important tool for studying metabolic fluxes is flux balance analysis (FBA), which is often used when there is not enough information to perform MFA. FBA uses an objective function (often maximizing growth or product formation), under certain constraints, such as substrate limitation or thermodynamic constraints. The result of FBA is an optimal set of fluxes, although there are several sets that would satisfy the system. Contrary to FBA, metabolic pathway analysis (MPA) determines all the possible flux vectors in a specific metabolic network, and no objective function or pre-set flux rates are necessary. Elementary mode analysis (EMA) is a type of MPA that is used to identify candidate genes for deletions or overexpression. There are several other computational tools that combine the described methodologies (Toya and Shimizu 2013, Machado and Herrgård 2015).

Corynebacterium glutamicum as an important industrial organism

In the years after World War II, Japanese scientists were seeking for a way to produce L-glutamate, a potentially useful amino acid to enhance the nutritional value of food. L-glutamate, in the form of monosodium glutamate, contributes to the taste of food and is responsible for the “umami” flavor. *C. glutamicum* was first isolated by the Japanese scientist Kinoshita and his team in 1956, as part of the research endeavor directed at discovering efficient L-glutamate producers. They found out that L-

glutamate accumulated when limiting concentration of biotin was present in the medium; additionally, mutagenized *C. glutamicum* strains were found to accumulate L-lysine, L-arginine, L-ornithine and L-threonine. Most of these amino acids are nowadays produced commercially using *C. glutamicum*, and more importantly, the development of the glutamate production process marked the starting point of amino acid fermentation industry (Kinoshita et al. 1957, Kinoshita 2005). The case of L-glutamate production by *C. glutamicum* is a good example of how biotechnological progress and basic research in microbiology and biochemistry are tightly connected. Due to the commercial interest of this bacterium, vast knowledge became available on its physiology, regulatory networks, genetics, etc. In the following text, some aspects of the broad knowledge on *C. glutamicum* metabolism will be summarized.

Central metabolism of *C. glutamicum*

C. glutamicum is a non-motile, non-sporulating, rod-shaped Gram-positive bacterium (Kinoshita et al. 1957). Until recently, it was believed that external electron acceptors, such as molecular oxygen or nitrate, were necessary for growth of this bacterium; however, a recent study reported limited growth under anoxic conditions (Liebl 2006, Nishimura et al. 2007, Michel et al. 2015). Phylogenetically, the genus *Corynebacterium* belongs to the eubacterial class Actinobacteria, order *Corynebacteriales*, which includes Gram-positive, high G+C content genera, such as *Nocardia*, *Mycobacterium* and *Rhodococcus* (Gao and Gupta 2012). The genome of *C. glutamicum* (3.28 Mbp, G+C content of 53.8%) has been fully

sequenced by two independent groups (Ikeda and Nakagawa 2003, Kalinowski et al. 2003).

C. glutamicum can grow on a variety of substrates, including sugars (glucose, fructose, and sucrose), organic acids (pyruvate, lactate, citrate, and acetate), and alcohols (ethanol), as single or mixed carbon and energy sources (Liebl 2006, Dominguez et al. 1997, Frunzke et al. 2008, Arndt et al. 2008). Interestingly, *C. glutamicum* is able to consume glucose concomitantly with other sugars or organic acids (e.g., fructose, gluconate, lactate or acetate) (Dominguez et al. 1997, Frunzke et al. 2008, Stansen et al. 2005, Wendisch et al. 2000). Up to now, diauxic growth was reported only for combinations of glucose/glutamate, acetate/ethanol and glucose/ethanol (Krämer et al. 1990, Arndt and Eikmanns 2007, Arndt et al. 2008).

A scheme of central metabolism of *C. glutamicum* growing on glucose or acetate is shown in Fig. 1.2 and a tabular view of genes coding for enzymes that catalyze the corresponding reactions is shown in Table 1.1.

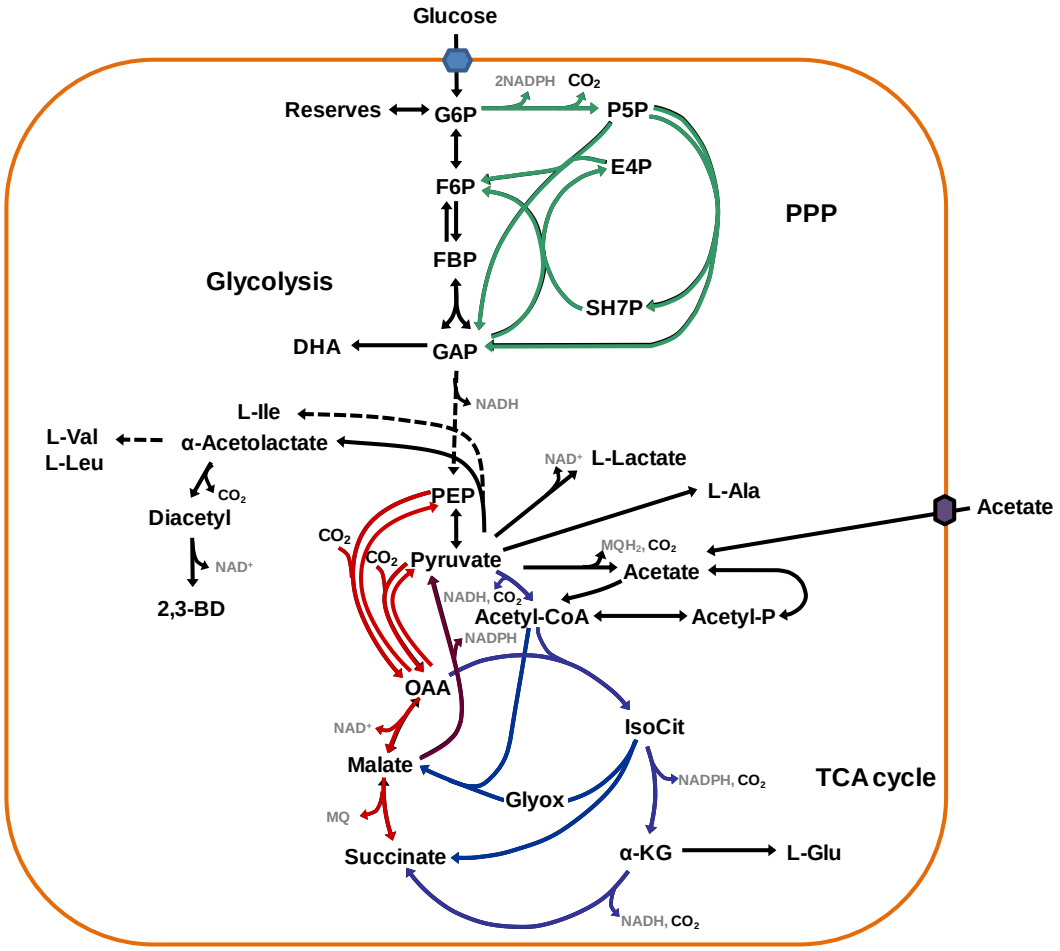

Fig. 1.2. Simplified scheme of central metabolism of *C. glutamicum* ATCC13032. Abbreviations: PPP, pentose phosphate pathway; TCA cycle, tricarboxylic acid cycle; G6P, glucose 6-phosphate; F6P, fructose 6-phosphate; FBP, fructose 1,6-bisphosphate; P5P, any of pentose 5-phosphate molecules; E4P, erythrose 4-phosphate; SH7P, sedoheptulose 7-phosphate; GAP, glyceraldehyde 3-phosphate; DHA, dihydroxyacetone; L-Ala, L-alanine; L-Val, L-valine; L-Leu, L-leucine; L-Ile, L-isoleucine; L-Glu, L-glutamate 2,3-BD, 2,3-butanediol; PEP, phosphoenolpyruvate; OAA, oxaloacetate; IsoCit, isocitrate; Glyox, glyoxylate; α-KG, α-ketoglutarate.

The main mode of glucose uptake is via the phosphotransferase (PTS) system. Uptake and phosphorylation of glucose into glucose 6-phosphate (G6P) are driven by hydrolysis of phosphoenolpyruvate (PEP) (Moon et al. 2007). The G6P pool is then partitioned between Embden-Meyerhof-Parnas (EMP) and Pentose Phosphate Pathway (PPP). Channeling carbon into the PPP provides metabolite precursors and NADPH for the anabolism, while processing carbon by the EMP results in synthesis of pyruvate and NADH (2 mol per mol of glucose).

Pyruvate formed in glycolysis can have different destinies. Under growth conditions, a major part of pyruvate is decarboxylated and activated to acetyl-CoA by the pyruvate dehydrogenase complex (PDHC). This multienzymatic complex consists of three subunits: pyruvate decarboxylase (E1p), dihydrolipoamide transacetylase (E2) and dihydrolipoamide dehydrogenase (E3) (Eikmanns 2005, Sauer and Eikmanns 2005). Deletion of the *aceE* gene encoding E1p (Table 1.1) leads to complete inactivation of PDHC and acetate auxotrophy, which can be circumvented by using substrates that enter central metabolism at the level of acetyl-CoA, such as acetate or ethanol (Schreiner et al. 2005, Blombach et al. 2009). Monocarboxylic acid transporter (MctC) is responsible for the import of acetate, while the activation to acetyl-CoA is carried out by acetate kinase (AK) and phosphotransacetylase (PTA) (Jolkver et al. 2009, Gerstmeir et al. 2003). Alternatively, acetate can be activated by CoA transferase (CtfA) (Veit et al. 2009). *C. glutamicum* also

possesses a pyruvate:quinone oxidoreductase (PQO), which converts pyruvate into acetate and CO_2, but cannot completely substitute the role of PDHC (Schreiner et al. 2006).

Acetyl-CoA is commonly channeled into the tricarboxylic acid (TCA) cycle by citrate synthase (CS) to provide energy and precursor molecules (Fig. 1.2). The electrons from NADH produced in glycolysis and the TCA cycle are used in the respiratory chain for adenosine triphosphate (ATP) generation (Bott and Niebisch 2003). Intermediates of the TCA cycle such as oxaloacetate (OAA) or α-ketoglutarate serve as precursors for the production of amino acids (L-aspartate and L-glutamate family, respectively). In addition, *C. glutamicum* possesses a TCA bypass in the form of a glyoxylate shunt with its key enzymes isocitrate lyase (ICL) and malate synthase (MS).

The relatively complex PEP-pyruvate-OAA node (Table 1.1, Fig. 1.2) plays a major role in carbon distribution within central metabolism (Eikmanns 2005, Sauer and Eikmanns 2005). Two CO_2/bicarbonate-fixing reactions, performed by PEP carboxylase (PEPCx) and pyruvate carboxylase (PCx), are mainly active during growth on sugars. During growth on gluconeogenic substrates, such as acetate, the PEP-pyruvate-OAA-node is actually the initial step of gluconeogenesis, performed by the GTP-dependent PEP-carboxykinase (PEPCk), malic enzyme (MalE) and by the OAA decarboxylase (ODx) (Riedel et al. 2001, Gourdon et al. 2000, Klaffl and Eikmanns 2010).

Pyruvate can be also converted directly into L-lactate under oxygen limiting conditions (Inui et al. 2004), or it can serve for the synthesis of amino acids of the pyruvate-family (L-alanine, L-leucine, and L-valine), initiated by the enzymes alanine aminotransferase (AlaT), valine-pyruvate aminotransferase (AvtA), and the key enzyme for the synthesis of branched-chain amino acids (BCAAs), the acetohydroxyacid synthase (AHAS). It is worth noting that other products from pyruvate metabolism, such as acetoin and 2,3-butanediol (2,3-BD), were detected in the wild-type *C. glutamicum* in trace amounts, suggesting minor alternative fates of pyruvate (Dickschat et al. 2010).

In addition, glycerol and dihydroxyacetone (DHA), the two “over-flow” metabolites, were detected in *C. glutamicum* under lysine production conditions (Kiefer et al. 2004). These metabolites come from dephosphorylation of glyceraldehyde-3-phosphate (GAP) or dihydroxyacetone phosphate (DHAP); as they represent loss of carbon, pathways for their synthesis were studied in detail (summarized in Table 1.1, Jojima et al. 2012, Lindner et al. 2012, Jojima et al. 2015).

Metabolic flux analysis of *C. glutamicum*

The reactions in central metabolism of *C. glutamicum* related to substrate uptake, glycolysis, PPP, TCA cycle, anaplerosis, glyoxylate cycle and product synthesis are well established, which facilitates the development of approaches for quantification of operating metabolic fluxes. Amino acid producer strains, i.e., for L-lysine, L-glutamate and L-valine, were

characterized; in addition**,** fluxes operating in cells grown on different substrates (acetate, glucose, acetate plus glucose, and fructose), under oxygen limitation, and stresses such as osmotic, have been described (Marx et al. 1996, Bartek et al. 2010, Vallino and Sephanopulos 1993, Kiefer et al. 2004, Uy et al. 2004, Wittman and Heinzle 2001, Wendisch et al. 2000, Dominguez et al. 1993, Varela et al. 2003).

Of particular interest to this work are studies on metabolic fluxes in growing cultures using glucose, acetate and a mixture of glucose and acetate as substrate (Wendisch et al. 2000). When grown on glucose, cells showed a high PPP flux (~89% of the total glucose uptake flux), which fueled glycolysis at the level of fructose-6-phosphate (F6P) and GAP. The TCA operated as a complete cycle in the forward direction and there was no activity of the glyoxylate shunt. The TCA cycle was replenished by the C_3 carboxylation reactions, and, interestingly, the shuffling between C_3 and C_4 compounds in the PEP-pyruvate-OAA node was particularly high (more than three times higher than the net flux from C_3 to the TCA cycle). As expected, cells grown on acetate showed a metabolic flux distribution different from those grown on glucose. As acetate enters metabolism at the level of acetyl-CoA, the activity of the TCA cycle and glyoxylate shunt increased drastically (TCA, four times higher on acetate than on glucose). C_4 precursors from the TCA were directed into gluconeogenesis via the PEP-pyruvate-OAA node. The flux through PPP was about six times lower in these cells compared to cells grown on glucose. Lastly, cells grown on acetate/glucose mixture exhibited substrate uptake rates which were twice

lower than the uptake rates on each individual carbon source alone. The PPP flux was comparable to that in cells growing on glucose and the TCA cycle flux was twice as high. The net direction of the anaplerosis was towards C_3 metabolites and particularly high metabolite shuffling occurred in the reductive TCA. This work showed that, unlike some other bacteria, such as *Lactococcus lactis* or *E. coli* (Görke and Stülke 2008), *C. glutamicum* is able to utilize the two carbon sources (acetate and glucose) simultaneously, indicating the lack of carbon catabolite repression. More importantly, MFA gives information on the redistribution of fluxes in different growth conditions, thus providing important insights into the physiology of this bacterium.

Table 1.1: Genes encoding the enzymes of central metabolism in *C. glutamicum*

Gene	Enzyme	Reaction	Reference
Glycolysis			
pgi	Phosphoglucoisomerase (PGI)	G6P ↔ F6P	Sugimoto and Shiio 1989
gapAl ***gapB***	Glyceraldehyde-3-phosphate dehydrogenases A and B (GAPDH)	GAP + NAD^+ +ATP → 1,3-Bisphosphoglycerate + NADH + ADP	Eikmanns 1992 Omumasaba et al. 2004
pyk	Pyruvate kinase (Pyk)	PEP + ADP → Pyruvate + ATP	Gubler et al. 1994
aceE ***aceF*** ***lpd***	E1p, E2 and E3 pyruvate dehydrogenase complex subunits (PDHC)	Pyruvate + NAD^+ + CoA→ Acetyl-CoA + CO_2 + NADH	Schreiner et al. 2006 Hoffelder et al. 2010 Schwinde et al. 2001
ldhA	NAD^+-dependent L-lactate dehydrogenase (LdhA)	Pyruvate + NADH ↔ L-Lactate + NAD^+	Inui et al. 2004
Pentose phosphate pathway			
zwf ***opcA***	Glucose-6-phosphate dehydrogenase (G6PDH)	G6P + $NADP^+$ → 6-Phosphoglucono-δ-Lactone + NADPH	Moritz et al. 2000 Sugimoto 1987
gnd	6-phosphogluconate dehydrogenase (6PGDH)	6PG + $NADP^+$ → Ribu5P + CO_2 + NADPH	Moritz et al. 2000
Transporters			
ptsI, ptsH ***ptsG***	Phosphotransferase system (glucose) (PTS)	$Glucose_{ext}$ + PEP → $G6P_{int}$ + Pyruvate (glucose uptake)	Moon et al. 2007

mctC	Monocarboxylic acid Transporter (MctC)	Uptake of pyruvate, propionate and acetate	Jolkver et al. 2009
sucE	Succinate exporter (SucE)	Export of succinate	Huhn et al. 2011
Acetate metabolism			
pqo	Pyruvate:quinone Oxidoreductase (PQO)	Pyruvate + MQ → Acetate + CO_2 + MQH_2	Schreiner 2005 Schreiner 2006
ackA	Acetate kinase (AK)	Acetate + ATP ↔ Acetyl-P + ADP Propionate + ATP ↔ Propionyl-P + ADP	Shiio et al. 1969
pta	Phosphotransacetylase (PTA)	Acetyl-P + CoA ↔ Acetyl-CoA + P_i Propionyl-P + CoA ↔ Propionyl-CoA + P_i	Shiio et al. 1969
cat	CoA transferase (CtfA)	Acetate + CoA ↔ Acetyl-CoA	Veit et al. 2009
TCA cycle and glyoxylate shunt			
gltA	Citrate synthase (CS)	OAA + Acetyl-CoA + H_2O → Citrate + CoA	Eikmanns et al. 1994
acn	Aconitase	Citrate ↔ Isocitrate	Baumgart et al. 2011
icd	Isocitrate dehydrogenase (ICD)	Isocitrate + $NADP^+$ → 2-Oxoglutarate + CO_2 + NADPH	Eikmanns et al. 1995
odhA ***aceF*** ***lpd***	Oxoglutarate dehydrogenase complex (ODHC)	2-Oxoglutarate + NAD^+ + CoA → Succinyl-CoA + CO_2 + NADH	Usuda et al. 1996 Kataoka et al. 2006 Hoffelder et al. 2010
sdhA, ***sdhB***, ***sdhC***	Succinate dehydrogenase (SDH)	Succinate + NAD^+/FAD ↔ NADH/$FADH_2$ + fumarate	Kurokawa and Sakamoto 2005
fum	Fumarase (Fum)	Fumarate ↔ Malate	Genda et al. 2006
mqo	Malate:quinone	Malate + MQ → OAA + MQH_2	Molenaar et al.

	oxidoreductase (MQO)		1998, 2000 Genda et al. 2003
mdh	Malate dehydrogenase (Mdh)	OAA + NADH → Malate + NAD^+	Molenaar et al. 2000
aceA	Isocitrate lyase (ICL)	Isocitrate → Glyoxylate + Succinate	Reinscheid et al. 1994a
aceB	Malate synthase (MS)	Glyoxylate + Acetyl-CoA → Malate + CoA	Reinscheid et al. 1994b
Anaplerotic reactions (PEP-pyruvate-OAA-node)			
ppc	Phosphoenolpyruvate carboxylase (PEPCx)	PEP + CO_2 → OAA + P_i	Eikmanns et al. 1989
pyc	Pyruvate carboxylase (PCx)	Pyruvate + CO_2 + ATP → OAA + ADP + P_i	Peters-Wendisch et al. 1997 Peters-Wendisch et al. 1998
pck	Phosphoenolpyruvate carboxykinase	OAA + ATP → PEP + ADP + CO_2	Jetten and Sinskey 1993 Riedel et al. 2001
odx	Oxaloacetate decarboxylase (ODx)	OAA → Pyruvate + CO_2	Klaffl and Eikmanns 2010
malE	Malic enzyme (MalE)	Malate + $NADP^+$ → Pyruvate + NADPH + CO_2	Gourdon et al. 2000
Amino acid production			
gdh	Glutamate dehydrogenase (GDH)	2-Oxoglutarate + $NADP^+$ + NH_4^+ ↔ L-Glutamate + NADPH	Shiio and Ujigawa 1978
gltB ***gltD***	Glutamate-2- oxoglutarate aminotransferase (GOGAT)	L-Glutamine + 2-Oxoglutarate + 2 NADH → 2 L-Glutamate + 2 NAD^+	Beckers et al. 2001

alaT	Alanine aminotransferase (AlaT)	L-Glutamate + Pyruvate ↔ L-Alanine + 2-Oxoglutarate	Marienhagen and Eggeling 2008
avtA	Valine-pyruvate aminotransferase (AvtA)	L-Alanine + α-KIV ↔ L-Valine + Pyruvate	Marienhagen and Eggeling 2008
ilvB ***ilvN***	Acetohydroxyacid synthase subunits (AHAS)	2 Pyruvate → α-Acetolactate + CO_2 Pyruvate + α-Ketobutyrate → α-Ketohydroxybutyrate + CO_2	Keilhauer et al. 1993
ilvC	Acetohydroxyacid isomeroreductase (AHAIR)	α-Acetolactate + $NADP^+$→ 2,3-Dihydroxyisovalerate + NADPH α-Acetohydroxybutyrate + $NADP^+$ → 2,3-Dihydroxy- 3-methylvalerate + NADPH	Keilhauer et al. 1993
ilvD	Dihydroxyacid Dehydratase (DHAD)	2,3-Dihydroxyisovalerate → α-KIV 2,3-Dihydroxy-3-methylvalerate → KMV	Radmacher et al. 2002
Other			
butA	Butanediol dehydrogenase (BDH)	Diacetyl + NADH → S-Acetoin+NAD^+ *S*-Acetoin + NADH ↔ (*2S,3S*)-2,3-BD + NAD^+ DHA + NADH ↔ Glycerol + NAD^+	Takusagawa et al. 2001 Jojima et al. 2015
hdpA	HAD superfamily phosphatase (HdpA)	GAP → Glyceraldehyde + P_i DHAP → DHA + P_i G3P → Glycerol + P_i	Jojima et al. 2012 Jojima et al. 2015
gpp	Glycerol-3-phosphate phosphatase (Gpp)	G3P → Glycerol + P_i	Lindner et al. 2012

Abbreviations: ATP, adenosine triphosphate; ADP, adenosine diphosphate; GAP, glyceraldehyde-3-phosphate; α-KIV, α -ketoisovalerate; KMV, 2-keto-3-methylvalerate; MQ, menaquinone oxidized; MQH_2, menaquinone reduced; OAA, oxaloacetate; PEP, phosphoenolpyruvate; P_i, inorganic phosphate; G3P, glycerol-3-phosphate; DHA, dihydroxyacetone; DHAP, dihydroxyacetone phosphate. Adapted from Wieschalka 2012.

Biotechnological production of bulk chemicals

One of the major issues of the modern era is the high growth rate of world population, concomitant increase in industrial production and, consequent limitation of resources, such as food, land, and energy. Industrial production processes are commonly associated with pollution, for example by accumulation of greenhouse gases, such as CO_2. Moreover, the raw initial material that is by far mostly used for the production of chemicals and fuels is petrol, a finite resource whose economy is unstable. Such limitations present a driving force in finding alternative ways to manufacture petroleum-derived products, and considerable effort was invested in white biotechnology to produce some of petroleum-based chemicals from biomass. This would, at least partially, ease the dependence on limited amounts of petrol and, on the other hand, decrease the pollution associated with petrol processing practices (Werpy and Petersen 2004, de Jong et al. 2012, Adom et al. 2014). In 2004, the US Department of Energy (DOE) issued the first of two reports stressing the need for research in the area of biobased products (Werpy and Petersen 2004). The first report contained a list of 15 chemicals that could be produced from biorefinery carbohydrates, based on multiple factors such as the existence of processes for the production of these chemicals, economics, industrial viability, size of markets, and the ability of a compound to serve as a platform for the production of derivatives. This list contained the following compounds: succinic, fumaric and malic acids, 2,5-furan dicarboxylic acid, 3-hydroxypropionic acid, aspartic acid, glucaric

acid, glutamic acid, itaconic acid, levulinic acid, 3-hydroxybutyrolactone, glycerol, sorbitol and xylitol/arabinitol (Table 1.2). A second group of building blocks that was also identified as potentially viable included: gluconic, lactic, malonic, propionic acid, the triacids, citric and aconitic, xylonic acid, acetoin, furfural, levoglucosan, lysine, serine and threonine.

In 2010, Bozell and Petersen published an updated set of potential target molecules using similar selection methodology (Table 1.2) (Bozell and Petersen 2010). The revised list excluded organic acids such as malic, fumaric, glucaric, itaconic, glutamic and aspartic acid, and included new chemicals such as ethanol, lactic acid and biohydrocarbons, such as isoprene. Importantly, both reports served as guides for subsequent research efforts and technology development in the chemical building blocks production sphere.

Table 1.2. Top chemical building blocks to be produced from carbohydrates according to the US DOE (Werpy and Petersen 2004, Bozell and Petersen 2010).

Building blocks from carbohydrates	
2004	**2010**
3-Hydroxypropionic acid	3-Hydroxypropionic acid/aldehyde
Glycerol	Glycerol and derivatives
3-Hydroxybutyrolactone	3-Hydroxybutyrolactone
Aspartic acid	Lactic acid
Succinic, fumaric and malic acids	Succinic acid
Glutamic acid	Ethanol
Itaconic acid	Isoprene
Levulinic acid	Levulinic acid
Xylitol/arabinitol	Xylitol
2,5-Furan dicarboxylic acid	Furans
Glucaric acid	Biohydrocarbons
Sorbitol	Sorbitol

Biobased production of succinate

One of the important chemical building blocks recognized by US DOE reports is succinic acid, a four-carbon dicarboxylic acid which can be used as a precursor of many industrially important chemicals. The bio-succinic acid market was estimated to be about US$ 240.3 million in 2011 and is expected to grow at a CAGR (Compound Annual Growth Rate) of 19.4% between 2012 and 2018 (Transparency Market Research 2012). Succinate is a promising molecule because it can be derivatized into other chemicals that are commonly petrol-derived, and that have a wide range of applications (Fig. 1.3) (Delhomme et al. 2009). Among potential important application of bio-based succinic acid could be the production of commodity chemical 1,4-butanediol ($3 billion market), which is a starting material for tetrahydrofuran (THF) and γ-butyrolactone; γ-butyrolactone can be used to produce *n*-methylpyrrolidinone (NMP) that could substitute petrochemical adipic acid in the production of polyester polyols to polyurethanes (Erickson et al. 2011). Another application of succinate is in the production of polybutylene succinate (PBS), a promising biodegradable polymer. Finally, succinate can be used in the production of detergents, surfactants, pigments, resins, biodegradable solvents, food, and pharmaceutical products (Zeikus et al. 1999).

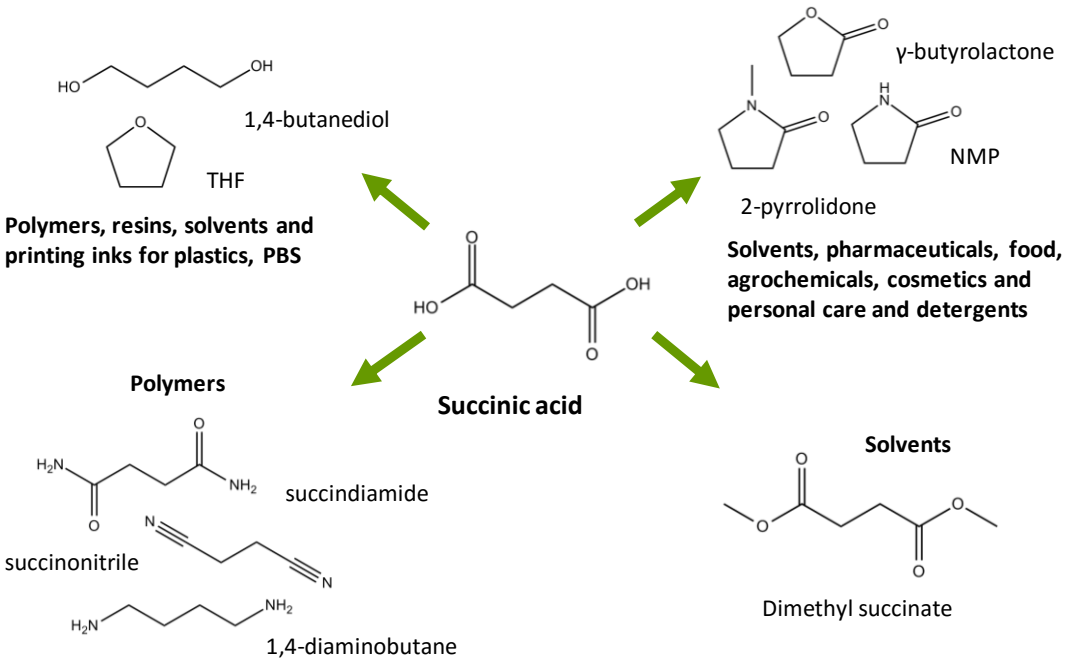

Fig. 1.3. Derivatives of succinic acid and their application. Abbreviations: THF, tetrahydrofuran; NMP, n-methylpyrrolidinone; PBS, polybutylene succinate.

With such wide range of applications and growing interest in this compound, it is not surprising that in the last decade, bio-based succinic acid production had moved from laboratory into industrial setting. Venture projects such as Bioamber Inc., Myriant Technologies LLC, Reverdia, and Succinity GmbH use organisms like *Escherichia coli*, *Saccharomyces cerevisiae* and *Basfia succiniciproducens* for the industrial scale production (reviewed in Litsanov et al. 2014). Importantly, production of bio-succinic acid has the potential to become an important component of petrol-independent industry (Erickson et al. 2012).

Specific microbial succinate producers

Tricarboxylic acid (TCA) cycle, which includes succinate as a metabolite, has a metabolic role in providing precursor molecules for anabolism, such as oxaloacetate and α-ketoglutarate, and redox equivalents for respiration. Under aerobic conditions, succinate is formed from succinyl-CoA via the succinyl-CoA synthetase (Fig. 1.4). Another pathway for succinate synthesis involves the reduction of oxaloacetate via malate and fumarate as intermediates. Oxaloacetate is a product of carboxylation of either phosphoenolpyruvate or pyruvate. Another carboxylation reaction that drains pyruvate into the TCA cycle is catalyzed by the malic enzyme, which forms malate that can be reduced into succinate as explained above. In addition, succinate can be produced from malate that comes from the glyoxylate shunt. As various pathways can be involved in the synthesis of succinate, an important tool for the optimization of production was metabolic flux analysis, which provided important guidelines for the design of efficient producer strains. In the following text, physiological aspects such as metabolic flux analysis and main steps in strain optimization of the most promising microbial producers will be described.

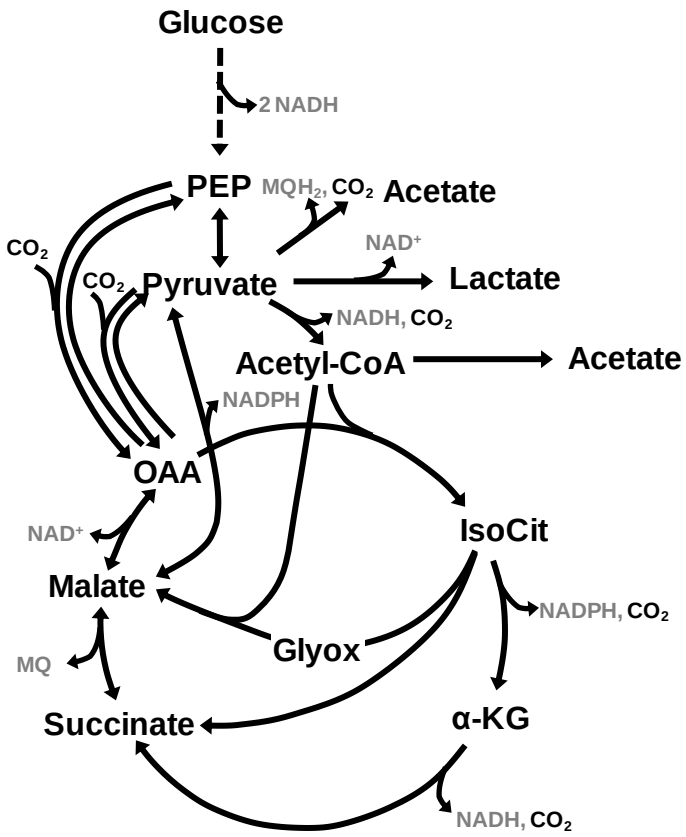

Fig. 1.4. Schematic overview of metabolic pathways that contribute to formation of succinate from glucose. Abbreviations: PEP, phosphoenolpyruvate; OAA, oxaloacetate; IsoCit, isocitrate; Glyox, glyoxylate; α-KG, α-ketoglutarate.

Actinobacillus succinogenes

Actinobacillus succinogenes is a natural succinate producer isolated from bovine rumen and known to be capnophilic (grows better in the presence of CO_2). Besides succinate, it produces formate, acetate and ethanol as the fermentation end-products. To study the formation of succinate from

glucose in this bacterium, enzyme assays and metabolic flux analysis were performed (McKinlay et al. 2007, McKinlay and Vielle 2008). *A. succinogenes* 130Z metabolizes glucose via the Embden-Meyerhof-Parnas (EMP) pathway, with a negligible contribution of the Entner-Doudoroff (ED) and a low activity of the Pentose Phosphate Pathway (PPP, between 1 and 4%). Succinate is formed through carboxylation of PEP into oxaloacetate and subsequent reduction via the reductive TCA branch. This pathway is crucial for succinate production, as *A. succinogenes* does not possess a complete TCA cycle (genes encoding citrate synthase and isocitrate dehydrogenase are missing in the genome), and the glyoxylate shunt did not seem to contribute to succinate formation. The model predicts a low back flux from C_4 to C_3 metabolites, via the oxaloacetate decarboxylase and malic enzyme (McKinlay et al. 2007, McKinlay and Vielle 2008).

Distribution of fluxes at four key points determined the succinate production in *A. succinogenes*: oxaloacetate, malate, PEP, and pyruvate. When CO_2 in the form of sodium bicarbonate ($NaHCO_3$) was provided, carboxylation of C_3 intermediates, and especially of pyruvate by the malic enzyme, was increased. The increased flux towards reduced compound, such as succinate, provoked an increase in NADH forming reactions (formate dehydrogenase and pyruvate dehydrogenase), and a decrease in NADH consuming reactions (ethanol production). Addition of H_2, on the other hand, decreased fluxes through formate and pyruvate dehydrogenase in response to lower reductant demand for succinate production. Authors conclude that these latter fluxes should be considered

for minimization in order to maximize carbon channeling towards succinate, however the future strategies would have to take into consideration the role of these pathways in provision of redox equivalents necessary for the succinate formation (McKinlay et al. 2007, McKinlay and Vielle 2008).

Mannheimia succiniciproducens

Mannheimia succiniciproducens is a rumen bacterium closely related to *A. succinogenes*, thus they share many metabolic traits. Soon after isolation of the bacterium in 2002, its genome was sequenced and genome-scale *in silico* metabolic model was assembled (Hong et al. 2004, Kim et al. 2007). Similarly to *A. succinogenes*, *M. succiniciproducens* possesses the EMP, PPP and ED pathways. There are three enzymes for the inter-conversion of C_3 and C_4 metabolites: PEP carboxykinase, PEP carboxylase and malic enzyme, the first being the most important one for the oxaloacetate formation. Unlike *A. succinogenes*, *M. succinicigenes* possesses citrate synthase and isocitrate dehydrogenase, but lacks succinyl-CoA synthetase to close the oxidative TCA cycle; the glyoxylate shunt is also absent. While acetate producing pathways are similar, *M. succiniciproducens* forms lactate rather than ethanol. With the development of genetic tools, it was possible to design strains unable to produce lactate and acetate by the inactivation of genes encoding the respective enzymes (Lee et al. 2006). Additionally, an *in silico* analysis of the effects of H_2 and CO_2 on the metabolism of the wild-type and the deletion mutants was performed to

estimate the organic acid production patterns (Kim et al. 2009). The model predicted that addition of H_2 affected positively the cell growth, CO_2 uptake rate, and succinic acid production rate, while the fluxes towards formic and acetic acid decreased. All mutants showed the dependence of succinate production on the CO_2 provided, but this trend was predicted to stand until the CO_2 uptake rate exceeds the glucose uptake rate, after which cells start to accumulate pyruvate, in accordance with experimental evidence (Song et al. 2007).

Basfia succiniciproducens

Basfia succiniciproducens is a less known rumen bacterium isolated by the German company BASF. Knowledge on this organism is scarce; however, the metabolic network of *B. succiniciproducens* was deduced from the genetic repertoire of its relative *M. succiniciproducens* (Hong et al. 2004, Becker et al. 2013). It comprises glycolysis, PPP, ED pathway, a full TCA cycle, anaplerotic carboxylation and decarboxylation, fermentation pathways, and anabolic routes into biomass. The end product spectrum includes the organic acids acetate, succinate and formate as major products, and low amounts of lactate and ethanol. Most of glucose is processed through EMP (92%) and by PPP to a low extent (7-8%). PPP provides NADPH for anabolic needs, and anabolic precursors to a lesser extent, as PPP intermediates were directed into the glycolysis. TCA cycle functions as two separate branches rather than as a cycle. Succinate was by far formed via the reductive branch, and almost negligibly by the

oxidative branch. Accordingly to the model predictions, pyruvate:formate lyase was inactivated as the first step of the engineering strategy. However, this resulted in increased lactate and a slight (5%) increase in succinate. Additional inactivation of lactate dehydrogenase resulted in 45% increase in the succinate yield compared to the wild-type. The double deletion mutant was predicted to be the most promising succinate producer of *B. succiniciproducens* (Becker et al. 2013).

Escherichia coli

Escherichia coli is an important industrial bacterium and a model organism for studying many aspects of bacterial physiology. Thus, there is a vast knowledge available on different features of *E. coli* metabolism, as well as a large set of genetic tools. *E. coli* is able to produce succinate in addition to acetate, lactate, ethanol and formate, but not up to high amounts as shown for rumen bacteria.

Various efforts were directed to turn succinate into the major fermentation product in *E. coli*. This bacterium has different central metabolism compared to the described natural producers; succinate can be formed from oxaloacetate (produced by two PEP carboxylating enzymes) and reductive TCA, oxidative TCA cycle, glyoxylate shunt and action of malic enzyme in carboxylation of pyruvate. Having this in mind, a stoichiometric metabolic model was constructed in the lab of Sang Yup Lee, with the aim to estimate flux operation which would secure maximal succinate yields (Hong et al. 2003). This model suggested that maximal succinate yield was

1.65 mol per mol glucose, without provision of external electron sources, and 2 mol per mol glucose if external electrons were provided. The uptake of CO_2 and the source of electrons for reduction reactions are two limiting factors for optimal succinate formation.

Accordingly, many metabolic engineering strategies were applied to make recombinant *E. coli* succinate producers (for a comprehensive review, see Thakker et al. 2012). An example of this is *E. coli* NZ111, a platform strain for succinate production in which lactate dehydrogenase and pyruvate:formate lyase were inactivated, leading to suppression of lactate, acetate and formate production and increase in succinate (Stols and Donnelly 1997). However, this strain grew poorly under anaerobic conditions and excreted pyruvate. Overproduction of the malic enzyme and inactivation of PTS system in NZY111 resulted in construction of *E. coli* AFP 111, a strain that exhibited restored growth and increased succinate formation due to the enhanced availability of PEP for the carboxylation (Vemuri et al. 2002). In another study, ^{13}C-labeling tracer experiments were coupled to metabolic flux analysis to determine the metabolic fluxes in non-growing *E. coli* AFP 111 cells under various CO_2 concentrations (Lu et al. 2009). Authors showed that CO_2 supported succinate formation and that about 90% of succinate was formed by incorporation of CO_2 by PEP carboxylase. Increase in CO_2 and succinate led to an increase in PPP, which served as a generator of reducing power in the form of NADPH. This was not unexpected having in mind that *E. coli* possesses two

transhydrogenases, which can interconvert NADPH and NADH and thus provide NADH necessary for succinate formation.

Another approach to produce succinate anaerobically involved engineering of the glyoxylate shunt since the production via this pathway requires less NADH (Sanchez et al. 2006). The strain with inactivated alcohol dehydrogenase, lactate dehydrogenase and phosphotransacetylase-acetate kinase, and with de-repressed glyoxylate pathway through deletion of a repressor protein gene, produced succinate with a yield of 1.6 mol per mol glucose. This strain used a combination of the glyoxylate shunt and the reductive TCA to produce succinate, for which 1.25 mol NADH was required, compared to 2 mol NADH per mol succinate required when solely the reductive TCA branch is used.

Saccharomyces cerevisiae

Saccharomyces cerevisiae is a well-studied and robust industrial host. The availability of a sophisticated toolbox for genetic engineering and tolerance to low pH and high osmotic pressure conditions make this organism an interesting host for the industrial production of succinate. The metabolic pathways for succinate formation are in principle the same as in bacteria such as *E. coli*. One of the possible strategies is to produce succinate via the reductive TCA cycle, however this requires complex metabolic engineering interventions as the yeast fumarase has 17-fold higher affinity towards fumarate than towards malate (Pines et al. 1996) and cytosolic malate dehydrogenase is subjected to proteolytic degradation in the

presence of glucose (Hung et al. 2004). In addition to this, succinate formation via the reductive TCA results in no net ATP production for cell growth and maintenance. Second option to produce succinate is through the oxidative TCA cycle; however, this can lead to maximal yield of 1 mol per mol glucose (half of that expected through the reductive TCA). ATP formed this way can be utilized to keep intracellular pH high at the low pH succinate producing conditions, which are desirable for more efficient product purification (Yuzbashev et al. 2011). Raab and Lang constructed a metabolic model that suggested that optimal production of succinate would happen when reductive TCA was used in combination with the glyoxylate shunt (designed as “oxido-reductive” route). Maximal yield predicted by this model was 1.71 mol succinate per mol glucose and it resulted in balanced electron production and positive net ATP yield (Raab and Lang 2011). A recent study by Otero et al. (2013) showed the importance of metabolic models and systems biology for efficient development of yeast succinate producers. In a systems metabolic engineering approach (*in silico* guided metabolic engineering, strain development and transcriptome guided metabolic engineering), yeast strains with significantly improved succinate production parameters were designed. The resulting strain showed a 30-fold improvement in succinate titer, and a 43-fold improvement in succinate yield on biomass, highlighting the significance of systems biology for identification of non-intuitive targets for metabolic engineering, such as serine-glycine metabolism (Otero et al. 2013). However, in the meantime Reverdia, a joint venture between two big biotech companies Roquette

Freres and DSM, developed yeast with impressive production characteristics (100 g/L succinate at pH 3), in a two-step approach that consisted of rational metabolic engineering and strain development. This strain had suppressed production of reduced by-products such as glycerol and ethanol, produced succinate via the combination of glyoxylate and reductive TCA branch, and transport of succinate was enhanced by transporter engineering (van den Tweel 2010).

Biobased production of 2,3-butanediol

2,3-Butanediol (2,3-BD) is a bulk chemical with a wide range of industrial applications (Fig. 1.5). It can be used as carrier for pharmaceuticals as well as for the production of moistening and softening agents, perfumes, fumigants, insecticides, explosives, plasticizers and printing inks; it is a promising fuel additive and a cryoprotectant (Magee and Kosaric 1987, Garg and Jain 1995, Ji et al. 2011).

The derivative of 2,3-BD, butanone (methyl ethyl ketone), is an important fuel additive with a combustion heat value higher than ethanol, solvent for resins and lacquers and a catalyst (Magee and Kosaric 1987, Villet 1981). 1,3-Butadiene, another derivative of 2,3-BD, is a building block of synthetic rubber (van Haveren et al. 2007, Syu 2001, Celińska and Grajek 2009). Diacetyl and acetoin, high-value food additives, are formed by dehydrogenation of 2,3-BD. Acetoin can be employed as flavoring agent due to its buttery taste; diacetyl is an important bacteriostatic food additive (Bartowsky and Henschke 2004, Macciola et al. 2008). Esterification

derivatives of 2,3-BD have application in cosmetic products, lotions, drugs, and antiperspirants (Garg and Jain 1995, Syu 2001).

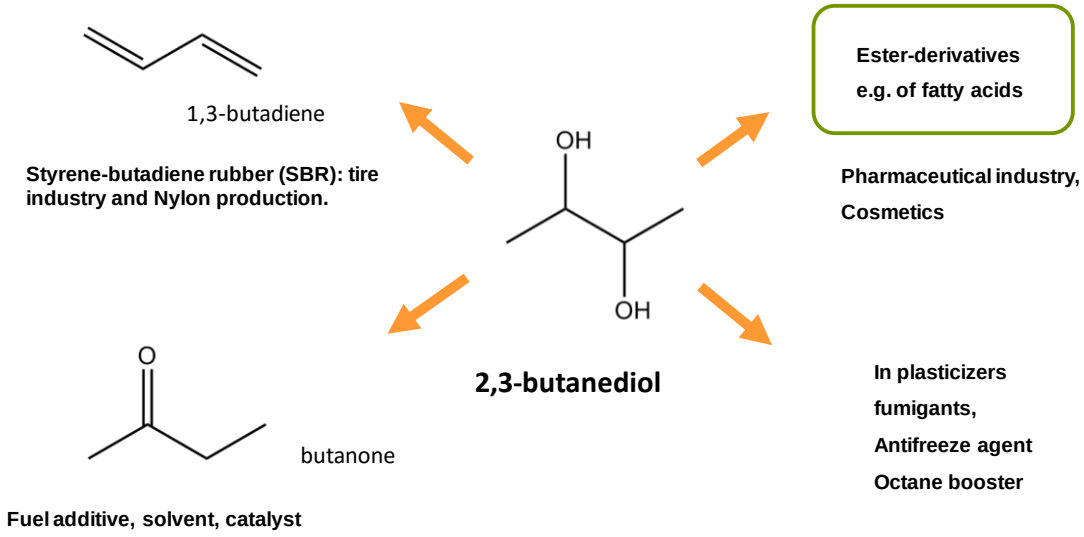

Fig. 1.5. Derivatives and applications of 2,3-butanediol.

So far, a partnership of two companies, LanzaTech and Invista, announced commercial production of 2,3-BD from CO (carbon monoxide) using acetogenic bacteria. 2,3-BD produced this way will be dehydrogenated into 1,3-butadiene, a precursor of synthetic rubber.

Specific microbial 2,3-butanediol producers

2,3-BD is a four-carbon polyol produced from pyruvate in a three-step pathway (Fig. 1.6). Two pyruvate molecules are combined into an α-acetolactate molecule by the catabolic acetolactate synthase (ALS) or the anabolic acetohydroxyacid synthase (AHAS); the following step, α-acetolactate decarboxylation into (*R*)-acetoin, is catalyzed by α-

acetolactate decarboxylase (ALDC). The last step, acetoin reduction into 2,3-BD, is performed by the butanediol dehydrogenase (BDH). An alternative and less efficient pathway is active in the presence of oxygen that causes spontaneous decarboxylation of α-acetolactate into diacetyl, which can be converted into (*R*)- or (*S*)-acetoin by the diacetyl reductase. Often it is BDH that can also catalyze reduction of diacetyl (Fig. 1.6).

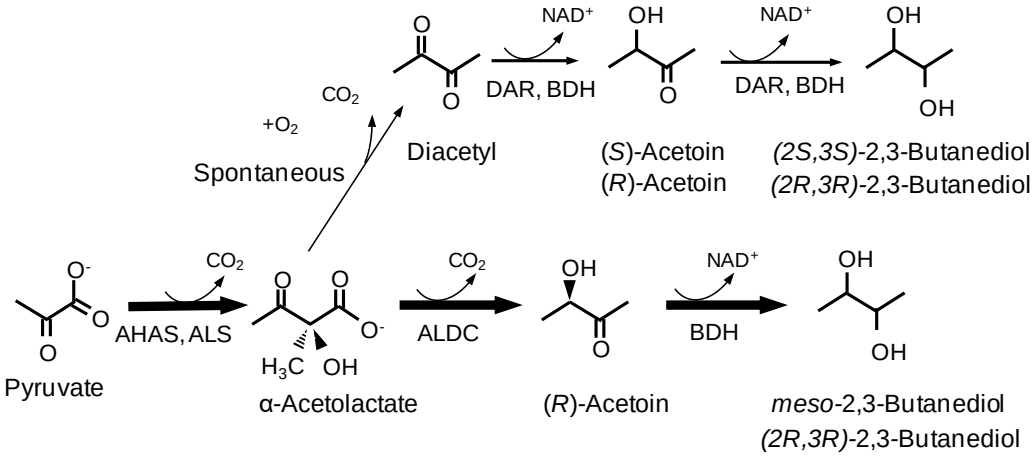

Figure 1.6. Scheme illustrating the pathways for the synthesis of 2,3-butanediol in bacteria: after it is synthesized from pyruvate, α-acetolactate can be either decarboxylated enzymatically into (*R*)-acetoin, which is reduced into 2,3-BD, or it can get spontaneously decarboxylated into diacetyl, which is reduced in two steps into 2,3-BD. The more efficient pathway via ALDC is shown in bold. Abbreviations: ALS, α-acetolactate synthase; ALDC, α-acetolactate decarboxylase; BDH, butanediol dehydrogenase; AHAS, acetohydroxyacid synthase, DAR, diacetyl reductase.

The molecule of acetoin contains a single chiral carbon and can exist as one of the two enantiomeric forms: (*R*)-acetoin or (*S*)-acetoin (Fig. 1.7). 2,3-BD possesses two chiral centers and three stereoisomers: (*2R,3R*)-

2,3-BD (or D-2,3-butanediol), (*2S,3S*)-2,3-BD (or L-2,3-butanediol), and the optically inactive (*2R,3S*)-2,3-BD (or *meso*-2,3-BD) (Fig. 1.7).

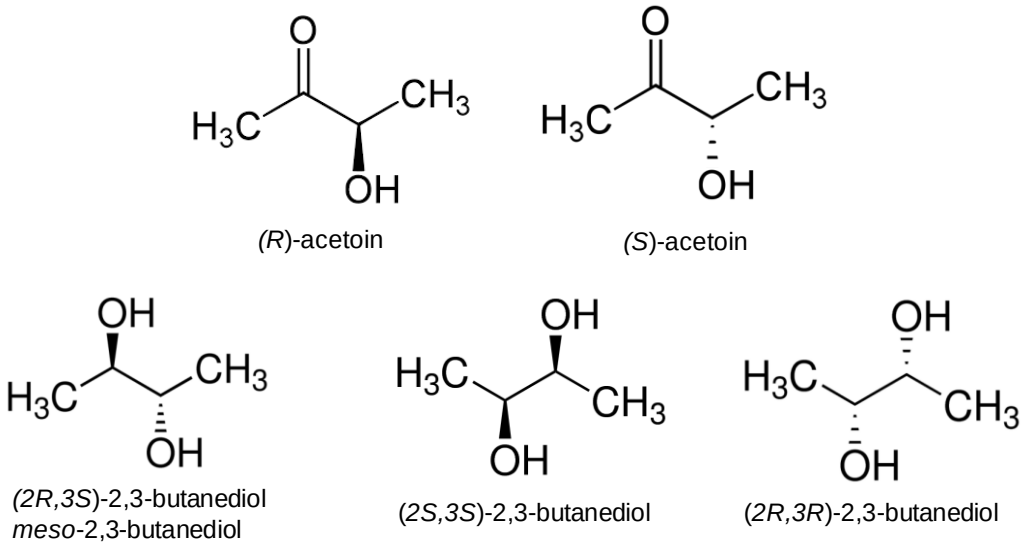

Figure 1.7. Molecular formulas of the two acetoin enantiomers: (*R*)- and (*S*)-acetoin, and the three stereoforms of 2,3-butanediol: optically inactive *meso*-2,3-butanediol and the two enantiomeric forms: (*2S,3S*)-, and (*2R,3R*)-2,3-butanediol.

In most cases, bacteria produce a mixture of 2,3-BD stereoisomers, which is not considered a disadvantage if bioproduced 2,3-BD is to be used as a bulk chemical; however, optically active forms are particularly important in chiral synthesis of pharmaceuticals and other high value chemicals. Also, (2*R,*3*R*)-butanediol is used as antifreeze agent and solvent due to its low freezing point (Gao et al. 2012, Qi et al. 2014). Since the production of pure stereoisomers of 2,3-BD is advantageous for many applications, it is important to study the stereospecific properties of BDHs and the respective catalytic mechanisms (Ji et al. 2011).

BDHs belong to the NAD(P)-dependent alcohol dehydrogenase family, generally divided into three large groups: i) Fe-dependent alcohol dehydrogenases, which belong to the smallest and the least studied group; ii) Zn-dependent alcohol dehydrogenases, also designated medium-chain dehydrogenase/reductase (MDR) family; and iii) short-chain dehydrogenase/reductase (SDR) family that are not metal-ion-dependent.

The BDHs of *K. pneumoniae*, *S. marescens*, and *E. cloacae* fall into the SDR family; these enzymes introduce the new hydroxyl group in the (*S*)-configuration, thus reducing (*R*)-acetoin to *meso*-2,3-BD and (*S*)-acetoin to (*2S,3S*)-2,3-BD (Fig. 1.7, also see Table 4.1). *C. glutamicum* (formerly *Brevibacterium saccharolyticum* C-1012), and *Rhodococcus erythropolis* possess BDHs that belong to the SDR family, and were found to be absolutely specific for (*S*)-acetoin and (*2S,3S*)-2,3-BD (Wang et al. 2013, Takusagawa et al. 2001). On the other hand, the BDHs of *B. subtilis*, *P. polymyxa* and *S. cerevisiae* belong to the MDR family, and generally introduce a hydroxyl group in the (*R*)-configuration; they use (*R*)-acetoin and (*S*)-acetoin to produce (*2R,3R*)-2,3-BD and *meso*-2,3-BD, respectively (Fig. 1.7; Table 4.1).

In the following text, major achievements in the biobased production of 2,3-BD using different organisms will be summarized, with a special focus on the stereochemistry of the 2,3-BD formation.

Klebsiella spp.

Klebsiella oxytoca and *Klebsiella pneumoniae* are natural 2,3-BD producers and among the top 2,3-BD producers. Engineering strategies consisted in elimination of the by-products; *Klebsiella oxytoca* strain with interrupted pathways for the production of ethanol, acetate and lactate achieved a particularly high yield, specific productivity, and titer (0.98 mol 2,3-BD per mol glucose, 1.2 $g \cdot L^{-1} \cdot h^{-1}$, and 117 $g \cdot L^{-1}$, respectively) (Jantama et al. 2015). However, the potential pathogenicity of these strains is still considered an obstacle for industrial scale production (Ji et al. 2011). Both *Klebsiella oxytoca* and *Klebsiella pneumoniae* are known to produce *meso*- and (*2S,3S*)-2,3-BD. One BDH, belonging to the SDR group, from *Klebsiella pneumoniae* was characterized and shown to catalyze reduction of (*S*)-acetoin into (*2S,3S*)-2,3-BD, or (*R*)-acetoin into *meso*-2,3-BD (Ui et al. 1997, Zhang et al. 2012). In addition, when 2,3-BD was produced from glycerol, (*2R,3R*)-2,3-BD was detected; this led to the discovery of a glycerol dehydrogenase with a dual role: it formed (*2R,3R*)-2,3-BD from (*R*)-acetoin, and *meso*-2,3-BD from (*S*)-acetoin, in addition to glycerol oxidation (Chen et al. 2014, Y Wang et al. 2014).

Paenibacillus polymyxa

Paenibacillus polymyxa is one of the most promising non-pathogenic natural 2,3-BD producers. Particularly successful is strain DSM 365, that produced 111 $g \cdot L^{-1}$ 2,3-BD within 54 h with high optical purity (98% (*2R,3R*)-form and 2% of *meso*-form) under oxygen limiting conditions, in

medium that contained yeast extract. 2,3-BD formation by this strain was lower (72 $g \cdot L^{-1}$ 2,3-BD and acetoin) in the medium with decreased content of yeast extract, since exopolysaccharide formation occurred. Optical purity was also affected (79% (*2R,3R*)-2,3-BD) (Haßler et al. 2011).

BDH of *P. polymyxa* ATCC12321 and ZJ-9 were purified and characterized; both enzymes belonged to the MDR group and showed strong preference for (*2R,3R*)-2,3-BD (Yu et al. 2011, Gao et al. 2013).

***Enterobacter* spp.**

Enterobacter cloacae and *Enterobacter aerogenes* are class II natural 2,3-BD producers. *E. cloacae* subsp. *dissolvens* SDM is able to produce 78.3 $g \cdot L^{-1}$ of 2,3-BD in 24 h using simultaneous saccharification and fermentation, with a yield of 0.42 g 2,3-BD per g cassava powder (0.84 mol per mol) and a specific productivity of 3.3 $g \cdot L^{-1} \cdot h^{-1}$. The produced 2,3-BD was mainly the *meso*-form (83.1%) with 5.2% of (2*R*,3*R*)-2,3-BD, and 11.7% of (2*S*,3*S*)-2,3-BD (Wang et al. 2012). An SDR-type BDH is responsible for *meso*- and (2*S*,3*S*)-2,3-BD formation (Carballo et al. 1991). *E. aerogenes* with inactivated lactate dehydrogenase gene produced 118.05 $g \cdot L^{-1}$ of 2,3-BD in 54 h, and even though the produced isomer was not specified, it was earlier shown that this bacterium produces mainly the *meso*-form of 2,3-BD with small contamination by the optically active form (Höhn-Bentz 1978).

Serratia marcescens

Serratia marcescens H30 is another class II natural 2,3-BD producer; formation of surface-active exolipid serrawettin W1 is characteristic for this strain. To avoid excessive addition of antifoam agent and microbial contamination, *S. marcescens* deficient in serrawettin W1 formation was constructed and employed for 2,3-BD production. The resulting strain produced 2,3-BD from sucrose at a concentration of 152 $g \cdot L^{-1}$ with a productivity of 2.67 $g \cdot L^{-1} \cdot h^{-1}$ and a yield of 93% (Zhang et al. 2010). This organism was also shown to possess an SDR-type BDH, responsible for the meso-2,3-BD production observed in fermentations (Zhang et al. 2014).

Lactococcus lactis

Lactococcus lactis belongs to the lactic acid bacteria that produce 2,3-BD as a part of the strategy to cope with low pH stress. Under anaerobic conditions, the triple lactate dehydrogenase-deficient mutant of *L. lactis* overexpressing the endogenous ALS and BDH achieved the theoretical yield of *meso*-2,3-BD under anaerobic conditions (0.67 mol per mol glucose) (Gaspar et al. 2012).

L. lactis possesses two BDH activities (Crow 1990). Curiously, Crow described that the two activities produce different forms of 2,3-BD (*meso*- and optically active form); Gaspar and co-workers assigned *butA* encoded activity as the *meso*-BDH; on the other hand, Nielsen et al. concluded that the *butB* encoded activity is the one responsible for *meso*-2,3-BD formation (Gaspar et al. 2012, Nielsen et al. 2010).

Bacillus spp.

The three non-pathogenic strains from the *Bacillus* genus, *Bacillus subtilis*, *Bacillus amyloliquefaciens* and *Bacillus licheniformis* are known to naturally produce 2,3-BD. All three strains are capable of producing 2,3-BD with high yield (~0.9 mol 2,3-BD per mol glucose), however, *B. amyloliquefaciens* and *B. licheniformis* are superior in terms of productivity and titer (specific productivities and yields of 1.16 $g \cdot L^{-1} \cdot h^{-1}$ and 102.3 $g \cdot L^{-1}$; and 2.10 $g \cdot L^{-1} \cdot h^{-1}$ and 74 $g \cdot L^{-1}$ achieved by the two strains, respectively) (Fu et al. 2014, Li et al. 2014, Yang et al. 2014). Due to the fact that MDR-type BDH of *B. subtilis* was described, this enzyme was employed in production of enantiopure (2*R*,3*R*)-2,3-BD by non-natural producers (Nicholson et al. 2008, Xu et al. 2014, Lian et al. 2014).

Escherichia coli

Even though *E. coli* lacks a functional pathway for the synthesis of 2,3-BD, it has been engineered for the production of this diol, due to its amenability for the industrial scale production and availability of information about this bacterium. There were several attempts to engineer *E. coli* to produce 2,3-BD and, in general, they consisted of overexpression of foreign pathways in *E. coli* hosts. Importantly, Xu and co-workers (Xu et al. 2014) carried out a systematic approach to choose the best genetic elements for the over-expression of the biosynthetic pathway (promoters and gene clusters), and optimized the fermentation conditions to obtain *E. coli* strains that produced 73.8 $g \cdot L^{-1}$ of 2,3-BD in 62 h, with an approximate yield of 0.82

mol per mol glucose. The most efficient production was achieved by using the genes from *Enterobacter cloacae*, a pathogenic natural 2,3-BD producer. The main product was *meso*-2,3-BD, with traces of the two optically active forms (Xu et al. 2014).

Saccharomyces cerevisiae

The industrial organism *Saccharomyces cerevisiae* possesses three pathways for 2,3-BD biosynthesis, but produces minimal amounts of this compound. Using the prediction of a genome scale model, a background strain was built in which alcohol dehydrogenases involved in ethanol production were inactivated; in addition, glycerol production was eliminated. In this background, heterologous pathways from *Enterobacter aerogenes* and *Bacillus subtilis* were introduced to produce 2,3-BD with increased efficiency (Ng et al. 2012).

In another study, ethanol production was eliminated by disabling pyruvate decarboxylases (Lian et al. 2014). Although this strain is unable to produce acetyl-CoA from glucose, it was enabled to grow on glucose by the means of adaptive evolution. A pathway consisting of yeast ALS and BDH, in addition to ALDC from *Bacillus subtilis* was introduced into the resulting strain. This strain produced 0.7 mol of enantiopure (*2R,3R*)-2,3-BD per mol substrate (mixture of glucose and galactose), around 100 $g \cdot L^{-1}$ in 300 h.

Only one BDH has been characterized in *S. cerevisiae;* this enzyme belongs to a MDR group, and produced a mixture of (*2R,3R*)-2,3-BD and *meso*-2,3-BD from *R/S*-acetoin (Gonzalez et al. 2000).

Acetogenic bacteria

The three non-pathogenic acetogenic *Clostridium* species, *Clostridium autoethanogenum*, *C. ljungdahlii*, and *C. ragsdalei* are able to use CO-containing industrial waste gases or syngas as the sole carbon and energy source to produce 2,3-BD (Köpke et al. 2011). In these organisms, CO and/or CO_2 enter the methyl (eastern) and carbonyl (western) branches of the Wood-Ljungdahl pathway, resulting in the formation of acetyl-CoA, which serves as the central precursor for all catabolic and anabolic processes. Pyruvate formed from acetyl-CoA by the pyruvate synthase, is a precursor for the synthesis of 2,3-BD. The major form of 2,3-BD produced is (*2R,3R*)-2,3-BD; a small contamination with *meso*-2,3-BD was observed. This corresponds to sequence analysis of the BDH genes in these three clostridia, which shows high similarity (60%) to the (*2R,3R*)-2,3-butanediol dehydrogenase of *Bacillus subtilis* (Köpke et al. 2011).

Cyanobacteria (*Synechococcus elongatus* PCC7942)

Cyanobacteria have the enzymatic machinery required to fix CO_2, but lack the 2,3-BD biosynthetic pathway. As a proof of principle for the 2,3-BD production from CO_2, *Synechococcus elongatus* PCC7942 was systematically engineered using various combinations of genes encoding enzymes in the 2,3-BD pathway (Oliver et al. 2012). Final strain, with a 2,3-BD forming pathway consisting of ALS from *B. subtilis*, ALDC from *Aeromonas hydrophila* and BDH from *Clostridium beijerinckii*, produced 2.4 $g \cdot L^{-1}$ of 2,3-BD directly from CO_2 and sunlight, in 21 days. The major

product was (*2R,3R*)-2,3-BD and a low amount of *meso*-2,3-BD was also detected.

CHAPTER 2

The effect of CO_2 on anaerobic succinate production by *Corynebacterium glutamicum*: carbon flux analysis by ^{13}C-NMR

This chapter is published in:

Radoš D, Turner DL, Fonseca LL, Carvalho AL, Blombach B, Eikmanns BJ, Neves AR and Santos H.
Carbon flux analysis by ^{13}C Nuclear Magnetic Resonance to determine the effect of CO_2 on anaerobic succinate production *by Corynebacterium glutamicum*. (2014) Applied and Environmental Microbiology 80:3015-3024.

Contents

Summary

Corynebacterium glutamicum wild-type produces a mixture of lactic, succinic and acetic acid from glucose under oxygen deprivation. We investigated the effect of CO_2 on the production of organic acids in a two-stage process: cells were grown aerobically in glucose and, subsequently, organic acid production by non-growing cells was studied under anaerobic conditions. The presence of CO_2 caused an up to 3-fold increase in the succinate yield (1 mol per mol of glucose), and about 2-fold increase in acetate, both at the expense of L-lactate production; moreover, dihydroxyacetone formation was abolished. The redistribution of carbon fluxes in response to CO_2 was estimated by using ^{13}C-labelled glucose and ^{13}C-NMR analysis of the labelling patterns in end-products. The flux analysis showed that 97% succinate was produced via the reductive part of the tricarboxylic acid cycle, the low activity of the oxidative branch being sufficient to provide the reducing equivalents needed for the redox balance. The flux via the pentose phosphate pathway was low (~5%) regardless of the presence or absence of CO_2. Moreover, there was a significant channelling of carbon to storage compounds (glycogen, trehalose), and concomitant catabolism of these reserves. The intracellular and extracellular pools of lactate and succinate were measured by *in vivo* NMR and the stoichiometry (H^+:organic acid) of the respective exporters was calculated. This study shows that it is feasible to take advantage of natural cellular regulation mechanisms to obtain high yields of succinate with *C. glutamicum* without genetic manipulation.

Introduction

Corynebacterium glutamicum is a facultatively anaerobic (Nishimura et al. 2007), Gram-positive bacterium that occupies a prominent position among industrial microorganisms, primarily due to its outstanding performance in the production of L-amino acids. In fact, over two million tons of L-glutamate and L-lysine are produced per year by *C. glutamicum* fermentation (Shimizu and Hirasava 2007, Becker and Wittmann 2012). In addition, this is a GRAS-organism (Generally Regarded as Safe), robust (osmotolerant and phage-resistant), extensively studied with respect to metabolism and regulation, and amenable to genetic manipulation for which a comprehensive toolbox is available (Eggeling and Reyes 2005). Under aerobic conditions, *C. glutamicum* is able to grow relatively fast to high cell densities in minimal medium. In contrast, in the absence of oxygen and nitrate, cell growth is negligible, while the ability to metabolize sugars is retained (Okino et al. 2005, Dominguez et al. 1993). Thus, cells of *C. glutamicum* can be grown aerobically and subsequently used for fermentation of desired products under anoxic conditions as demonstrated for L-alanine, L-valine or isobutanol (Yamamoto et al. 2012, Hasegawa et al. 2013, Yamamoto et al. 2013, Blombach et al. 2013).

It is well known that *C. glutamicum* converts glucose into organic acids under oxygen deprivation, i.e., L-lactic, succinic and acetic acids (Okino et al. 2005, Dominguez et al. 1993, Inui et al. 2004). Lactate and succinate are important bulk chemicals with increasing industrial demand, hence it is not surprising that a considerable research effort has been made to

optimize their production from renewable feedstocks, such as biomass (Bozell and Petersen 2010). Wild type *C. glutamicum* is able to produce L-lactate from glucose with high yield (1.79 mol per mol glucose) (Inui et al. 2004); moreover, it has been successfully engineered for the production of D-lactate and derived polyesters (Okino et al. 2008b, Song et al. 2012). In contrast, succinate is a minor product of glucose metabolism by wild type *C. glutamicum* (Okino et al. 2005, Dominguez et al. 1993, Inui et al. 2004). Studies have shown that the presence of bicarbonate increases succinate production considerably (Okino et al. 2005, Inui et al. 2004), and this finding prompted a variety of genetic and environmental manipulations aiming at further production enhancement (Litsanov et al. 2012a, Okino et al. 2008a). In particular, a high yield of succinate (1.67 mol per mol glucose) was achieved by using formate as electron and CO_2 donor, but there is still need for improvement with regard to productivity and cost-efficiency (Litsanov et al. 2012a).

Obviously, the maximization of organic acid production implies the reduction of by-products, namely by metabolic engineering strategies. As demonstrated for the construction of effective amino acid producers, the success of engineering approaches depends on detailed knowledge of cellular metabolism, which necessarily includes quantitative information on carbon flux distribution throughout the network of metabolic pathways **(**Kiefer et al. 2004, Bartek et al. 2011). Over the last two decades our team has taken advantage of the analytical power of Nuclear Magnetic Resonance (NMR) and its unique non-invasive characteristics to study

different aspects of metabolism directly in living cell suspensions (Neves et al. 1999, Neves et al. 2002a, Carvalho et al. 2013). We set out to apply this methodology and characterize *C. glutamicum* metabolism in the anaerobic production phase, in the presence and absence of CO_2, to obtain pointers for the design of strains with maximal succinate production.

Herein we report the use of ^{13}C-NMR combined with specifically ^{13}C-labelled glucose to assess the impact of CO_2 on the metabolic flux distribution in wild type *C. glutamicum* in the anaerobic production phase. Moreover, the intracellular pools of organic acids were monitored *in vivo* during the production phase. Our analysis shows that the flux through the pentose phosphate pathway (PPP) is small and not significantly altered by CO_2 supply. In addition, succinate production proceeds largely via the reductive branch of the tricarboxylic acid (TCA) cycle, but a significant flux via the oxidative branch provides the reducing equivalents needed for the redox balance.

Materials and Methods

Growth conditions

Corynebacterium glutamicum strain ATCC13032 (Kinoshita et al. 1958) was the only organism used in this work. Cells were grown aerobically in the CGXII minimal medium described by Eikmanns et al. (Eikmanns et al. 1991a), modified as follows: 5 $g \cdot L^{-1}$ $(NH_4)_2SO_4$, 21 $g \cdot L^{-1}$ MOPS (3-[N-morpholino] propanesulfonic acid), 0.2 $mg \cdot L^{-1}$ biotin. The medium was

supplemented with 4% (wt/vol) glucose. Growth experiments were performed at 30°C with constant agitation at 140 rpm in 2-liter baffled shake flasks. The medium was inoculated by addition of a pre-culture to an initial optical density at 600 nm (OD_{600}) of approximately 0.5; the initial pH value was 7.0. Pre-cultures were grown for 8 h under the same conditions as the main cultures, except that 250 mL baffled shake flasks were used. In all cases the medium volume was 1/10 of the flasks' total capacity. Growth was monitored by measuring the OD_{600}. A factor of 0.24 ± 0.01, determined from a CDW ($mg \cdot mL^{-1}$) versus OD_{600} curve, was used to convert OD_{600} into dry weight (mg biomass$\cdot mL^{-1}$).

Preparation of cell suspensions

Cells were grown as described above and harvested 16 h after inoculation, at the beginning of the stationary phase (OD_{600} of 40- 45), centrifuged (9,924 × *g*, 10 min, 4°C), and washed twice with an appropriate buffer (MES - 2-(N-morpholino)ethanesulfonic acid or PIPES - piperazine-N,N′-bis(2-ethanesulfonic acid), 10 mM at pH 7). The resulting cell suspension was centrifuged (11,325 × *g*, 10 min, 4°C) and the pellet re-suspended to an OD_{600} of 100 (dense cell suspension) or 7.5 (diluted cell suspension) in 50 mM buffer (PIPES at pH 7 or MES at pH 5.7); SAG 5693 antifoam (approx. 15-20 µL per 50 mL of cell suspension) and D_2O (6% vol/vol) were added to the dense cell suspensions for the *in vivo* NMR measurements.

In vivo NMR experiments

The experiments were performed using the on-line system described by Neves et al. (Neves et al. 1999), which consists of an 80 mL-bioreactor coupled to the NMR tube with a circulating system that allows for non-invasive studies of metabolism under controlled conditions of pH, gas atmosphere and temperature. Dense cell suspensions (OD_{600} of 100) were placed in the bioreactor and kept at 30ºC. The pH was controlled at 7.0 or 5.7 by the automatic addition of 5 M NaOH. To achieve anaerobic conditions, argon, carbon dioxide (CO_2) or a mixture of CO_2 and nitrogen (20% CO_2; vol/vol), was bubbled through the cell suspension in the bioreactor and also provided to the headspace of the NMR tube. Glucose specifically labelled with ^{13}C on carbon one (20 mM) was added to the cell suspension at time-point zero. The time course of glucose consumption, product formation and changes in the pools of intracellular organic acids were monitored *in vivo*. When the substrate was exhausted, an NMR-sample extract was prepared as described previously (Neves et al. 1999, Neves et al. 2002a). In brief, an aliquot of the cell suspension (6 mL) was passed through a French press: the resulting cell extract was incubated at 82°C (10 min) in a stoppered tube, cooled down on ice and cell debris and denatured macromolecules were removed by centrifugation (45,696 × *g,* 10 min at 4°C). The supernatant (NMR-sample extract) was used for quantification of end products and minor metabolites. Samples were stored at -20ºC until further analysis.

Quantification of end-products and intracellular organic acids

Lactate was quantified in the NMR-sample extract by ^{1}H-NMR in an AMX300 (Bruker BioSpin GmbH) spectrometer. Formic acid (sodium salt) was added to the samples and used as an internal concentration standard. The concentration of other metabolites was determined in fully relaxed ^{13}C spectra of the NMR-sample extracts as described by Neves et al. (Neves et al. 1999). Due to the fast pulsing conditions used for acquiring *in vivo* ^{13}C-spectra, correction factors were determined to convert peak intensities into concentrations. The correction factors for the resonances due to C_3 of intracellular lactate (0.60 ± 0.04) and C_2-C_3 of intracellular succinate (0.60 ± 0.02) were determined from the acquisition of fully and partially relaxed spectra of an NMR-extract. The correction factors for C_3 of extracellular lactate (0.55 ± 0.02) and C_2-C_3 of extracellular succinate (0.57 ± 0.02) were determined as above, except that PIPES buffer (50 mM, pH 7.0) containing succinate (50 mM) and lactate (60 mM) was used. The quantitative kinetic data for intracellular metabolites were calculated as described elsewhere (Neves et al. 1999, Neves et al. 2002, Carvalho et al. 2013). Intracellular concentrations were calculated using a value of 1.4 µL per mg CDW^{-1} for the intracellular volume of *C. glutamicum* (Krämer et al. 1990). Although individual experiments are illustrated in each figure, each experiment was repeated at least twice. The values reported are averages of two experiments and the uncertainty varied from ± 2 to ± 15% for metabolite concentration and from ± 1% to ± 10% for maximal glucose consumption rate (GCR).

Analysis of metabolic fluxes in the anaerobic phase (non-growing cells)

Diluted cell suspensions (OD_{600} of 7.5) prepared as described above were used to estimate the fluxes through the metabolic pathways operating under oxygen deprivation. The cell suspensions were kept at 30ºC under controlled pH of 7.0 and anaerobic conditions were ensured by bubbling argon or CO_2 through the suspension. Glucose (50 mM) specifically labelled with ^{13}C on carbon one, carbon two, simultaneously labelled on C_1 and C_2, or uniformly labelled, was added to the cell suspension at time-point zero. Samples (1 mL) were withdrawn at time-point zero and periodically for 32 h, centrifuged (10,000 × *g*, 2 min at 4ºC), and the supernatant solutions saved at −20°C until further analysis. ^{13}C-labeled end-products were quantified in the supernatants by ^{13}C-NMR using as concentration standard tetramethylurea (99%) contained in a capillary, or by ^{1}H-NMR using sodium formate as an internal standard. The total quantities of end-products were determined from averages of 6 independent experiments and have a typical standard deviation of 3%.

^{13}C-glucose isotopomers were selected specifically to resolve the contributions of different pathways (Schrader et al. 1993, Klapa et al. 1999). The labelling pattern of end products was analyzed and a scheme including central metabolic pathways was constructed (Fig 2.1 and Table 2.1). This comprised glycolysis, PPP, reductive TCA cycle down to succinate and oxidative TCA cycle also ending at succinate, lactate and acetate production from pyruvate, pyruvate (Pyr) / phosphoenolpyruvate

(PEP) carboxylation and oxaloacetate/malate conversion to pyruvate. The efflux of carbon at the level of glucose-6-phosphate towards carbon reserves (glycogen, trehalose, etc), and respective mobilization to glycolysis are also considered. PEP/Pyr carboxylation reactions are lumped together since the labelling patterns of PEP and pyruvate are indistinguishable; similarly a single flux was considered for the decarboxylation reactions from oxaloacetate or malate. The two possible acetate forming pathways from pyruvate are combined into a single one. All reactions in the reductive TCA were considered as reversible. The contribution of the glyoxylate shunt was neglected (see Discussion).

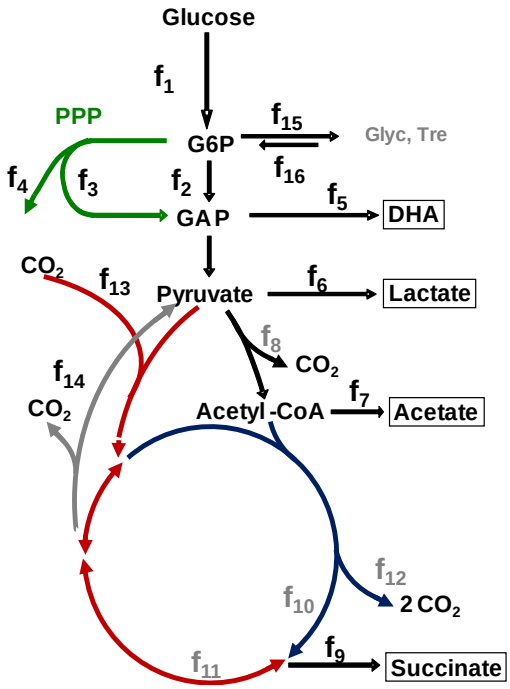

Fig 2.1. Scheme representing the reactions in the metabolic model used to estimate the flux distribution in non-growing cells of *C. glutamicum*. For more information on the metabolic fluxes, see Table 2.1.

Table 2.1. The equations used to calculate respective carbon fluxes.

Flux	Equation	Glc isotopomer
f_1	$f_1=Glc_{in}$	
f_2	$f_2=(f_1-f_{15}+f_{16})*4*[2\text{-}^{13}C]Lac/(4*[2\text{-}^{13}C]Lac+5*[3\text{-}^{13}C]Lac)$	[2-^{13}C]Glc
f_3	$f_3= (f_1-f_{15}+f_{16})*5*[3\text{-}^{13}C]Lac/(4*[2\text{-}^{13}C]Lac+5*[3\text{-}^{13}C]Lac)$	[2-^{13}C]Glc
f_4	$f_4=f_3/5$	
f_5	$f_5=DHA_{out}$	
f_6	$f_6=Lac_{out}$	
f_7	$f_7=Ac_{out}$	
f_8	$f_8=f_7/2 + f_{10}/4$	
f_9	$f_9=Suc_{out}$	
f_{10}	$f_{10}=f_9*[1,4\text{-}^{13}C]Suc/[2,3\text{-}^{13}C]Suc$	[2-^{13}C]Glc
f_{11}	$f_{11}=f_9*$ $([2,3\text{-}^{13}C]Suc-[1,4\text{-}^{13}C]Suc)/[2,3\text{-}^{13}C]Suc$	[2-^{13}C]Glc
f_{12}	$f_{12}=f_{10}/2$	
f_{13}	$f_{13}=f_9/4$	
f_{14}	$f_{14}= f_6 *[2,3\text{-}^{13}C]Lac / [1\text{-}2\text{-}3\text{-}^{13}C]Lac$	[U-^{13}C]Glc
f_{15}[a]	$f_{15}=(1\text{-}^{13}Cbalance)*f_1$	
f_{16}	$f_{16}=^{12}Cbalance -f_1-f_{13}+f_4+f_5+f_6+f_7+f_8+f_9+f_{12}+f_{15}$	
	$f_2+f_3=f_5+f_6+3*f_{10}/2+3*f_{11}/4+3*Ac_{out}/2$	
	$^{12}Cbalance=(f_1+f_{13}+f_{16})- (f_4+f_5+f_6+f_7+f_8+f_9+f_{12}+f_{15})$	

[a] ^{13}C-balance value was corrected for the loss of ^{13}C-label from the C1 of glucose as CO_2 in the PPP in the experiments which used [1-^{13}C]Glc or [1,2-^{13}C]Glc. Glc_{in}, supplied glucose; DHA_{out}, dyhydroxyacetone; Lac_{out}, lactate; Ac_{out}, acetate; Suc_{out}, succinate.

Deconvolution of overlapping intra- and extracellular organic acid resonances

Partial overlap of the resonances due to internal and external lactate hampered direct integration. Therefore, deconvolution of the relevant spectral region was performed by fitting the sum of Lorentzian and Gaussian functions using Matlab V7.1 (The Math Works, Natick, MA, USA).

Determination of *n*, number of protons exported concomitantly with each molecule of organic acid

The total amounts of internal and external organic acids were fitted to exponential curves which were used to calculate the *n*-value numerically, as in Carvalho *et al.* (Carvalho et al. 2013). The intracellular pH was determined by ^{31}P-NMR and the relative concentrations of the ionised forms were obtained using pK_{a1}=4.2 and pK_{a2}=5.6 for succinic acid.

NMR spectroscopy

All carbon-13 spectra were acquired at 125.77 MHz on a Bruker AVANCE II 500 MHz spectrometer (Bruker BioSpin GmbH) at 30ºC. *In vivo* experiments were run using a quadruple nuclei probe head, as described earlier (Neves et al. 1999). ^{13}C-NMR spectra of supernatants derived from diluted cell suspensions (OD_{600} of 7.5) were recorded using a ^{13}C-selective probe head, 32 K data points, a 68° flip angle and a repetition delay of 90.5 s. Tetramethylurea contained in a capillary was used as concentration standard and also as a reference for chemical shifts (δ=38.7 ppm).

Quantification of end-products by HPLC

End-products in supernatants derived from diluted cell suspensions or NMR-sample extracts (dense cell suspensions) were also quantified by HPLC, using an apparatus equipped with a refractive index detector (Shodex RI-101, Showa Denko K. K., Japan) and an HPX-87H anion exchange column (Bio-Rad Laboratories Inc., California, USA) at 60ºC, with 5 mM H_2SO_4 as the elution fluid and a flow rate of 0.5 mL·min^{-1}.

Chemicals

[1-^{13}C]glucose, [2-^{13}C]glucose, [1,2-^{13}C]glucose and [U-^{13}C]glucose were obtained from Cambridge Isotope Laboratories, Inc. The SAG 5693 antifoam agent was from Union Carbide Chemicals & Plastics. Formic acid (sodium salt) and tetramethylurea were purchased from Merck Sharp & Dohme and Sigma-Aldrich, respectively. All other chemicals were reagent grade (Sigma-Aldrich and Merck Sharp & Dohme).

Results

The effect of CO_2 on succinate production

In vivo ^{13}C-NMR was used to characterise the metabolism of glucose in *C. glutamicum* ATCC 13032 at OD_{600} = 100 and pH = 7 under anaerobic conditions in: i) the absence of CO_2, ii) 20% (vol/vol) CO_2, and iii) pure CO_2 (Fig. 2.2). In the absence of CO_2, *C. glutamicum* produced lactate, succinate and acetate from glucose, with lactate accounting for 1.22 mol per mol of glucose consumed (i.e., 61%) (Fig. 2.2A and Table 2.2). Replacement of argon by 20% (vol/vol) CO_2 (Fig. 2.2B), led to a decrease in lactate by about one third (from 24.5 $\pm$ 3.1 mM to 14.6 $\pm$ 0.2 mM), while succinate production doubled (from 5.9 $\pm$ 0.2 to 11.8 $\pm$ 1.0 mM) (Fig. 2.2). This trend was even more pronounced when the pure CO_2 was bubbled through the cell suspension (Fig. 2.2C and Table 2.2): lactate accounted for 21% of the glucose consumed (0.42 $\pm$ 0.01 mol per mol), corresponding to *circa* three times lower yield than in the absence of CO_2.

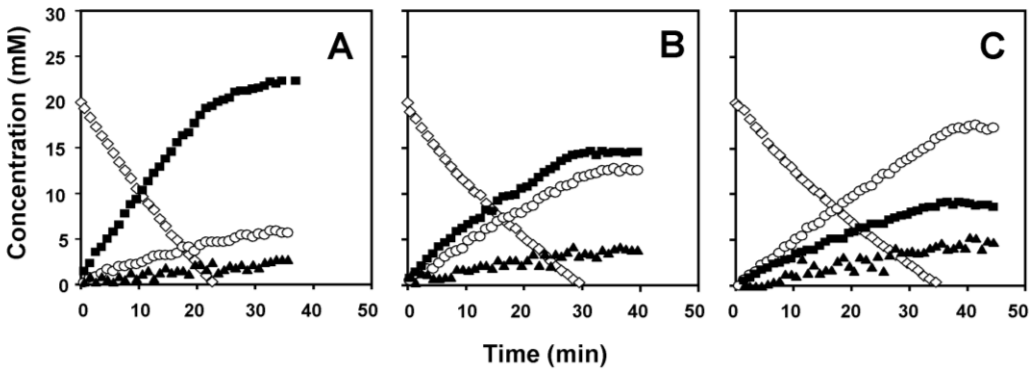

Figure 2.2. Time courses of glucose consumption and product accumulation during the metabolism of 20 mM [1-^{13}C]glucose in non-growing cell suspensions of *C. glutamicum* (OD_{600} = 100). The experiments were monitored by *in vivo* ^{13}C-NMR and carried out at 30 ºC, with pH controlled at 7.0 and bubbling (**A**) no CO_2, (**B**) 20% CO_2 or (C) 100% CO_2. Glucose consumption rates: (A) 34.5 (B) 22.5 (**C**) 21.2 nmol·min^{-1}·mg CDW^{-1}. Symbols: grey diamonds, glucose; open circles, succinate; black squares, lactate; black triangles, acetate. Each panel represents a single experiment from a set of at least two similar replicates.

Under pure CO_2, succinate was the major end-product, reaching a maximal concentration of 17.5 ± 0.3 mM. CO_2 also had a positive effect on the acetate yield, which increased approximately two-fold in the presence of 100% CO_2 as compared to no added CO_2 (Table 2.2). Other minor products, including L-glutamate, L-alanine, α-ketoglutarate, trehalose and glycogen were detected under all conditions examined. A negative correlation was observed between CO_2 supply and the glucose consumption rate (GCR), which dropped from 34.5 ± 0.7 nmol·min^{-1}·mg CDW^{-1} to 22.5 ± 2.1 and 21.2 ± 0.1 nmol·min^{-1}·mg CDW^{-1} when 20% (vol/vol) CO_2 or 100% CO_2 were used, respectively (Table 2.2).

Table 2.2. The effect of CO_2 availability on the anaerobic metabolism of glucose by *C. glutamicum* ATCC13032. The initial concentration of glucose was 20 and 50 mM for the experiments with dense and diluted cell suspensions, respectively. In dense cell suspensions (OD_{600} =100), end-products and glucose were determined online by *in vivo* NMR while in diluted cell suspensions (OD_{600} =7.5), they were measured by NMR and HPLC off-line in the sample supernatants. The pH of the cell suspension was maintained at 7.0 or 5.7.

pH	% CO_2	**Yield** (mol·mol^{-1} Glc)			**GCR** (nmol·min^{-1} mg^{-1}·CDW)	^{13}**C balance**[b] (%)	**Total C balance**[c] (%)
		Lactate[a]	Succinate[a]	Acetate[a]			
OD_{600} =100							
7.0	0	1.22 ± 0.16	0.29 ± 0.01	0.13 ± 0.02	34.5 ± 0.7	90.1 ± 6.5	141 ± 2
	20	0.73 ± 0.01	0.59 ± 0.05	0.19 ± 0.01	22.5 ± 2.1	83.8 ± 0.4	163 ± 21
	100	0.42 ± 0.01	0.87 ± 0.02	0.28 ± 0.01	21.2 ± 0.1	87.5 ± 1.2	173± 13
5.7	0	1.19 ± 0.06	0.15 ± 0.01	0.06 ± 0.01	19.7 ± 0.4	86.5 ± 0.9	110 ± 11
	100	0.83 ± 0.04	0.41 ± 0.01	0.13 ± 0.01	18.4 ± 0.2	77.2 ± 3.4	111 ± 3
OD_{600} = 7.5							
7.0	0	1.24 ± 0.06	0.03 ± 0.01	0.03 ± 0.01	25.0 ± 3.6	89.0 ± 2.8	103 ± 4
	100	0.56 ± 0.12	0.91 ± 0.11	0.26 ± 0.02	21.3 ± 1.4	79.7 ± 5.2	91 ± 6

[a]Product yields were calculated assuming that [1-^{13}C]glucose was processed via the EMP pathway and produces a labelled and an unlabelled pyruvate molecule as follows: lactate yield = [3-^{13}C]lactate×2/[1-^{13}C]glucose; acetate yield = [2-^{13}C]acetate×2/[1-^{13}C]glucose; succinate yield = ([2,3-^{13}C]succinate×2 + [1,4-^{13}C]succinate)/ [1-^{13}C]glucose; [b] ^{13}C balance is the percentage of carbon in metabolized ^{13}C-glucose that is recovered in the fermentation products; [c] total carbon balances were calculated summing up the end product concentrations. Abbreviations: GCR, glucose consumption rate.

Carbon flux analysis in non-growing cells based on ^{13}C-NMR

The fundamental as well as biotechnological interest of finding that the succinate yield was strongly increased by CO_2 motivated us to characterize the redistribution of carbon fluxes induced by CO_2 in non-growing cells (production stage). To this end, we relied on isotopomeric ^{13}C-NMR analysis of end-products from the anaerobic metabolism of glucose specifically labelled in suitable positions. The set of experiments was performed with diluted cell suspensions (OD_{600} of 7.5, as compared to 100 used for *in vivo* NMR). The use of diluted cell suspensions was dictated by the need to reduce the contribution of unlabelled end products attributed to the concomitant metabolism of internal reserves, which would complicate the analysis of labelling patterns in end-products. Indeed, in dense cell suspensions the total amount of carbon recovered in end-products was up to 70% greater than that expected from the supplied glucose (Table 2.2). Curiously, in the absence of CO_2, the succinate yield was around 10 times higher in the experiments with dense cell suspensions as compared to diluted cell suspensions. We speculate that this difference is related with a higher concentration of endogenous bicarbonate in thick suspensions since CO_2 removal is less efficient.

Considering the fate of ^{13}C-label derived from the several glucose isotopomers led to the conclusion that [2-^{13}C]glucose should provide optimal information on the activity of anaerobic pathways. Other isotopomers of glucose ([1-^{13}C]glucose, [1,2-^{13}C]glucose and [U-^{13}C]glucose) gave additional information: by using [1-^{13}C]glucose and [U-

^{13}C]glucose we were able to track backflux from the TCA cycle (oxaloacetate/malate) to 3-carbon units (PEP/Pyr); [1,2-^{13}C]glucose confirmed the PPP activity provided by the analysis of [2-^{13}C]glucose metabolism; all experiments were used to estimate the extent of metabolization of internal reserves. Because we were unable to analyse metabolites other than end-products, namely lactate, acetate, succinate, dihydroxyacetone (DHA) and glycerol, the model is necessarily highly simplified. Nonetheless, using this model we were able to estimate and compare the activity of main pathways in response to CO_2, including the split PPP/glycolysis and the proportions of the reductive and oxidative branches in the TCA cycle.

NMR analysis of end-products derived from metabolism of [2-^{13}C]glucose (Fig. 2.3, Table 2.3), provided a straightforward and accurate way to determine division between the Embden-Meyerhof-Parnas (EMP) and PPP using the ^{13}C-enrichments in C_2 and C_3 of lactate or DHA (Schrader et al. 1993). Our data showed that the majority of glucose was metabolized via the EMP pathway, in the absence of CO_2, while the activity of PPP accounted for about 2% of the carbon taken up in glucose (Fig. 2.4A). The PPP flux was 5% in the presence of pure CO_2 (Fig. 2.4B). Without added CO_2, we observed a high production of DHA (21% of the total glucose carbon), while addition of CO_2 abolished DHA formation. Moreover, the presence of CO_2 had a strong impact on the distribution of fluxes at the pyruvate node, i.e., lactate production was reduced (from 65 to 25% of carbon input), while the remaining fluxes towards pyruvate dehydrogenase

and PEP/Pyr carboxylation reactions were clearly enhanced (about 6- and 16- fold, respectively).

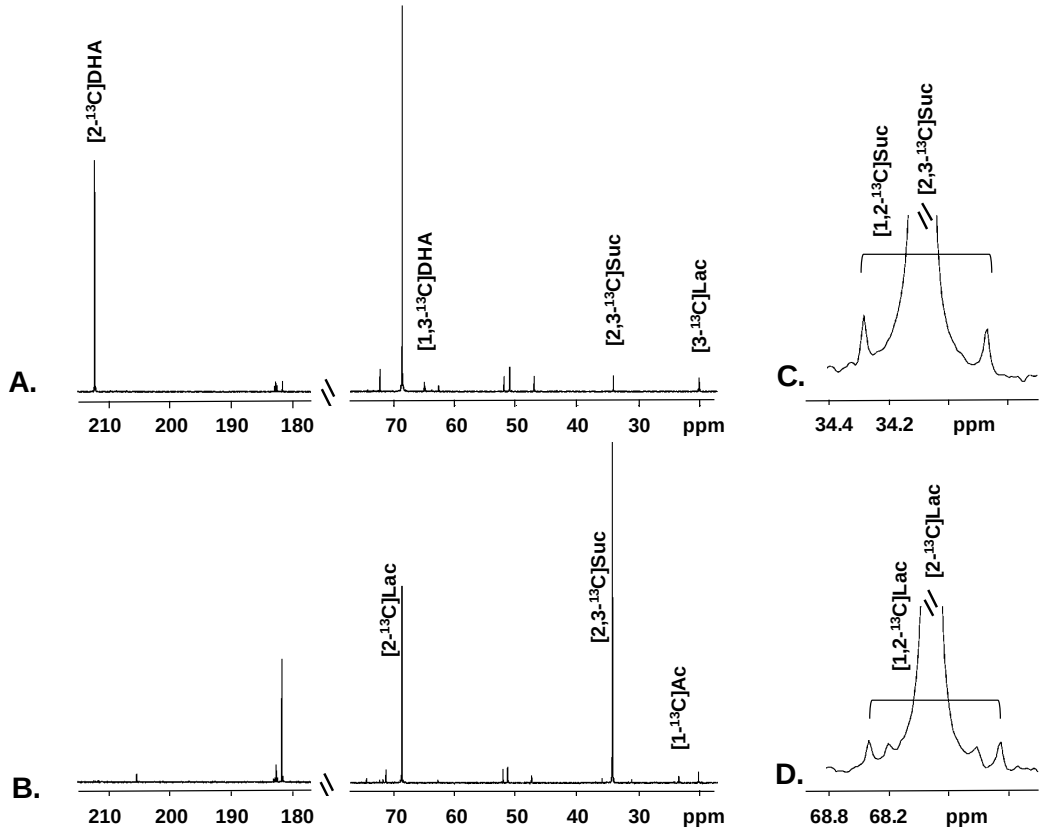

Figure 2.3. Relevant sections of ^{13}C-NMR spectra of end-products derived from the anaerobic metabolism of [2-^{13}C]glucose by diluted cells suspensions (OD_{600} = 7.5) of *C. glutamicum* in the absence of CO_2 (**A**) or presence of 100% CO_2 (**B**, **C** and **D**). **C** and **D** are expansions of the resonance patterns, respectively due to [2,3-^{13}C]succinate and [2-^{13}C]lactate in spectrum B. Symbols: DHA, dihydroxyacetone; Lac, lactate; Suc, succinate; Ac, acetate. A representative experiment is depicted from a set of three replicates.

Cells produced a low amount of [1,2-^{13}C]lactate (about 1% of total lactate) from the metabolism of [2-^{13}C]glucose, regardless of the CO_2 content in the atmosphere (Fig. 2.3D). The appearance of labelling on contiguous carbon atoms can originate from the reversible reactions catalysed by transketolase and transaldolase in the PPP (Schrader et al. 1993), or from the decarboxylation of four-carbon dicarboxylic acids (oxaloacetate/malate), that are labelled in adjacent carbons (back-flux from oxaloacetate/malate to PEP/Pyr). To clarify the origin of [1,2-^{13}C]lactate (derived from [2-^{13}C]glucose), we performed experiments with supply of [1-^{13}C]glucose and [1,2-^{13}C]glucose: small amounts (about 0.5 mM) of [1-^{13}C]lactate and [1,2,3-^{13}C]lactate were detected, respectively (data not shown). This labelling pattern can be explained by a small percentage of fructose 6-phosphate produced through EMP that is directed to the reactions catalysed by transketolase and transaldolase in PPP. To confirm or rule out the occurrence of back-flux from oxaloacetate/malate to PEP/Pyr, the alternative path that would produce the same labelling, we looked for [2-^{13}C]lactate in the end-products derived from [1-^{13}C]glucose, and also for [2,3-^{13}C]lactate derived from the metabolism of [U-^{13}C]glucose, following an approach eloquently described by McKinley and Vieille 2008 (McKinlay and Vieille 2008). The analysis showed only vestigial amounts of [2-^{13}C]lactate or [2,3-^{13}C]lactate (data not shown), meaning that the back-flux to pyruvate under 100% CO_2 atmosphere is insignificant.

Table 2.3. ^{13}C-labelling in the end-products derived from anaerobic metabolism of [2-^{13}C]glucose. Concentrations were determined by ^{13}C-NMR and corrected for natural abundance (1.1%). Values are average of three independent experiments. n.d., not detected or no greater than natural abundance. The total concentrations were obtained by HPLC and are the average of five independent experiments.

Metabolite	**Concentration** (mM)	
	0% CO_2	**100% CO_2**
Lactate C3	0.48	0.51
Lactate C2	27.28	11.31
Lactate C1	0.13	0.10
Lactate C3-C2	n.d.	n.d.
Lactate C2-C1	0.29	0.19
Total lactate	64.88	24.73
Succinate C2,3	0.56	18.92
Succinate C1,4	n.d.	0.58
Succinate C1-2	n.d.	0.21
Total succinate	4.09	67.44
Acetate C2	n.d.	0.27
Acetate C1	0.64	5.51
Acetate C1-C2	n.d.	n.d.
Total acetate	1.75	10.38
DHA C1,C3	0.20	n.d.
DHA C2	10.70	n.d.
DHA C1-C2	0.13	n.d.
Total DHA	21.09	n.d.
Glycerol C1,C3	0.28	0.15
Glycerol C2	1.61	0.20
Total glycerol	3.25	0.36

Abbreviation: DHA, dihydroxyacetone

Table 2.4. Values calculated for the metabolic fluxes.

Carbon flux	0% CO_2	100% CO_2
	% of carbon per 100 carbon atoms taken up in glucose	
f_1	100.00	100.00
f_2	90.04	88.40
f_3	1.92	4.81
f_4	0.38	0.96
f_5	21.09	0.00
f_6	64.88	24.73
f_7	1.76	10.38
f_8	0.84	5.65
f_9	4.10	67.44
f_{10}	-0.14	1.83
f_{11}	4.24	65.61
f_{12}	-0.07	0.91
f_{13}	1.02	16.86
f_{14}	0.60	0.53
$(f_{16}-f_{15})$	-8.04	-6.79
f_{15}	11.97	19.30
f_{16}	3.94	12.51
^{13}C balance	87.87	80.70
^{12}C balance	91.83	102.55

In the absence of added CO_2, the production of succinate was too low to estimate fluxes within the TCA cycle. However, the increase in succinate production induced by CO_2 enabled the characterisation of the TCA cycle reactions in more detail. Approximately 97 % (18.84 out of 19.58 mM, Table 2.3) of the labelled succinate pool was enriched in either of the inner carbons (C_2 or C_3) (Table 2.3), reflecting the prominent contribution of the reductive branch of the TCA cycle. The low proportion of succinate labelled on either C_1 or C_4 (3%) indicated a small but statistically significant contribution of the oxidative branch of the TCA cycle (see Discussion).

The proportions of succinate produced via the oxidative versus the reductive TCA cycles determined the amount of CO_2 released (1%, three

mol per mol of succinate via oxidative TCA) and the amount incorporated through PEP/Pyr carboxylation reactions (ca. 17%, one mol per mol of total succinate). Decarboxylation of pyruvate into acetate or acetyl-CoA and of 6-phosphogluconate (in PPP) added to the loss of carbon through CO_2 (about 7% in total) (Fig. 2.4B). In experiments where pure CO_2 was provided, it is reasonable to assume that all of the incorporated CO_2 was unlabelled, whereas about one third of the CO_2 lost in decarboxylation reactions was labeled on average across the various experiments. The gain (carboxylation reactions) and loss of carbon (decarboxylation reactions) was accounted for in both the ^{13}C and total carbon balances. The remaining loss of ^{13}C of about 10-20% was attributed to channelling of ^{13}C-glucose to reserve materials (glycogen, trehalose, etc). The flux towards glycogen and trehalose was confirmed by *in vivo* NMR experiments that showed increasing resonances of glycogen and trehalose from the metabolism of C_1-labeled glucose (data not shown). The difference between total and ^{13}C balances, after accounting for incorporation of unlabelled CO_2, was attributed to catabolism of unlabelled intracellular reserves that had accumulated during growth (ca. 4% without CO_2 and 13% with 100% CO_2 experiments) (Fig. 2.4A and B). Therefore, there is carbon exchange with internal reserves and a net channelling of supplied glucose to the formation of storage compounds. The equations used to obtain the fluxes shown in Figure 3 are listed in Table 2.1.

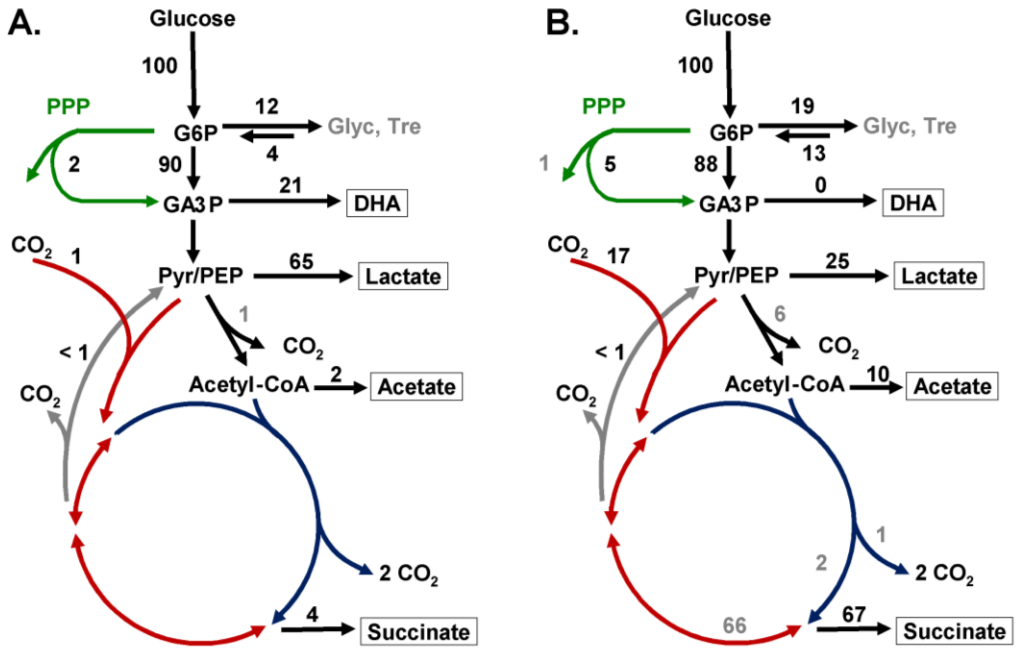

Figure 2.4. Scheme representing the reactions in the metabolic model used to estimate the flux distribution in non-growing cells of *C. glutamicum* (OD_{600} =7.5), with no supply of CO_2 (**A**); and 100% CO_2 (**B**) at pH 7.0. To extract the minimal set of reactions operating under these conditions we analyzed the ^{13}C labelling in end-products from anaerobic metabolism of [1-^{13}C]glucose, [2-^{13}C]glucose, [1,2-^{13}C]glucose and [U-^{13}C]glucose. Fluxes are shown as a percentage in relation to the number of carbon atoms taken up as glucose. Lines with arrows represent respective fluxes in the central metabolism: PPP (green), EMP (black), reductive TCA (red), oxidative TCA (blue), oxaloacetate/malate decarboxylation into PEP/Pyr (grey). More precise values for fluxes are shown in Table 2.4.

Intracellular pools of lactate and succinate determined by *in vivo* ^{13}C-NMR

Production of organic acids by fermentation at low pH is highly desirable to facilitate downstream processing and minimize waste products (Straathof 2013). Moreover, high intracellular pools of succinic and lactic acids may inhibit protein activity (Carvalho et al. 2013, Reinscheid 1994a). Therefore, we examined the effect of CO_2 on succinate production at a lower pH. Furthermore, at acidic pH it is possible to monitor intracellular pools of organic acids non-invasively by ^{13}C-NMR (Carvalho et al. 2013). The species of weak organic acids in solution are in fast exchange on the NMR timescale, thus giving rise to a single resonance whose chemical shift is determined by the proportion of the protonated and non-protonated species, i.e., by pH. When the pH values of the intracellular and extracellular compartments are sufficiently different, the internal and external pools originate distinct resonances in the NMR spectrum. Herein the pH of the external solution was set at 5.7 based on the pH dependence of the chemical shift of succinate (C_2/C_3 resonance), and considering the neutrophilic character of *C. glutamicum*. A typical sequence of ^{13}C-NMR spectra obtained during the metabolism of [1-^{13}C]glucose (Fig. 2.5) shows intense resonances due to extracellular succinate (δ, 33.4 ppm) and lactate (δ, 20.6 ppm). More importantly, two small resonances appear at 33.7 ppm and 20.7 ppm, which arise from these organic acids inside the cell (internal pH approx. 6.3 as determined by ^{31}P-NMR, data not shown).

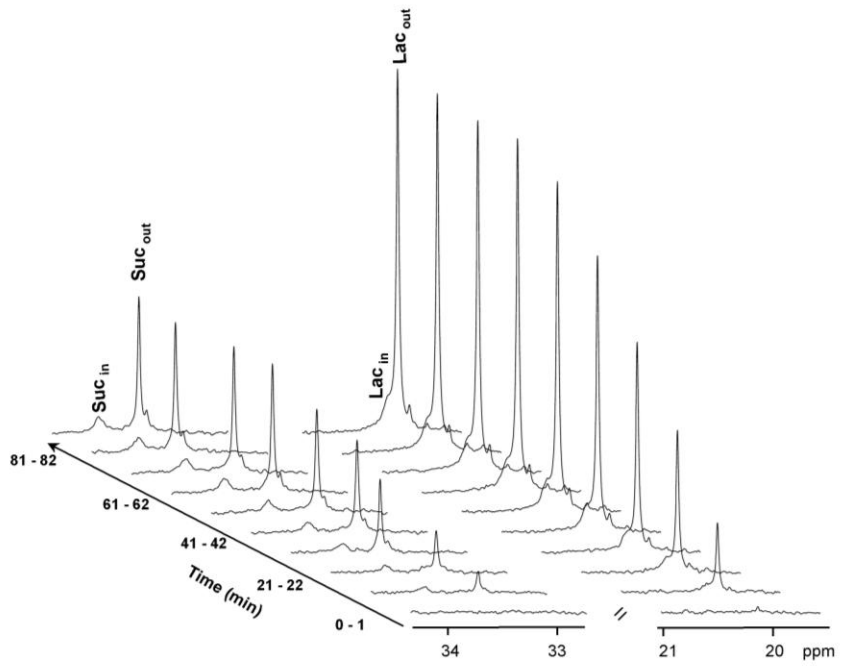

Figure 2.5. Sequences of ^{13}C-NMR spectra acquired during glucose metabolism by dense cell suspensions (OD_{600} =100), of *C. glutamicum* at pH 5.7 under 100% CO_2 atmosphere. The resonances due to intra- and extracellular succinate and lactate are depicted. Suc_{in}, intracellular succinate; Suc_{out}, extracellular succinate; Lac_{in}, intracellular lactate; Lac_{out}, extracellular lactate. A single experiment is depicted from two independent replicates with high reproducibility.

The kinetics of glucose consumption and the build-up of intra- and extracellular pools under anaerobic conditions (with and without CO_2) are shown in Fig. 2.6. A shift in the external pH from 7.0 to 5.7 did not alter the nature of end-products but led to a clear change in their proportions (Table 2.2). As for pH 7.0, CO_2 had a positive effect on succinate production (8.3 $\pm$ 0.2 mM as compared to 3.1 $\pm$ 0.3 mM without CO_2), but lactate was the

major end-product at the lower pH regardless the presence of pure CO_2 in the atmosphere. At pH 5.7, GCR was impaired and this negative effect was more pronounced in the absence of CO_2 (Table 2.2). Intracellular succinate and lactate pools increased steadily during glucose metabolism, reaching their maximal concentrations at the onset of glucose exhaustion. In the absence of CO_2, succinate and lactate reached intracellular levels of 17.2 ± 0.9 mM and 196.1 ± 28.4 mM, respectively (Fig. 2.6A). Under CO_2 the intracellular lactate pool decreased to 123.3 ± 18.4 mM, while the intracellular succinate concentration increased to 57.1 ± 1.7 mM. Except for small resonances assigned to fructose-1,6-bisphosphate, intermediate metabolite pools were below the detection limit of these experiments (around 3 mM).

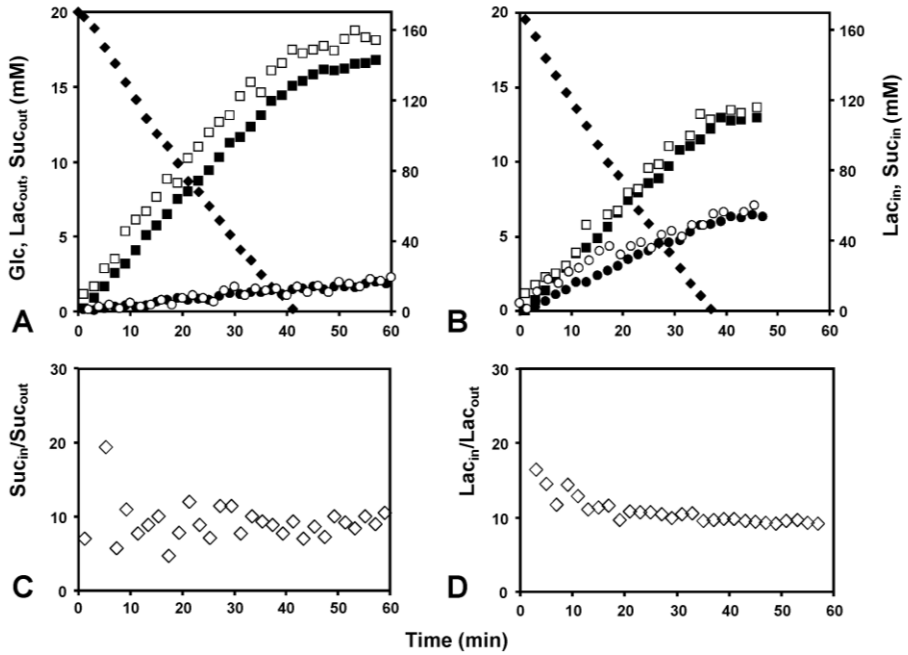

Figure 2.6. Time courses for consumption of glucose (20 mM), and build-up of intra- and extracellular pools of lactate and succinate determined from the sequences of spectra shown in Figure 4, in the absence of CO_2 (**A**) and in the presence of 100% CO_2 (**B**). Symbols: black diamonds, glucose; full squares, extracellular lactate; empty squares, intracellular lactate; full circles, extracellular succinate; empty circles, intracellular succinate. (**C**) Plot of the ratio intracellular succinate/extracellular succinate, and intracellular lactate/extracellular lactate (**D**). Each panel represents a single experiment from a set of at least two similar replicates.

Discussion

In this study we investigated the effect of CO_2 on anaerobic organic acid formation by wild type *C. glutamicum* and found that the succinate yield increased 3-fold to 1 mol succinate per mole glucose in the presence of

CO_2. This experimental yield is significantly higher than those reported in the literature for wild type *C. glutamicum*, which do not exceed 0.44 mol succinate per mol glucose (Inui et al. 2004, Yamamoto et al. 2011). Moreover, it is significant even when compared with engineered *C. glutamicum* strains that show succinate yields between 1.02 and 1.67 mol per mol glucose (Litsanov et al. 2012a, Okino et al. 2008a, Wieschalka et al. 2012b, Zhu et al. 2014).

The increase in the succinate yield prompted us to characterize the underlying redistribution of carbon fluxes. Analysis of enrichment on C_2 and C_3 of lactate derived from [2-^{13}C]glucose showed a low proportion of flux through PPP in relation to glycolysis, and this split ratio was only slightly increased in the presence of CO_2. To our knowledge, this is the first estimation of the contribution of PPP in *C. glutamicum* under oxygen depletion conditions. The low contribution of the PPP flux corroborates the view that in *C. glutamicum* the activity of this pathway is controlled by the demand for NADPH (Marx et al. 1999)), which is naturally low in non-growing cells producing mainly organic acids. Accordingly, during the valine production phase of a recombinant L-valine-producing strain of *C. glutamicum* (non-growing cells, oxygen supplied), the carbon flux was fully directed to PPP to match the high demand for NADPH associated with the synthesis of this amino acid (two mol NADPH per valine produced) (Bartek et al. 2011).

In the absence of added CO_2, besides lactate, cells produced considerable amounts of DHA, which indicate the presence of a metabolic bottleneck at

the level of glyceraldehyde-3-phosphate dehydrogenase, most likely due to enzyme inhibition by a high $NADH/NAD^+$ ratio (Even et al. 1999). Significantly, this redox imbalance was abolished under succinate producing conditions since the reductive part of the TCA cycle provides a sink for reducing equivalents, and hence DHA was not produced.

Succinate production occurred mainly *via* PEP/Pyr carboxylation and reductive TCA cycle. However, the detection of ^{13}C-labelling on the outer carbons of succinate (Fig. 2.3, Table 2.3), denotes the operation of the oxidative path and/or the glyoxylate shunt. These two pathways lead to identical labelling patterns on succinate, and so their individual contributions cannot be resolved. We assumed that the flux through the glyoxylate shunt is negligible under the experimental conditions used in this study, based on the following information: the activity of isocitrate lyase is absent in *C. glutamicum* during anaerobic glucose metabolism (Inui et al. 2004); succinate is an effective inhibitor of isocitrate lyase (inhibition constant of 1.48 mM) (Reinscheid et al. 1994a). Therefore, it seems reasonable to neglect the glyoxylate shunt contribution in our metabolic model, which was designed for cells producing high levels of succinate, under anaerobic non-growing conditions.

Activity of the full oxidative branch of the TCA cycle makes sense in view of the overall redox balance. For calculation of the redox balance, all three reduced cofactors (NADH, NADPH and MQH_2), were considered as equivalent electron reducing units (Bott 2003, Genda et al. 2003). It is rewarding to find that the small flux through the oxidative TCA cycle (2

C-atoms succinate for each 100 C-atoms glucose taken up), estimated from the ^{13}C-enrichment on C_1/C_4 of succinate, provides the balance of reducing power needed for succinate production. Indeed, the calculation of the overall redox balance would be exactly 100% with a flux of 3.5 (instead of 2) carbons through the oxidative TCA cycle, which is a difference within the uncertainty of the data. However, a large deficit in reducing capacity (up to 20%) would occur if the glyoxylate shunt was active and the oxidative branch inoperative. Low contributions of the oxidative branch to anaerobic succinate production have also been reported in *Basfia succinoproducens* and appear to be required for optimal production in non-growing cells (Becker et al. 2013). The operation of the oxidative branch of the TCA cycle implies a cost in terms of CO_2 loss, thus Zhu et al., (Zhu et al. 2014) constructed a *C. glutamicum* strain with overexpression of the genes involved in the glyoxylate shunt, but this strategy alone was not satisfactory as the yield was essentially unchanged (1.21 to 1.23 mol per mol glucose).

The experiments with [1-^{13}C]glucose and [U-^{13}C]glucose showed that back-flux from oxaloacetate/malate to PEP/Pyr is insignificant under 100% CO_2 atmosphere. This was unexpected knowing that the PEP/Pyr/oxaloacetate node shows great flexibility in *C. glutamicum* cells, at least in the presence of oxygen (Bartek et al. 2011, Wendisch et al. 2000). There are three possible routes through which oxaloacetate/malate can be decarboxylated into PEP/Pyr: i) oxaloacetate decarboxylase, which is inhibited by succinate (Jetten and Sinskey 1995); ii) PEP carboxykinase which is down-

regulated under oxygen deprivation (Inui et al. 2007); iii) and the malic enzyme, which is over-expressed under oxygen deprivation (Inui et al. 2007). Therefore, it appears that the malic enzyme has very low activity in the decarboxylating direction, probably because of low requirement for NADPH. Actually, having the malic enzyme acting in the malate-forming direction as previously suggested (Gourdon et al. 2000), would provide a sink for NADPH produced in PPP, a useful feature since this bacterium lacks NADPH:NAD^+ transhydrogenase activity (Blombach et al. 2011, Kabus et al. 2007).

The difference between the recovery of ^{13}C and total carbon (Table 2.2) deserves further discussion. In addition to the obvious dilution of label resulting from ^{12}C incorporation from CO_2 in PEP/PYR carboxylation reactions, one should consider the contribution of unlabelled internal reserves. *C. glutamicum* can store glycogen and maltodextrins during growth (Seibold et al. 2007), as well as trehalose (Wolf et al. 2003) and the catabolism of these components concomitantly with the metabolism of added labeled glucose will lead to ^{13}C dilution, as demonstrated by the presence of unlabeled end-products when uniformly labeled glucose was provided. This phenomenon has been observed in bacteria and yeast which showed fast mobilization of carbohydrate storage pools (Matheron et al. 1998, Aboka et al. 2009). Moreover, the reverse flux from labeled glucose to reserves was apparent from the build-up of labeled glycogen and trehalose (data not shown). Therefore, our model takes into account that both the utilization of internal reserves and storage of labeled glucose

occur in the presence and absence of CO_2. According to this model, 12% and 19% of labelled glucose was stored, and unlabelled reserves (4% and 13% of C-atoms taken up as glucose) were channelled to catabolism.

Lowering pH from neutral to 5.7 had a strong negative effect on the GCR. Furthermore, the decrease in metabolic efficiency was accompanied by decline in the succinate yield. As cells were grown under identical conditions, transcriptional or proteomic effects are unlikely to occur and the metabolic effects are ascribed to immediate impact of pH on the efficiency of glucose transporters and/or cytoplasmic enzymes. The lack of effect at the transcriptional level has been demonstrated in *Lactococcus lactis* under similar experimental conditions (Carvalho et al. 2013). Despite the poor performance of *C. glutamicum* at acidic pH we decided to measure the intracellular pools of organic acids, seeking information on eventual constraints at the level of organic acid export systems. The average number, *n*, of protons exported with the lactate or succinate anions was determined directly from the kinetics of accumulation of intra and extracellular organic acids (Carvalho et al. 2013). During glucose consumption in a CO_2 atmosphere, *n* was maintained close to 1.4 in the case of lactate, and varied only slightly (between 2.7 and 2.3) in the case of succinate, indicating lack of inhibition of exporters by the acid intracellular pools, which are actually much lower than those observed in *L. lactis* (up to 0.7 M lactate). Both for lactate and succinate, the ratio intracellular/extracellular pools tended rapidly to about 10 during glucose utilization (Fig. 2.6). Succinate exporters have been identified in several *C.*

glutamicum strains but their detailed characterization is lacking (Huhn et al. 2011, Fukui et al. 2011). We speculate that, although cultivated at neutral pH, the organism is well adjusted to sustain the observed production fluxes at pH 5.7; moreover, the ability to maintain a high concentration gradient across the cell membrane creates a favourable contribution to the energetics of the efflux processes.

In conclusion, this study demonstrates that the supply of CO_2 to wild type *C. glutamicum* caused an important redistribution of the central metabolic fluxes, resulting in an up to 3-fold improvement in succinate yield without involvement of genetic manipulation. Succinate was produced largely via the reductive part of the TCA cycle, but there was also a significant flux through the oxidative part to meet the redox balance. Under production conditions (no-growth, lack of oxygen), the split ratio between PPP and glycolysis was low (around 5%), and independent of CO_2 availability indicating that the flux via PPP is primarily controlled by NADPH demand. The metabolism of glucose-grown cells of *C. glutamicum* seemed well tuned to produce succinate at high yield with straightforward manipulation of environmental conditions and taking advantage of cellular regulation mechanisms. However, further effort should be directed at improving the rate of glucose consumption.

Acknowledgements and work contributions

Authors want to acknowledge Ana Mingote for technical assistance.

DR was involved in designing the study, all stages of experimental work and writing the manuscript. DLT provided the metabolic model. LLF and ALC helped to perform the ^{13}C-tracer experiments and analyze data. HS, DLT, BJE, BB and ARN contributed to study design, supervision and manuscript preparation.

CHAPTER 3

Engineering *Corynebacterium glutamicum* for the production of 2,3-butanediol

This chapter is published in:

Radoš D, Carvalho AL, Wieschalka S, Neves AR, Blombach B, Eikmanns BJ and Santos H.

Engineering *Corynebacterium glutamicum* for the production of 2,3-butanediol. (2015) Microbial Call Factories 14:171.

Contents

Summary

2,3-Butanediol is an important bulk chemical with a wide range of applications. In bacteria, this metabolite is synthesized from pyruvate via a three-step pathway involving α-acetolactate synthase, α-acetolactate decarboxylase and 2,3-butanediol dehydrogenase. Thus far, the best producers of 2,3-butanediol are pathogenic strains, hence, the development of more suitable organisms for industrial scale fermentation is needed. Herein, 2,3-butanediol production was engineered in the Generally Regarded As Safe (GRAS) organism *Corynebacterium glutamicum*. A two-stage fermentation process was implemented: first, cells were grown aerobically on acetate; in the subsequent production stage cells were used to convert glucose into 2,3-butanediol under non-growing and oxygen-limiting conditions.

A gene cluster, encoding the 2,3-butanediol biosynthetic pathway of *Lactococcus lactis*, was assembled and expressed in background strains, *C. glutamicum* Δ*ldhA*, *C. glutamicum* Δ*aceE*Δ*pqo*Δ*ldhA* and *C. glutamicum* Δ*aceE*Δ*pqo*Δ*ldhA*Δ*mdh*, tailored to minimize pyruvate-consuming reactions, i.e., to prevent carbon loss in lactic, acetic and succinic acids. Producer strains were characterized in terms of activity of the relevant enzymes in the 2,3-butanediol forming pathway, growth, and production of 2,3-butanediol under oxygen-limited conditions. Productivity was maximized by manipulating the aeration rate in the production phase. The final strain, *C. glutamicum* Δ*aceE*Δ*pqo*Δ*ldhA*Δ*mdh*(pEKEx2-*als,aldB,*P_{tuf}*butA*), under optimized conditions produced 2,3-butanediol with

a 0.66 $mol \cdot mol^{-1}$ yield on glucose, an overall productivity of 0.2 $g \cdot L^{-1} \cdot h^{-1}$ and a titer of 6.3 $g \cdot L^{-1}$.

We have successfully developed *C. glutamicum* into an efficient cell factory for 2,3-butanediol production. The use of the engineered strains as a basis for production of acetoin, a widespread food flavour, is proposed.

Introduction

Concern over exhaustion of fossil fuel resources, emission of CO_2 linked with petroleum-derived products, and accumulation of non-degradable synthetic polymers urged the development of environmentally friendly processes for production of chemicals. A solution offered by the rising field of white biotechnology is to produce chemical building blocks by microbial fermentation of sugars derived from renewable biomass (Bozell and Petersen 2010).

2,3-Butanediol (2,3-BD) is an important chemical used in the production of plasticizers and fumigants, as an antifreeze agent, a fuel and octane booster, among other applications (Celińska and Grajek 2009). The range is still expanding and the market size is expected to reach 74 kilo tons by 2018 (Transparency Market Research 2012). Significantly, the 2,3-BD derivative, 1,3-butanediene, can be used in synthetic rubber production, while 2-butanone (methyl ethyl ketone) is a fuel additive and solvent for resins and lacquers. Additionally, ester-derivatives are used in the pharmaceutical and cosmetics industries. The world annual market for 2,3-BD derivatives is estimated at around $43 billion (Köpke et al. 2011).

2,3-BD has three stereoisomeric forms: the enantiomers (*2S,3S*)-2,3-BD and (*2R,3R*)-2,3-BD, and the optically inactive form (*2R,3S*)-2,3-BD (*meso*-2,3-BD). 2,3-BD is an end-product of the metabolism of many bacteria, synthesized from pyruvate via a three step pathway (Fig. 3.1). The first reaction involves the condensation of two pyruvate molecules into α-acetolactate, which is catalyzed by α-acetolactate synthase (ALS, EC 2.2.1.6), the enzyme committed to pyruvate catabolism. Alternatively, as in *Corynebacterium glutamicum*, α-acetolactate can be synthesized by the action of acetohydroxyacid synthase (AHAS, EC 2.2.1.6, encoded by *ilvBN*), and used as precursor for the synthesis of branched chain amino acids (L-valine, L-leucine and L-isoleucine). In the catabolic route, α-acetolactate is decarboxylated by α-acetolactate decarboxylase (ALDC, EC 4.1.1.5, encoded by *aldB*) to yield (*R*)-acetoin. In the presence of oxygen, α-acetolactate can undergo spontaneous decarboxylation to form diacetyl, which is subsequently reduced to (*R*)- or (*S*)-acetoin by diacetyl reductases (EC 1.1.1.303; EC 1.1.1.304). Acetoin is finally reduced to 2,3-BD by butanediol dehydrogenases (BDH, EC 1.1.1.76; EC 1.1.1.4). In some cases, such as *C. glutamicum* or *L. lactis*, BDH is promiscuous and recognizes as substrates diacetyl as well as acetoin, thus diacetyl can be reduced to acetoin via this activity (Takusagawa et al. 2001, Crow 1990).

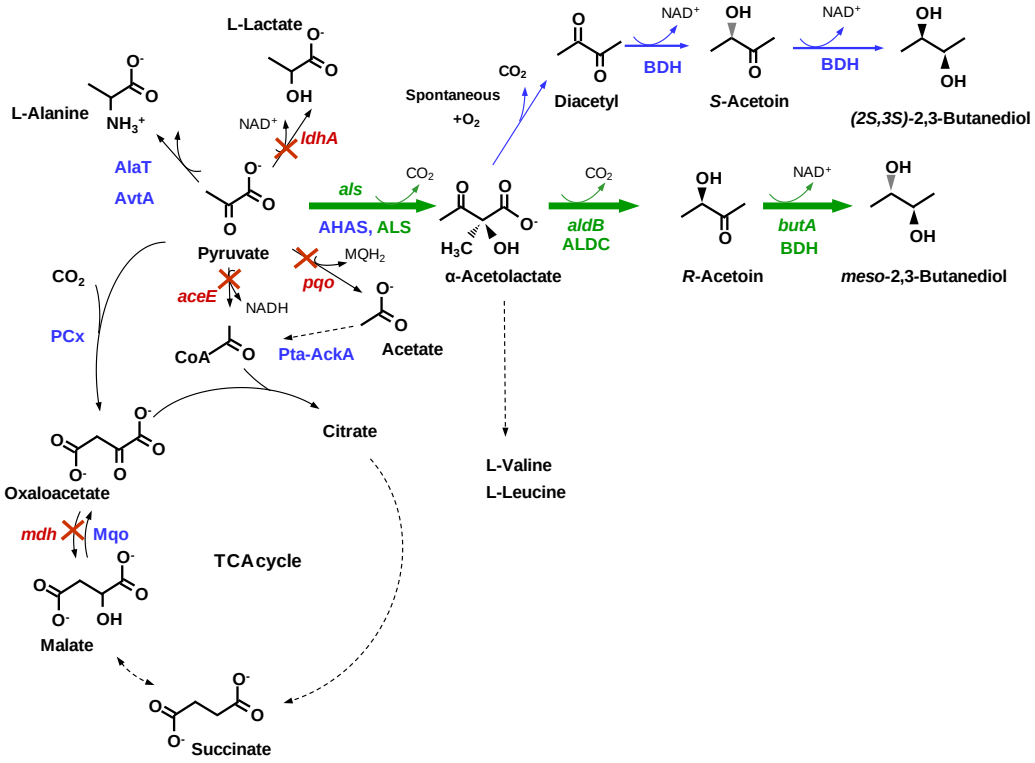

Figure 3.1. A scheme depicting major pyruvate consuming reactions, including the proposed pathway for synthesis of optically active 2,3-BD in *C. glutamicum* and the strategy for engineering *meso*-2,3-BD synthesis. *L. lactis* genes of the 2,3-BD biosynthetic pathway (green) were introduced into *C. glutamicum*. Endogenous genes of interest are presented in blue; the red cross marks indicate genes that were inactivated in host strains to prevent the production of lactic acid (*ldhA*) and acetic acid (*aceE* and *pqo*); suppression of succinic acid was attempted by deletion of *mdh*. Abbreviations: *mdh*, malate dehydrogenase gene; *mqo*, malate:quinone oxidoreductase gene; ALS, α-acetolactate synthase (encoded by *als*); ALDC, α-acetolactate decarboxylase (encoded by *aldB*); BDH, butanediol dehydrogenase (encoded by *butA*), AHAS, acetohydroxyacid synthase; LDH, lactate dehydrogenase (encoded by *ldhA*); PQO, pyruvate:quinone oxidoreductase (encoded by *pqo*); AlaT, alanine-glutamate transaminase; AvtA, alanine-valine transaminase; AceE, E1-subunit of the pyruvate dehydrogenase complex (encoded by *aceE*); Pta-Ack, phosphotransacetylase and acetate kinase; PCx, pyruvate carboxylase.

Thus far, the best producers of 2,3-BD are pathogenic strains, such as *Klebsiella pneumoniae*, *Klebsiella oxytoca*, *Enterobacter aerogenes*, and *Serratia marcescens (*Wang et al. 2010, Jantama et al. 2015, Jung et al. 2013, Zhang et al. 2010), hence, a considerable research effort has been directed to the development of more suitable organisms for industrial scale fermentation. *Lactococcus lactis*, *Bacillus subtilis*, *Paenibacillus polymyxa*, *Saccharomyces cerevisiae* and *Escherichia coli* have been used for this purpose, but the low production efficiency or complex nutritional requirements of the engineered strains make the overall process unsatisfactory (Gaspar et al. 2011, Fu et al. 2014, Häßler et al. 2012, Lian et al. 2014, Xu et al. 2014). Therefore, the search goes on for more appropriate host strains and more efficient fermentation processes. A few years ago, some of us engineered *L. lactis* for the production of 2,3-BD by overexpression of two endogenous genes (*als*, *butA*) (Gaspar et al. 2011); theoretical product yields were reached, but the fastidious nutritional requisites of this bacterium precludes its utilization as an industrial producer of bulk chemicals.

In this work, we selected *Corynebacterium glutamicum* as an industrially established host strain and aimed to develop an efficient 2,3-BD producer. *C. glutamicum* is an important industrial microorganism, widely known for the million-ton scale production of L-glutamate and L-lysine (Ajinomoto Co., Inc. 2011). Therefore, the existing knowledge of the industrial fermentation of this bacterium could be exploited for the production of bulk chemicals, such as 2,3-BD. In addition, *C. glutamicum* is a facultative

anaerobic organism with GRAS (Generally Regarded As Safe) status, robust (osmotolerant, phageresistant, organic solvent tolerant), extensively studied with respect to metabolism and regulation, and for which a comprehensive toolbox for genetic manipulation has been developed (Wendisch et al. 2006, Eggeling and Bott 2005, Burkovski 2008). Considerable research effort has been invested in metabolic engineering of *C. glutamicum,* resulting in the construction of producer strains for a broad spectrum of compounds, such as biofuels (isobutanol), polymer precursors (diaminopentane, cadaverine and putrescine), sugar alcohols (xylitol) and organic acids (Blombach et al. 2011, Yamamoto et al. 2013, Mimitsuka et al. 2007, Kind et al. 2010, Schneider and Wendisch 2010, Sasaki et al. 2010, Okino et al. 2008a, Litsanov et al. 2012a, Okino et al. 2008b). As a result of this research endeavour, platform strains of *C. glutamicum* have been established. More specifically, strains deficient in L-lactate dehydrogenase (LDH, encoded by *ldhA*) have been proven to be a useful starting point for strain development since deletion of the *ldhA* gene eliminates L-lactate formation, concomitantly increasing NADH availability (Okino et al. 2008a, Okino et al. 2008b). In addition, strains deficient in the *aceE*-encoded E1 subunit of the pyruvate dehydrogenase complex (PDHC) were also shown to be suitable hosts for the production of pyruvate and pyruvate-derived products, L-valine, L-lysine, 2-ketoisovalerate, succinate and isobutanol (reviewed in (Eikmanns and Blombach 2014). Typically, PDHC-deficient strains are unable to grow on glucose as sole carbon source unless the medium is supplemented with

acetate or ethanol (Schreiner et al. 2005, Blombach et al. 2009). However, in the absence of the latter substrates, *C. glutamicum* Δ*aceE* remains metabolically active and converts glucose to pyruvate, L-alanine and L-valine under aerobic conditions (Eikmanns and Blombach 2014). Combined activities of pyruvate:quinone oxidoreductase, acetate kinase and phosphotransacetylase (Fig. 3.1) do not provide sufficient acetyl-CoA to replace the PDHC reaction in glucose containing medium, however, deletion of the respective *pqo* gene was shown to be beneficial for the production of pyruvate and its derived products L-valine and 2-ketoisovalerate (Blombach et al. 2008, Krause et al. 2010). In this framework, we constructed and tested three strains as potential hosts for efficient 2,3-BD production. In addition to *C. glutamicum* Δ*ldhA*, and *C. glutamicum* Δ*aceE*Δ*pqo*Δ*ldhA*, designed to minimize lactate and acetate formation, a third strain, *C. glutamicum* Δ*aceE*Δ*pqo*Δ*ldhA*Δ*mdh*, was constructed with an extra deletion of the malate dehydrogenase gene to reduce succinate formation (Fig. 3.1). In these strains we expressed *als*, *aldB*, *butA* from *L. lactis* and devised a two-stage process for efficient production of 2,3-BD. In the first stage cells were grown aerobically on acetate or glucose for biomass formation; in the second stage (production stage), biomass was used to convert glucose into 2,3-BD under non-growing and oxygen-limiting conditions.

Materials and Methods

Bacterial strains and growth conditions

Strains and plasmids used in this work are shown in Table 3.1. Cells were grown aerobically in the 2×TY medium described by Green and Sambrook (Green and Sambrook 2012). Medium was supplemented either with 0.5% (wt/vol) glucose or with 1% (wt/vol) potassium acetate. Plasmid-harbouring strains were selected using kanamycin (25 $\mu g \cdot mL^{-1}$). Gene expression was induced by using 0.5 mM isopropyl β-D-1-thiogalactopyranoside (IPTG). Cultivations were performed at 30°C with constant agitation at 160 rpm and were initiated by addition of a pre-culture to an optical density at 600 nm (OD_{600}) of about 0.3. Growth was monitored by measuring the OD_{600}. Specific growth rates (μ) were calculated through linear regression of the plots of $\ln(OD_{600})$ *versus* time during the exponential growth phase. For growth characterization, samples (1 mL) were taken periodically and pH was measured.

For the molecular biology procedures, *E. coli* DH5α was grown in test tubes containing 5 mL of 2×TY medium at 37˚C and 180 rpm. Plasmid selection was achieved using 50 μg kanamycin per mL.

Table 3.1. Bacterial strains and plasmids used in this study.

Strains	Description	Ref
E. coli DH5α	Plasmid-free *E. coli*	Amersham Biosciences
C. glutamicum ATCC13032	Wild-type strain	Kinoshita et al. 1958
C. glutamicum Δ*ldhA*	ATCC13032 with deletion of lactate dehydrogenase gene *ldhA*	This work
C. glutamicum Δ*aceE*Δ*pqo*Δ*ldhA*	ATCC13032 with deletions of the genes for the E1 subunit of pyruvate dehydrogenase complex, the pyruvate:quinone oxidoreductase and the lactate dehydrogenase	Wieschalka et al. 2012a
C. glutamicum Δ*aceE*Δ*pqo* Δ*ldhA*Δ*mdh*	ATCC13032 with deletions of the genes for the E1 subunit of pyruvate dehydrogenase complex, the pyruvate:quinone oxidoreductase, lactate dehydrogenase and malate dehydrogenase	This study
C. glutamicum Δ*aceE*Δ*pqo*Δ*ldhA* (pEKEx2)	*C. glutamicum* Δ*aceE*Δ*pqo*Δ*ldhA* harboring plasmid pEKEx2	This work
C. glutamicum Δ*ldhA* (pEKEx2)	*C. glutamicum* Δ*ldhA* harboring plasmid pEKEx2	This work
C. glutamicum Δ*aceE*Δ*pqo* Δ*ldhA*Δ*mdh* (pEKEx2)	*C. glutamicum* Δ*aceE*Δ*pqo*Δ*ldhA*Δ*mdh* harboring plasmid pEKEx2	This work
C. glutamicum ldhA (pEKEx2- *als,aldB,butA*)	*C. glutamicum* Δ*ldhA* harboring plasmid pEKEx2 *als,aldB,butA*	This work
C. glutamicum Δ*aceE*Δ*pqo*Δ*ldhA* (pEKEx2-*als,aldB,butA*)	*C. glutamicum* Δ*aceE*Δ*pqo*Δ*ldhA* harboring plasmid pEKEx2-*als,aId,BbutA*	This work
C. glutamicum Δ*aceE*Δ*pqo*Δ*ldhA*Δ*mdh* (pEKEx2-*als,aldB,butA*)	*C. glutamicum* Δ*aceE*Δ*pqo*Δ*ldhA*Δ*mdh* harboring plasmid pEKEx2-*als,aldB,butA*	This work
C. glutamicum Δ*aceE*Δ*pqo*Δ*ldhA* (pEKEx2-*als,aldB,*$_{Ptuf}$*butA*)	*C. glutamicum* Δ*aceE*Δ*pqo*Δ*ldhA* harboring plasmid pEKEx2-*als,aldB,*$_{Ptuf}$*butA*	This work
C. glutamicum Δ*aceE*Δ*pqo*Δ*ldhA*Δ*mdh* (pEKEx2-*als,aldB,*$_{Ptuf}$*butA*)	*C. glutamicum* Δ*aceE*Δ*pqo*Δ*ldhA*Δ*mdh* harboring plasmid pEKEx2-*als,aldB,*$_{Ptuf}$*butA*	This work
Plasmids		
pEKEx2	kan^R from pUC4K; P_{trc}, *lacI*, pUC18 mcs, induced by addition of IPTG	Eikmanns et al. 1991a
pEKEx2-*als*	pEKEx2 with cloned *als* from *L. lactis*	This study
pEKEx2-*als,aldB,butA*	pEKEx2-*als* with *aldB* and *butA* from *L. lactis*	This work
pEKEx2-*als,aldB,*$_{Ptuf}$*butA*	pEKEx2-*als* wit *aldB* and P_{tuf}-*butA* from *L. lactis*	This work

Abbreviations: *als*, α-acetolactate synthase gene; *aldB,* α-acetolactate decarboxylase gene; *butA*, butanediol dehydrogenase gene; P_{tuf}, a 185 bp region upstream of *tuf* gene of *C. glutamicum;* kan^R, kanamycin resistance; P_{trc}, trc promoter; *lacI*, lac repressor gene.

Construction of strains and plasmids

All primers used are listed in Table 3.2. To construct control strain *C. glutamicum* Δ*ldhA*, deletion of *ldhA* (cg3219) gene was performed according to (Wieschalka et al. 2012a), using the primer pairs described there. Deletion of the *mdh* (cg2613) gene in *C. glutamicum* Δ*aceE*Δ*pqo*Δ*ldhA* (*aceE*, cg2466; *pqo*, cg2891) was performed as described in (Blombach et al. 2011). Chromosomal DNA of *L. lactis* MG1363, isolated according to (Johansen and Kibenich 1992), was used as template in PCR amplifications. In the first cloning step, the α-acetolactate synthase gene (*als*) was amplified from *L. lactis* chromosome using primer pair als-FW and als-RE and cloned into plasmid pEKEx2. In the second step, genes encoding the α-acetolactate decarboxylase (*aldB*) and 2,3-butanediol dehydrogenase (*butA*) of *L. lactis* were amplified using primers aldB-FW, aldB-RE, butA-FW and butA-RE, ligated, and subsequently inserted into pEKEx2-*als*, giving pEKEx2-*als,aldB,butA*. Alternatively, gene *butA* fused with 185 bp region upstream of *tuf* gene (P_{tuf}) was synthesized by NZYTech (Lisbon, Portugal). Plasmid pUC57 containing P_{tuf}-*butA* fusion was amplified in *E. coli* DH5α and restricted using *BamH*I and *Kpn*I. The P_{tuf}-*butA* fragment was purified from agarose gel and ligated to *aldB*, after which joint DNA fragment was inserted into pEKEx2-*als*, yielding pEKEx2-*als,aldB,*$_{Ptuf}$*butA.* Plasmids were obtained and maintained in *E. coli* DH5α. After verification of the correctness of the insert by sequencing (GATC, Konstanz, Germany), plasmids were isolated from *E. coli* and electroporated into competent *C. glutamicum* cells using

the procedure described in (Liebl et al. 1989) and (Van der Rest et al. 1999). Then, plasmids were isolated from *C. glutamicum* in the following way: 5 mL of overnight culture was centrifuged for 1 min at 16,100 × *g* and room temperature, to be re-suspended in 0.2 mL of solution A (50 mM glucose, 25 mM Tris-HCl, 10 mM EDTA, pH 8.0, freshly prepared). One µL of RNase A (10 $mg \cdot mL^{-1}$), and 15 $mg \cdot mL^{-1}$ (final concentration) lysozyme were added, and the lysis was performed for 1.5 h at 55°C. After the initial lysis step, isolation was continued with comercially available kits according to supplier instructions (Qiagen MiniPrep or Illustra Plasmid Mini Preparation Kit, GE Healthcare). Isolated plasmids were used as templates for PCR amplification of the inserted genes. Amplified region sequence was confirmed to be correct by sequencing (GATC, Konstanz, Germany).

Table 3.2. Primers used in this study

Primer name	5' - 3' sequence	Restriction site
als-FW	AAAACTGCAGTTTAAAAGGAGCCTCATATGTCTGAGAAACAA TTTGGGGC	*Pst*I
als-RE	ACGCGTCGACTCAGTAAAATTCTTCTGGCAAT	*Sal*I
aldB-FW	ACGCGTCGACTTTAAAAGGAGCCTCATATGTCAGAAATCACA CAAC	*Sal*I
aldB-RE	CGCGGATCCTCATTCAGCTACATCAATATCTTTTTTCAAAGC CTC	*BamH*I
butA-FW	CGCGGATCCTTTAAAAGGAGCCTCATATGTCTAAAGTTGCAG CAG	*BamH*I
butA-RE	CGGGGTACCTTAATGAAATTGCATTCACCATC	*Kpn*I

Preparation of cell suspensions

Cells grown as described above were harvested 14 h after inoculation, centrifuged (3,214 × *g*, 10 min, 4°C), and washed once with 0.9 % (wt/vol) NaCl. The resulting cell suspension was centrifuged (3,214 × *g*, 10 min, 4°C) and the pellet was re-suspended in a minimal CGXII basal solution at pH 7.0, that contained per liter: 1 g KH_2PO_4, 1 g K_2HPO_4, 21 g MOPS (3-[N-morpholino] propanesulfonic acid), 0.25 g $MgSO_4 \cdot 7\ H_2O$, 10 mg $CaCl_2 \cdot 2\ H_2O$ (Eikmanns et al. 1991b). Nitrogen sources (urea and $(NH_4)_2SO_4$) were omitted, in order to minimize the biosynthesis of amino acids during the production phase.

Two-stage fermentations processes

C. glutamicum strains were grown and cell suspensions prepared as described above. For the second fermentation stage (production phase), 50 mL of cell suspension (OD_{600} of 15 - 20) were placed in an 80-mL fermenter (mini-fermenter), kept at 30°C with a water bath and mixed with a magnetic stirrer at 200 rpm. Aeration was performed by sparging sterile air at a rate of 5, 10 or 20 $mL \cdot min^{-1}$. The oxygen electrode (InPro® 6100/320/T/N, Mettler Toledo), was used to attempt monitoring dissolved oxygen during the production stage. The electrode was calibrated to 0% and 100% after equilibration with pure argon and air, respectively. Glucose was provided to a final concentration of 2% (wt/vol) and samples were collected over a period of 30 h. For the first round evaluation of the performance of the several constructs, 25 mL of concentrated cell suspension (OD_{600} of between 20 and 30) were placed in

50 mL closed falcon tubes kept at 30°C in a rotary shaker (180 rpm). Glucose was provided to a final concentration of 2% (wt/vol) and the fermentation was allowed to proceed for 48 h. Samples (1 mL) were centrifuged for 5 minutes at room temperature and 16,100 × *g*; supernatants were then separated and kept at -20°C until further analysis. End-products of metabolism were quantified by using ^{1}H-NMR.

Enzymatic activities

C. glutamicum strains were grown as described above and cell suspensions prepared in 50 mM PIPES at pH 7.0. Crude cell extracts were prepared by using glass beads (<106 µm) in a MiniBeadbeater-8 cell disrupter (Biospec Products) in 3 cycles of 1 min, with breaks of 3 min during which the extracts were kept on ice. After disruption, extracts were centrifuged at 16,100 × g for 20 min at 4°C. All enzyme activities were assayed at 30°C in a Beckman Coulter DU 800 spectrophotometer in 50 mM PIPES (pH 7.0). One unit of enzyme activity corresponds to 1 µmol of substrate/product converted/formed per minute under the experimental conditions applied. The protein concentration was determined using Pierce BCA Protein Assay Kit (Thermo Scientific). Specific activity was expressed as units (µmol min^{-1}) per milligram of protein [U · (mg of protein)$^{-1}$]. α-Acetolactate synthase activity was determined as described by (Hugenholtz and Starrenburg 1992). The reaction was stopped by the addition of 100 µL of 6N H_2SO_4, and acetoin was quantified colorimetrically at 525 nm as described by Westerfeld (Westerfeld 1945). Butanediol dehydrogenases were assayed as described by Stormer (Stormer 1975),

in a modified reaction mixture containing 50 mM buffer, 0.2 mM NADH and 2.5 mM racemic acetoin.

NMR spectroscopy

All ^{1}H-NMR spectra were acquired on a Bruker AVANCE II+ 400 MHz spectrometer (Bruker BioSpin GmbH) at 27º C, using a BBO-F probe head. Pre-saturation of the residual water signal was applied. Acquisition parameters: flip angle of 90º; 32K acquisition data points; repetition delay of 31.5 s. Formate was used as a concentration standard.

Chemicals and reagents

For the molecular biology purposes, RNase A and Pwo polymerase were purchased from Roche Life Science; lysozyme (Fluka) was purchased from Sigma-Aldrich, while all other enzymes were from New England Biolabs. Acetoin used in enzymatic assays was from Sigma-Aldrich. All other chemicals were commercially available reagent-grade (Sigma-Aldrich or Merck Sharp & Dohme).

Results

Design of a synthetic pathway for 2,3-BD and functional analysis

The first step in engineering *C. glutamicum* for the synthesis of 2,3-BD was to construct an artificial operon comprising *als*, *aldB*, and *butA* that form the 2,3-BD biosynthetic pathway of *L. lactis*. The three genes were cloned into pEKEx2 expression vector under control of the isopropyl β-D-1-thiogalactopyranoside (IPTG)-inducible P_{tac} promoter (Fig. 3.2), and transformed into the three selected background strains *C. glutamicum* Δ*ldhA*, Δ*aceE*Δ*pqo*Δ*ldhA* and Δ*aceE*Δ*pqo*Δ*ldhA*Δ*mdh* (Table 3.1).

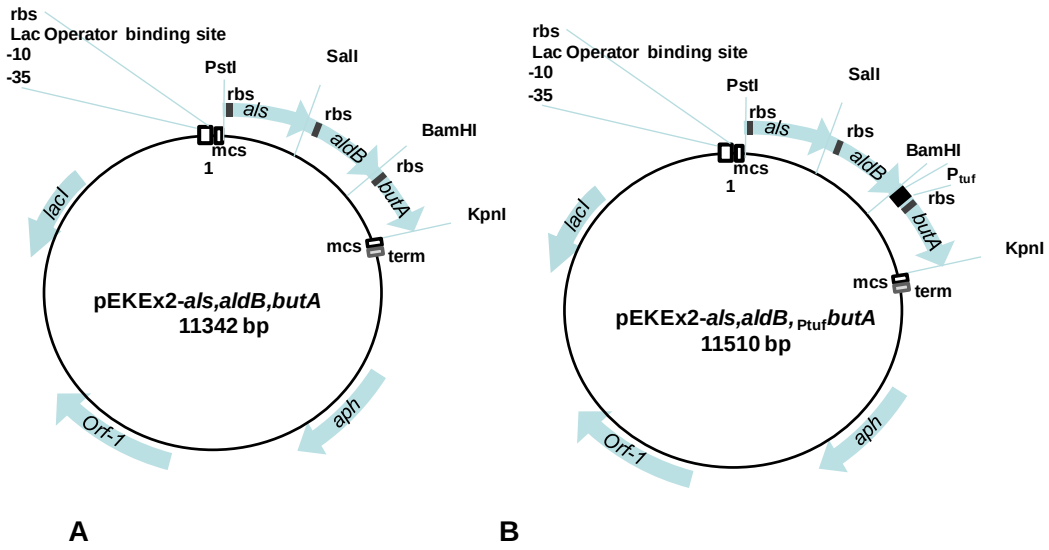

Figure 3.2. Plasmid maps of pEKEx2-*als,aldB,butA* and of pEKEx2-*als,aldB,* $_{Ptuf}$*butA.* Abbreviations: mcs, multiple cloning site; rbs, ribosomal binding site; term, transcriptional terminator; *als*, acetolactate synthase; *aldB*, acetolactate decarboxylase; *butA*, butanediol dehydrogenase; *aph*, aminoglycoside resistance determinant; *Orf-1*, open reading frame 1; *lacI* – Lac repressor.

To evaluate whether the target enzymes were functionally produced, specific activities were determined in cell extracts (Table 3.3). Induced expression of *als* and *aldB* genes in *C. glutamicum* Δ*ldhA*(pEKEx2-*als,aldB,butA*) led to 61- and 15-fold increase in ALS/ALDC activity when compared to control *C. glutamicum* Δ*ldh*(pEKEx2) grown on glucose and acetate, respectively; this corresponded to an increase from 0.024 ± 0.003 to 1.47 ± 0.42 U·(mg of protein)$^{-1}$ in glucose grown cells, and from 0.037 ± 0.002 to 0.54 ± 0.09 U·(mg of protein)$^{-1}$ in acetate grown cells. For *C. glutamicum* Δ*aceE*Δ*pqo*Δ*ldhA*(pEKEx2-*als,aldB,butA*), ALS/ALDC

activity was increased 17-fold (0.034 ± 0.001 compared to 0.58 ± 0.12 U·(mg of protein)$^{-1}$), and for Δ*aceE*Δ*pqo*Δ*ldhA*Δ*mdh*(pEKEx2-*als,aldB,butA*) the activity was 8-fold higher (0.055 ± 0.019 compared to 0.43 ± 0.04 U·(mg of protein)$^{-1}$). The activity of BDH in strain Δ*ldhA*(pEKEx2-*als,aldB,butA*) doubled in glucose grown cells, and, unexpectedly, decreased 2-fold (from 0.2 to 0.1 U·(mg of protein)$^{-1}$) in acetate-grown cells, when compared to the control strain cultivated under the same conditions. Acetate grown *C. glutamicum* Δ*aceE*Δ*pqo*Δ*ldhA*(pEKEx2-*als,aldB,butA*) and Δ*aceE*Δ*pqo*Δ*ldhA*Δ*mdh*(pEKEx2-*als,aldB,butA*) showed 3- and 8-fold increase in BDH activity, compared to the control strain. Maximal specific activity values of 0.97 ± 0.19 U·(mg of protein)$^{-1}$) were obtained. In an attempt to increase BDH activity further we cloned the constitutive P_{tuf} promoter (Litsanov et al. 2012a, Fukui et al. 2011) in front of *butA*, yielding pEKEx2-*alsaldB*P_{tuf}*butA* (Fig. 3.2). However, this increased BDH activity only slightly (Table 3.3).

Table 3.3. Overexpression and specific activities of enzymes for the synthesis of 2,3-butanediol as determined in crude cell extracts. Cells were grown for 14 h in 2×TY medium supplemented with acetate, unless stated otherwise. Values shown are averages ± SD of at least three independent experiments and two technical replicates.

Strain	**ALS/ALDC activity** U·(mg of protein)$^{-1}$	**BDH activity** U·(mg of protein)$^{-1}$	**ALS/ALDC over-expression** (-fold)	**BDH over-expression** (-fold)
Δ*ldhA* (pEKEx2)*	0.02 ± 0.00	0.66 ± 0.03	-	-
Δ*ldhA* (pEKEx2-*als,aldB,butA*)*	1.47 ± 0.42	1.18 ± 0.26	61	2
Δ*ldhA* (pEKEx2)	0.04 ± 0.00	0.20 ± 0.03	-	-
Δ*ldhA* (pEKEx2-*als,aldB,butA*)	0.54 ± 0.09	0.10 ± 0.03	15	-
Δ*aceE*Δ*pqo*Δ*ldhA* (pEKEx2)	0.03 ± 0.01	0.24 ± 0.04	-	-
Δ*aceE*Δ*pqo*Δ*ldhA* (pEKEx2-*als,aldB,butA*)	0.58 ± 0.12	0.67 ± 0.01	17	3
Δ*aceE*Δ*pqo*Δ*ldhA* (pEKEx2-*als,aldB,*$_{Ptuf}$*butA*)	1.42 ± 0.24	0.53 ± 0.17	31	2
Δ*aceE*Δ*pqo*Δ*ldhA*Δ*mdh* (pEKEx2)	0.06 ± 0.02	0.11 ± 0.04	-	-
Δ*aceE*Δ*pqo*Δ*ldhA*Δ*mdh* (pEKEx2-*als,aldB,butA*)	0.43 ± 0.04	0.97 ± 0.19	8	8
Δ*aceE*Δ*pqo*Δ*ldhA*Δ*mdh* (pEKEx2-*als,aldB,*$_{Ptuf}$*butA*)	0.47 ± 0.14	1.21 ± 0.01	9	10

Abbreviations: *, cells grown on glucose; ALS, α-acetolactate synthase; ALDC, α-acetolactate decarboxylase; BDH, butanediol dehydrogenase.

Growth profiles of engineered strains

First, we characterized growth and biomass formation of the engineered strains in shake-flasks in 2×TY medium containing glucose or acetate (Fig. 3.3 and Table 3.4). The Δ*aceE* strains (PDHC-deficient) are unable to grow on glucose as sole carbon source, therefore, they were grown aerobically on acetate alone. Strains *C. glutamicum* Δ*ldh*(pEKEx2) and Δ*ldhA*(pEKEx2-*als,aldB,butA*) were grown on glucose and also on acetate for comparison purposes. While the control strain *C. glutamicum* Δ*ldh*(pEKEx2) had similar specific growth rates when grown on glucose or acetate (0.52 ± 0.02 and 0.51 ± 0.05 h^{-1}, respectively), Δ*ldhA*(pEKEx2-*als,aldB,butA*) displayed a lower growth rate on acetate (0.46 ± 0.01 versus 0.58 ± 0.01 h^{-1}). The pH profiles were also dependent on the substrate used for growth as glucose-grown cells presented a sharper decrease in pH at the onset of stationary phase (Fig. 3.3). The biomass formation was fairly similar for *C. glutamicum* Δ*ldh*(pEKEx2) and producer strain Δ*ldhA*(pEKEx2-*als,aldB,butA*) regardless of the substrate used for growth (maximal OD_{600} values in the range 21 to 24).

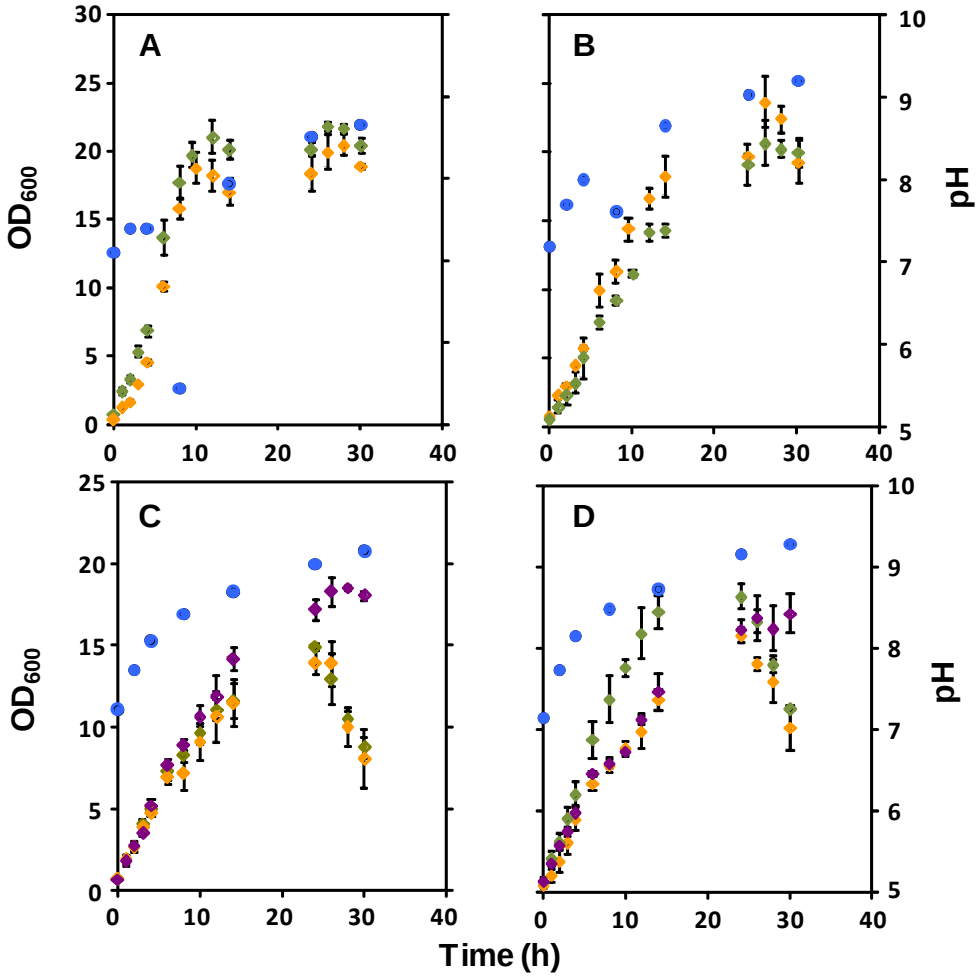

Figure 3.3. Growth curves and pH profiles of the 2,3-BD producer and parental strains, grown in 2×TY medium for 30 h at 160 rpm and 30 °C. The pH profiles for each set of producer and control strains are identical. The Δ*aceE* strains were unable to grow on glucose as sole carbon source, thus they were grown only on acetate. For comparison, *C. glutamicum* Δ*ldh*(pEKEx2) and *ΔldhA*(pEKEx2-*als,aldB,butA*) were grown on glucose (**A**) or acetate (**B**). Remaining panels show *C. glutamicum* Δ*aceE*Δ*pqo*Δ*ldhA* derived strains (**C**) and *C. glutamicum* Δ*aceE*Δ*pqo*Δ*ldhA*Δ*mdh* derived strains (**D**) grown on acetate. Legend: blue, pH; green, control strains; orange, strains with pEKEx2-*als,aldB,butA*; purple, strains with pEKEx2-*als,aldB,*$_{Ptuf}$*butA*.

The *C. glutamicum* Δ*aceE*Δ*pqo*Δ*ldhA*-derived producers showed growth and pH profiles identical to those of the control strain Δ*aceE*Δ*pqo*Δ*ldhA*(pEKEx2). The specific growth rate of *C. glutamicum* Δ*aceE*Δ*pqo*Δ*ldhA*Δ*mdh*(pEKEx2-*als,aldB,butA*) was higher as compared to the control strain Δ*aceE*Δ*pqo*Δ*ldhA*Δ*mdh*(pEKEx2) (0.55 ± 0.04 vs 0.46 ± 0.01 h^{-1}); on the other hand, the growth rate of Δ*aceE*Δ*pqo*Δ*ldhA*Δ*mdh*(pEKEx2-*als,aldB,*$_{Ptuf}$*butA*) was comparable to that of the control strain (0.44 ± 0.01 vs 0.46 ± 0.01 h^{-1}). For all Δ*aceE*Δ*pqo*Δ*ldhA*- and Δ*aceE*Δ*pqo*Δ*ldhA*Δ*mdh*-derived strains, the initial and final pH values were 7.1 and 9.2, respectively, and maximal OD_{600} values were in the range 15 to 19. In summary, cell growth was not impaired by the expression of heterologous genes (Table 3.4), reflecting the robustness of these platform strains.

Characterization of 2,3-BD production under low-oxygen conditions

The production of reduced compounds, such as 2,3-BD, is expected to be maximal under oxygen limiting conditions. Having this in mind, we devised a strategy for the production of 2,3-BD in which aerobically grown cells are collected, washed, re-suspended in minimal medium and provided with glucose under oxygen limiting conditions. Oxygen concentration was not measured, but the observed formation of organic acids indicated restricted oxygen availability (Fig. 3.4).

In a first attempt to reduce pyruvate consuming reactions leading to end-products other than 2,3-BD, we used as background *C. glutamicum* Δ*ldhA*.

Table 3.4. Growth parameters of producer strains as compared to the control strains. Cultures were grown in 2×TY medium supplemented with 1% (wt/vol) potassium acetate, unless stated otherwise. Values shown are means ± SD of three independent experiments

Strain	Specific growth rate μ (h^{-1})	OD_{max}
Δ*ldhA* (pEKEx2)*	0.52 ± 0.02	22.0 ± 0.3
Δ*ldhA* (pEKEx2-*als,aldB,butA*)*	0.58 ± 0.01	20.7 ± 0.8
Δ*ldhA* (pEKEx2)	0.51 ± 0.05	20.8 ±1.5
Δ*ldhA* (pEKEx2-*als,aldB,butA*)	0.46 ± 0.01	23.7 ± 2.7
Δ*aceE*Δ*pqo*Δ*ldhA* (pEKEx2)	0.46 ± 0.04	15.0 ± 0.2
Δ*aceE*Δ*pqo*Δ*ldhA* (pEKEx2-*als,aldB,butA*)	0.46 ± 0.03	15.2 ± 1.2
Δ*aceE*Δ*pqo*Δ*ldhA* (pEKEx2-*als,aldB,*$_{Ptuf}$*butA*)	0.46 ± 0.01	18.7 ± 0.5
Δ*aceE*Δ*pqo*Δ*ldhA*Δ*mdh* (pEKEx2)	0.46 ± 0.01	19.4 ± 1.9
Δ*aceE*Δ*pqo*Δ*ldhA*Δ*mdh* (pEKEx2-*als,aldB,butA*)	0.55 ± 0.04	15.8 ± 0.5
Δ*aceE*Δ*pqo*Δ*ldhA*Δ*mdh* (pEKEx2-*als,aldB,*$_{Ptuf}$*butA*)	0.44 ± 0.01	17.5 ± 0.8

*Strain was grown on 0.5% (wt/vol) glucose. All other strains are grown on acetate. For experimental details see Materials and methods.

During the production phase, glucose-grown cells produced 2,3-BD with a yield of 0.05 mol per mol of glucose (Tables 3.5 and S3.1); the yield was even lower for cells grown on acetate (0.02 mol per mol of glucose). The glucose consumption rate (GCR) was low, i.e., 2.5 ± 0.4 nmol·min^{-1}·mg CDW^{-1}. For comparison purposes, the GCR of the wild type strain (grown on acetate) was determined in a similar experimental set-up to give 24.6 ± 0.5 nmol·min^{-1}·mg CDW^{-1}. Actually, this value agrees

perfectly with 25 nmol·min^{-1}·mg CDW^{-1}, the GCR reported earlier for wild type *C. glutamicum* with a different experimental set-up (Chapter 2). Importantly, the introduction of the lactoccocal pathway had a positive effect on GCR in glucose grown *C. glutamicum* Δ*ldhA*(pEKEx2-*als,aldB,butA*) (4.4 ± 0.4 nmol·min^{-1}·mg CDW^{-1} compared to 2.5 ± 0.4 nmol·min^{-1}·mg CDW^{-1} in the control strain), and no effect on acetate grown cells (3.4 ± 0.4 compared to 3.0 ± 0.2 nmol·min^{-1}·mg CDW^{-1} in the control strain). 2,3-BD produced by the engineered strain Δ*ldhA*(pEKEx2-*als,aldB,butA*) grown on glucose and acetate was, respectively, 34 ± 3 mM (yield of 0.34 ± 0.04 mol per mol glucose, a 7-fold increase compared to the control strain), and 19.5 ± 0.7 mM (0.27 ± 0.06 mol per mol glucose; 11-fold increase). Other major products of metabolism were acetate, succinate, and glycerol at respective concentrations of 29 ± 2, 22 ± 2, 10 ± 1 mM in cells grown on acetate, and 25 ± 6, 20 ± 1, 19 ± 6 mM in glucose grown cells (Fig. 3.4, Table S3.1).

The inactivation of the PDHC and PQO in the producer strain Δ*aceE*Δ*pqo*Δ*ldhA*(pEKEx2-*als,aldB,butA*) had a drastic effect on 2,3-BD yield that increased from 0.27 ± 0.06 in Δ*ldhA*(pEKEx2-*als,aldB,butA*), to 0.66 ± 0.05 mol per mol, reflecting primarily the reduction of acetate formation (from 29 mM to below 0.5 mM). Moreover, the GCR increased about 1.6-fold and there was a 7-fold increase in overall productivity. Glycerol and succinate were the major side-products (12 ± 1 and 8 ± 1 mM, respectively) (Fig. 3.4).

Table 3.5. Glucose (Glc) consumption rate (GCR), molar yield and productivity of 2,3-butanediol (2,3-BD), and carbon recovery (CR) by the control and engineered *C. glutamicum* strains. In the first phase, cells were grown aerobically on 1% (wt/vol) potassium acetate except for the strains indicated with an asterisk for which 0.5% (wt/vol) glucose was used instead. Second phase fermentations were carried out for 48 h, using 25 mL of cell suspension in closed 50-mL falcon flasks with glucose as substrate. The cardinal symbol indicates that optically active 2,3-BD was produced; remaining strains produced *meso*-form of 2,3-BD. Values are averages of at least three independent experiments. A single NMR spectrum was acquired for each sample.

Strain	**GCR** (nmol·min^{-1}·mg CDW^{-1})	**Yield** (mol 2,3-BD per mol Glc)	**Productivity** (nmol·min^{-1}·mg CDW^{-1})	**CR** (%)
Δ*ldhA* (pEKEx2)*	2.5 ± 0.4	0.05 ± 0.00$^{\#}$	0.12 ± 0.01	81 ± 3
Δ*ldhA* (pEKEx2-*als,aldB,butA*)*	4.4 ± 0.4	0.34 ± 0.04	1.28 ± 0.09	79 ± 9
Δ*ldhA*(pEKEx2)	3.0 ± 0.2	0.02 ± 0.01$^{\#}$	0.06 ± 0.03	77 ± 1
Δ*ldhA* (pEKEx2-*als,aldB,butA*)	3.4 ± 0.4	0.27 ± 0.06	0.53 ± 0.13	82 ± 3
Δ*aceE*Δ*pqo*Δ*ldhA*(pEKEx2)	1.6 ± 0.3	0.22 ± 0.01$^{\#}$	0.30 ± 0.00	87 ± 1
Δ*aceE*Δ*pqo*Δ*ldhA* (pEKEx2-*als,aldB,butA*)	5.4 ± 0.7	0.66 ± 0.05	3.55 ± 0.58	84 ± 7
Δ*aceE*Δ*pqo*Δ*ldhA* (pEKEx2-*als,aldB,*$_{Ptuf}$*butA*)	6.1 ± 0.1	0.61 ± 0.06	3.13 ± 0.22	87 ± 3
Δ*aceE*Δ*pqo*Δ*ldhA*Δ*mdh* (pEKEx2)	1.6 ± 0.3	0.34 ± 0.05$^{\#}$	0.53 ± 0.00	91 ± 6
Δ*aceE*Δ*pqo*Δ*ldhA*Δ*mdh* (pEKEx2-*als,aldB,butA*)	6.0 ± 0.3	0.64 ± 0.09	4.34 ± 0.16	90 ± 4
Δ*aceE*Δ*pqo*Δ*ldhA*Δ*mdh* (pEKEx2-*als,aldB,*$_{Ptuf}$*butA*)	6.5 ± 0.5	0.64 ± 0.10	4.25 ± 0.41	91 ± 7

Further engineering aimed at succinate reduction (MDH inactivation by deletion of the cg2613-encoded activity), left both yield and GCR essentially unchanged while productivity was slightly improved in *C.*

glutamicum Δ*aceE*Δ*pqo*Δ*ldhA*Δ*mdh*(pEKEx2-*als,aldB,butA*) (4.3 ± 0.2 compared to 3.6 ± 0.6 nmol·min^{-1}·mg CDW^{-1}). Strains in which the lactococcal *butA* gene was placed under the control of P_{tuf} promoter showed similar behavior to those which had this gene under P_{tac} control in terms of all production parameters (Table 3.5, Fig. 3.4). In summary, *C. glutamicum* Δ*aceE*Δ*pqo*Δ*ldhA*(pEKEx2-*als,aldB,butA*), Δ*aceE*Δ*pqo*Δ*ldhA*Δ*mdh*(pEKEx2-*als,aldB,butA*) and Δ*aceE*Δ*pqo*Δ*ldhA*Δ*mdh* (pEKEx2-*als,aldB,*$_{Ptuf}$*butA*) showed the highest yield of about 0.65 mol 2,3-BD per mol of glucose with the latter two strains exhibiting the highest productivities of about 4.3 nmol 2,3-BD per min and mg CDW (Table 3.5). All control strains produced optically active 2,3-BD, while only the *meso*-form was found as end-product of the producer strains (Fig. 3.4; Table S3.1).

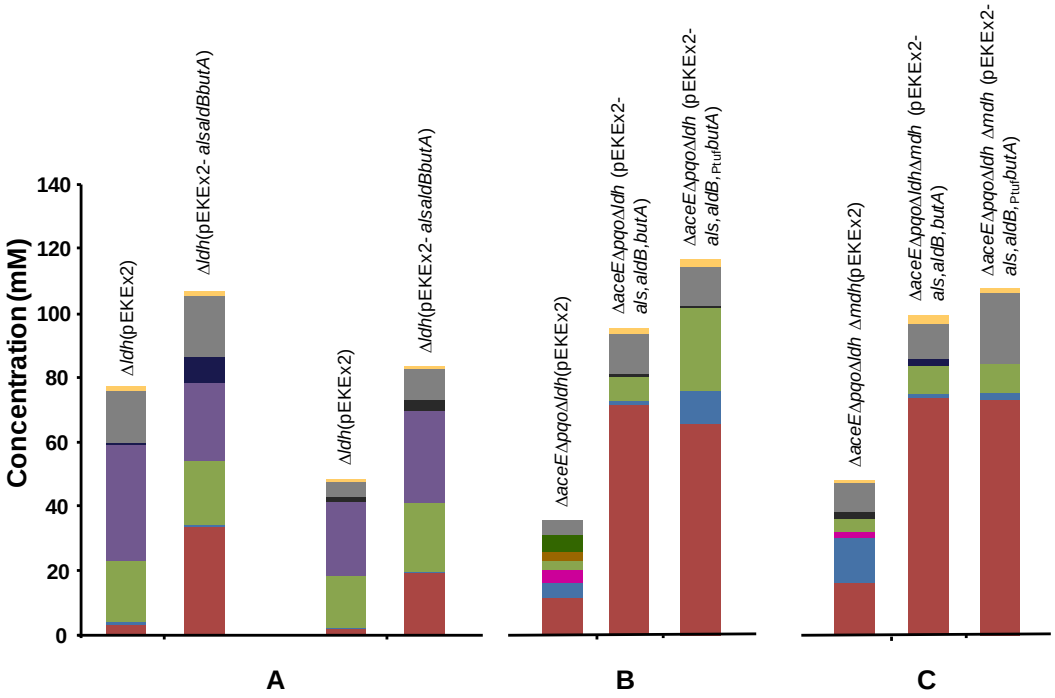

Figure 3.4. End-products of glucose metabolism in 2,3-BD producers and control strains under oxygen limiting conditions: 25 mL of cell suspension in stoppered 50-mL flasks incubated with 2% (wt/vol) glucose for 48 h at 180 rpm and 30ºC. Control strains produced optically active 2,3-BD (most likely (*2S*,*3S*)-2,3-BD), while the engineered strains produced *meso*-2,3-BD. For simplicity, a single color is used to represent any form of 2,3-BD. Lactate dehydrogenase negative strains (**A**) grown on glucose (left) and acetate (right); triple deletion mutants *C. glutamicum* Δ*aceE*Δ*pqo*Δ*ldhA*(pEKEx2-*als,aldB,butA*), *C. glutamicum* Δ*aceE*Δ*pqo*Δ*ldhA*(pEKEx2-*als,aldB,*$_{Ptuf}$*butA*) (**B**) and quadruple deletion mutants *C. glutamicum* Δ*aceE*Δ*pqo*Δ*ldhA*Δ*mdh*(pEKEx2-*als,aldB,butA*) and *C. glutamicum* Δ*aceE*Δ*pqo*Δ*ldhA*Δ*mdh*(pEKEx2-*als,aldB,*$_{Ptuf}$*butA*) (**C**). Legend: ■, 2,3-BD; ■, acetoin; ■, acetolactate; ■, succinate; ■, acetate; ■, pyruvate; ■, α-ketoisovalerate; ■, DHA; ■, glycerol; ■, L-alanine.

It is important to note that pH was not controlled during the production phase. All fermentations started at pH 7.0, but the final pH value varied as mutants exhibited different acidifying properties due to their differential ability to produce organic acids. At the end of 48 h-fermentation, pH was between 5.1 and 5.3 for *ldhA*-negative strains. As expected, reduction of succinate and acetate, and accumulation of neutral compounds led to higher final pH values: 6.6, 6.4, 5.7 and 6.6 for *C. glutamicum* Δ*aceE*Δ*pqo*Δ*ldhA*(pEKEx2-*als,aldB,butA*), Δ*aceE*Δ*pqo*Δ*ldhA*Δ*mdh* (pEKEx2-*als,aldB,butA*), Δ*aceE*Δ*pqo*Δ*ldhA*(pEKEx2-*als,aldB,*$_{Ptuf}$*butA*) and Δ*aceE*Δ*pqo*Δ*ldhA*Δ*mdh*(pEKEx2-*als,aldB,*$_{Ptuf}$*butA*), respectively. Earlier work has shown that a decrease in pH results in considerably lower GCR in resting cells of wild-type *C. glutamicum* (Chapter 2).

Optimization of 2,3-BD production by manipulation of oxygen supply

Engineered strains of *C. glutamicum* converted up to two thirds of glucose into 2,3-BD (Table 3.5), however the consumption rate of glucose was not satisfactory when compared to other *C. glutamicum* strains, such as those manipulated for the production of isobutanol and succinate (Blombach et al. 2011, Litsanov et al. 2012). The accumulation of reduced compounds, such as succinate and glycerol, hinted that the low GCR in the engineered strains could result from a high NADH:NAD^+ ratio, as previously proposed (Tsuge et al. 2015). Oxygen can be an alternative acceptor of electrons from NADH, via the electron transfer chain, hence we performed fermentations under different controlled oxygen supply conditions (sparging rates of 5, 10 or 20 mL air min^{-1}) in the mini-fermenter as

described in Methods, to determine the conditions that would support maximal yield, GCR and productivity (Tables 3.6 and S3.2, Fig. 3.5). Strains *C. glutamicum* Δ*aceE*Δ*pqo*Δ*ldhA*(pEKEx2-*als,aldB,*$_{Ptuf}$*butA*) and Δ*aceE*Δ*pqo*Δ*ldhA*Δ*mdh*(pEKEx2-*als,aldB,*$_{Ptuf}$*butA*) were selected for this optimization step as they showed particularly high ALS/ALDC and BDH activity, respectively.

Table 3.6. Glucose (Glc) consumption rate (GCR), molar yield and productivity of 2,3-butanediol (2,3-BD), and carbon recovery (CR) achieved with *C. glutamicum* Δ*aceE*Δ*pqo*Δ*ldhA*(pEKEx2-*als,aldB,*$_{Ptuf}$*butA*) and *C. glutamicum* Δ*aceE*Δ*pqo*Δ*ldhA*Δ*mdh*(pEKEx2-*als,aldB,*$_{Ptuf}$*butA*) strains under different aeration conditions. Cells were grown aerobically on 1% (wt/vol) potassium acetate. The second, production phase was performed in a 80-mL fermenter at 30°C for 30 h with glucose as substrate. The cell suspension was sparged with air at the flow rates indicated. *Meso*-2,3-BD was by far the major stereoisomer. At the optimal aeration rate (10 mL·min^{-1}), there was 95% of the *meso*-form. Values are averages of three independent experiments; a single NMR spectrum was acquired for each sample.

Strain	**Airflow** (mL·min^{-1})	**GCR** (nmol·min^{-1}· mg CDW^{-1})	**Yield** (mol 2,3-BD per mol Glc)	**Productivity** (nmol·min^{-1}· mg CDW^{-1})	**CR** (%)
Δ*aceE*Δ*pqo*Δ*ldhA* (pEKEx2-*als,aldB,*$_{Ptuf}$*butA*)	5	7.2 ± 0.6	0.44 ± 0.04	3.4 ± 0.3	89 ± 6
	10	15.8 ± 1.7	0.57 ± 0.03	8.1 ± 0.4	91 ± 4
	20	14.7 ± 1.1	0.36 ± 0.06	5.0 ± 0.9	83 ± 10
Δ*aceE*Δ*pqo*Δ*ldhA* Δ*mdh* (pEKEx2-*als,aldB,*$_{Ptuf}$*butA*)	5	11.1 ± 1.0	0.52 ± 0.03	5.5 ± 0.7	85 ± 2
	10	21.1 ± 0.8	0.66 ± 0.01	10.9 ± 1.8	90 ± 8
	20	22.8 ± 1.6	0.46 ± 0.02	8.0 ± 0.7	78 ± 7

Cell suspensions of *C. glutamicum* Δ*aceE*Δ*pqo*Δ*ldhA*(pEKEx2-*als,aldB,*$_{Ptuf}$*butA*) and Δ*aceE*Δ*pqo*Δ*ldhA*Δ*mdh*(pEKEx2-*als,aldB,*$_{Ptuf}$*butA*) under constant air flow of 5 mL·min^{-1} showed an increased GCR (7.2 ± 0.6 and 11.1 ± 1.0 nmol·min^{-1}·mg CDW^{-1} in mini-fermenter for the two respective strains (Table 3.6), compared to 6.1 ± 0.1 and 6.5 ± 0.5 nmol·min^{-1}·mg CDW^{-1} in flasks (Table 3.5)); the productivity in mini-fermenter was 3.4 ± 0.3 and 5.5 ± 0.7 nmol·min^{-1}·mg CDW^{-1} compared to 3.1 ± 0.2 and 4.3 ± 0.4 nmol·min^{-1}·mg CDW^{-1} in flasks, but the yield was higher for fermentations in closed flasks (Tables 3.5 and 3.6). Upon doubling of the air flow to 10 mL·min^{-1}, GCR and the productivity of *C. glutamicum* Δ*aceE*Δ*pqo*Δ*ldhA*(pEKEx2-*als,aldB,*$_{Ptuf}$*butA*) and Δ*aceE*Δ*pqo*Δ*ldhA*Δ*mdh*(pEKEx2-*als,aldB,*$_{Ptuf}$*butA*) increased two-fold; both strains produced 2,3-BD at highest yields (0.57 ± 0.03 and 0.66 ± 0.01 mol 2,3-BD per mol glucose). Interestingly, further increase in the flow rate to 20 mL·min^{-1} resulted in significantly lower yields and productivities (Table 3.6).

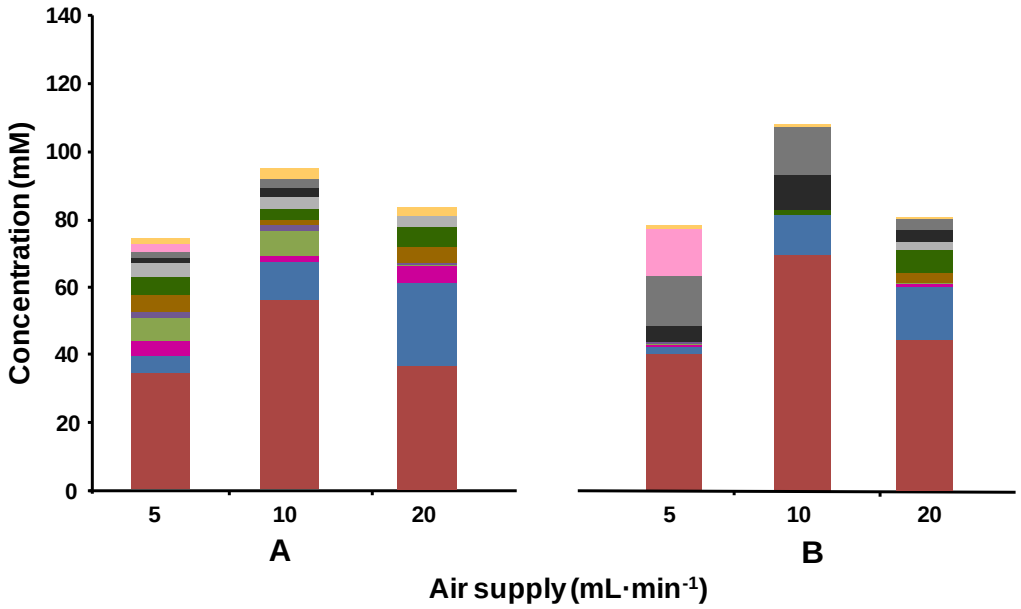

Figure 3.5. Effect of aeration rate on end-products of glucose metabolism in the triple deletion mutant *C. glutamicum* Δ*aceE*Δ*pqo*Δ*ldhA*(pEKEx2-*als,aldB,*$_{Ptuf}$*butA*) (**A**) and the quadruple deletion mutant Δ*aceE*Δ*pqo*Δ*ldhA*Δ*mdhA* (pEKEx2-*als,aldB,*$_{Ptuf}$*butA*) (**B**). Fifty mL of cell suspension in 80-mL fermenter incubated with 2% (wt/vol) glucose for 30 h at 30^0C. The air flow was 5, 10 or 20 mL/min. Legend: ■, 2,3-BD; ■, acetoin; ■, acetolactate; ■, succinate; ■, acetate; ■, pyruvate; ■, α-ketoisovalerate; ■, α-ketoglutarate; ■, DHA; ■, glycerol; ■, ethanol; ■, L-alanine.

Ethanol was produced by both strains in experiments using 5 mL·min^{-1} air, and glycerol was absent only in the experiment using 20 mL·min^{-1} air with the Δ*aceE*Δ*pqo*Δ*ldhA*(pEKEx2-*als,aldB,*$_{Ptuf}$*butA*) strain. Other side products in these experiments were acetoin, succinate, dihydroxyacetone (DHA), pyruvate, acetate, L-alanine, α-acetolactate, α-ketoglutarate, and α-ketoisovalerate (Fig. 3.5, Table S3.2). Among these, acetoin formation

showed a clear dependence on oxygen availability, increasing about 3- and 5-fold when the air flow was increased from 5 to 10 mL·min^{-1} and from 5 to 20 mL·min^{-1}, respectively. Dissolved oxygen was not controlled, but we confirmed that the oxygen concentration was below the detection limit of the oxygen electrode even at the highest aeration rate. The time course for glucose consumption and end-product formation is illustrated in Figure 3.6 for the best producer strain. In summary, under an air flow of 10 mL·min^{-1} *C. glutamicum* Δ*aceE*Δ*pqo*Δ*ldhA*Δ*mdh*(pEKEx2-*als,aldB,*$_{Ptuf}$*butA*) produced 70 ± 8 mM 2,3-BD with a yield of 0.66 mol per mol of glucose and productivity of 11 nmol·min^{-1}·mg CDW^{-1}, which represent a notable improvement (Fig. 3.7).

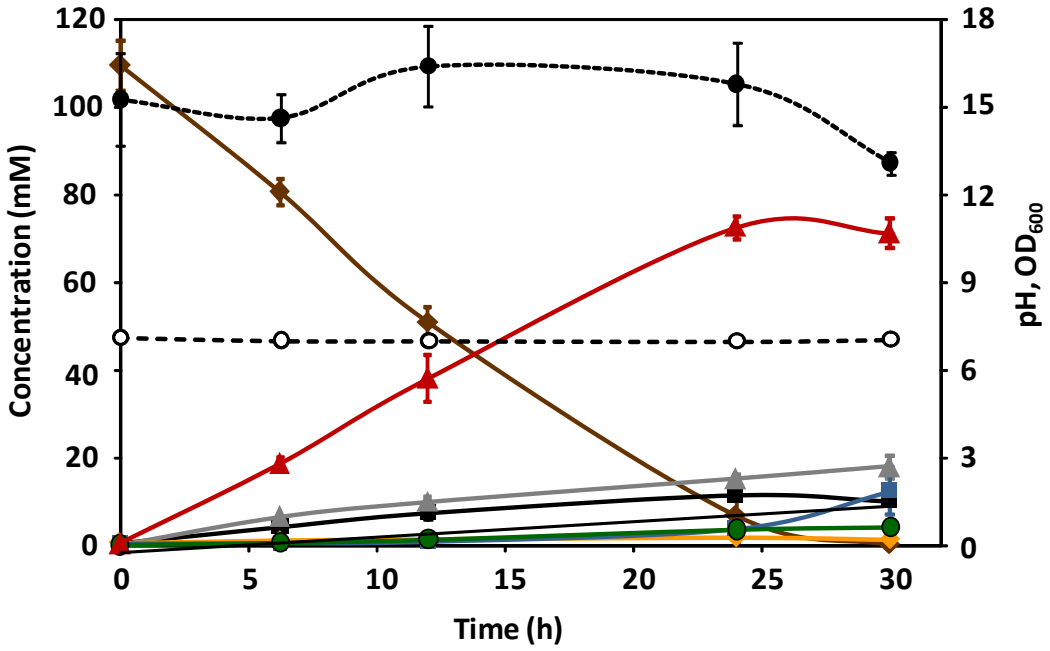

Figure 3.6. Fermentation profile of the best 2,3-BD producer strain *C. glutamicum* Δ*aceE*Δ*pqo*Δ*ldhA*Δ*mdh*(pEKEx2-*als,aldB,*$_{Ptuf}$*butA*) as a function of time. Fifty mL of cell suspension in 80-mL fermenter incubated with 2% (wt/vol) glucose for 30 h at 30ºC. The air flow was 10 mL·min^{-1}. Error bars are shown as standard deviation of three independent replicates. Legend: ●, biomass as OD_{600}; ○, pH value; ▲, 2,3-BD; ■, acetoin; ♦, glucose; ●, α-ketoisovalerate; ■, DHA; ▲, glycerol; ♦, L-alanine.

Discussion

The wild-type *C. glutamicum* produces vestigial amounts of 2,3-BD (Dickschat et al. 2010). Accordingly, low levels of 2,3-BD were also found in the end-products of glucose metabolism by the control strain *C. glutamicum* Δ*ldhA*(pEKEx2), the initial host in this work (Table 3.5). *C.*

glutamicum was the favored candidate for 2,3-BD production given its high performance as an industrial organism and its GRAS status. Moreover, we verified that 2,3-BD has low toxicity to *C. glutamicum* as cell growth was not affected by 2% 2,3-BD (data not shown). 2,3-BD producing bacteria, such as *Klebsiella spp*., synthesize this diol from pyruvate in a sequence of three reactions catalyzed by α-acetolactate synthase, α-acetolactate decarboxylase and butanediol dehydrogenase. In this work, we constructed an artificial operon with the three relevant genes of *L. lactis* and introduced this heterologous pathway into *C. glutamicum* (Fig. 3.2).

C. glutamicum is able to synthesize α-acetolactate from pyruvate via the action of the anabolic enzyme, AHAS; however, this enzyme is highly inhibited by the branched chain amino acids derived from α-acetolactate (Elisáková et al. 2005). Therefore, our engineering strategy endowed the host strain with a heterologous ALS, i.e., the catabolic enzyme from *L. lactis*, which is not susceptible to amino acid inhibition (Snoep et al. 1992). The enhanced activity of ALS should also be beneficial for directing the flux towards 2,3-BD.

The second step in the biosynthetic pathway, decarboxylation of α-acetolactate into (*R*)-acetoin, is carried out by α-acetolactate decarboxylase. A homologue of this enzyme is not predicted in the genome of *C. glutamicum*, and indeed the ALS/ALDC activity was low in cell extracts of all control strains (Table 3.3). The third step, reduction of acetoin, is performed by BDH, and a relatively high activity (0.2-0.3 $U \cdot (mg\ protein)^{-1}$) was detected in the control strains (Table 3.3).

Actually, this is not surprising given that *C. glutamicum* possesses (*2S,3S*)-BDH, which is claimed to be absolutely stereospecific for (*S*)-acetoin (Takusagawa et al. 2001). Like all known ALDCs, the enzyme from *L. lactis* produces exclusively (*R*)-acetoin (Marlow et al. 2013), thus a BDH with suitable stereospecific properties needed to be included.

^{1}H-NMR can distinguish the optically active from the *meso*-form of 2,3-BD (Fig. 4.5). Control strains produced only optically active 2,3-BD (Table 3.5), most likely derived from diacetyl formed via spontaneous decarboxylation of α-acetolactate in the presence of oxygen. Diacetyl is then converted to 2,3-(*2S,3S*)-BD in two reduction reactions catalyzed by the endogenous BDH (Fig. 3.1). In contrast to the control strains, *meso*-2,3-BD was by far the main form synthesized by the producer strains, the optically active form (around 5% of total 2,3-BD), being detected only in fermentations performed at the highest aeration rates, in agreement with the oxygen dependence of the spontaneous decarboxylation of α-acetolactate. Given that *C. glutamicum* lacks α-acetolactate decarboxylase, the presence of BDH in this bacterium is rather puzzling. Moreover, according to a recent study, *C. glutamicum* BDH is a promiscuous enzyme that besides acetoin recognizes DHA as substrate, though with a low affinity (30 mM or higher DHA concentration needed for activity) (Jojima et al. 2015). Further work should be directed to clarify the physiological role of BDH in *C. glutamicum.*

The *L. lactis* genes (*als*, *aldB*, *butA*) were functionally expressed in the three host strains. The combined activity ALS/ALDC was in the range 0.4 - 1.4 U·(mg of protein)$^{-1}$ for producer strains grown on acetate, corresponding to overexpression levels of 8 to 31-fold. Opportunely, the heterologous activities are comparable to those of glycolytic enzymes measured in crude extracts of *C. glutamicum* (Yamamoto et al. 2012). Overexpression of *butA* (encoding BDH activity) was similarly successful, yielding final BDH activity up to 1.2 U·(mg of protein)$^{-1}$, which confirms the suitability of using the lactococcal genes for 2,3-BD production in *C. glutamicum*.

The introduction of the assembled pathway in *C. glutamicum* Δ*ldhA* enabled efficient redirection of the flux from pyruvate into 2,3-BD. However, the yield was relatively low (0.3 mol per mol glucose) and the two major products were succinate and acetate. Hence, the next engineering step had the objective of suppressing acetate pathways; this proved to be crucial in the by-product elimination strategy, as the 2,3-BD yield doubled in the Δ*aceE*Δ*pqo*Δ*ldhA*-derived producer strains (Table 3.5; Fig. 3.7). Additional inactivation of *mdh* did not improve the yield significantly, but there was a slight increase in productivity (Table 3.5).

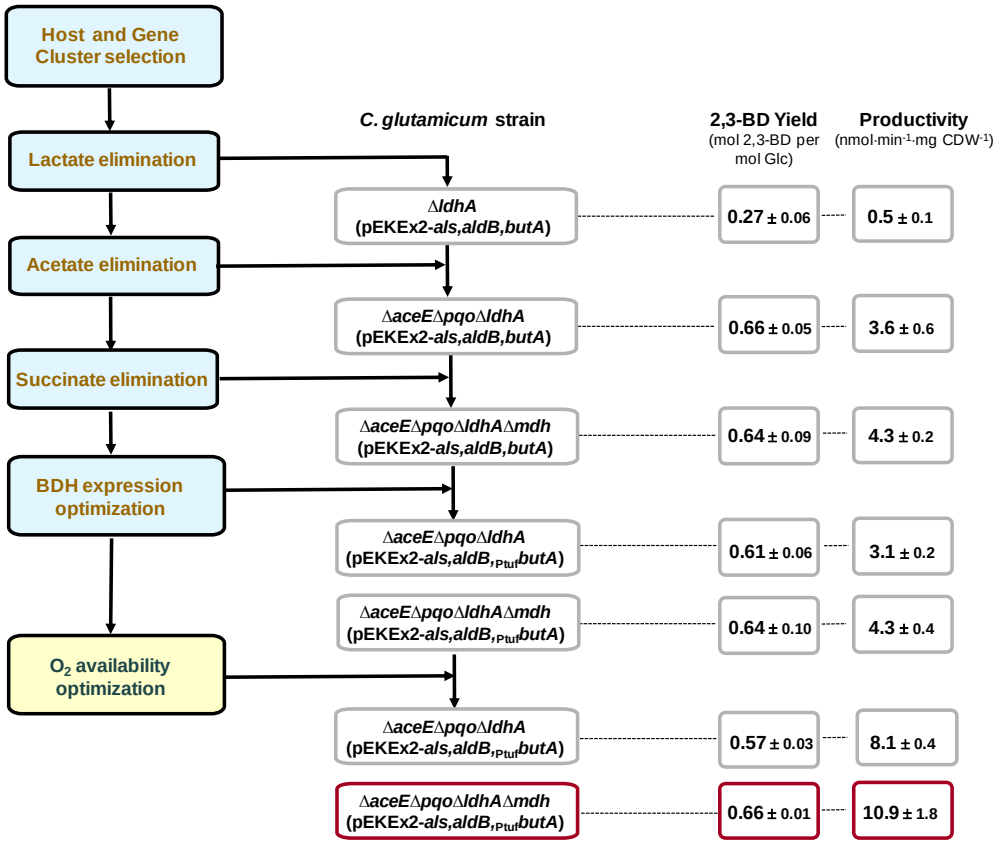

Figure 3.7. A summary of the stepwise systematic approach used to engineering *C. glutamicum* for the production of 2,3-BD. The values reflect the impact of the several steps on yield and productivity. Blue boxes refer to strain optimization steps, while the yellow box indicates the process optimization step. Abbreviations: 2,3-BD, 2,3-butanediol; Glc, glucose.

Curiously, the strains derived from *C. glutamicum* Δ*aceE*Δ*pqo*Δ*ldhA*Δ*mdh* produced substantial amounts of succinate despite the intended suppression of succinate formation via the reductive branch of the TCA cycle. The genome of *C. glutamicum* includes *mdhB* (cg0763), putatively assigned as malate/L-lactate dehydrogenase, hence

this second activity may contribute to succinate formation. On the other hand, involvement of the glyoxylate shunt and/or the oxidative branch of the TCA cycle cannot be ruled out.

Glycerol was the second major side-product detected in *C. glutamicum* Δ*aceE*Δ*pqo*Δ*ldhA*- and Δ*aceE*Δ*pqo*Δ*ldhA*Δ*mdh*-derived strains. Two pathways have been proposed for the synthesis of this polyol in *C. glutamicum* (Jojima et al. 2015, Lindner et al. 2012). Jojima and coworkers (Jojima et al. 2015) proposed that under oxygen-deprivation conditions glycerol is formed through reduction of DHA by the activity of endogenous BDH. On the other hand, DHA is a product of dihydroxyacetone-phosphate (DHAP) dephosphorylation via the respective phosphatase (Jojima et al. 2012). Therefore, endogenous BDH and DHAP phosphatase are obvious targets for inactivation in further attempts to minimize side products. In this way, the electrons that are used for glycerol formation could be directed to acetoin reduction. The elimination of BDH would also be advantageous for the stereochemical purity of the desired end-product, since the small contamination with the optically active form would vanish, though at the expense of some carbon loss in the form of diacetyl.

Under production conditions (oxygen limitation), it is anticipated that the BDH activity plays an important role in satisfying the redox balance via cofactor recycling. Further enhancement of BDH activity was attempted by including an additional promoter, but the BDH activity remained unchanged (Tables 3.3 and 3.5). However, a high BDH activity would not fix the redox imbalance since the synthesis of 2,3-BD results in net production of 1 mol

NADH per mol of glucose consumed, and an additional sink for the reducing power becomes mandatory. Accordingly, providing controlled amounts of oxygen significantly improved GCR and 2,3-BD productivity.

Manipulation of oxygen availability had no clear impact on 2,3-BD yield, but was crucial to increase GCR, which reached maximal values of approx. 21 nmol·min^{-1}·mg CDW^{-1}, comparable to those of *C. glutamicum* strains engineered for isobutanol production (Blombach et al. 2011). This optimization step was more effective for *C. glutamicum* Δ*aceE*Δ*pqo*Δ*ldhA*Δ*mdh*(pEKEx2-*als,aldB,*$_{Ptuf}$*butA*) than for Δ*aceE*Δ*pqo*Δ*ldhA*(pEKEx2-*als,aldB,*$_{Ptuf}$*butA*) (Table 3.6). The reason could be related with the different BDH activity in these two strains (Table 3.3). The stronger activity in *C. glutamicum* Δ*aceE*Δ*pqo*Δ*ldhA*Δ*mdh*(pEKEx2-*als,aldB,*$_{Ptuf}$*butA*) would pull the flux towards 2,3-BD more efficiently, with concomitant benefit on the rate of NAD^+ regeneration, and hence on the GCR. Further increase in the air supply (from 10 to 20 mL·min^{-1}) had a negative impact on 2,3-BD yield, which is in conformity with the equivalent accumulation of acetoin. This shift in end-products towards compounds less reduced than 2,3-BD indicates that the competition of oxygen as an electron sink became excessive.

Thus far, *Klebsiella* spp., *E. aerogenes* and *S. marcescens* are the top producers of 2,3-BD (reviewed in (Ji et al. 2011)), however, the pathogenicity of these strains is regarded as a disadvantage and hinders large-scale production. The best non-pathogenic producer is *Paenibacillus*

polymyxa (72 $g \cdot L^{-1}$ and about 2 $g \cdot L^{-1} \cdot h^{-1}$), which grows in complex medium and has the drawback of producing exopolysaccharides that increase the viscosity of the fermentation broth (Häßler et al. 2012). Engineered *S. cerevisiae* has a 0.29 $g \cdot L^{-1} \cdot h^{-1}$ productivity and a yield of 0.70 mol 2,3-BD per mol glucose, while engineered *E. coli* produces 1.19 $g \cdot L^{-1} \cdot h^{-1}$ with a yield of 0.82 $mol \cdot mol^{-1}$ (Lian et al. 2014, Xu et al. 2014). The theoretical maximal yield of 2,3-BD from glucose is 1 mol per mol (0.5 g per g), and it was almost reached with pathogenic (*Klebsiella* spp.), and non-pathogenic producers (*Bacillus* spp.) (see General discussion). Compared with these non-native producers, the best *C. glutamicum* 2,3-BD producer, Δ*aceE*Δ*pqo*Δ*ldhA*Δ*mdh*(pEKEx2-*als,aldB,*$_{Ptuf}$*butA*), has a productivity close to the lower limit (10.9 $nmol \cdot min^{-1} \cdot mg\ CDW^{-1}$ corresponding to 0.21 $g \cdot L^{-1} \cdot h^{-1}$), and a good yield (0.66 mol 2,3-BD per mol glucose). Our work used cell suspensions at a relatively low OD_{600} (20 - 30, corresponding to about 5 g $CDW \cdot L^{-1}$), but *C. glutamicum* can easily be grown to much higher cell density, allowing for higher 2,3-BD productivity during the production phase. For example, the utilization of a high density bioreactor (50 g $CDW \cdot L^{-1}$), as in (Okino et al. 2008a), would lead to one order of magnitude greater productivity (around 2 $g \cdot L^{-1} \cdot h^{-1}$), which compares well with that of the non-pathogenic natural producer (Häßler et al. 2012). Further increase in GCR of engineered *C. glutamicum* strains might be possible with a more fine manipulation of the oxygen supply conditions.

While this manuscript was in a late stage of preparation, a study was published by Yang et al. (Yang et al. 2015) with the same purpose as ours,

albeit using different engineering strategies, host strains and production process. The 2,3-BD yield obtained was lower than that presented here (0.47 vs 0.66 mol per mol glucose), but a more extended comparison is hampered by the very different production processes used in the two studies.

By using a systematic approach *C. glutamicum* was successfully engineered for the production of 2,3-BD (Fig. 3.7). Organic acid production was strongly reduced or eliminated and adequate activities of the 2,3-BD biosynthetic pathway were achieved. By means of genetic engineering and manipulation of production conditions, productivity and yield were optimized. Characterization of production provided insight into metabolic features of producer strains, and indicated directions for further rounds of strain improvement. Future work should aim at increasing 2,3-BD yield by eliminating the side-products DHA and glycerol. By using the full potential of *C. glutamicum*, improvement of productivity and titer is also feasible. Additionally, we propose that the optimized construct, under adequate aeration conditions, can be used as a GRAS-platform for production of acetoin, another valuable chemical widespread in the food industry as flavor enhancer. Alternatively, straightforward developments, e.g., omission of the *butA* gene in the artificial operon and disruption of endogenous BDH, are expected to yield efficient acetoin producers.

Acknowledgements and work contributions

We thank D. L. Turner for a critical reading of the manuscript, Nuno Borges for helpful advice, and Sara Rebelo for technical assistance.

DR was involved in designing the study, all stages of experimental work and writing the manuscript. ALC contributed to construction of producer strains and enzymatic activities measurements. SW was involved in strain construction. HS, BB, BJE, and ARN contributed to study design, supervision and manuscript preparation.

Table S3.1. End-products of glucose metabolism and residual glucose measured in supernatants of cell suspensions of parent and producer strains incubated under oxygen limiting conditions (closed falcon tubes) for 48 h. All concentrations are in mM. Results are shown as means ± SD of three independent experiments.

Strain	Glc	2,3-BD	Acn	DA	Succ	Ac	Pyr	α-KIV	DHA	Gly	Eth	Isobut	Ala
Δ*ldhA* (pEKEx2)*	55±2	2.1±0.4	0.7±0.1	0.5±0.0	17.3±0.1	26±2	0.0	0.0	1.5±0.1	8±1	0.0	0.0	0.8±0.4
Δ*ldhA*(pEKEx2-*als,aldB,butA*)*	14±5	34±3	0.6±0.1	0.0	20±1	25±6	0.0	0.0	8±3	19±6	1.6±0.2	0.0	1.2±0.1
Δ*ldhA*(pEKEx2)	39±11	3.0±0.3	1.1±0.3	0.0	20±1	35.5±0.3	0.0	0.0	1±0.1	16±2	0.0	0.0	1.4±0.2
Δ*ldhA*(pEKEx2-*als,aldB,butA*)	44±11	20±1	0.4±0.1	0.0	22±2	29±2	0.0	0.0	3.4±0.6	10±1	1.0±0.3	0.0	1.3±0.3
Δ*aceE*Δ*pqo*Δ*ldhA* (pEKEx2)	68±6	11±1	5.1±0.2	4.1±0.3	3±1	0.0	5.6**	9.9**	0.0	5±1	0.0	0.0	0.0
Δ*aceE*Δ*pqo*Δ*ldhA* (pEKEx2-*als,aldB,butA*)	4.7±4.2	72±11	1.0±0.2	0.0	7.6±0.5	0.2±0.1	1.1±0.6	0.9±0.1	1.2±1.1	12±1	0.9±0.3	4±2	1.8±0.6
Δ*aceE*Δ*pqo*Δ*ldhA* (pEKEx2-*als,aldB,*$_{Ptuf}$*butA*)	0.0	66±12	10±2	0.0	26.2±0.4	0.2±0.1	0.0	0.0	1.0±0.6	11.8±0.3	1.3±0.2	0.0	2.2±0.4
Δ*aceE*Δ*pqo*Δ*ldhA* Δm*dh*(pEKEx2)	61±3	16±4	14±3	4.0**	4.1±5.5	0.0	0.0	0.0	5.9**	9±1	0.0	0.0	1.5**
Δ*aceE*Δ*pqo*Δ*ldhA* Δ*mdh*(pEKEx2-a*ls,aldB,butA*)	9±6	74±3	1.4±0.5	0.0	9±1	0.2±0.1	1.2±0.1	2.9±0.3	2.3±0.3	11±7	0.0	1.7±1.3	3±1
Δ*aceE*Δ*pqo*Δ*ldhA* Δ*mdh* (pEKEx2-*als,aldB,*$_{Ptuf}$*butA*)	0.0	73±7	2.0±1.5	0,0	8.8±0.4	0.2±0.1	0.0	0.0	0.4±0.1	22±3	0.9±0.1	0.0	1.6±0.2

*, cells grown on glucose; ** detected only in one experiment. Abbreviations: 2,3-BD, 2,3-butanediol; Acn, acetoin; DA, diacetyl; Succ, succinate; Ac, acetate; Pyr, pyruvate; α-KIV, α-ketoisovalerate; DHA, dihydroxyacetone; Gly, glycerol; Isobut, isobutanol; α-KG, α-ketoglutarate; Ala, L-alanine.

Table S3.2. End-products of glucose metabolism and residual glucose measured in supernatants of cell suspensions of producer strains incubated under different aeration conditions for 30 h. All concentrations are in mM, air is in mL·min^{-1}. Results are shown as means ± SD of three independent experiments.

Strain	Air	Glc	2,3-BD	Acn	DA	Succ	Ac	Pyr	α-KIV	α-KG	DHA	Gly	Eth	Isobut	Ala
Δ*aceE*Δ*pqo*Δ*ldhA* (pEKEx2-*als,aldB,* $_{Ptuf}$*butA*)	5	25±10	34±5	5±4	4.2±0.7	7.1±0.6	1.9±0.7	5±2	5.4±1.5	3.0±0.1	2±1	1.3±0.7	2.2±0.1	0.0	2.0±0.3
	10	0.0	56±1	11±3	0.6±0.1	7.6±0.8	1.7±1.1	1.1±0.6	3±1	3.1±0.1	2.2±0.6	2.7±0.2	0.0	1.1±0.1	3.2±0.2
	20	0.0	36±7	25±6	0.0	1.0**	0.5±0.2	5±3	6±1	2.5±0.4	0.2±0.2	0.0	0.0	0.0	2.4±0.4
Δ*aceE*Δ*pqo*Δ*ldhA*Δ*mdh* (pEKEx2-*als,aldB,* $_{Ptuf}$*butA*)	5	25±10	40±5	2.6±0.5	0.4±0.1	0.6±0.1	0.3±0.1	0.4±0.3	0.0	0.0	4±1	15±1	13.7±0.4	0.0	1.3±0.3
	10	0.0	70±8	12±5	0.0	0.0	0.1±0.1	0.0	1.0±0.5	0.0	10±1	17±3	0.0	0.0	1.1±0.3
	20	0.0	44±5	15.5±5.7	1.2±1.0	0.7±0.6	0.2±0.1	2.8±4.2	6.3±0.3	2.0±0.2	3.6±1.3	2.9±0.1	0.0	0.0	0.8±0.2

*, cells grown on glucose; ** detected only in one experiment. Abbreviations: 2,3-BD, 2,3-butanediol; Acn, acetoin; DA, diacetyl; Succ, succinate; Ac, acetate; Pyr, pyruvate; α-KIV, α-ketoisovalerate; DHA, dihydroxyacetone; Gly, glycerol; Isobut, isobutanol; α-KG, α-ketoglutarate; Ala, L-alanine.

CHAPTER 4

Stereospecificity of *Corynebacterium glutamicum* 2,3-butanediol dehydrogenase and implications for the stereoform composition of bioproduced 2,3-butanediol

This chapter is part of a manuscript in preparation:

Radoš D, Turner DL, Borges N, Catarino T, Neves AR, Eikmanns BJ, Blombach B, and Santos H.

Stereospecificity of *Corynebacterium glutamicum* 2,3-butanediol dehydrogenase and implications for the stereoform composition of bioproduced 2,3-butanediol.

Contents

Summary

The stereochemistry of 2,3-butanediol (2,3-BD) synthesis in microbial fermentations is industrially relevant as it determines the range of applications of this bio-based product. In this work, *Corynebacterium glutamicum* was engineered for the production of 2,3-BD using the following strategy: the activities of α-acetolactate synthase and decarboxylase were introduced by heterologous expression of the *Lactococcus lactis* genes encoding these two activities; additionally, the endogenous 2,3-butanediol dehydrogenase (BDH) was overproduced. The engineered strain produced *meso*-2,3-BD, suggesting that (*R*)-acetoin is a substrate for the endogenous 2,3-BDH. This observation challenged the reported absolute stereospecificity of *C. glutamicum* BDH for (*S*)-acetoin (Takusagawa et al. 2001. *Biosc. Biotechnol. Biochem*. 65:1876-8). Therefore, we decided to investigate the stereospecific properties of this enzyme to explain the apparent contradiction. The BDH of *C. glutamicum* (encoded by gene *butA*) was produced in *E. coli* and purified. Activity assays monitored online by ^{1}H-NMR using as substrates racemic acetoin and excess of NADH showed an initial, fast and complete reduction of (*S*)-acetoin to (*2S,3S*)-2,3-BD, followed by a slow (~20-fold lower apparent rate) conversion of (*R*)-acetoin into *meso*-2,3-BD. In experiments with limitation of NADH the initial behavior was similar but the subsequent slow synthesis of *meso*-2,3-BD proceeded at the expense of the (*2S,3S*)-2,3-BD pool, until equilibrium between the two forms was reached. Kinetic

parameters (V_{max} and K_m) for R/S-acetoin, *meso*-2,3-BD and (2*S*,3*S*)-BD were determined by specrophotometric assays. Our results show that *C. glutamicum* BDH is not absolutely specific for (*S*)-acetoin though this is by far the preferred substrate.

Introduction

2,3-Butanediol (2,3-BD) is an important chemical building block with multiple applications (Celińska and Grajek 2009). This C_4-diol is a product of the metabolism of bacteria, such as *Klebsiella pneumoniae, Klebsiella oxytoca, Enterobacter aerogenes, Enterobacter cloacae, Paenibacillus polymyxa, Serratia marcescens,* and *Lactococcus lactis* (Höhn-Bentz and Radler 1978, Chen et al. 2014, Park et al. 2013, Stormer 1975, Jung et al. 2012, Wang et al. 2012, Häßler et al. 2012, Zhang et al. 2010, Gaspar et al. 2011). The 2,3-BD biosynthetic pathway consists of three steps, with α-acetolactate and acetoin (or diacetyl), as intermediate metabolites (Fig. 4.1). In the first step, two pyruvate molecules are joined by the α-acetolactate synthase (ALS) into α-acetolactate, which is subsequently decarboxylated by the α-acetolactate decarboxylase (ALDC) to yield (*R*)-acetoin. In the presence of oxygen, α-acetolactate can undergo spontaneous decarboxylation to form diacetyl, which is reduced to (*R*)- or (*S*)-acetoin by diacetyl reductases. Acetoin is finally reduced to 2,3-BD by 2,3-butanediol dehydrogenase (BDH). Some BDHs, such as those of *Corynebacterium glutamicum* or *L. lactis*, recognize as substrates diacetyl

as well as acetoin, hence diacetyl can be reduced to acetoin via this activity (Crow 1990, Takusagawa et al. 2001).

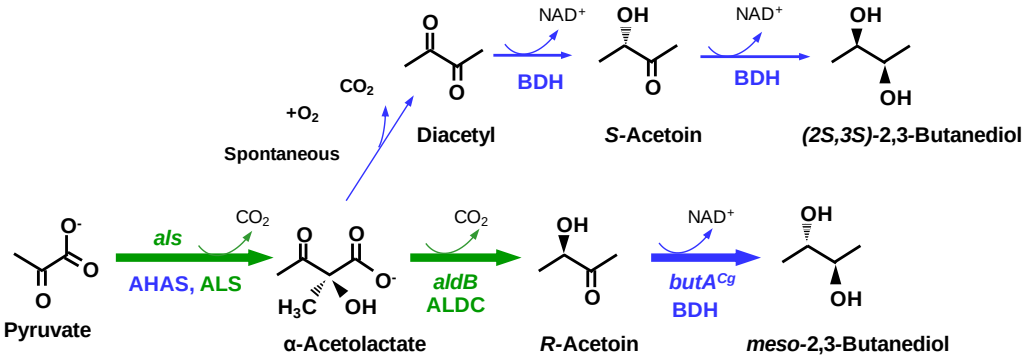

Figure 4.1. Scheme illustrating the pathways for the synthesis of 2,3-butanediol in bacteria. The strategy used in this work for engineering 2,3-BD synthesis in *C. glutamicum* is also depicted. Endogenous genes and enzymes are indicated in blue, while exogenous genes/enzymes are indicated in green. The first two genes of the 2,3-butanediol biosynthetic pathway were introduced from *L. lactis*; the third gene was *butA*^{Cg} encoding the endogenous butanediol dehydrogenase of *C. glutamicum*. Abbreviations: ALS, α-acetolactate synthase (encoded by *als*); ALDC, α-acetolactate decarboxylase (encoded by *aldB*); BDH, butanediol dehydrogenase (encoded by *butA*^{Cg}), AHAS, acetohydroxyacid synthase.

The acetoin molecule contains a single chiral carbon and can exist as (*R*)-acetoin or (*S*)-acetoin). The molecule of 2,3-BD possesses two chiral centers resulting in three stereoisomers: (*2R,3R*)-2,3-BD (or D-2,3-butanediol), (*2S,3S*)-2,3-BD (or L-2,3-butanediol), and the optically inactive (*2R,3S*)-2,3-BD also designated *meso*-2,3-BD (Fig. 4.2). In most cases, bacteria produce a mixture of 2,3-BD stereoisomers, which is generally ascribed to the presence of several BDHs with different stereospecific

properties or to a single enzyme that can recognize both stereoforms of acetoin (see Chen et al. 2014).

The stereochemical purity of 2,3-BD is not a primary concern if it is used as a bulk chemical; however, optically active forms are specially important reagents to provide chiral groups for synthesis of pharmaceuticals and other high value chemicals (Qi et al. 2014). In particular, (2*R*,3*R*)-butanediol is used as an antifreeze agent and solvent due to its low freezing point (Gao et al. 2013). Therefore, the production of pure stereoisomers of 2,3-BD is highly desirable for many applications; to this end, it is important to study the stereospecific properties of BDHs and the respective catalytic mechanisms (Ji et al. 2011). The number of fully characterized BDHs is very small, probably because of the high cost and limited availability of the pure enantiomers of acetoin. To our knowledge, the stereospecificity of BDH with respect to (*R*)- and (*S*)-acetoin has been studied only with the enzymes of *C. glutamicum*, *K. pneumonia* and *K. terrigena* (Takusagawa et al. 2001).

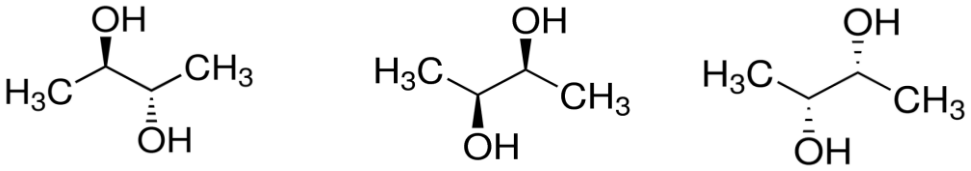

(2R,3S)-2,3-butanediol
meso-2,3-butanediol

(*2S,3S*)-2,3-butanediol

(*2R,3R*)-2,3-butanediol

Figure 4.2. Skeletal formulas of the three stereoforms of 2,3-butanediol: optically inactive *meso*-2,3-butanediol and the two enantiomeric forms: (*2S,3S*)-, and (*2R,3R*)-2,3-butanediol.

BDHs belong to the NAD(P)-dependent alcohol dehydrogenase family, generally divided into three large groups: i) Fe-dependent alcohol dehydrogenases, which belong to the smallest and the least studied group; ii) Zn-dependent alcohol dehydrogenases, also designated the medium-chain dehydrogenase/reductase (MDR) family; and iii) the short-chain dehydrogenase/reductase (SDR) family that includes metal-ion-independent enzymes.

The BDHs of *K. pneumoniae*, *S. marescens*, and *E. cloacae* belong to the SDR family; these enzymes introduce the new hydroxyl group in the (*S*)-configuration, thus reducing (*R*)-acetoin to *meso*-2,3-BD and (*S*)-acetoin to (*2S,3S*)-2,3-BD (Table 4.1). *C. glutamicum* (formerly *Brevibacterium saccharolyticum* C-1012), and *Rhodococcus erythropolis* possess BDHs that belong to the SDR family, with claimed absolute specificity for (*S*)-acetoin and (*2S,3S*)-2,3-BD (Z Wang et al. 2014, Takusagawa et al. 2001). On the other hand, the BDHs of *Bacillus subtilis*, *P. polymyxa* and *Saccharomyces cerevisiae* belong to the MDR family, and generally catalyze the introduction of a hydroxyl group in the (*R*)-configuration; they use (*R*)-acetoin and (*S*)-acetoin to produce (*2R,3R*)-2,3-BD and *meso*-2,3-BD, respectively (Table 4.1).

K. pneumoniae, which is considered a model organism for studying the mechanism of 2,3-BD stereoisomer formation, produces a high proportion of *meso*-2,3-BD and minor amounts of (*2S,3S*)-2,3-BD (Chen et al. 2014). The BDH enzyme is designated *meso*-BDH when the *meso*-form of 2,3-BD is preponderant. However, under certain conditions, such as growth on

glycerol, (*2R,3R*)-2,3-BD appears as end-product of *K. pneumoniae* fermentation: proportions of 90:9:1 (*meso*-2,3-BD : (*2R,3R*)-2,3-BD : (*2S,3S*)-2,3-BD) are typically found. Formation of the third stereoisomer is attributed to a secondary activity of glycerol dehydrogenase (Y. Wang et al. 2014). Enzyme promiscuity with regard to substrate utilization was also observed in *C. glutamicum* BDH, which besides reducing acetoin to 2,3-BD can also reduce dihydroxyacetone (DHA) to glycerol (Jojima et al. 2015).

Previously we engineered *C. glutamicum* to produce 2,3-BD by transforming it with the complete 2,3-BD-forming pathway from *L. lactis* (Chapter 3). As expected, under anaerobic conditions, the *meso*-form was the only stereoform of 2,3-BD that was detected. On the other hand, we were intrigued by the formation of *meso*-2,3-BD in a strain engineered to overexpress the endogenous *C. glutamicum* BDH along with ALS and ALDC from *L. lactis* (this work). This observation is difficult to explain, having in mind the stringent stereospecificity reported for *C. glutamicum* BDH (Takusagawa et al. 2001) and the information that (*R*)-acetoin is the sole product of *L. lactis* ALDC. Thus, we set out to investigate the origin of this paradox. The recombinant BDH of *C. glutamicum* was purified and assays were performed to determine the stereospecificity of the enzyme in relation to the substrates (*R*)-acetoin and (*S*)-acetoin. We showed that *C. glutamicum* BDH is not absolutely specific for (*S*)-acetoin, and uses (*R*)-acetoin at a rate approx. 20-fold lower than that of the preferred substrate.

Table 4.1. Stereospecificity properties of microbial 2,3-butanediol (2,3-BD) dehydrogenases.

Organism	BDH type (Family)	Substrate (oxidation)	Substrate (reduction)	Reference
K. pneumoniae XJ-Li	*meso*-2,3-BDH (SDR)	(*2S,3S*)-2,3-BD (4) *meso*-2,3-BD (100)	ND ND	Zhang et al. 2012
E. cloacae ssp. *dissolvens* strain SDM	*meso*-2,3-BDH (SDR)	(*2S,3S*)-2,3-BD (ND) *meso*-2,3-BD (ND)	(*S*)-acetoin (*R*)-acetoin	Carballo et al. 1991
S. marcescens H30	*meso*-2,3-BDH (SDR)	(*2S,3S*)-2,3-BD (11) *meso*-2,3-BD (100)	(*S*)-acetoin (*R*)-acetoin	Zhang et al. 2014
C. glutamicum	(*2S,3S*)-2,3-BDH (SDR)	(*2S,3S*)-2,3-BD (100)	(*S*)-acetoin	Takusagawa et al. 2001
R. erythropolis WZ010	(*2S,3S*)-2,3-BDH (SDR)	(*2S,3S*)-2,3-BD (100)	(*S*)-acetoin	Z Wang et al. 2014
R. erythropolis WZ010	(*2R,3R*)-2,3-BDH (MDR)	*meso*-2,3-BD* (ND) (*2R,3R*)-2,3-BD (ND)	(*S*)-acetoin (*R*)-acetoin	Yu et al. 2015
Mycobacterium tuberculosis	(*2R,3R*)-2,3-BDH (MDR)	(*2S,3S*)-2,3-BD (4) *meso*-2,3-BD (61) (*2R,3R*)-2,3-BD (100)	ND ND ND	Takeda et al. 2011
P. polymyxa ATCC12321	(*2R,3R*)-2,3-BDH (MDR)	*meso*-2,3-BD (72) (*2R,3R*)-2,3-BD(100)	(*S*)-acetoin (*R*)-acetoin	Yu et al. 2011
S. cerevisiae	(*2R,3R*)-2,3-BDH (MDR)	*meso*-2,3-BD (43) (*2R,3R*)-2,3-BD (100)	(*S*)-acetoin (*R*)-acetoin	González et al. 2000

Abbreviations: SDR, short-chain dehydrogenase/reductase; MDR, medium-chain dehydrogenase/reductase; ND, not determined; the relative activities of pure enzymes in the oxidation reaction are given in parenthesis.

Materials and Methods

Bacterial strains and growth conditions

Strains and plasmids used in this work are shown in Table 4.2. *C. glutamicum* cultures were grown aerobically in the 2×TY medium described by Sambrook and Green (Sambrook and Green 2012). Medium was supplemented either with 0.5% (wt/vol) potassium acetate or with 0.5% (wt/vol) potassium acetate plus 2% (wt/vol) glucose. Plasmid-harboring strains were selected using kanamycin (25 $\mu g \cdot mL^{-1}$); gene expression was induced by using 0.5 mM Isopropyl β-D-1-thiogalactopyranoside (IPTG). Cultivations were performed in shake flasks (50 mL of culture in 500 mL flasks), at 30°C with constant agitation at 160 rpm. Cultures were initiated by addition of a pre-culture to an optical density at 600 nm (OD_{600}) of about 0.3. Growth was monitored by measuring the OD_{600}. Specific growth rates (μ) were calculated through linear regression of the plots of $\ln(OD_{600})$ *versus* time during the exponential growth phase. For growth characterization, samples (1 mL) were taken periodically and analyzed by High Performance Liquid Chromatography (HPLC).

For the molecular biology procedures, *Escherichia coli* DH5α was grown in test tubes containing 5 mL of 2×TY medium at 37˚C and 180 rpm. Plasmid selection was achieved using 50 μg kanamycin$\cdot mL^{-1}$. For the protein production, *Escherichia coli* BL21(DE3) (200 mL) was grown in LB medium supplemented with 100 μg ampicillin$\cdot mL^{-1}$ at 37˚C and 180 rpm. Protein production was induced using 1 mM IPTG at an OD_{600} of 0.7; cells were collected 5 h after induction.

Construction of strains and plasmids

All primers used are listed in Table 4.3. Chromosomal DNA of *L. lactis* MG1363 or *C. glutamicum* ATCC13032, isolated according to Johansen and Kibenich 1992 and as described in Chapter 3, respectively, were used as templates in PCR amplifications. To obtain the expression vector of the 2,3-BD synthetic pathway, gene $butA^{Cg}$ (cg2958) was amplified from chromosomal DNA of *C. glutamicum* using primers RESTR-SOE7-FW and SOE7-RE and ligated to *L. lactis aldB* amplified by using aldB-FW and RESTR-SOE1-RE. Then, the *aldB*-$butA^{Cg}$ fragment was inserted in pEKEx2-*als* (Chapter 3), generating pEKEx2-*als,aldB,*$butA^{Cg}$ (Table 4.2). After confirmation of the correctness of the insert by sequencing (StabVida, Lisbon), plasmids were isolated from *E. coli* DH5α and electroporated into *C. glutamicum* strains using the procedure described in Liebl et al. 1989 and van der Rest et al. 1999.

To obtain the expression vector for recombinant protein production, gene $butA^{Cg}$ was amplified from the genomic DNA of *C. glutamicum* using primer pair butA-His-FW and butA-His-RE, and inserted into pET19b. Plasmid was obtained and maintained in *E. coli* BL21(DE3).

Table 4.2. Bacterial strains and plasmids used in this study.

Strain	Description	Reference
E. coli DH5α	Plasmid-free *E. coli* strain used for cloning purposes	Amersham Biosciences
E. coli BL21(DE3)	Plasmid-free *E. coli* strain used for protein expression	Stratagene
C. glutamicum ATCC13032	Wild-type strain	Kinoshita et al. 1958
E. coli pET19b-*butA*^{Cg}	*E. coli* BL21(DE3) carrying pET19b-*butA*^{Cg}	This work
C. glutamicum Δ*aceE*Δ*pqo*Δ*ldhA*	ATCC13032 with deletions of the genes encoding the E1 subunit of pyruvate dehydrogenase complex, the pyruvate:quinone oxidoreductase and the lactate dehydrogenase	Wieschalka et al. 2012
C. glutamicum Δ*aceE*Δ*pqo*Δ*ldhA*Δ*mdh*	ATCC13032 with deletions of the genes encoding the E1 subunit of pyruvate dehydrogenase complex, pyruvate:quinone oxidoreductase, lactate dehydrogenase and malate dehydrogenase	This work
C. glutamicum Δ*aceE*Δ*pqo*Δ*ldhA* (pEKEx2)	*C. glutamicum* Δ*aceE*Δ*pqo*Δ*ldhA* harboring plasmid pEKEx2	This work
C. glutamicum Δ*aceE*Δ*pqo*Δ*ldhA*Δ*mdh* (pEKEx2)	*C. glutamicum* Δ*aceE*Δ*pqo*Δ*ldhA*Δ*mdh* harboring plasmid pEKEx2	This work
C. glutamicum Δ*aceE*Δ*pqo*Δ*ldhA* (pEKEx2-*als,aldB,butA*^{Cg})	*C. glutamicum* Δ*aceE*Δ*pqo*Δ*ldhA* harboring plasmid pEKEx2-*als,aldB,butA*^{Cg}	This work
C. glutamicum Δ*aceE*Δ*pqo*Δ*ldhA*Δ*mdh* (pEKEx2-*als,aldB,butA*^{Cg})	*C. glutamicum* Δ*aceE*Δ*pqo*Δ*ldhA*Δ*mdh* harboring plasmid pEKEx2-*als,aldB,butA*^{Cg}	This work
Plasmid	**Description**	**Reference**
pET19b	amp^{R}, T7*lac*, N-terminal Histidine-tag with the enterokinase cutting site	Novagen
pET19b-*butA*^{Cg}	pET19b with cloned *butA*^{Cg}	This work
pEKEx2	kan^{R} from pUC4K; P_{trc}, *lacI*, pUC18 mcs, induced by addition of IPTG	Eikmanns et al. 1994
pEKEx2-*als*	pEKEx2 with cloned *als* from *L. lactis*	This work
pEKEx2- *als,aldB,butA*^{Cg}	pEKEx2-*als* with cloned *aldB (L. lactis)* and *butA* from *C. glutamicum*	This work

Abbreviations: *als*, α-acetolactate synthase gene; *aldB,* α-acetolactate decarboxylase gene; *butA*^{Cg}, butanediol dehydrogenase gene of *C. glutamicum*; kan^{R}, kanamycin resistance; amp^{R}, amplicillin resistance; P_{trc}, trc promoter; T7,

T7 RNA polymerase promoter sequence; *lac*, lac operator sequence; *lacI*, lac repressor gene.

Table 4.3. Primers used in this study

Primer name	5' - 3' sequence	Restriction site
butA-His-FW	GGAATTCCATATGATGAGCAAAGTTG	*Nde*I
butA-His-RE	CGCGGATCCCTAGTTGTAGAGC	*BamH*I
aldB-FW*	ACGCGTCGACTTTAAAAGGAGCCTCATATGTC AGAAATCACACAAC	*Sal*I
RESTR-SOE1-RE	CCCGCTCGAGTCATTCAGCTACATCAATATC	*Xho*I
RESTR-SOE7-FW	ATTCTCGAGTTTAAAAGGAGCCTCATATGAGC AAAGTTGCAATG	*Xho*I
SOE7-RE	CGGGGTACCCCGCTAGTTGTAGAGCATGCC	*Kpn*I

*see Table 3.2.

Preparation of cell suspensions

Cells grown as above were harvested 16 h after inoculation at OD_{600} of 16 – 20 for *C. glutamicum* Δ*aceE*Δ*pqo*Δ*ldhA* derived strains, and at OD_{600} of 13 – 15 for *C. glutamicum* Δ*aceE*Δ*pqo*Δ*ldhA*Δ*mdh* derived strains, centrifuged (9,924 × *g*, 10 min, 4°C), and washed once with an appropriate buffer (PIPES - piperazine-N,N′-bis(2-ethanesulfonic acid), 10 mM at pH 7.0). The resulting cell suspension was centrifuged (11,325 × *g*, 10 min, 4°C) and the pellet re-suspended in 50 mM PIPES buffer at pH 7.0.

Two-stage fermentations using 2,3-BD producing strains

C. glutamicum strains were grown and cell suspensions prepared as described above. The second fermentation step was initiated by placing 50 mL of concentrated cell suspension (OD_{600} of 30 - 40) in a 50 mL shake

flask or by placing 50 mL of cell suspension (OD_{600} of 15 - 20) into an 80-mL fermenter (mini-fermenter). Shake flasks were kept in a rotary shaker at 30°C and 160 rpm; temperature in the mini-fermenter was kept at 30°C using a water bath and stirring was done using a magnetic stirrer. The gas atmosphere in the mini-fermenter was established by sparging sterile air at a rate of 5, 10 or 15 $mL \cdot min^{-1}$. The cell suspension was provided with glucose to a final concentration of 2% (wt/vol) and samples were collected over a period of 72 h in the case of shake flask experiments, and after 53 h in the case of mini-fermenter experiments. Samples (1 mL) were centrifuged for 5 minutes at room temperature and 16,100 × *g*; supernatants were kept at -20°C until further analysis. Products of metabolism were quantified by using ^{1}H-NMR on a Bruker Avance400 (Bruker BioSpin GmbH).

Enzymatic activities in cell extracts

For the enzymatic assays, *C. glutamicum* strains were grown as described above and cell suspensions prepared in 50 mM PIPES at pH 7.0. Crude cell extracts were prepared by using glass beads (<106 µm) in a MiniBeadbeater-8 cell disrupter (Biospec Products) in 3 cycles of 1 min, with breaks of 3 min during which the extracts were kept on ice. After disruption, extracts were centrifuged at 16,100 × g for 20 min at 4°C. All enzyme activities were assayed at 30°C in a Beckman Coulter DU 800 spectrophotometer. One unit of enzyme activity is the amount of enzyme catalyzing the conversion of 1 µmol of substrate per minute under the experimental conditions used. The protein concentration was determined

using Pierce BCA Protein Assay Kit (Thermo Scientific). Specific activity was expressed as units (μmol · min^{-1}) per milligram of protein (U · mg of $protein^{-1}$). Acetolactate synthase activity was determined as described by Hugenholtz and Starrenburg (Hugenholtz and Starrenburg 1992). The reaction was stopped by the addition of 100 μl of 6N H_2SO_4, and acetoin was quantified colorimetrically at 525 nm as described by Westerfeld (Westerfeld 1945). Butanediol dehydrogenase was assayed as described by Stormer (Stormer 1975), in a modified reaction mixture containing 50 mM PIPES at pH 7.0, 0.2 mM NADH and 2.5 mM of racemic acetoin. The kinetics of oxidation of different forms of 2,3-BD was studied in 50 mM CAPS buffer (N-cyclohexyl-3-aminopropanesulfonic acid) at pH 10.5, using 5 mM 2,3-BD and 0.2 mM NAD^+.

Protein purification

Cells of *E. coli* pET19b*butA*^{Cg} grown as described above, were collected, centrifuged (9,924 × *g*, 10 min, 4°C), and washed once with an appropriate buffer (Tris-HCl, 2-amino-2-hydroxymethyl-propane-1,3-diol hydrochloride), 10 mM at pH 7.5. The resulting cell pellet was re-suspended in 2 mL of 50 mM Tris-HCl at pH 7.5; the cell suspension was passed through a French press 3 times (120 MPa), and centrifuged (12,857 × *g*, 20 min, 4°C). The supernatant was applied to 5 mL-HisTrap HP column (GE Healthcare Life Sciences) and eluted according to the instruction of the manufacturer. The most pure fraction (see Fig. 4.3), was dialysed against 50 mM PIPES pH 7.0 and concentrated using an Amicon concentrator. The purified protein was kept at 4°C.

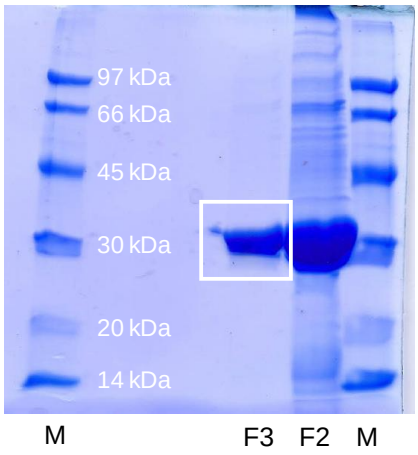

Figure 4.3. SDS-PAGE gel of different fractions eluted from the His-Trap column used for purification of recombinant *C. glutamicum* butanediol dehydrogenase. Fraction 3 (F3) was used for determination of kinetic parameters by spectrophotometric assays and for monitoring reaction kinetics by NMR. Abbreviations: M, marker; F2, fraction 2.

Kinetic parameters of the recombinant BDH

Kinetic parameters of the purified recombinant BDH were determined using *R/S*-acetoin (0.105, 0.206, 0.412, 0.618, 0,824, 1.648, 4.11, 8.22, 16.44 and 41.1 mM), *meso*-2,3-BD (0.491, 0.982, 2.455, 4.91, 7.37, 9.82, and 19.64 mM), and (*2S,3S*)-2,3-BD (0.030, 0.054, 0.109, 0.217, 0.435, 0.870, 2.174, 4.348, 6.522, 8.696 mM) as substrates. Acetoin reduction reactions were performed in the presence of 0.2 mM NADH in buffer PIPES (50 mM at pH 7.0), and the oxidation of each form of 2,3-BD was followed in the presence of 0.2 mM NAD^+ in 50 mM CAPS buffer at pH 10.5. The kinetics of NADH reduction or NAD^+ was determined from absorbance measurements at 340 nm. The K_i, K_m and V_{max} values were calculated by a

computer-aided direct fit to the Michaelis-Menten equation. All reactions followed Michaelis-Menten-type kinetics.

Kinetics of *R*/*S*-acetoin reduction monitored by NMR spectroscopy

The time courses for acetoin reduction, NADH oxidation, and production of 2,3-BD were followed online by ^{1}H-NMR. The reaction was studied using either excess or limitation of NADH with respect to racemic acetoin. Reaction mixtures contained either 21 mM *R/S*-acetoin and 9 mM NADH or 9 mM *R/S*-acetoin and 21 mM NADH in 40 mM PIPES at pH 7.0. Two µL of NaN_3 (4%, wt/vol) were added to the mixture to prevent microbial contamination. A lock signal was provided by addition of 60 µL of D_2O. The total volume was 550 µL. The reaction was started by addition of 1.5 µg of pure recombinant *C. glutamicum* BDH at time zero, and carried out at 30°C.

The time courses for substrate utilization and product build-up were studied by sequential acquisition of ^{1}H-NMR spectra on a Bruker AVANCE II+ 500 MHz spectrometer (Bruker BioSpin GmbH), using a QXI-Z H C/N/P-D (5 mm) probe head. Acquisition parameters: flip angle of 60º; 32K acquisition data points; repetition delay of 1.5 s, number of scans, 4. Pre-saturation of the residual water signal was applied. For quantification, 10 µL of 50 mM DSS was used as internal standard. Fully relaxed spectra were acquired (flip angle of 60º; 32K acquisition data points; repetition delay of 60 s, number of scans, 4), to determine correction factors that were applied to the areas measured in non-relaxed spectra.

NMR quantification of fermentation products in non-growing cells

^{1}H-NMR spectra were acquired on a Bruker AVANCE II+ 400 MHz spectrometer at 27ºC, using a BBO-F probe head. Pre-saturation of the residual water signal was applied. Acquisition parameters: flip angle of 90º; 32K acquisition data points; repetition delay of 61.5 s. Formate was used as an internal concentration standard.

Quantification of products during growth by HPLC

End-products of metabolism in growing cultures were quantified by HPLC using an apparatus equipped with a refractive index detector (Shodex RI-101, Showa Denko K. K., Japan) and an HPX-87H anion exchange column (Bio-Rad Laboratories Inc., California, USA) at 60ºC, with 5 mM H_2SO_4 as the elution fluid and a flow rate of 0.5 mL·min^{-1}.

Chemicals and reagents

For molecular biology purposes, RNAse A and Pwo polymerase were purchased from Roche Life Science; lysozyme (Fluka) was purchased from Sigma-Aldrich, while all other enzymes were from New England Biolabs. Acetoin (≥98%), *meso*-2,3-BD (99%) and (*2S,3S*)-2,3-BD (97%, 99% optical purity) used in enzymatic assays were purchased from Sigma-Aldrich. All other chemicals were commercially available reagent-grade (Sigma-Aldrich or Merck Sharp & Dohme).

Results

Functional analysis of engineered activities

Artificial operon comprising three genes encoding the 2,3-BD biosynthetic pathway (*als*, *aldB*, and $butA^{Cg}$) was assembled in the pEKEx2 expression vector and transformed into the two selected background strains, *C. glutamicum* Δ*aceE*Δ*pqo*Δ*ldhA* and Δ*aceE*Δ*pqo*Δ*ldhA*Δ*mdh* (Table 4.2). To evaluate whether the target enzymes were functionally produced, specific activities were determined in cell extracts (Table 4.4). Induced expression of *als* and *aldB* genes in *C. glutamicum* Δ*aceE*Δ*pqo*Δ*ldhA*(pEKEx2-*als,aldB,butA*^{Cg}) led to 45-fold increase in ALS/ALDC activity when compared to control *C. glutamicum* Δ*aceE*Δ*pqo*Δ*ldhA*(pEKEx2), while the increase was 20-fold for Δ*aceE*Δ*pqo*Δ*ldhA*Δ*mdh*(pEKEx2-*als,aldB,butA*^{Cg}) compared to Δ*aceE*Δ*pqo*Δ*ldhA*Δ*mdh*(pEKEx2). ALS/ALDC activity in crude extracts of the two engineered strains reached values of 1.2 - 1.4 U·(mg of protein)$^{-1}$. BDH activity doubled in strain Δ*aceE*Δ*pqo*Δ*ldhA*(pEKEx2-*als,aldB,butA*^{Cg}) and increased 7-fold in Δ*aceE*Δ*pqo*Δ*ldhA*Δ*mdh*(pEKEx2-*als,aldB,butA*^{Cg}) compared to their respective controls.

Table 4.4. Overexpression and specific activities of enzymes for the synthesis of 2,3-butanediol as determined in crude cell extracts. Cells were grown for 14 h in 2×TY medium supplemented with acetate and glucose. BDH activity was measured with *R*/*S*-acetoin as substrate. Values are averages ± SD of at least three independent experiments and two technical replicates.

Strain	**ALS-ALDC activity** U · mg of protein^{-1}	**BDH activity** U · mg of protein^{-1}	**ALS/ALDC over-expression** (fold)	**BDH over-expression** (fold)
Δ*aceE*Δ*pqo*Δ*ldhA* (pEKEx2)	0.03 ± 0.01	0.30 ± 0.03	-	-
Δ*aceE*Δ*pqo*Δ*ldhA* (pEKEx2-*als,aldB,butA*^{Cg})	1.35 ± 0.05	0.81 ± 0.08	45	2
Δ*aceE*Δ*pqo*Δ*ldhA*Δ*mdh* (pEKEx2)	0.06 ± 0.02	0.19 ± 0.01	-	-
Δ*aceE*Δ*pqo*Δ*ldhA*Δ*mdh* (pEKEx2-*als,aldB,butA*^{Cg})	1.17 ± 0.18	1.36 ± 0.05	20	7

Growth characterization

The two host strains *C. glutamicum* Δ*aceE*Δ*pqo*Δ*ldhA* and *C. glutamicum* Δ*aceE*Δ*pqo*Δ*ldhA*Δ*mdh* require acetate for growth, since all the pathways for acetate formation from glucose have been abolished. When grown on 2% (wt/vol) glucose plus 0.5% (wt/vol) acetate, both strains showed a growth profile different from wild-type *C. glutamicum,* in accordance with previous reports (Eikmanns and Blombach 2014). The deletion strains used primarily acetate for growth, while glucose was consumed mainly once acetate was exhausted; moreover, the OD_{600} did not change significantly after acetate depletion, indicating that glucose was converted preferentially into products other than biomass (Fig. 4.4). Growth parameters, such as specific growth rate (μ) and maximal OD (OD_{max}) are presented in Table 4.5. All cultures grew relatively fast with μ values of about 0.5 h^{-1}, with the growth rate of the producer strains being slightly lower than that of the control strains. OD_{max} values showed very small variation, being slightly higher in the producer strains as compared to control strains (OD_{600} of about 26 – 28 for the producer strains and 22 – 23 for the control strains).

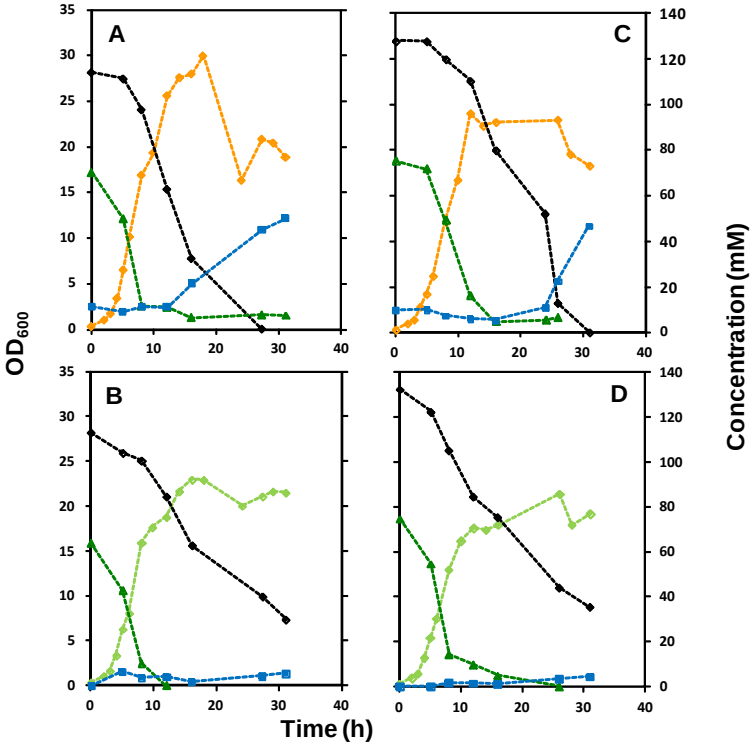

Figure 4.4. Growth curves, substrate consumption and acetoin production by the 2,3-BD producers and control strains, grown in 2×TY medium for 31 h at 160 rpm and 30 °C. The Δ*aceE* strains were unable to grow on glucose as sole carbon source, thus they were grown on a mixture of acetate (0.5% wt/vol) and glucose (2% wt/vol). Panels refer to strains derived from either *C. glutamicum* Δ*aceE*Δ*pqo*Δ*ldhA* (A and B) or *C. glutamicum* Δ*aceE*Δ*pqo*Δ*ldhA*Δ*mdh* (C and D). Legend: ♦, control strains; ♦, strains with pEKEx2-*als,aldB,butA*^{Cg}; ■, acetoin; ▲, acetate; ♦, glucose.

Growing cultures of control strains accumulated mostly pyruvate and dihydroxyacetone (DHA) (data not shown), while acetoin was a minor product (~5 mM) (Table 4.5). The two producer strains accumulated about 50 mM acetoin and trace amounts of 2,3-BD. The control strains

consumed all acetate after 31 h, but about 33 mM glucose remained in the culture; the producer strains consumed all glucose, but ~5 mM acetate remained in the culture supernatants.

Table 4.5. Growth parameters of producer strains, as compared to the control strains, and acetoin, glucose and acetate concentrations in supernatant solutions collected 31 h after the inoculation. Values shown are means ± SD of at least three independent experiments.

Strain	**Specific growth rate μ** (h^{-1})	**OD_{max}**	**Acetoin** (mM)	**Residual glucose** (mM)
Δ*aceE*Δ*pqo*Δ*ldhA* (pEKEx2)	0.57 ± 0.02	23.0 ± 0.0	5.2 ± 0.1	32.5 ± 3.2
Δ*aceE*Δ*pqo*Δ*ldhA* (pEKEx2-*als,aldB,butA*^{Cg})	0.51 ± 0.12	28.8 ± 2.0	52.2 ± 5.5	0.0
Δ*aceE*Δ*pqo*Δ*ldhA*Δ*mdh* (pEKEx2)	0.54 ± 0.04	22.1 ± 0.5	4.8 ± 0.3	33.9 ± 4.0
Δ*aceE*Δ*pqo*Δ*ldhA*Δ*mdh* (pEKEx2-*als,aldB,butA*^{Cg})	0.48 ± 0.02	26.0 ± 1.7	45.2 ± 4.4	0.0

Characterization of 2,3-BD production under oxygen-limiting conditions

C. glutamicum was grown in the presence of oxygen, while the production of 2,3-BD is expected to be maximal under oxygen limiting conditions. Having this in mind, we have employed a two-stage fermentation strategy for the production of 2,3-BD in which aerobically grown cells are collected, washed, re-suspended in appropriate buffer and used under oxygen deprivation conditions in the subsequent production step. The results of the

two-stage fermentations with *C. glutamicum* Δ*aceE*Δ*pqo*Δ*ldhA*(pEKEx2-*als,aldB,butA*^{Cg}), Δ*aceE*Δ*pqo*Δ*ldhA*Δ*mdh*(pEKEx2-*als,aldB,butA*^{Cg}) and their respective control strains, are shown in the Tables 4.6 and 4.7.

When the second fermentation stage was performed in shake flasks, the two control strains *C. glutamicum* Δ*aceE*Δ*pqo*Δ*ldhA*(pEKEx2) and Δ*aceE*Δ*pqo*Δ*ldhA*Δ*mdh*(pEKEx2) consumed glucose at a slow rate (1.8 ± 0.1 and 1.4 ± 0.0 nmol·min^{-1}·mg CDW^{-1}); 20 - 28 % of glucose was used for the synthesis of 2,3-BD, which was produced in the optically active form (Fig. 4.5C). Introduction of 2,3-BD biosynthetic pathway increased GCR in both producer strains to 4.2 nmol·min^{-1}·mg CDW^{-1}, and more importantly, *meso*-2,3-BD was the main form produced in shake flask fermentations (Fig. 4.5B), with a yield of 0.62 ± 0.04 and 0.70 ± 0.02 mol per mol glucose for Δ*aceE*Δ*pqo*Δ*ldhA*(pEKEx2-*als,aldB,butA*^{Cg}) and Δ*aceE*Δ*pqo*Δ*ldhA*Δ*mdh*(pEKEx2-*als,aldB,butA*^{Cg}), respectively. Optically active 2,3-BD was below the detection limit (0.1 mM). Glycerol was by far the major side product in both strains (25 ± 9 mM and 20 ± 6 mM for Δ*aceE*Δ*pqo*Δ*ldhA*(pEKEx2-*als,aldB,butA*^{Cg}) and Δ*aceE*Δ*pqo*Δ*ldhA*Δ*mdh*(pEKEx2-*als,aldB,butA*^{Cg}), respectively), followed by acetoin (17 ± 6 mM and 4 ± 3 mM for Δ*aceE*Δ*pqo*Δ*ldhA*(pEKEx2-*als,aldB,butA*^{Cg}) and Δ*aceE*Δ*pqo*Δ*ldhA*Δ*mdh*(pEKEx2-*als,aldB,butA*^{Cg}), respectively).

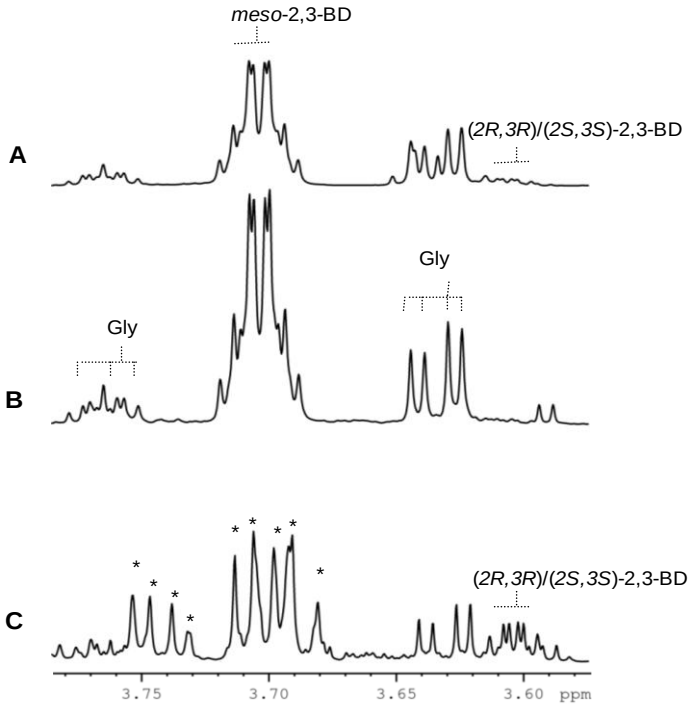

Figure 4.5. ^{1}H-NMR spectra of fermentation products of *C. glutamicum* Δ*aceE*Δ*pqo*Δ*ldhA*(pEKEx2-*als,aldB,butA*^{Cg}) under aeration of 10 mL·min^{-1} (**A**), in shake flasks (**B**), or the control strain *C. glutamicum* Δ*aceE*Δ*pqo*Δ*ldhA*(pEKEx2) in shake flasks (**C**). Legend: *meso*-2,3-BD, *meso*-2,3-butanediol; (*2S,3S*)/(*2R,3R*)-2,3-BD, optically active 2,3-butanediol; Gly, glycerol. Resonances of residual glucose are labeled with an asterisk.

Performing the production step in the mini-fermenter, with the strain Δ*aceE*Δ*pqo*Δ*ldhA*(pEKEx2-*als,aldB,butA*^{Cg}) under controlled aeration (sparging air at 5, 10 or 15 mL·min^{-1}), led to increased GCR and decreased yield of 2,3-BD. The optimal performance was achieved under an air flow rate of 10 mL·min^{-1} (GCR of 11.6 ± 0.6 nmol·min^{-1}·mg CDW^{-1} and yield of 0.52 ± 0.01 mol 2,3-BD per mol glucose).

The major form of 2,3-BD was *meso*-2,3-BD, and the ratio *meso*-2,3-BD : optically active 2,3-BD was 95:5 (Fig. 4.5A). The main side-products were glycerol (28 ± 9 mM), ethanol (11 ± 6 mM) and acetoin (7 ± 3 mM). Further attempts to optimize production parameters by manipulating growth conditions (growing cells only in acetate) did not influence the 2,3-BD production significantly (Tables 4.6 and 4.7).

Table 4.6. Glucose consumption rate and molar yield of 2,3-BD achieved in the second stage of fermentation under oxygen limited conditions by the control and producer *C. glutamicum* strains. Unless otherwise stated, cells were grown on a mixture of 2% (wt/vol) glucose and 0.5% (wt/vol) potassium acetate and the second stage was performed in glass shake flasks for 72 h or in the mini-fermenter for 53 h.

Strain	**Air** (mL·min^{-1})	**GCR** (nmol·min^{-1}· mg CDW^{-1})	**Yield** (mol 2,3-BD per mol Glc)	**Productivity** (nmol·min^{-1}· mg CDW^{-1})	**CR** (%)
Δ*aceE*Δ*pqo*Δ*ldhA* (pEKEx2)	NA	1.8 ± 0.1	0.20 ± 0.05	0.24 ± 0.03	78 ± 2
Δ*aceE*Δ*pqo*Δ*ldhA* (pEKEx2-*als,aldB,butA*^{Cg})	NA	4.2 ± 0.3	0.62 ± 0.04	0.93 ± 0.06	96 ± 10
Δ*aceE*Δ*pqo*Δ*ldhA* (pEKEx2-*als,aldB,butA*^{Cg})	5	6.2 ± 0.3	0.46 ± 0.03	3.46 ± 0.64	80 ± 5
Δ*aceE*Δ*pqo*Δ*ldhA* (pEKEx2-*als,aldB,butA*^{Cg})	10	11.6 ± 0.4	0.52 ± 0.01	6.07 ± 1.20	83 ± 5
Δ*aceE*Δ*pqo*Δ*ldhA* (pEKEx2-*als,aldB,butA*^{Cg})	15	10.4 ± 1.9	0.39 ± 0.3	3.81 ± 0.76	77 ± 8
Δ*aceE*Δ*pqo*Δ*ldhA* (pEKEx2-*als,aldB,butA*^{Cg})*	NA	3.8 ± 0.8	0.68 ± 0.07	2.41 ± 0.21	85 ± 4
Δ*aceE*Δ*pqo*Δ*ldhA* (pEKEx2-*als,aldB,butA*^{Cg})*	10	11.2 ± 3.2	0.58 ± 0.16	5.8 ± 0.8	73 ± 5
Δ*aceE*Δ*pqo*Δ*ldhA*Δ*mdh* (pEKEx2)	NA	1.4 ± 0.0	0.28 ± 0.07	0.34 ± 0.08	100 ± 4
Δ*aceE*Δ*pqo*Δ*ldhA*Δ*mdh* (pEKEx2-*als,aldB,butA*^{Cg})	NA	4.2 ± 0.2	0.70 ± 0.02	1.13 ± 0.04	94 ± 5

Abbreviations: GCR, glucose consumption rate; Glc, glucose; 2,3-BD, 2,3-butanediol; CR, carbon recovery; NA, not applicable, designates experiments performed in shake flasks. * Strain was grown on 0.5% (wt/vol) potassium acetate and no glucose. For experimental details see Materials and Methods. The values are averages of three independent experiments.

Table 4.7. End-products of glucose metabolism and residual glucose in fermentations of control and producer strains incubated under oxygen limiting conditions. All concentrations are mM. *Strain grown on 0.5% (wt/vol) potassium acetate and no glucose; **metabolite detected in a single experiment. NA, not applicable, indicates experiments performed in shake flasks**.** Abbreviations: 2,3-BD, 2,3-butanediol; Acn, acetoin; DA, diacetyl; Succ, succinate; Ac, acetate; Pyr, pyruvate; α-KIV, α-ketoisovalerate; DHA, dihydroxyacetone; Gly, glycerol; Isobut, isobutanol; α-KG, α-ketoglutarate; Ala, L-alanine.

Strain	Air	Glc	2,3-BD	Acn	DA	Succ	Ac	Pyr	α-KIV	DHA	Gly	Isobut	Eth	α-KG	Ala
Δ*aceE*Δ*pqo*Δ*ldhA* (pEKEx2)	NA	42±8	17±2	7.6±0.4	13.2**	5±2	0.0	6±4	11±6	1.0±0.3	2.7**	0.0	0.0	0.0	1±1
Δ*aceE*Δ*pqo*Δ*ldhA* (pEKEx2-*als,aldB,butA*^{Cg})	NA	0.0	67±4	17±6	0.0	2±1	0.0	0.0	0.0	3±3	25±9	4±2	0.0	0.0	1.4±0.2
Δ*aceE*Δ*pqo*Δ*ldhA* (pEKEx2-*als,aldB,butA*^{Cg})	5	27±14	40±6	3.1±0.7	2±1	0.8±0.3	2±1	1±1	0.0	4±1	18±5	1.8±0.2	5±3	2±1	0.0
Δ*aceE*Δ*pqo*Δ*ldhA* (pEKEx2-*als,aldB,butA*^{Cg})	10	0.0	65±14	7±3	1.4±0.3	0.6±0.3	0.4±0.4	0.0	0.0	9±2	28±9	1.5±0.4	11±6	4±1	0.0
Δ*aceE*Δ*pqo*Δ*ldhA* (pEKEx2-*als,aldB,butA*^{Cg})	15	0.7±0.0	43±14	25±8	4±1	8.8±0.4	0.2±0.2	1.7±0.3	0.0	6±2	6±5	1.5±0.6	2.5±2.2	3±2	0.0
Δ*aceE*Δ*pqo*Δ*ldhA* (pEKEx2-*als,aldB,butA*^{Cg})*	NA	0.0	75±1	8±7	0.6±0.1	2.7±0.4	0.0	0.3±0.0	0.0	2.0±0.5	8±5	0.5±0.1	0.0	0.0	1.3±0.6
Δ*aceE*Δ*pqo*Δ*ldhA* (pEKEx2-*als,aldB,butA*^{Cg})*	10	0.0	62±11	1.0±0.2	0.0	7.6±0.5	0.2±0.1	1.1±0.6	0.9±0.1	1.2±1.1	12±1	4±2	0.0	0.0	1.8±0.6
Δ*aceE*Δ*pqo*Δ*ldhA* Δ*mdh* (pEKEx2)	NA	45±2	24±6	22±2	12.0**	8±6	0.0	1±1	9.1**	5±6	0.0	0.0	0.0	0.0	2.1±0.1
Δ*aceE*Δ*pqo*Δ*ldhA* Δ*mdh* (pEKEx2-*als,aldB,butA*^{Cg})	NA	0.0	83±2	4±3	0.7±0.2	3±2	0.0	0.7**	0.0	0.0	20±6	2.7±0.5	0.0	0.0	1.4±0.2

Stereospecificity of the recombinant BDH of *C. glutamicum*

Interestingly, *meso*-2,3-BD was the major form produced in fermentations using a producer that over-expressed ALS/ALDC of *L. lactis*, and BDH of *C. glutamicum.* Decarboxylation of α-acetolactate yields (*R*)-acetoin, thus the production of *meso*-2,3-BD indicates that the BDH of *C. glutamicum* can use (*R*)-acetoin in contrast with earlier studies reporting absolute stereospecificity for (*S*)-acetoin (Marlow et al. 2013, Takusagawa 2001). Therefore, we decided to produce the recombinant BDH and clarify this inconsistency. The pure enantiomers of acetoin are not available commercially, but this drawback was overcome by using NMR that can distinguish between *meso*-2,3-BD and optically active 2,3-BD (Fig. 4.5 and 4.6). *meso*-2,3-BD is necessarily formed from (*R*)-acetoin, because the *C. glutamicum* BDH belongs to the SDR family, introducing the hydroxyl-group to yield an *S*-stereocenter (Table 4.1). Moreover, the utilization of (*S*)-acetoin by this BDH will produce optically active (*2S,3S*)-2,3-BD. In this way, NMR provides indirect information on the utilization of individual enantiomers of acetoin present in the racemic mixture provided as substrate. In other words, it is able to “separate” the enantiomers in the racemic mixture.

The time courses for product formation are especially informative in assays using an excess of NADH, i.e., 21 mM NADH : 9 mM *R/S*-acetoin (Fig. 4.7). The trace for acetoin utilization showed two phases: an initial rapid consumption (77.4 ± 4.0 μmol·min^{-1}·mg protein^{-1}) matched the rate of optically active 2,3-BD formation (70.2 ± 15.2 μmol·min^{-1}·mg protein^{-1}). The

formation of *meso*-2,3-BD proceeded at a rate about 20-fold lower (maximal value of 3.7 ± 0.5 μmol·min^{-1}·mg protein^{-1}). Significantly, the level of optically active 2,3-BD leveled-off at the time half of the initial amount of acetoin was consumed. The production of *meso*-2,3-BD continued slowly until acetoin was exhausted and the two forms of 2,3-BD reached equal concentrations.

In the experiments with deficit of NADH versus acetoin, i.e., 9 mM NADH: 21 mM *R/S*-acetoin (Fig. 4.8), initially acetoin was consumed rapidly at a maximal rate of 92.7 ± 6.2 μmol·min^{-1}·mg protein^{-1}, and optically active 2,3-BD was produced at a comparable rate (74.2 ± 0.6 μmol·min^{-1}·mg protein^{-1}). After about 10 minutes of reaction, *meso*-2,3-BD was detected and increased slowly (maximal rate 2.5 ± 0.2 μmol·min^{-1}·mg protein^{-1}). Interestingly, after depletion of the reducing agent, NADH, the build-up of *meso*-2,3-BD was concomitant with an equivalent decrease in optically active 2,3-BD, this trend proceeding until the two stereoforms reached approximately equal concentrations. The incubation was prolonged up to 7 days. At equilibrium, the molar ratio, optically active 2,3-BD: *meso*-2,3-BD was 1.25 ± 0.3.

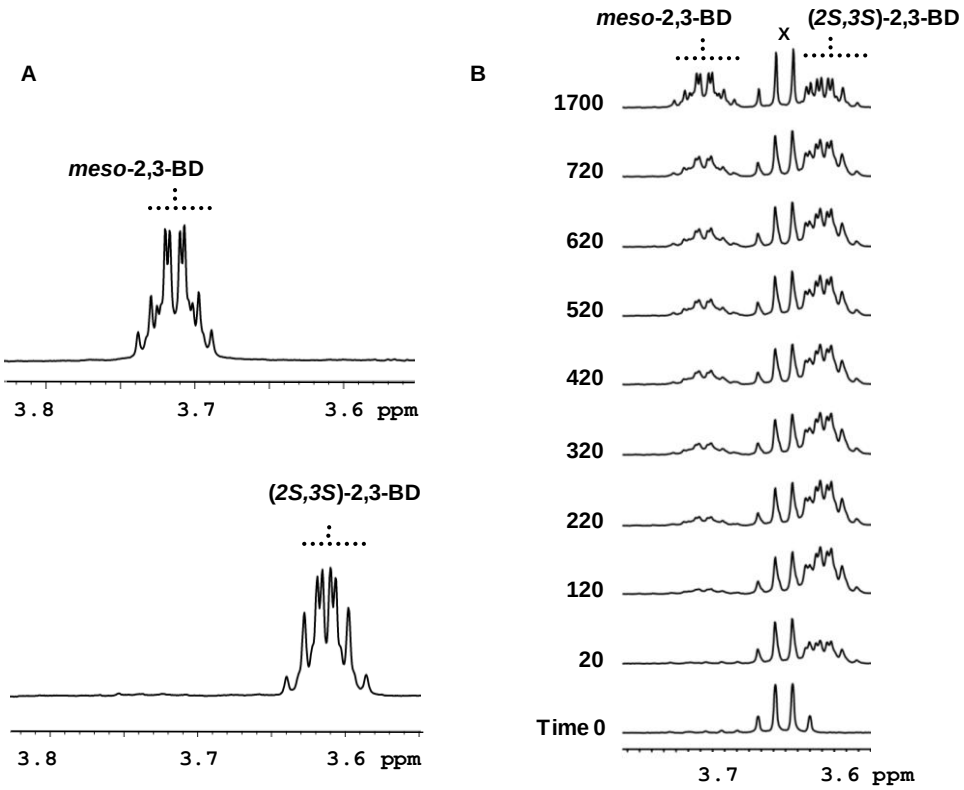

Figure 4.6. Sections of ^{1}H-NMR spectra of 2,3-butanediol forms, *meso*-2,3-BD and (*2S,3S*)-2,3-BD: pure compounds used as standards (**A**); and produced from R/S-acetoin by the purified recombinant butanediol dehydrogenase of *C. glutamicum* at 30°C (**B**). The mixture contained 9 mM NADH and 21 mM racemic acetoin in 40 mM PIPES buffer, pH 7.0. The reaction was started at time zero by addition of 1.5 µg of pure protein. Legend: X, methylene group of ethanol, a contaminant of commercial NADH.

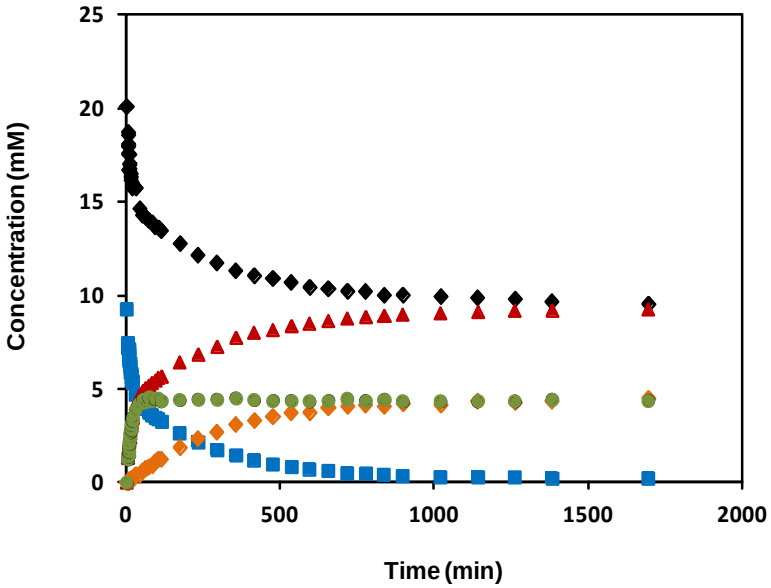

Figure 4.7. Time course of *R/S*-acetoin consumption, NADH consumption, and 2,3-butanediol formation by the butanediol dehydrogenase of *C. glutamicum*. Reaction mixture consisting of 9 mM acetoin and 21 mM NADH in 40 mM PIPES buffer (pH 7.0), was incubated with recombinant butanediol dehydrogenase at 30°C. The reaction kinetics was followed in real time by ^{1}H-NMR. Symbols: ■, acetoin; ▲, total 2,3-butanediol, ♦, NADH; ●, optically active 2,3-butanediol; ♦, *meso*-2,3-butanediol. This is a representative data set from at least three replicates.

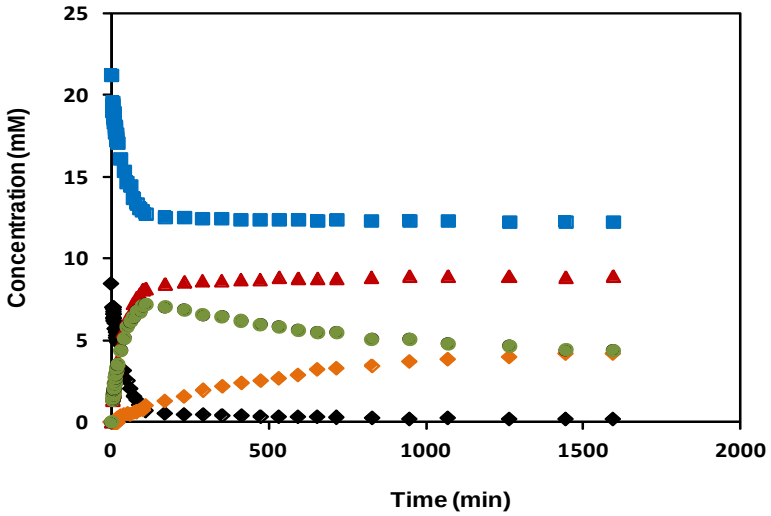

Figure 4.8. Time course of *R/S*-acetoin and NADH consumption, and 2,3-butanediol formation by butanediol dehydrogenase of *C. glutamicum*. The reaction mixture, consisting of 21 mM acetoin and 9 mM NADH in 40 mM PIPES buffer (pH 7.0), was incubated with recombinant butanediol dehydrogenase at 30°C. The reaction kinetics was followed in real time by ^{1}H-NMR. Symbols: ■, acetoin; ▲, total 2,3-butanediol, ♦, NADH; ●, optically active (2*S*,3*S*)-2,3-butanediol. This is a representative data set from three replicates.

Table 4.8. Kinetic properties of *C. glutamicum* butanediol dehydrogenase determined by NMR. Values are averages ± SD of three independent experiments.

Substrate or product	**Reaction rate (w/ excess NADH** (μmol·min^{-1} ·mg protein^{-1})	**Reaction rate (w/ limited NADH)** (μmol·min^{-1} ·mg protein^{-1})
S-Acetoin	77.4 ± 4.0	92.7 ± 6.2
(2*S*,3*S*)-2,3-BD	70.2 ± 15.2	74.2 ± 0.6
R-Acetoin	3.7 ± 0.5	2.5 ± 0.2

Kinetic parameters of the recombinant BDH of *C. glutamicum*: spectrophotometric assays

To determine the kinetic parameters V_{max} and K_m for the substrates commercially available, the oxidation (or reduction) of NADH was monitored spectrophotometrically (Table 4.9). Under the experimental conditions used in this work (50 mM PIPES buffer at pH 7.0 and 30°C), K_m for *R/S*-acetoin was 0.10 ± 0.03 mM, and V_{max} was 112 ± 15 μmol·min^{-1} ·mg protein^{-1}. Interestingly, a slight inhibition of the enzyme by acetoin was observed, for which an inhibition constant of 11.0 ± 0.4 mM was calculated. The K_m values for (2*S*,3*S*)-2,3-BD and *meso*-2,3-BD determined in 50 mM CAPS buffer at pH 10.5, were 0.052 ± 0.005 mM and 2.01 ± 0.40 mM, respectively, while the respective V_{max} values were 22 ± 1 and 4.1 ± 0.3 μmol·min^{-1}·mg protein^{-1}.

Table 4.9. Kinetic properties of *C. glutamicum* butanediol dehydrogenase determined by spectrophotometry. Values are averages ± SD of at least three independent experiments. See Materials and Methods for experimental conditions.

Substrate	V_{max} (μmol·min^{-1} ·mg protein^{-1})	K_m (mM)	k_{cat}/K_m (mM^{-1}·s^{-1})	K_i (mM)
(*S*)-Acetoin**	112 ± 15	0.10 ± 0.03	ND	11.0 ± 0.4
(2*S*,3*S*)-2,3-BD	22 ± 1	0.052 ± 0.005	187.5	ND
meso-2,3-BD	4.1 ± 0.3	2.01 ± 0.40	0.9	ND
(*S*)-Acetoin*	ND	0.44	ND	ND

*from (Takusagawa et al. 2001); ND, not determined; **, Racemic acetoin was provided but (*S*)-acetoin is the major isomer utilized in this time scale.

As the recombinant *C. glutamicum* BDH carries an N-terminal histidine tag with 10 residues and this could affect in some way the structure and stereoselectivity properties of the protein, we decided to compare the stereoselectivity of the purified enzyme with that of the BDH activity overproduced in the 2,3-BD-producer strain (Table 4.10). The results show that the enzyme prefers by far (*2S,3S*)-2,3-BD and the pattern is not significantly affected by heterologous expression of the His-tagged protein in *E. coli*.

Table 4.10. Stereoselective oxidation of the three stereoisomers of 2,3-BD by *C. glutamicum* BDH. Activity measurements were carried out with preparations of the purified recombinant protein and also with crude cell extracts of the 2,3-BD producer and control strains. Relative activities appear in parentheses. Assays were performed at 30°C and pH 10.5, in CAPS buffer (50 mM) containing 0.2 mM NAD^+ and 5 mM 2,3-BD. All experiments were performed three times.

	Substrate	**Activity** (U·mg protein^{-1})
C. glutamicum Δ*aceE*Δ*pqo*Δ*ldhA*Δ*mdh*	(*2S,3S*)-2,3-BD (100)	0.233 ± 0.019
	(*2R,3R*)-2,3-BD (3)	0.008 ± 0.002
	meso-2,3-BD (1)	0.003 ± 0.000
C. glutamicum Δ*aceE*Δ*pqo*Δ*ldhA*Δ*mdh* (pEKEx2-*als,aldB,butA*^{Cg})	(*2S,3S*)-2,3-BD (100)	0.452 ± 0.017
	(*2R,3R*)-2,3-BD (3)	0.012 ± 0.002
	meso-2,3-BD (1)	0.005 ± 0.001
Purified *C. glutamicum* BDH	(*2S,3S*)-2,3-BD (100)	74.3 ± 17.2
	(*2R,3R*)-2,3-BD (1.6)	1.154 ± 0.007
	meso-2,3-BD (0.4)	0.279 ± 0.036

Discussion

In an early study Takusagawa et al (2001) over-produced the BDH of *C. glutamicum* in *E. coli* and characterized the kinetic parameters of the enzyme with different substrate stereoisomers, both for the oxidation and the reduction reactions (Takusagawa et al. 2001). The authors found no significant activity with (*R*)-acetoin, (2*R*,3*R*)-BD or meso-2,3-BD, but the enzyme catalyzed the reduction of (*S*)-acetoin as well as the oxidation of (2*S*,3*S*)-BD. The absolute stereoselectivity of BDH for (*S*)-acetoin was put in doubt by recent results with *C. glutamicum* hosts engineered for the production of 2,3-BD (this work, and Yang et al. 2015). These authors showed that the best production was obtained with a strain overproducing ALS/ALDC from *K. pneumoniae*, but without an exogenous BDH. Therefore, the endogenous BDH of *C. glutamicum* must be responsible for the reduction of enzymatically produced (*R*)-acetoin.

In our work, the endogenous BDH was overproduced along with ALS and ALDC of *L. lactis*. Under limited oxygen conditions (shake flaks), this engineered strain produced 2,3-BD in the *meso*-form, which was necessarily derived from (*R*)-acetoin. On the other hand, optically active 2,3-BD, certainly (*2S,3S*)-2,3-BD, was the sole stereoform detected in the fermentation products of the control strain. Indeed, as *C. glutamicum* lacks ALDC activity, the synthesis of 2,3-BD in the control strain should proceed via spontaneous decarboxylation of α-acetolactate; the resulting product, diacetyl, is reduced to (*S*)-acetoin by *C. glutamicum* BDH, as this SDR enzyme typically introduces a stereocenter in the *S*-configuration.

Likewise, subsequent reduction of (*S*)-acetoin yields (*2S,3S*)-2,3-BD (Fig. 4.1). This description also agrees with the observed production of (*2S,3S*)-2,3-BD from diacetyl in *E. coli* engineered to express *C. glutamicum* BDH (Ui et al. 2004).

In summary, work from us and others shows that *C. glutamicum* BDH uses (*R*)-acetoin to some extent *in vivo*. This has been fully corroborated by our *in vitro* studies with the recombinant enzyme. The assays monitored by online NMR clearly showed that (*R*)-acetoin was used, though at an apparent rate approx. 20 times lower than (*S*)-acetoin (Table 4.8). As for the reverse catalysis (oxidation), the specificity constant (k_{cat}/K_m) for meso-2,3-BD is about two-orders of magnitude lower than for (*2S,3S*)-2,3-BD, but still clearly measurable (Table 4.9). Even so, these values should be regarded with caution since the pH used for the assay, 10.5, is far from the physiological range. More reliable parameters will be obtained directly with (*R*)-acetoin, when this compound becomes available (on-demand synthesis, Enamine, Ukraine).

The discrepancy between our results and those of Takusagawa et al (2001), with the recombinant *C. glutamicum* BDH, is difficult to explain. We used a His-tagged protein, while they used an untagged protein; one could argue that the presence of the His-tag might affect the enzyme stereospecificity. This was proven untrue, by comparing the BDH activity in cell extracts of the engineered strain and in preparations of the pure enzyme (Table 4.10). So, perhaps those authors overlooked the low activities obtained with (*R*)-acetoin, *meso*-2,3-BD and (*2R,3R*)-2,3-BD.

Still, this minor activity towards (*R*)-acetoin is responsible for a reasonable 2,3-BD productivity of *C. glutamicum* Δ*aceE*Δ*pqo*Δ*ldhA*(pEKEx2-*als,aldB,butA*^{Cg}) when compared with that of the strain optimally engineered with the full biosynthetic pathway from *L. lactis*, (Δ*aceE*Δ*pqo*Δ*ldhA*(pEKEx2-*als,aldB,*$_{Ptuf}$*butA*), which contains a BDH specific for (*R*)-acetoin (Gaspar et al. 2011, also see Chapter 3). The 2,3-BD productivity values for these strains, at an aeration rate of 10 mL·min^{-1}, are 5.8 ± 0.8 (Table 4.6) and 8.1 ± 0.4 nmol·min^{-1}·mg CDW^{-1} (Table 3.6, Chapter 3). Moreover, the corresponding GCR values are also surprisingly similar, i.e., 11.2 ± 3.2 nmol·min^{-1}· mg CDW^{-1} and 15.8 ± 1.7 nmol·min^{-1}·mg CDW^{-1}. Furthermore, strain Δ*aceE*Δ*pqo*Δ*ldhA* (pEKEx2-*als,aldB,butA*^{Cg}) has a BDH activity of about 40 nmol·min^{-1}·mg protein^{-1} with respect to (*R*)-acetoin (one twentieth of the total activity, Tables 4.4 and 4.10), which is much lower than 0.53 ± 0.17 µmol·min^{-1}·mg protein^{-1} present in strain Δ*aceE*Δ*pqo*Δ*ldhA*(pEKEx2-*als,aldB,*$_{Ptuf}$*butA*) (see Table 3.3, chapter 3), yet GCR and productivity are not substantially different. This indicates that the metabolic bottleneck for 2,3-BD production does not reside at the level of *C. glutamicum* BDH, despite its relatively low activity for the less preferred substrate, (*R*)-acetoin). In conclusion, the main handicap of the producer strains is the low GCR, and the underlying reason is unrelated with the level of BDH activity.

A mixture of 2,3-BD-forms is produced by many natural producers (Chen et al. 2014, Haßler et al. 2011, Qi et al. 2014). Before the genomic era this was ascribed to the existence of acetoin racemase (Voloch et al. 1983).

However, it is now generally accepted that this multi-form production is due to the presence of more than one BDH activity. This multiplicity of BDHs has been shown for *B. subtilis*, *Bacillus licheniformis*, *L. lactis*, *R. erythropolis*, and several other bacteria (Zhang et al. 2013, Qi et al. 2014, Crow 1990, Z Wang et al. 2014, Yu et al. 2015). Several homologs of Zn-dependent alcohol dehydrogenase are predicted in the genome of *C. glutamicum*, thus it is surprising that the BDH activity with (2*R,*3*R*)-2,3-BD was very low in crude cell extracts of producer and control strains (2-3% of the activity with (2*S,*3*S*)-2,3-BD). Moreover, this result is comparable to what was found with the purified BDH of *C. glutamicum* (Table 4.10). Therefore, it seems that the *butA*-encoded enzyme is the only BDH expressed under these conditions. It is also interesting to note that the activity for (*2R,3R*)-2,3-BD is higher than for *meso*-2,3-BD, so it will be pertinent to determine the kinetic parameters of the enzyme for (*2R,3R*)-2,3-BD. Definite proof about the presence or other BDHs implies the construction and characterization of a *butA*-deletion (cg2958) mutant.

Acknowledgements and work contributions

Technical assistance by Sara Rebelo is gratefully acknowledged. We thank Dr. Paula Gaspar for providing DNA templates for amplification of *L. lactis* genes.

DR was involved in designing the study, all stages of experimental work and writing the manuscript. BB provided the deletion strains. NB was involved in protein production and purification. HS, DLT, TC, BJE, BB and ARN contributed to study design, supervision and manuscript preparation.

CHAPTER 5

General discussion

Contents

Anaerobic succinate production in *Corynebacterium glutamicum*

Confronted with the exhaustion of petroleum resources and the negative environmental impact associated with the use of fossil fuels, fermentative production of bulk chemicals from renewable biomass is becoming an appealing alternative to traditional petrochemical processes. More specifically, the bio-based production of succinate and 2,3-butanediol (2,3-BD), have received substantial attention lately, as they are good examples of how science and technology cooperate to overcome the limitations of microbial production and move towards an industrial setting.

In this work, we describe our contribution to metabolic engineering of the industrial bacterium *C. glutamicum* for the production of the two bulk chemicals, succinate and 2,3-BD. The first part of the work focuses on the characterization of anaerobic succinate production by the wild-type organism.

C. glutamicum is well known for the industrial production of amino acids under aerobic conditions, hence this aspect of metabolism has been extensively studied using various approaches. In particular, the metabolic fluxes of L-lysine and L-glutamate producer strains were characterized in detail (Vallino and Sephanopulos 1993, Kiefer et al. 2004, Uy et al. 2004, Wittman and Heinzle 2001, Marx et al. 1997, Shirai et al. 2007, Dominguez et al. 1998). In contrast, at the beginning of this thesis work, knowledge on the fluxes operating under anaerobic conditions was very limited, thus we

deemed it important to take a systems biology approach and study anaerobic glucose metabolism in this bacterium.

Our first attempt involved the use of *in vivo* ^{13}C-NMR, which is a powerful technique for measurements of intracellular metabolites. The non-invasive character of this methodology is highly advantageous, but the intrinsic low sensitivity of the NMR technique restricts the range of applications (Neves et al. 1999, Neves et al. 2002a, Carvalho et al. 2013). In cell suspensions of *C. glutamicum* we were able to detect and quantify fructose 1,6-bisphosphate (FBP), glycogen (data not shown), and succinic and lactic acids (Fig. 2.5). The low intracellular pools of other metabolites precluded their detection *in vivo*. On the other hand, the experimental set-up developed in our lab for *in vivo* NMR requires the establishment of a defined gas atmosphere, and this requisite led us to discover a prominent increase in succinate production upon changing the gas atmosphere from argon to CO_2 (Fig. 2.2).

Lactate and dihydroxyacetone (DHA) were the two major end-products of glucose metabolism when CO_2 was not supplied. While lactate is a common product of *C. glutamicum* anaerobic metabolism (Inui et al. 2004, Dominguez et al. 1993), the accumulation of DHA is rarely reported. It was observed in a lysine-producing strain, and the authors speculated the existence of a glycolytic bottleneck at the level of glyceraldehyde 3-phosphate dehydrogenase (GAPDH), an enzyme inhibited by a high NADH/NAD^+ ratio (Dominguez et al. 1998, Kiefer et al. 2004). In our hands, under high CO_2 conditions and production of a reduced compound

such as succinate, DHA was abolished, most probably due to a decreased NADH/NAD^+ ratio.

Upon switching the atmosphere to pure CO_2, succinate yield increased to almost 1 mol per mol glucose, with lactate and acetate as major side-products (Table 2.2). As succinate production yields net 1 mol NAD^+ per mol succinate, the main focus of engineering strategies has been to increase NADH availability. Eliminating lactate production is a common first step to redirect carbon and electrons towards succinate (Okino et al. 2008, Litsanov et al. 2012a). To satisfy the redox balance, carbon is theoretically distributed between succinate (-2 NADH) and acetate production (+4 NADH per mol glucose) in a ratio succinate:acetate of 2:1. Further reduction of acetate, a source of ATP and NADH, may impair anaerobic growth, as observed in *E. coli* (Stols and Donnelly 1997, Vemuri et al. 2002). More importantly, other sources of NADH to support succinate production have to be found. Litsanov et al. (2012) observed that, once acetate and lactate production were abolished, the maximal yield of succinate was 1 mol per mol glucose, meaning that succinate formation was constrained by insufficient reducing power (Litsanov et al. 2012a). In the same study, the authors tested formate oxidation as a source of CO_2 and electrons for succinate production in a *C. glutamicum* strain engineered with formate dehydrogenase; the anaerobic metabolism of glucose in the presence of formate and bicarbonate yielded 1.67 mol succinate per mol glucose (Litsanov et al. 2012a).

The model for anaerobic metabolism developed in this thesis showed that the flux via the Pentose Phosphate Pathway was low (~5% of the total glycolytic flux), in the presence or absence of CO_2. Similarly, a low PPP flux was found under succinate producing conditions in *Actinobacillus succinogenes* (1 - 4%) and *Basfia succiniciproducens* (7 - 8%) (McKinlay et al. 2007, McKinlay and Vielle 2008, Becker et al. 2013). Interestingly, in *Escherichia coli* AFP111, the fraction of carbon going through PPP changed from 4 to 17% when the atmosphere was switched from 3% to 50% CO_2, and succinate production increased accordingly. This *E. coli* strain responded to an increase in NADH consumption with an increase in NADPH production, since it has a transhydrogenase activity, which enables interconversion of these two reduced co-factors (Lu et al. 2009). *C. glutamicum* is known to respond to high NADPH demand by increasing the flux via PPP, but does not possess a functional transhydrogenase (Marx et al. 1999, Bartek et al. 2011, Blombach et al. 2011, Kabus et al. 2007). However, the existence of a transhydrogenase-like cycle, consisting of pyruvate carboxylase and/or PEP carboxylase, malate dehydrogenase, and malic enzyme, has been described. This cycle was proposed to be responsible for at least part of the NADPH supply in the isobutanol producing *C. glutamicum* strain (Blombach et al. 2011).

There were attempts to increase the PPP flux in a succinate producer strain by overproducing the first two enzymes of the PPP, which are insensitive to feedback inhibition by their reaction products, however this had only a slight positive effect on the GCR and succinate yield (Wiechalka

2012). PPP is a relevant source of reducing power, but due to the absence of transydrogenase and consequent lack of efficient interconversion between NADH and NADPH, employing this pathway to generate the reducing equivalents needed for anaerobic succinate production did not meet expectations.

By analyzing the ^{13}C-label in succinate derived from [2-^{13}C]glucose metabolism, we concluded that succinate production occurred mainly *via* PEP/Pyr carboxylation and the reductive tricarboxylic acid (TCA) cycle, with a small contribution of the oxidative branch, which was responsible for provision of NADH necessary for closing the redox balance. Similarly low activity of the oxidative TCA branch was observed in *B. succiniciproducens* (Becker et al. 2013). In our metabolic model, we assume that the flux through the glyoxylate shunt is negligible since the activity of isocitrate lyase is absent in *C. glutamicum* during anaerobic glucose metabolism (Inui et al. 2004), and because succinate is an effective inhibitor of isocitrate lyase (K_i of 1.48 mM) (Reinscheid et al. 1994a). Accordingly, Zhu et al. (2013) constructed a *C. glutamicum* strain with overexpression of the genes involved in the glyoxylate shunt, but this strategy alone turned out unsatisfactory as the yield was essentially unchanged (Zhu et al. 2014). Also, overproduction of isocitrate lyase and malate synthase has a minor positive effect in aerobic succinate production (Litsanov et al. 2012b).

In *E. coli,* strain AFP111, the flux via the glyoxylate shunt contributes about 6 – 8 % for succinate production (Lu et al. 2009), but in strain SBS990MG (pHL413), optimal succinate yields (1.6 – 1.7 mol per mol glucose) were

obtained when about one third of oxaloacetate was directed to the glyoxylate shunt (Sánchez et al. 2006). In fact, it is important to consider the glyoxylate shunt since it uses less NADH than the reductive branch of TCA for succinate formation (Hong et al. 2003). A combination of the glyoxylate shunt and the reductive TCA requires 1.25 mol NADH, compared to 2 mol NADH per mol succinate when only the reductive TCA branch is used. Moreover, the maximal succinate yield achievable in the absence of external electron donors (1.65 mol per mol glucose) is only possible with the contribution of the glyoxylate shunt (Hong et al. 2003). Top succinate producers, yeast and *E. coli*, use the glyoxylate shunt in combination with the reductive TCA branch (Sánchez et al. 2006, van den Tweel 2010).

Possible engineering of the glyoxylate shunt for succinate production in *C. glutamicum* should consider the following information: i) in glucose grown cells, transcription of the isocitrate lyase and malate synthase genes is repressed (Gertsmeir et al. 2004); and ii) isocitrate lyase activity is inhibited by several metabolites (3-phosphoglycerate, 6-phosphogluconate, PEP, fructose-1,6-bisphosphate, succinate, and glyoxylate, with K_i values between 0.5 and 1.5 mM) (Reinscheid et al. 1994a). Perhaps over-producing an isocitrate lyase with more suitable properties could be a useful strategy to take advantage of the glyoxylate shunt.

The experiments with [1-^{13}C]glucose and [U-^{13}C]glucose showed that back-flux from oxaloacetate/malate to PEP/Pyr was insignificant under 100% CO_2 atmosphere. This was unexpected knowing that the

PEP/Pyr/oxaloacetate node shows great flexibility in *C. glutamicum*, at least in the presence of oxygen (Bartek et al. 2011, Wendisch et al. 2000). However, having this reaction practically unidirectional was beneficial for succinate production. Pyruvate and PEP carboxylase overproduction enhanced the succinate yield (Okino et al. 2008a, Litsanov et al. 2012a, Sánchez et al. 2006). According to Lu et al. (2009) the activity of the carboxylating enzymes limits CO_2 utilization at high CO_2 concentrations, and this could explain the beneficial effect of overexpressing pyruvate and PEP carboxylase genes (Okino et al. 2008a, Litsanov et al. 2012a, Litsanov et al. 2012b, Sánchez et al. 2006).

In conclusion, our efforts to study succinate production resulted in high succinate yields in the wild-type strain without genetic manipulation. This strain produced 1 mol succinate per mol glucose, which is significant even when compared with the highest yield obtained thus far (1.7 mol per mol glucose). The model of anaerobic glucose metabolism provided useful hints for strain development. Forcing flux via PPP or glyoxylate shunt could be useful approaches to further improve the succinate yield.

Engineering 2,3-butanediol production in *C. glutamicum*

We transformed *C. glutamicum* into a cell factory for the production of 2,3-BD. Herein, we compare our engineering strategies and strain performance with those of other microbial producers; special attention was directed to the stereochemistry of 2,3-BD formation.

Because under oxygen limiting conditions *C. glutamicum* produces organic acids (lactic, acetic and succinic), host strains with minimized accumulation of these organic acids were selected. Actually, elimination of reduced side-products is a common strategy employed to create efficient 2,3-BD producers. A few examples: lactate elimination in *Klebsiella pneumoniae* and *Enterobacter aerogenes*; lactate, acetate and ethanol elimination in *Klebsiella oxytoca*; acetate, glycerol, and ethanol elimination in *S. cerevisiae* (Kim et al. 2014, Jung et al. 2012, Lian et al. 2014, Ng et al. 2012, Jantama et al. 2015). Our strategy was successful, as the best producer strain under optimized conditions accumulated only traces of acetate (0.1 mM), and succinate and lactate were below this level (Table S3.2). In particular, elimination of acetate had a crucial impact on the yield of 2,3-BD (Fig 3.7).

Acetate formation by the 2,3-BD producer strains is curious, as all known acetate-forming pathways were inactivated (Tables S3.2 and 4.7). The results of ^{13}C-tracer experiments using a similar strain showed that acetate was derived from glucose (Appendix I). A possible candidate for acetate synthesis is the α-ketoglutarate dehydrogenase complex, whose catalytic subunit shows a low activity with pyruvate (Hoffelder et al. 2010).

C. glutamicum host strains were transformed with the 2,3-BD biosynthetic pathway from *L. lactis* that consists of three genes: *als,* encoding α-acetolactate synthase (ALS); *aldB,* encoding α-acetolactate decarboxylase; and *butA,* encoding butanediol dehydrogenase (BDH). Typical ALS/ALDC

activities in crude cell extracts were 0.5 U·mg protein^{-1} (about 0.25 U·mg CDW^{-1}) and, for BDH, 1 U·mg protein^{-1} (about 0.5 U·mg CDW^{-1}). These values are one order of magnitude higher than the productivity of 2,3-BD (0.011 µmol·min^{-1}·mg CDW^{-1}, Table 3.3), hence these activities should be sufficient to support the cellular fluxes. And indeed, in the best producer strain, 98% of pyruvate was directed towards the 2,3-BD pathway and transformed into acetoin and 2,3-BD (Table S3.2). We conclude that the activity of ALS and ALDC were not limiting for the 2,3-BD production.

Most of the carbon that was not processed to pyruvate (24% of the total glucose provided), was converted into DHA and glycerol (Table S3.2). DHA accumulation was also observed in L-lysine producer, suggesting that DHA elimination could be a goal common to metabolic engineering strategies of *C. glutamicum* (Kiefer et al. 2004). Dihydroxyacetone phosphate phosphatase and BDH, responsible for DHA and glycerol formation, respectively, are apparent engineering targets (Jojima et al. 2012). Another useful strategy to prevent loss of carbon in the over-flow metabolites from glycolysis was applied in the anaerobic L-alanine production; it consisted of over-producing the glycolytic enzymes, GAPDH, pyruvate kinase, phosphofructokinase and glucose-6-phosphate isomerase. This strategy led to a decreased concentration of metabolites upstream of GAPDH and a 5-fold increase in the GCR. Therefore, this could also be a useful strategy to further improve productivity of 2,3-BD in *C. glutamicum* (Yamamoto et al. 2012).

Despite high BDH activity in crude cell extracts, the accumulation of acetoin was observed in all 2,3-BD producer strains, both with BDH of *L. lactis* and of *C. glutamicum* (Tables S3.2 and 4.7). Acetoin accumulation was higher in strains with the overproduction of endogenous BDH, probably reflecting the lower preference for (*R*)-acetoin of the enzyme. As expected, the acetoin accumulation increased with oxygen availability.
The strain with overproduction of the endogenous BDH accumulated much higher levels of glycerol than the strain with the lactococcal enzyme. BDH of *C. glutamicum*, active in all strains, can use DHA and produce glycerol, although with a very low affinity (Jojima et al. 2015). If the same enzyme is involved in both reactions, then concomitant accumulation of acetoin and glycerol are contradictory and difficult to explain. It is likely that under our experimental conditions the endogenous BDH is not the only enzyme responsible for glycerol formation. On the other hand, the slow reaction rate of (*R*)-acetoin reduction by BDH of *C. glutamicum*, and consequent slow NADH oxidation, could lead to inhibition of GAPDH, accumulation of DHA and glycerol.

Under strict anaerobic conditions, the theoretical yield is 0.67 mol 2,3-BD per mol glucose. Addition of oxygen as an electron acceptor increases the theoretical yield to one mol of 2,3-BD per one mol of glucose (0.5 g per g). In our experiments, the most important step towards increasing productivity was the optimization of oxygen availability. This confirmed that excess NADH influenced negatively the GCR and the productivity. Under optimal

air supply (10 mL·min^{-1}), the productivity increased over two-fold (10.9 nmol·min^{-1}·mg CDW^{-1}, Fig. 3.7) compared to the fermentation in shake flasks (4.3 nmol·min^{-1}·mg CDW^{-1}). Elimination of DHA and glycerol, as well as the fine tuning of oxygen supply should help to further increase the yield of 2,3-BD.

The introduction of an NADH oxidase, as done in PDHC-negative 2,3-BD producing yeast, could be considered (Kim et al. 2015). However, as NADH oxidase has very high affinity for NADH (K_m of 25 µM in *L. lactis*), compared with BDH (K_m of 100 µM), it would be difficult to optimize 2,3-BD production. This strategy has proven very useful when acetoin is the desired end-product (Neves et al. 2002b, Sun et al. 2012, Ji et al. 2013, Bao et al. 2014).

Thus far, the best producers of 2,3-BD are pathogenic organisms, such as *K. pneumoniae*, *K. oxytoca*, *E. aerogenes* and *Serratia marcescens* (Table 5.1). Typical productivities are in the range 1 – 4 g·L^{-1}·h^{-1}, and titers of 100 – 150 g·L^{-1}, reaching almost theoretical yields of 2,3-BD from glucose. However, the potential pathogenicity of these organisms is still a major obstacle for large-scale production. One of the best non-pathogenic alternatives is *Paenibacillus polymyxa* (2 g·L^{-1}·h^{-1} and 72 g·L^{-1}), however this bacterium produces exopolysaccharides, which drains carbon and increases the viscosity of the fermentation broth; only upon temperature increase was the formation of exopolysaccharides decreased, but not completely (Häßler et al. 2012). Significant progress was made towards developing production processes for *Bacillus amyloliquefaciens* and

Bacillus licheniformis, which form 2,3-BD at a specific productivity of 1 – 2 $g \cdot L^{-1} \cdot h^{-1}$ and titer of 74 – 100 $g \cdot L^{-1}$, reaching almost theoretical yields (T Yang et al. 2015, Li et al. 2014).

The two common industrial hosts, *E. coli* and *S. cerevisiae*, fall behind the natural producers in terms of production parameters; however, advance was achieved over the years, especially through engineering *E. coli*, which produces up to 74 $g \cdot L^{-1}$ with a productivity of 1.2 $g \cdot L^{-1} \cdot h^{-1}$ and a yield that is 82% of the theoretical one. Yeast, on the other hand, produces 100 $g \cdot L^{-1}$ in about 300 h of fermentation, with a yield of 0.35 $g \cdot g^{-1}$, which is in the range of productivities and yields of the best *C. glutamicum* producer, *C. glutamicum* Δ*aceE*Δ*pqo*Δ*ldhA*Δ*mdh*(pEKEx2-*als,aldB,*$_{Ptuf}$*butA*), that formed 2,3-BD with a yield of 0.33 $g \cdot g^{-1}$ and a productivity of 0.21 $g \cdot L^{-1} \cdot h^{-1}$ (this work). The GCR reached by this strain (21 $nmol \cdot min^{-1} \cdot mg\ CDW^{-1}$, corresponding to 1.3 $mmol \cdot h^{-1} \cdot g\ CDW^{-1}$) is good, when compared to a similar strain that produced isobutanol under oxygen-limiting conditions (1.1 $mmol \cdot h^{-1} \cdot g\ CDW^{-1}$) and twice lower than that of the succinate producer (2.6 $mmol \cdot h^{-1} \cdot g\ CDW^{-1}$) developed in the lab of Michael Bott (Blombach et al. 2011, Litsanov et al. 2012).

Our strains were grown on acetate due to auxotrophy caused by the pyruvate dehydrogenase complex (PDHC) inactivation. Growth on glucose is known to increase the level of glycolytic enzymes in *C. glutamicum* (Muffler et al. 2002). Instead of full inactivation of PDHC it would be useful to manipulate this activity to levels that would allow for growth on glucose,

as this strategy showed beneficial impact on the production of L-lysine, L-valine, α-ketoisovalerate by *C. glutamicum* (Buchholz et al. 2013). Glucose also supports growth to higher optical densities, which is desirable to reach enhanced volumetric productivity.

Interestingly, under growth conditions, strains that over-expressed endogenous BDH produced up to 52 mM acetoin from glucose, which is about 4.6 $g \cdot L^{-1}$ in 31 h (0.23 $g \cdot g^{-1}$) (Table 4.5). This is a reasonable yield of acetoin if we take into account that optimization was not carried out. Therefore, *C. glutamicum* appears like a promising platform for production of this food additive because of its GRAS status. Omission of the *butA* gene in the 2,3-BD biosynthetic operon and disruption of endogenous BDH are expected to yield efficient acetoin producers. So far, *B. subtilis* is the most studied producer of acetoin, reaching yields of 0.36 $g \cdot g^{-1}$ and a titer of 54 $g \cdot L^{-1}$ in 144 h (Zhang et al. 2013).

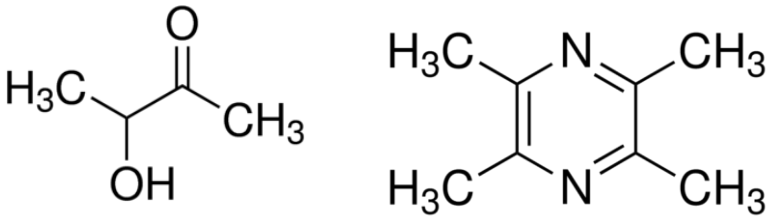

Acetoin Tetramethylpyrazine

Fig 5.1. Acetoin and tetramethylpyrazine molecules.

Another potential application of the strains constructed in this work is the production of tetramethylpyrazine (TMP), a derivative of acetoin (Fig. 5.1). Thus far, two reports mentioned TMP production in *C. glutamicum*: i)

traces of TMP were detected in the fermentation headspace of wild-type strain; and ii) considerable amounts of TMP were produced by a mutant strain that accumulated α-acetolactate; upon cooling, TMP formed crystals in the fermentation broth (Dickschat et al. 2010, Demain et al. 1967). TMP is a biologically active alkaloid that has a potent effect on neurovascularization and is prescribed as a complementary treatment for glaucoma (N Yu et al. 2014, Gong et al. 2014). The mechanism of TMP synthesis is not fully understood, but spontaneous formation from acetoin and ammonium salts has been proposed. Cultures of *B. subtilis* produce up to 7.5 $g \cdot L^{-1}$ TMP (Huang et al. 1996, Zhu et al. 2010).

Table 5.1. Summary of the best 2,3-butanediol (2,3-BD) producers.

Strain	2,3-BD isomer	Substrate	Method	Yield ($g \cdot g^{-1}$)	Productivity ($g \cdot L^{-1} \cdot h^{-1}$)	Titer ($g \cdot L^{-1}$)	Ref
Klebsiella pneumoniae	*Meso*-2,3-BD; (*2S, 3S*)-2,3-BD	Glucose	Fed-batch	0.43	4.21	150	Ma et al. 2009
Klebsiella oxytoca	*Meso*-2,3-BD; (*2S, 3S*)-2,3-BD	Glucose	Fed-batch	0.49	1.20	117.4	Jantama et al. 2015
Enterobacter aerogenes	*Meso*-2,3-BD; (*2S, 3S*)-2,3-BD	Sugarcane molasses	Fed-batch	0.37	2.74	98.7	Jung et al. 2013
Serratia marescens	*Meso*-2,3-BD	Sucrose	Fed-batch	0.41	2.67	152	Zhang et al. 2010
Paenibacillus polymyxa	(*2R,3R*)-2,3-BD	Glucose + yeast extract	Batch	Not specified	2.0	72.0	Häßler et al. 2012
Bacillus subtilis	(*2R,3R*)-2,3-BD	Glucose	Batch	0.47	0.22	49.3	Fu et al. 2014
Bacillus licheniformis	(*2R,3R*)-2,3-BD; *meso*-2,3-BD	Corn stover hydrolysate	Fed-batch	0.47	2.10	74.0	Li et al. 2014
Bacillus amyloliquefaciens	(*2R,3R*)-2,3-BD; *meso*-2,3-BD	Glycerol	Fed-batch	0.44	1.16	102.3	Yang et al. 2014
Escherichia coli	(*2R,3R*)-2,3-BD; (*2S, 3S*)-2,3-BD; *meso*-2,3-BD	Glucose	Fed-batch	0.41	1.19	73.8	Xu et al. 2014
Saccharmyces cerevisiae	(*2R,3R*)-2,3-BD	Glucose+ galactose	Fed-batch	0.35	0.29	100	Lian et al. 2014
C. glutamicum	Not specified	Glucose	Batch, growth coupled	0.24*	0.24	18.9	Yang et al. 2015
C. glutamicum	*Meso*-2,3-BD; optically active (*2S, 3S*)-2,3-BD	Glucose	Batch, growth decoupled	0.33	0.21	6.3	This work

* Calculated from data reported in (Yang et al. 2015).

Stereochemistry of 2,3-butanediol biosynthesis

Most microorganisms produce mixtures of 2,3-BD isomers with variable proportions. This is a consequence of i) existence of BDHs with different stereochemical properties; and/or ii) existence of more than one BDH in a particular organism. As for some applications it is essential to have the enantiopure 2,3-BD, the stereochemical properties of BDHs should be investigated (Gao et al. 2013, Qi et al. 2014, Ji et al. 2011). Available data on BDHs are summarized in Table 4.1; in addition, the nature of the 2,3-BD stereoforms found as fermentation products is shown in Table 5.2.

The focus of this part of our work was to study the stereochemical properties of *C. glutamicum* BDH. Takusagawa et al. (2001) characterized the kinetic parameters of this enzyme and showed that it catalyzed the reduction of (*S*)-acetoin as well as the oxidation of (2*S*,3*S*)-BD and had no significant activity with (*R*)-acetoin, (2*R*,3*R*)-BD or meso-2,3-BD (Takusagawa et al. 2001). However, when this BDH was overproduced in *C. glutamicum* together with ALS and ALDC of *L. lactis*, *meso*-2,3-BD was observed as a major end-product of glucose metabolism under limited oxygen conditions (this work). As this SDR enzyme typically introduces a chiral center in the *S*-configuration, the *meso*-form detected was necessarily derived from (*R*)-acetoin. While our work was in progress, an article appeared in the literature reporting 2,3-BD production by *C. glutamicum* using ALS and ALDC from *K. pneumoniae*, but without a heterologous BDH (Yang et al. 2015). Therefore, an endogenous BDH of *C. glutamicum* must be responsible for the reduction of enzymatically

produced (*R*)-acetoin. It is important to point out that known ALDC enzymes specifically decarboxylate α-acetolacteate into (*R*)-acetoin (Marlow et al. 2013).

The assays with pure preparations of the recombinant BDH of *C. glutamicum* showed that (*R*)-acetoin (present in the racemic mixture), was reduced into *meso*-2,3-BD, though at an apparent rate 20 times lower than (*S*)-acetoin (Table 4.8). This work will be complemented with the determination of the kinetic parameters with (*R*)-acetoin, as soon as this compound becomes available (on-demand synthesis, Enamine, Ukraine).

Studying the properties of BDHs suggested some guidelines for the construction of better producers. SDRs typically introduce a new hydroxyl group in *S*-configuration and form *meso*-2,3-BD from enzymatically produced (*R*)-acetoin, or (*2S*,*3S*)-2,3-BD from (*S*)-acetoin formed by spontaneous decarboxylation of α-acetolactate in the presence of oxygen. This means that strains that employ SDRs for 2,3-BD production will always form a mixture of *meso*- and (*2S*,*3S*)-2,3-BD in the presence of oxygen; (*2S*,*3S*)-2,3-BD will be the minor product under oxygen limiting conditions as the substrate (*S*)-acetoin is less efficiently accumulated. Relevant examples are *E. coli* engineered with the pathway from *E. cloacae*, or *K. pneumoniae* with native pathway, both using SDRs (Tables 4.1 and 5.2). This also means that under aerated conditions, it will not be possible to produce pure *meso*-2,3-BD by *C. glutamicum* with a pathway that contains the lactococcal *butA* gene, which encodes an SDR. Our data

(Appendix II) corroborates this conclusion as it shows that this enzyme produced a mixture of *meso*- and (*2S*,*3S*)-2,3-BD. Table 5.2 shows that, when enantiopure 2,3-BD is desired, a more suitable strategy is to employ MDRs that introduce the new hydroxyl group in an *R*-configuration; consequently, the only product that can be formed from diacetyl and (*R*)-acetoin is (*2R,3R*)-2,3-BD. This strategy was implemented in *S. cerevisiae* overproducing BDH from *B. subtilis,* and led to production of enantiopure (*2R,3R*)-2,3-BD (Table 5.2).

Curiously, *butB*-encoded BDH (BDHB) of *L. lactis*, an MDR-type enzyme, produced traces of *meso*-2,3-BD, rather than (2*R*,3*R*)-2,3-BD upon incubation with racemic acetoin. Similarly, Nielsen et al. found that *E. coli* that overexpressed lactococcal *butB* formed *meso*-2,3-BD (Nielsen et al. 2010). It seems that this enzyme is different from other MDRs, thus it would be interesting to further optimize the production of BDHB and confirm these preliminary results.

Table 5.2. 2,3-Butanediol forms produced by different bacteria. The relative proportion of each 2,3-BD form is given in parenthesis.

Organism	Pathway used	Fermentation conditions	2,3-BD produced	Ref
E. coli BL21/pET-RABC	*Complete pathway from E. cloacae*	Fed-batch; pH 7; 400 rpm and aeration rate 1.5 vvm	meso-2,3-BD (95.5) (2S,3S)-2,3-BD (3.9) (2R,3R)-2,3-BD (0.5)	Xu et al. 2014
S. cerevisiae JL0432	Endogeneous BDH and ALS; ALDC from *B. subtilis*	Fed-batch; pH 5; DO 10-15%	(*2R,3R*)-2,3-BD (99.9) (*2S,3S*)-2,3-BD (0) *meso*-2,3-BD (0)	Lian et al. 2014
K. pneumoniae Δ*ldhA pGEM*	Endogenous pathway	Fed-batch; pH 6 and aeration rate 1.5 vvm	*meso*-2,3-BD (90) (*2S,3S*)-2,3-BD (10)	Park et al. 2013
P. polymyxa DSM 365	Endogenous pathway	Fed-batch; pH 6; stirring 300 rpm and aeration rate 1.67 vvm	(*2R,3R*)-2,3-BD (98) *meso*-2,3-BD (1)	Haßler et al. 2011
P. polymyxa DSM 365	Endogenous pathway	Fed-batch; pH 6; stirring 800 rpm and aeration rate 0.1 vvm	(*2R,3R*)-2,3-BD (94) *meso*-2,3-BD (6)	Haßler et al. 2011
C. glutamicum Δ*aceE*Δ*pqo*Δ*ldhA*Δ *mdh* (pEKEx2-*als,aldB,*$_{Ptuf}$*butA*)	*Complete pathway from L. lactis MG1363*	Batch; pH 7 and aeration 5 mL·min^{-1}	*meso*-2,3-BD (100) (*2S,3S*)-2,3-BD (0)	This work
C. glutamicum Δ*aceE*Δ*pqo*Δ*ldhA*Δ *mdh* (pEKEx2-*als,aldB,*$_{Ptuf}$*butA*)	*Complete pathway from L. lactis MG1363*	Batch; pH 7 and aeration 10 mL·min^{-1}	*meso*-2,3-BD (95) (*2S,3S*)-2,3-BD (5)	This work
C. glutamicum Δ*aceE*Δ*pqo*Δ*ldhA*Δ *mdh* (pEKEx2-*als,aldB,butA*^{Cg})	*Endogenous BDH, ALS and ALDC from L. lactis MG1363*	Batch; pH 7 and aeration 10 mL·min^{-1}	*meso*-2,3-BD (90) (*2S,3S*)-2,3-BD (10)	This work

Abbreviations: ALS, α-acetolactate synthase; ALDC, α-acetolactate decarboxylase; BDH, 2,3-butanediol dehydrogenase; vvm, gas volume flow per unit of liquid volume per minute; DO, dissolved oxygen.

Finally, the physiological role of the 2,3-BD pathway and the function of BDH in *C. glutamicum* are interesting questions which deserve some discussion. In *L. lactis* IL1403, ALS was found to be upregulated under low pH conditions and the 2,3-BD pathway was speculated to be involved in preventing intracellular acidification by redirecting carbon to neutral compounds rather than to organic acids (Zuljan et al. 2014). This pathway was also proposed to be part of the response to low pH in the pathogens *S. marcescens* MG1 and *Serratia plymuthica* RVH1 (Van Houdt et al. 2006). Furthermore, the acquisition of heterologous ALS and ALDC improved growth of *E. coli* due to lesser extent of external acidification (Vivijs et al. 2014). Over-expression of the 2,3-BD-forming lactococcal pathway in *C. glutamicum* caused cells to grow slightly better on acetate, compared to control strains, and also to survive better during the stationary phase (Fig. 3.3). This puzzling result is not associated with a response to low pH, since the pH of the culture medium was higher than 7.0 in both cases.

Interestingly, it was recently shown that bacterial volatiles such as 2,3-BD and acetoin produced by *E. aerogenes* increase maize resistance to pathogens and herbivores (D'Alessandro et al. 2014). Similarly, in *Arabidopsis* seedlings exposed to bacterial volatiles from *B. subtilis* GB03 and *B. amyloliquefaciens* IN937a, disease severity by the bacterial pathogen *Erwinia carotovora* was significantly reduced compared with

seedlings not exposed to bacterial volatiles (Song and Ryu 2013). Furthermore, the same study revealed that (*2R*,*3R*)-2,3-BD promoted growth, while the application of the racemic mixture was found to induce systemic resistance to pathogenesis (Song and Ryu 2013).

The occurrence of BDH in *C. glutamicum* is peculiar, since *C. glutamicum* does not possess any ALDC activity, and the production of 2,3-BD by the wild-type and LDH-negative strain is rather inefficient (Table 3.5, Dickschat et al. 2010). Furthermore, it was found that *butA* expression is upregulated in nitrogen limitation (Silberbach et al. 2005). A study aimed at identifying proteins affected by high salt stress, also found upregulation of *butA* (Franzel et al. 2010). In an attempt to establish a comprehensive transcriptome map of *C. glutamicum*, Pfeifer-Sancar et al. (2013) detected three transcripts of the *butA* gene, differing in the 5′-untranslated region, which indicates that this gene is under complex transcriptional control (Pfeifer-Sancar et al. 2013). Furthermore, our measurements show high BDH activity in crude cell extracts (Table 3.3). Having in mind that *C. glutamicum* is a soil-born bacterium that lacks ALDC, a key-enzyme for the biosynthesis of 2,3-BD, a major role in acidification prevention can be ruled out. It is tempting to speculate that 2,3-BD could play a role in interaction with other organisms.

Final remarks

Major achievements of this thesis work:

- The *in vivo* NMR methodology was successfully applied to *C. glutamicum* for the first time.
- Intracellular and extracellular pools of organic acids (lactic and succinic) were measured non-invasively. To the best of our knowledge, this is the most reliable methodology to measure organic acid gradients across intact cells.
- The first metabolic model of the anaerobic glucose metabolism in the wild-type *C. glutamicum* was constructed.
- First demonstration of *C. glutamicum* as a host for industrial production of 2,3-BD was accomplished (proof of concept).
- The use of *C. glutamicum* 2,3-BD producers as a GRAS platform for the development of new producer strains of acetoin was proposed.
- The ability of BDH from *C. glutamicum* to use (*R*)-acetoin and produce *meso*-2,3-BD was proven *in vivo* and *in vitro*.

References

REFERENCES

Aboka FO, Heijnen JJ, Van Winden WA. 2009. Dynamic ^{13}C-tracer study of storage carbohydrate pools in aerobic glucose-limited *Saccharomyces cerevisiae* confirms a rapid steady-state turnover and fast mobilization during a modest stepup in the glucose uptake rate. FEMS Yeast Res. 9:191–201.

Adom F, Dunn JB, Han J, Sather N. 2014. Life-cycle fossil energy consumption and greenhouse gas emissions of bioderived chemicals and their conventional counterparts. Environ. Sci. Technol. 48:14624–31.

Ajinomoto Co., Inc. Financial Report 2011. https://www.ajinomoto.com/en/ir/pdf/Aji_FR2011.pdf. Accessed 7 Jun 2015.

Arndt A, Eikmanns BJ. 2007. The alcohol dehydrogenase gene *adhA* in *Corynebacterium glutamicum* is subject to carbon catabolite repression. J. Bacteriol. 189:7408–16.

Arndt A, Auchter M, Ishige T, Wendisch VF, Eikmanns BJ. 2008. Ethanol catabolism in *Corynebacterium glutamicum*. J. Mol. Microbiol. Biotechnol. 15:222–33.

Bao T, Zhang X, Rao Z, Zhao X, Zhang R, Yang T, Xu Z, Yang S. 2014. Efficient whole-cell biocatalyst for acetoin production with NAD+ regeneration system through homologous co-expression of 2,3-butanediol dehydrogenase and NADH oxidase in engineered *Bacillus subtilis*. PLoS One 9:e102951. doi:10.1371/journal.pone.0102951.

Bartek T, Blombach B, Zonnchen E, Makus P, Lang S, Eikmanns BJ, Oldiges M. 2010. Importance of NADPH supply for improved L-valine formation in *Corynebacterium glutamicum*. Biotechnol. Prog. 26:361–71.

Bartek T, Blombach B, Lang S, Eikmanns BJ, Wiechert W, Oldiges M, Nöh K, Noack S. 2011. Comparative ^{13}C-metabolic flux analysis of PDHC-deficient L-valine producing *Corynebacterium glutamicum*. Appl. Environ. Microbiol. 77:6644-52.

Baumgart M, Mustafi N, Krug A, Bott M. 2011. Deletion of the aconitase gene in *Corynebacterium glutamicum* causes strong selection pressure for secondary mutations inactivating citrate synthase. J. Bacteriol. 193(24):6864-73.

Becker J, Reinefeld J, Stellmacher R, Schäfer R, Lange A, Meyer H, Lalk M, Zelder O, von Abendroth G, Schröder H, Haefner S, Wittmann C. 2013. Systems-wide analysis and engineering of metabolic pathway fluxes in bio-succinate producing *Basfia succiniciproducens*. Biotechnol. Bioeng. 9999:1–11.

Becker J, Wittmann C. 2012. Bio-based production of chemicals, materials and fuels - *Corynebacterium glutamicum* as versatile cell factory. Curr. Opin. Biotechnol. 23:631–40.

Beckers G, Nolden L, Burkovski A. 2001. Glutamate synthase of *Corynebacterium glutamicum* is not essential for glutamate synthesis and is regulated by the nitrogen status. Microbiology 147:2961–70.

Blombach B, Arndt A, Auchter M, Eikmanns BJ. 2009. L-Valine production during growth of pyruvate dehydrogenase complex-deficient *Corynebacterium glutamicum* in the presence of ethanol or by inactivation of the transcriptional regulator SugR. Appl. Environ. Microbiol. 75:1197–200.

Blombach B, Schreiner ME, Bartek T, Oldiges M, Eikmanns BJ. 2008. *Corynebacterium glutamicum* tailored for high-yield L-valine production. Appl. Microbiol. Biotechnol. 79:471–9.

Blombach B, Riester T, Wieschalka S, Ziert C, Youn J-W, Wendisch VF, Eikmanns BJ. 2011. *Corynebacterium glutamicum* tailored for efficient isobutanol production. Appl. Environ. Microbiol. 77:3300–10.

Blombach B, Buchholz J, Busche T, Kalinowski J, Takors R. 2013. Impact of different CO_2/HCO_3^- levels on metabolism and regulation in *Corynebacterium glutamicum*. J. Biotechnol. 168:331–40.

Bozell JJ, Petersen GR. 2010. Technology development for the production of biobased products from biorefinery carbohydrates—the US Department of Energy's "Top 10" revisited. Green Chem. 12:539-54.

Bott M, Niebisch A. 2003. The respiratory chain of *Corynebacterium glutamicum*. J. Biotechnol. 104:129–53.

Bott M, Niebich A. 2005. Respiratory energy metabolism. *In* Eggeling L, Bott M (eds), Handbook of *Corynebacterium glutamicum*. CRC Press. Taylor & Francis Group, Boca Raton FL. p. 305–32.

Buchholz J, Schwentner A, Brunnenkan B, Gabris C, Grimm S, Gerstmeir R, Takors R, Eikmanns BJ, Blombach B. 2013. Platform engineering of *Corynebacterium glutamicum* with reduced pyruvate dehydrogenase complex activity for improved production of L-lysine, L-valine, and 2-ketoisovalerate. Appl. Environ. Microbiol. 79:5566–75.

Burkovski, A. 2008. Corynebacteria: Genomics and Molecular Biology. 1st ed. Norfolk, UK: Caister Academic Press.

Carballo J, Martin R, Bernardo A, Gonzalez J. 1991. Purification, characterization and some properties of diacetyl(acetoin) reductase from *Enterobacter aerogenes*. Eur. J. Biochem. 198:327–32.

Carvalho AL, Turner DL, Fonseca LL, Solopova A, Catarino T, Kuipers OP, Voit EO, Neves AR, Santos H. 2013. Metabolic and transcriptional analysis of acid stress in *Lactococcus lactis*, with a focus on the kinetics of lactic acid pools. PLoS One 8:e68470. doi:10.1371/journal.pone.0068470.

Celińska E, Grajek W. 2009. Biotechnological production of 2,3-butanediol - current state and prospects. Biotechnol. Adv. 27:715–25.

Chen C, Wei D, Shi J, Wang M, Hao J. 2014. Mechanism of 2,3-butanediol stereoisomer formation in *Klebsiella pneumoniae*. Appl. Microbiol. Biotechnol. 98:4603–13.

Cocaign-Bousquet M, Guyonvarch A, Lindley ND. 1996. Growth Rate-Dependent Modulation of Carbon Flux through Central Metabolism and the Kinetic Consequences for Glucose-Limited Chemostat Cultures of *Corynebacterium glutamicum*. Appl. Environ. Microbiol. 62:429–36.

Crow VL. 1990. Properties of 2,3-butanediol dehydrogenases from *Lactococcus lactis* subsp. *lactis* in relation to citrate fermentation. Appl. Environ. Microbiol. 56:1656–65.

D'Alessandro M, Erb M, Ton J, Brandenburg A, Karlen D, Zopfi J, Turlings TCJ. 2014. Volatiles produced by soil-borne endophytic bacteria increase plant pathogen resistance and affect tritrophic interactions. Plant Cell Environ. 37:813–26.

Delhomme C, Weuster-Botz D, Kühn FE. 2009. Succinic acid from renewable resources as a C4 building-block chemical - a review of the catalytic possibilities in aqueous media. Green .Chem. 11:13–26.

Demain AL, Jackson M, Trenner NR. 1967. Thiamine-dependent accumulation of tetramethylpyrazine accompanying a mutation in the isoleucine-valine pathway. J. Bacteriol. 94:323–6.

Dickschat JS, Wickel S, Bolten CJ, Nawrath T, Schulz S, Wittmann C. 2010. Pyrazine biosynthesis in *Corynebacterium glutamicum*. Eur. J. Org. Chem. 2010:2687–95.

Dominguez H, Nezondet C, Lindley ND, Cocaign M, National I, De Rangueil CS. 1993. Modified carbon flux during oxygen limited growth of *Corynebacterium glutumicum* and the consequences for amino acid overproduction. Biotechnol. Lett. 15:449-54.

Dominguez H, Cocaign-Bousquet M, Lindley ND. 1997. Simultaneous consumption of glucose and fructose from sugar mixtures during batch growth of *Corynebacterium glutamicum*. Appl. Microbiol. Biotechnol. 47:600–3.

Dominguez H, Rollin C, Guyonvarch A, Guerquin-Kern JL, Cocaign-Bousquet M, Lindley ND. 1998. Carbon-flux distribution in the central metabolic pathways of *Corynebacterium glutamicum* during growth on fructose. Eur. J. Biochem. 254:96–102.

Eggeling L, Bott M. 2005. Handbook of *Corynebacterium glutamicum*. CRC Press. Taylor & Francis Group, Boca Raton FL.

Eggeling L, Reyes O. 2005. Part VII - Experiments. *In* Eggeling L, Bott M (eds), Handbook of *Corynebacterium glutamicum*. CRC Press. Taylor & Francis, Boca Raton FL. p. 535–66.

Eikmanns BJ, Follettie MT, Griot MU, Sinskey AJ. 1989. The phosphoenolpyruvate carboxylase gene of *Corynebacterium glutamicum*: molecular cloning, nucleotide sequence, and expression. Mol. Gen. Genet. 218:330–9.

Eikmanns BJ, Kleinertz E, Liebl W, Sahm H. 1991b. A family of *Corynebacterium glutamicum*/*Escherichia coli* shuttle vectors for cloning, controlled gene expression, and promoter probing. Gene. 102:93–8.

Eikmanns BJ, Metzger M, Reinscheid D, Kircher M, Sahm H. 1991a. Amplification of three threonine biosynthesis genes in *Corynebacterium glutamicum* and its influence on carbon flux in different strains. Appl. Microbiol. Biotechnol. 34:617–22.

Eikmanns BJ. 1992. Identification, sequence analysis, and expression of a *Corynebacterium glutamicum* gene cluster encoding the three glycolytic enzymes glyceraldehyde-3-phosphate dehydrogenase, 3-phosphoglycerate kinase, and triosephosphate isomerase. J. Bacteriol. 174:6076–86.

Eikmanns BJ, Thum-Schmitz N, Eggeling L, Lüdtke KU, Sahm H. 1994. Nucleotide sequence, expression and transcriptional analysis of the *Corynebacterium glutamicum gltA* gene encoding citrate synthase. Microbiol. 140:1817–28.

Eikmanns BJ, Rittmann D, Sahm H. 1995. Cloning, sequence analysis, expression, and inactivation of the *Corynebacterium glutamicum icd* gene encoding isocitrate dehydrogenase and biochemical characterization of the enzyme. J. Bacteriol. 177:774–82.

Eikmanns B. 2005. Central Metabolism Tricarboxylic Acid Cycle and Anaplerotic Reactions. *In* Eggeling L, Bott M (eds), Handbook of *Corynebacterium glutamicum*. CRC Press. Taylor & Francis Group, Boca Raton FL. p. 241–76.

Eikmanns BJ, Blombach B. 2014. The pyruvate dehydrogenase complex of *Corynebacterium glutamicum*: an attractive target for metabolic engineering. J. Biotechnol. 192:339–45.

Elisáková V, Pátek M, Holátko J, Nesvera J, Leyval D, Goergen J-L, Delaunay S. 2005. Feedback-resistant acetohydroxy acid synthase increases valine production in *Corynebacterium glutamicum*. Appl. Environ. Microbiol. 71:207–13.

Erickson B, Nelson, Winters P. 2012. Perspective on opportunities in industrial biotechnology in renewable chemicals. Biotechnol. J. 7:176–85.

Even S, Garrigues C, Loubiere P, Lindley ND, Cocaign-Bousquet M. 1999. Pyruvate metabolism in *Lactococcus lactis* is dependent upon glyceraldehyde-3-phosphate dehydrogenase activity. Metab. Eng. 1:198–205.

Fisher AK, Freedman BG, Bevan DR, Senger RS. 2014. A review of metabolic and enzymatic engineering strategies for designing and optimizing performance of microbial cell factories. Comput. Struct. Biotechnol. J. 11:91–9.

Franzel B, Trötschel C, Rückert C, Kalinowski J, Poetsch A, Wolters DA. 2010. Adaptation of *Corynebacterium glutamicum* to salt-stress conditions. Proteomics 10:445–57.

Frunzke J, Engels V, Hasenbein S, Gätgens C, Bott M. 2008. Co-ordinated regulation of gluconate catabolism and glucose uptake in *Corynebacterium glutamicum* by two functionally equivalent transcriptional regulators, GntR1 and GntR2. Mol. Microbiol. 67:305–22.

Fu J, Wang Z, Chen T, Liu W, Shi T, Wang G, Tang Y, Zhao X. 2014. NADH plays the vital role for chiral pure D-(-)-2,3-butanediol production in *Bacillus subtilis* under limited oxygen conditions. Biotechnol. Bioeng. 111:2126–31.

Fukui K, Koseki C, Yamamoto Y, Nakamura J, Sasahara A, Yuji R, Hashiguchi K, Usuda Y, Matsui K, Kojima H, Abe K. 2011. Identification of succinate exporter in *Corynebacterium glutamicum* and its physiological roles under anaerobic conditions. J. Biotechnol. 154:25-34.

Gao B, Gupta RS. 2012. Phylogenetic framework and molecular signatures for the main clades of the phylum Actinobacteria. Microbiol. Mol. Biol. Rev. 76:66–112.

Gao J, Yang H-H, Feng X-H, Li S, Xu H. 2013. A 2,3-butanediol dehydrogenase from *Paenibacillus polymyxa* ZJ-9 for mainly producing R,R-2,3-butanediol: purification, characterization and cloning. J. Basic Microbiol. 53:733–41.

Garg SK, Jain A. 1995. Fermentative production of 2,3-butanediol: A review. Bioresour. Technol. 51:103–9.

Gaspar P, Neves AR, Gasson MJ, Shearman CA, Santos H. 2011. High yields of 2,3-butanediol and mannitol in *Lactococcus lactis* through engineering of NAD^+ cofactor recycling. Appl. Environ. Microbiol. 77:6826–35.

Genda T, Nakamatsu T, Ozak H. 2003. Purification and characterization of malate dehydrogenase from *Corynebacterium glutamicum*. J. Biosci. Bioeng. 95:562–6.

Genda T, Watabe S, Ozaki H. 2006. Purification and characterization of fumarase from *Corynebacterium glutamicum*. Biosci. Biotechnol. Biochem. 70:1102–9.

Gerstmeir R. 2003. Acetate metabolism and its regulation in *Corynebacterium glutamicum*. J. Biotechnol. 104:99–122.

Gerstmeir R, Cramer A, Dangel P, Schaffer S, Eikmanns BJ. 2004. RamB, a novel transcriptional regulator of genes involved in acetate metabolism of *Corynebacterium glutamicum*. J. Bacteriol. 186:2798–809.

Ghiaci P, Norbeck J, Larsson C. 2013. Physiological adaptations *of Saccharomyces cerevisiae* evolved for improved butanol tolerance. Biotechnol. Biofuels 6:101.

Gong G, Yuan L, Cai L, Ran M, Zhang Y, Gong H, Dai X, Wu W, Dong H. 2014. Tetramethylpyrazine suppresses transient oxygen-glucose deprivation-induced connexin32 expression and cell apoptosis via the ERK1/2 and p38 MAPK pathway in cultured hippocampal neurons. PLoS One 9:e105944. doi:10.1371/journal.pone.0105944.

González E, Fernández MR, Larroy C, Solà L, Pericàs MA, Parés X, Biosca JA. 2000. Characterization of a (*2R,3R*)-2,3-butanediol dehydrogenase as the *Saccharomyces cerevisiae* YAL060W gene product. Disruption and induction of the gene. J. Biol. Chem. 275:35876–85.

González-Ramos D, van den Broek M, van Maris AJ, Pronk JT, Daran J-MG. 2013. Genome-scale analyses of butanol tolerance in *Saccharomyces cerevisiae* reveal an essential role of protein degradation. Biotechnol. Biofuels 6:48.

Gourdon P, Baucher MF, Lindley ND, Guyonvarch A. 2000. Cloning of the malic enzyme gene from *Corynebacterium glutamicum* and role of the enzyme in lactate metabolism. Appl. Environ. Microbiol. 66:2981–7.

Green MR, Sambrook J. 2012. Molecular cloning: a laboratory manual. 4th ed. Cold Spring Harbor, NY:Cold Spring Harbor Laboratory Press.

Gubler M, Jetten M, Lee SH, Sinskey AJ. 1994. Cloning of the pyruvate kinase gene (*pyk*) of *Corynebacterium glutamicum* and site-specific inactivation of *pyk* in a lysine-producing *Corynebacterium lactofermentum* strain. Appl. Environ. Microbiol. 60:2494–500.

Görke B, Stülke J. 2008. Carbon catabolite repression in bacteria: many ways to make the most out of nutrients. Nat. Rev. Microbiol. 6:613–24

Hasegawa S, Suda M, Uematsu K, Natsuma Y, Hiraga K, Jojima T, Inui M, Yukawa H. 2013. Engineering of *Corynebacterium glutamicum* for high-yield L-valine production under oxygen deprivation conditions. Appl. Environ. Microbiol. 79:1250–7.

Hoffelder M, Raasch K, van Ooyen J, Eggeling L. 2010. The E2 domain of OdhA of *Corynebacterium glutamicum* has succinyltransferase activity dependent on lipoyl residues of the acetyltransferase AceF. J. Bacteriol. 192:5203–11.

Hong SH, Moon SY, Lee SY. 2003. Prediction of maximum yields of metabolites and optimal pathways for their production by metabolic flux analysis. J. Microbiol. Biotechnol. 13:571–577.

Hong SH, Kim JS, Lee SY, In YH, Choi SS, Rih J-K, Kim CH, Jeong H, Hur CG, Kim JJ. 2004. The genome sequence of the capnophilic rumen bacterium *Mannheimia succiniciproducens*. Nat. Biotechnol. 22:1275–81.

Huang T-C, Fu H-Y, Ho C-T. 1996. Mechanistic studies of tetramethylpyrazine formation under weak acidic conditions and high hydrostatic pressure. J. Agric. Food Chem. 44:240–6.

Hugenholtz J, Starrenburg MC. 1992. Diacetyl production by different strains of *Lactococcus lactis* subsp. *lactis* var. diacetylactis and *Leuconostoc spp*. Appl. Microbiol. Biotechnol. 38:17–22.

Hung GC, Brown CR, Wolfe AB, Liu J, Chiang HL. 2004. Degradation of the gluconeogenic enzymes fructose-1,6-bisphosphatase and malate dehydrogenase is mediated by distinct proteolytic pathways and signaling events. J. Biol. Chem. 279:49138–50.

Huhn S, Jolkver E, Krämer R, Marin K. 2011. Identification of the membrane protein SucE and its role in succinate transport in *Corynebacterium glutamicum*. Appl. Microbiol. Biotechnol. 89:327–35.

Häßler T, Schieder D, Pfaller R, Faulstich M, Sieber V. 2012. Enhanced fed-batch fermentation of 2,3-butanediol by *Paenibacillus polymyxa* DSM 365. Bioresour. Technol. 124:237–44.

Höhn-Bentz H, Radler F. 1978. Bacterial 2,3-butanediol dehydrogenases. Arch. Microbiol. 116:197–203.

Ikeda M, Nakagawa S. 2003. The *Corynebacterium glutamicum* genome: features and impacts on biotechnological processes. Appl. Microbiol. Biotechnol. 62:99–109.

Inui M, Murakami S, Okino S, Kawaguchi H, Vertès AA, Yukawa H. 2004. Metabolic analysis of *Corynebacterium glutamicum* during lactate and succinate productions under oxygen deprivation conditions. J. Mol. Microbiol. Biotechnol. 7:182–96.

Inui M, Suda M, Okino S, Nonaka H, Puskás LG, Vertès AA, Yukawa H. 2007. Transcriptional profiling of *Corynebacterium glutamicum* metabolism during organic acid production under oxygen deprivation conditions. Microbiology 153:2491–504.

Jantama K, Polyiam P, Khunnonkwao P, Chan S, Sangproo M, Khor K, Jantama SS, Kanchanatawee S. 2015. Efficient reduction of the formation of by-products and improvement of production yield of 2,3-butanediol by a combined deletion of alcohol dehydrogenase, acetate kinase-phosphotransacetylase, and lactate dehydrogenase genes in metabolically engineered *Klebsiella oxytoca* in mineral salts medium. Metab. Eng. 30:16–26.

Jetten MS, Sinskey AJ. 1995. Purification and properties of oxaloacetate decarboxylase from *Corynebacterium glutamicum*. Antonie Van Leeuwenhoek 67:221–7.

Ji X-J, Huang H, Ouyang P-K. 2011. Microbial 2,3-butanediol production: a state-of-the-art review. Biotechnol. Adv. 29:351–64.

Ji X-J, Xia Z-F, Fu N-H, Nie Z-K, Shen M-Q, Tian Q-Q, Huang H. 2013. Cofactor engineering through heterologous expression of an NADH oxidase and its impact on metabolic flux redistribution in *Klebsiella pneumoniae*. Biotechnol. Biofuels 6:7.

Johansen E, Kibenich A. 1992. Isolation and characterization of IS1165, an insertion sequence of *Leuconostoc mesenteroides* subsp. *cremoris* and other lactic acid bacteria. Plasmid 27:200–6.

Jojima T, Igari T, Gunji W, Suda M, Inui M, Yukawa H. 2012. Identification of a HAD superfamily phosphatase, HdpA, involved in 1,3-dihydroxyacetone production during sugar catabolism in *Corynebacterium glutamicum*. FEBS Lett. 586:4228–32.

Jojima T, Igari T, Moteki Y, Suda M, Yukawa H, Inui M. 2015. Promiscuous activity of (*S,S*)-butanediol dehydrogenase is responsible for glycerol production from 1,3-dihydroxyacetone in *Corynebacterium glutamicum* under oxygen-deprived conditions. Appl. Microbiol. Biotechnol. 99:1427–33.

Jolkver E, Emer D, Ballan S, Krämer R, Eikmanns BJ, Marin K. 2009. Identification and characterization of a bacterial transport system for the uptake of pyruvate, propionate, and acetate in *Corynebacterium glutamicum*. J. Bacteriol. 191:940–8.

de Jong E, Higson A, Walsh P, Wellisch M. 2012. Product developments in the bio-based chemicals arena. Biofuels Bioprod. Biorefining. 6:606-24.

Jung M-Y, Ng CY, Song H, Lee J, Oh M-K. 2012. Deletion of lactate dehydrogenase in *Enterobacter aerogenes* to enhance 2,3-butanediol production. Appl. Microbiol. Biotechnol. 95:461–9.

Jung M-Y, Park B-S, Lee J, Oh M-K. 2013. Engineered *Enterobacter aerogenes* for efficient utilization of sugarcane molasses in 2,3-butanediol production. Bioresour. Technol. 139:21–7.

Kabus A, Georgi T, Wendisch VF, Bott M. 2007. Expression of the *Escherichia coli pntAB* genes encoding a membrane-bound transhydrogenase in *Corynebacterium glutamicum* improves L-lysine formation. Appl. Microbiol. Biotechnol. 75:47–53.

Kalinowski J. 2003. The complete *Corynebacterium glutamicum* ATCC 13032 genome sequence and its impact on the production of L-aspartate-derived amino acids and vitamins. J. Biotechnol. 104:5–25.

Kataoka M, Hashimoto K-I, Yoshida M, Nakamatsu T, Horinouchi S, Kawasaki H. 2006. Gene expression of *Corynebacterium glutamicum* in response to the conditions inducing glutamate overproduction. Lett. Appl. Microbiol. 42:471–6.

Keilhauer C, Eggeling L, Sahm H. 1993. Isoleucine synthesis in *Corynebacterium glutamicum*: molecular analysis of the *ilvB-ilvN-ilvC* operon. J. Bacteriol. 175:5595–603.

Kiefer P, Heinzle E, Zelder O, Wittmann C. 2004. Comparative metabolic flux analysis of lysine-producing *Corynebacterium glutamicum* cultured on glucose or fructose. Appl. Environ. Microbiol. 70:229–39.

Kim B, Lee S, Jeong D, Yang J, Oh M-K, Lee J. 2014. Redistribution of carbon flux toward 2,3-butanediol production in *Klebsiella pneumoniae* by metabolic engineering. PLoS One 9:e105322. doi: 10.1371/journal.pone.0105322.

Kim J-W, Seo S-O, Zhang G-C, Jin Y-S, Seo J-H. 2015. Expression of *Lactococcus lactis* NADH oxidase increases 2,3-butanediol production in Pdc-deficient *Saccharomyces cerevisiae*. Bioresour. Technol. 191:512–9.

Kim TY, Kim HU, Park JM, Song H, Kim JS, Lee SY. 2007. Genome-scale analysis of *Mannheimia succiniciproducens* metabolism. Biotechnol. Bioeng. 97:657–71.

Kim TY, Kim HU, Song H, Lee SY. 2009. *In silico* analysis of the effects of H_2 and CO_2 on the metabolism of a capnophilic bacterium *Mannheimia succiniciproducens*. J. Biotechnol. 144:184–9.

Kind S, Jeong WK, Schröder H, Wittmann C. 2010. Systems-wide metabolic pathway engineering in *Corynebacterium glutamicum* for bio-based production of diaminopentane. Metab. Eng. 12:341–51.

Kind S, Neubauer S, Becker J, Yamamoto M, Völkert M, Abendroth G von, Zelder O, Wittmann C. 2014. From zero to hero - production of bio-based nylon from renewable resources using engineered *Corynebacterium glutamicum*. Metab. Eng. 25:113–23.

Kinoshita S, Nakayama K, Akita S. 1958. Taxonomical study of glutamic acid accumulating bacteria, *Micrococcus glutamicus* nov. sp. Bull. Soc. Chem. Soc. Japan 22:176–85.

Kinoshita S. 2005. A short history of the birth of the amino acid industry in Japan. *In* Eggeling L, Bott M (eds), Handbook of *Corynebacterium glutamicum*. CRC Press. Taylor & Francis Group, Boca Raton FL.p. 3-9.

Klaffl S, Eikmanns BJ. 2010. Genetic and functional analysis of the soluble oxaloacetate decarboxylase from *Corynebacterium glutamicum*. J. Bacteriol. 192:2604–12.

Klapa M, Park S, Sinskey A, Stephanopoulos G. 1999. Metabolite and isotopomer balancing in the analysis of metabolic cycles: I. Theory. Biotechnol. Bioeng. 62:375–91.

Krause FS, Blombach B, Eikmanns BJ. 2010. Metabolic engineering of *Corynebacterium glutamicum* for 2-ketoisovalerate production. Appl. Environ. Microbiol. 76:8053–61.

Krämer R, Lambert C, Hoischen C, Ebbighausen H. 1990. Uptake of glutamate in *Corynebacterium glutamicum*. Kinetic properties and regulation by internal pH and potassium. Eur. J. Biochem. 194:929-35.

Kurokawa T, Sakamoto J. 2005. Purification and characterization of succinate:menaquinone oxidoreductase from *Corynebacterium glutamicum*. Arch. Microbiol. 183:317–24.

Köpke M, Mihalcea C, Liew F, Tizard JH, Ali MS, Conolly JJ, Al-Sinawi B, Simpson SD. 2011. 2,3-Butanediol production by acetogenic bacteria, an alternative route to chemical synthesis, using industrial waste gas. Appl. Environ. Microbiol. 77:5467–75.

Lee JW, Na D, Park JM, Lee J, Choi S, Lee SY. 2012. Systems metabolic engineering of

microorganisms for natural and non-natural chemicals. Nat. Chem. Biol. 8:536–46.

Lee SJ, Song H, Lee SY. 2006. Genome-based metabolic engineering of *Mannheimia succiniciproducens* for succinic acid production. Appl. Environ. Microbiol. 72:1939–48.

Lee SY, Kim HU. 2015. Systems strategies for developing industrial microbial strains. Nat. Biotechnol. 33:1061–72.

Lessard P. 1996. Metabolic engineering, the concept coalesces. Nat. Biotechnol. 14: 1654-5.

Li L, Li K, Wang K, Chen C, Gao C, Ma C, Xu P. 2014. Efficient production of 2,3-butanediol from corn stover hydrolysate by using a thermophilic *Bacillus licheniformis* strain. Bioresour. Technol. 170:256–61.

Lian J, Chao R, Zhao H. 2014. Metabolic engineering of a *Saccharomyces cerevisiae* strain capable of simultaneously utilizing glucose and galactose to produce enantiopure (*2R,3R*)-butanediol. Metab. Eng. 23:92–9.

Liebl W, Bayerl A, Schein B, Stillner U, Schleifer KH. 1989. High efficiency electroporation of intact *Corynebacterium glutamicum* cells. FEMS Microbiol. Lett. 53:299–303.

Liebl W. 2006. The genus *Corynebacterium*—nonmedical. *In:* Dworkin M, Falkow S, Rosenberg E, Schleifer KH, and Stackebrandt E (eds), The Prokaryotes. 3rd ed, vol. 3. *Springer*. New York. pp 796–818.

Lindner SN, Meiswinkel TM, Panhorst M, Youn J-W, Wiefel L, Wendisch VF. 2012. Glycerol-3-phosphatase of *Corynebacterium glutamicum*. J. Biotechnol. 159:216–24.

Litsanov B, Brocker M, Bott M. 2012a. Toward homosuccinate fermentation: metabolic engineering of *Corynebacterium glutamicum* for anaerobic production of succinate from glucose and formate. Appl. Environ. Microbiol. 78:3325–37.

Litsanov B, Kabus A, Brocker M, Bott M. 2012b. Efficient aerobic succinate production from glucose in minimal medium with *Corynebacterium glutamicum*. Microb. Biotechnol. 5:116–28.

Litsanov B, Brocker M, Oldiges M, Bott M. 2014. Succinic Acid. *In:* Bisaria VS, Kondo A. (eds), Bioprocessing of Renewable Resources to Commodity Bioproducts. John Wiley & Sons, Inc. p. 435-72.

Lu S, Eiteman MA, Altman E. 2009. Effect of CO_2 on succinate production in dual-phase *Escherichia coli* fermentations. J. Biotechnol. 143:213–23.

Ma C, Wang A, Qin J, Li L, Ai X, Jiang T, Tang H, Xu P. 2009. Enhanced 2,3-butanediol production by *Klebsiella pneumoniae* SDM. Appl. Microbiol. Biotechnol. 82:49–57.

Machado D, Herrgård M. 2015. Co-evolution of strain design methods based on flux balance and elementary mode analysis. Metab. Eng. Commun. 2:85–92.

Magee R, Kosaric N. 1987. The microbial production of 2,3-butanediol. Adv. Appl. Microbiol. 32:89-161.

Marlow VA, Rea D, Najmudin S, Wills M, Fülöp V. 2013. Structure and mechanism of acetolactate decarboxylase. ACS Chem. Biol. 8:2339–44.

Matheron C, Delort A, Gaudet G. 1998. ^{13}C and ^{1}H Nuclear Magnetic Resonance study of glycogen futile cycling in strains of the genus *Fibrobacter*. Appl. Environ. Microbiol. 64:74-81.

Marienhagen J, Eggeling L. 2008. Metabolic function of *Corynebacterium glutamicum* aminotransferases AlaT and AvtA and impact on L-valine production. Appl. Environ. Microbiol. 74:7457–62.

Marx A, Striegel K, de Graaf AA, Sahm H, Eggeling L. 1997. Response of the central metabolism of *Corynebacterium glutamicum* to different flux burdens. Biotechnol. Bioeng. 56:168–80.

Marx A, Eikmanns BJ, Sahm H, de Graaf AA, Eggeling L. 1999. Response of the central metabolism in *Corynebacterium glutamicum* to the use of an NADH-dependent glutamate dehydrogenase. Metab. Eng. 1:35–48.

McKinlay JB, Shachar-Hill Y, Zeikus JG, Vieille C. 2007. Determining *Actinobacillus succinogenes* metabolic pathways and fluxes by NMR and GC-MS analyses of ^{13}C-labeled metabolic product isotopomers. Metab. Eng. 9:177–92.

McKinlay JB, Vieille C. 2008. ^{13}C-metabolic flux analysis of *Actinobacillus succinogenes* fermentative metabolism at different $NaHCO_3$ and H_2 concentrations. Metab. Eng. 10:55–68.

Michel A, Koch-Koerfges A, Krumbach K, Brocker M, Bott M. 2015. Anaerobic growth of *Corynebacterium glutamicum* by mixed-acid fermentation. Appl. Environ. Microbiol. 81:7496-508.

Mimitsuka T, Sawai H, Hatsu M, Yamada K. 2007. Metabolic engineering of *Corynebacterium glutamicum* for cadaverine fermentation. Biosci. Biotechnol. Biochem. 71:2130–5.

Molenaar D, van der Rest ME, Petrović S. 1998. Biochemical and genetic characterization of the membrane-associated malate dehydrogenase (acceptor) from *Corynebacterium glutamicum*. Eur. J. Biochem. 254:395–403.

Molenaar D, van der Rest ME, Drysch A, Yücel R. 2000. Functions of the membrane-associated and cytoplasmic malate dehydrogenases in the citric acid cycle of *Corynebacterium glutamicum*. J. Bacteriol. 182:6884–91.

Moon M-W, Park S-Y, Choi S-K, Lee J-K. 2007. The phosphotransferase system of *Corynebacterium glutamicum*: features of sugar transport and carbon regulation. J.

Mol. Microbiol. Biotechnol. 12:43–50.

Moritz B, Striegel K, De Graaf AA, Sahm H. 2000. Kinetic properties of the glucose-6-phosphate and 6-phosphogluconate dehydrogenases from *Corynebacterium glutamicum* and their application for predicting pentose phosphate pathway flux in vivo. Eur. J. Biochem. 267:3442–52.

Muffler A, Bettermann S, Haushalter M, Hörlein A, Neveling U, Schramm M, Sorgenfrei O. 2002. Genome-wide transcription profiling of *Corynebacterium glutamicum* after heat shock and during growth on acetate and glucose. J. Biotechnol. 98:255–68.

Neves AR, Ramos A, Nunes MC, Kleerebezem M, Hugenholtz J, De Vos WM, Almeida J, Santos H. 1999. *In vivo* nuclear magnetic resonance studies of glycolytic kinetics in *Lactococcus lactis*. Biotechnol. Bioeng. 64:200–12.

Neves AR, Ventura R, Mansour N, Shearman C, Gasson MJ, Maycock C, Ramos A, Santos H. 2002a. Is the glycolytic flux in *Lactococcus lactis* primarily controlled by the redox charge? Kinetics of NAD(+) and NADH pools determined *in vivo* by ^{13}C NMR. J. Biol. Chem. 277:28088–98.

Neves AR, Ramos A, Costa H, van Swam II, Hugenholtz J, Kleerebezem M, de Vos W, Santos H. 2002b. Effect of different NADH oxidase levels on glucose metabolism by *Lactococcus lactis*: kinetics of intracellular metabolite pools determined by *in vivo* nuclear magnetic resonance. Appl. Environ. Microbiol. 68:6332–42.

Ng CY, Jung M-Y, Lee J, Oh M-K. 2012. Production of 2,3-butanediol in *Saccharomyces cerevisiae* by *in silico* aided metabolic engineering. Microb. Cell Fact. 11:68.

Nicholson WL. 2008. The *Bacillus subtilis ydjL* (*bdhA*) gene encodes acetoin reductase/2,3-butanediol dehydrogenase. Appl. Environ. Microbiol. 74:6832–8.

Nielsen DR, Yoon S-H, Yuan CJ, Prather KLJ. 2010. Metabolic engineering of acetoin and *meso*-2,3-butanediol biosynthesis in *E. coli*. Biotechnol. J. 5:274–84.

Nishimura T, Vertès AA, Shinoda Y, Inui M, Yukawa H. 2007. Anaerobic growth of *Corynebacterium glutamicum* using nitrate as a terminal electron acceptor. Appl. Microbiol. Biotechnol. 75:889–97.

Okino S, Inui M, Yukawa H. 2005. Production of organic acids by *Corynebacterium glutamicum* under oxygen deprivation. Appl. Microbiol. Biotechnol. 68:475–80.

Okino S, Suda M, Fujikura K, Inui M, Yukawa H. 2008b. Production of D-lactic acid by *Corynebacterium glutamicum* under oxygen deprivation. Appl. Microbiol. Biotechnol. 78:449–54.

Okino S, Noburyu R, Suda M, Jojima T, Inui M, Yukawa H. 2008a. An efficient succinic acid production process in a metabolically engineered *Corynebacterium glutamicum* strain. Appl. Microbiol. Biotechnol. 81:459–64.

Oliver JWK, Machado IMP, Yoneda H, Atsumi S. 2013. Cyanobacterial conversion of carbon dioxide to 2,3-butanediol. Proc. Natl. Acad. Sci. U S A 110:1249–54.

Omumasaba CA, Okai N, Inui M, Yukawa H. 2004. *Corynebacterium glutamicum* glyceraldehyde-3-phosphate dehydrogenase isoforms with opposite, ATP-dependent regulation. J. Mol. Microbiol. Biotechnol. 8:91–103.

Otten A, Brocker M, Bott M. 2015. Metabolic engineering of *Corynebacterium glutamicum* for the production of itaconate. Metab. Eng. 30:156–65.

Otero JM, Cimini D, Patil KR, Poulsen SG, Olsson L, Nielsen J. 2013. Industrial systems biology of Saccharomyces cerevisiae enables a novel succinic acid factory. PLoS One. 8:e54144. doi: 10.1371/journal.pone.0054144.

Park C, Lu M, Yun S, Park K, Lee J. 2013. Effect of pH on the metabolic flux of *Klebsiella oxytoca* producing 2,3-butanediol in continuous cultures at different dilution rates. Bioprocess. Biosyst. Eng. 36: 845-55.

Peters-Wendisch PG, Wendisch VF, Paul S, Eikmanns BJ, Sahm H. 1997. Pyruvate carboxylase as an anaplerotic enzyme in *Corynebacterium glutamicum*. Microbiology 143:1095–103.

Peters-Wendisch PG, Kreutzer C, Kalinowski J, Pátek M, Sahm H, Eikmanns BJ. 1998. Pyruvate carboxylase from *Corynebacterium glutamicum*: characterization, expression and inactivation of the *pyc* gene. Microbiology 144:915–27.

Pfeifer-Sancar K, Mentz A, Rückert C, Kalinowski J. 2013. Comprehensive analysis of the *Corynebacterium glutamicum* transcriptome using an improved RNAseq technique. BMC Genomics 14:888.

Pines O, Even-Ram S, Elnathan N, Battat E, Aharonov O, Gibson D, Goldberg I. 1996. The cytosolic pathway of L-malic acid synthesis in *Saccharomyces cerevisiae*: the role of fumarase. Appl. Microbiol. Biotechnol. 46:393–99.

Qi G, Kang Y, Li L, Xiao A, Zhang S, Wen Z, Xu D, Chen S. 2014. Deletion of *meso*-2,3-butanediol dehydrogenase gene *budC* for enhanced D-2,3-butanediol production in *Bacillus licheniformis*. Biotechnol Biofuels 7:16.

Raab AM, Lang C. 2011. Oxidative versus reductive succinic acid production in the yeast *Saccharomyces cerevisiae*. Bioeng. Bugs 2:120–3.

Radmacher E, Vaitsikova A, Burger U, Krumbach K, Sahm H, Eggeling L. 2002. Linking central metabolism with increased pathway flux: L-valine accumulation by *Corynebacterium glutamicum*. Appl. Environ. Microbiol. 68:2246–50.

Riedel C, Rittmann D, Dangel P, Möckel B, Petersen S, Sahm H, Eikmanns BJ. 2001. Characterization of the phosphoenolpyruvate carboxykinase gene from *Corynebacterium glutamicum* and significance of the enzyme for growth and amino acid production. J. Mol. Microbiol. Biotechnol. 3:573–83.

Royal Belgian Academy Council of Applied Science. 2004. “Industrial Biotechnology and Sustainable Chemistry”.

Reinscheid DJ, Eikmanns BJ, Sahm H. 1994a. Characterization of the isocitrate lyase gene from *Corynebacterium glutamicum* and biochemical analysis of the enzyme. J. Bacteriol. 176:3474–83.

Reinscheid DJ, Eikmanns BJ, Sahm H. 1994b. Malate synthase from *Corynebacterium glutamicum*: sequence analysis of the gene and biochemical characterization of the enzyme. Microbiol. 140:3099–108.

Sánchez AM, Bennett GN, San K-Y. 2006. Batch culture characterization and metabolic flux analysis of succinate-producing *Escherichia coli* strains. Metab. Eng. 8:209–26.

Sasaki M, Jojima T, Inui M, Yukawa H. 2010. Xylitol production by recombinant *Corynebacterium glutamicum* under oxygen deprivation. Appl. Microbiol. Biotechnol. 86:1057–66.

Sauer U, Eikmanns BJ. 2005. The PEP-pyruvate-oxaloacetate node as the switch point for carbon flux distribution in bacteria. FEMS Microbiol. Rev. 29:765–94.

Schneider J, Wendisch VF. 2010. Putrescine production by engineered *Corynebacterium glutamicum.* Appl. Microbiol. Biotechnol. 88:859–68.

Schrader MC, Eskey CJ, Simplaceanu V, Ho C. 1993. A carbon-13 nuclear magnetic resonance investigation of the metabolic fluxes associated with glucose metabolism in human erythrocytes. Biochim. Biophys. Acta 1182:162-78.

Schreiner ME, Fiur D, Holátko J, Pátek M, Eikmanns BJ. 2005. E1 enzyme of the pyruvate dehydrogenase complex in *Corynebacterium glutamicum*: molecular analysis of the gene and phylogenetic aspects. J. Bacteriol. 187:6005–18.

Schreiner ME, Eikmanns BJ. 2005. Pyruvate:quinone oxidoreductase from *Corynebacterium glutamicum*: purification and biochemical characterization. J. Bacteriol. 187:862–71.

Schreiner ME, Riedel C, Holátko J, Pátek M, Eikmanns BJ. 2006. Pyruvate:quinone oxidoreductase in *Corynebacterium glutamicum*: molecular analysis of the pqo gene, significance of the enzyme, and phylogenetic aspects. J. Bacteriol. 188:1341–50.

Schwinde JW, Hertz PF, Sahm H, Eikmanns BJ, Guyonvarch A. 2001. Lipoamide dehydrogenase from *Corynebacterium glutamicum*: molecular and physiological analysis of the *lpd* gene and characterization of the enzyme. Microbiology 147:2223–31.

Seibold G, Dempf S, Schreiner J, Eikmanns BJ. 2007. Glycogen formation in *Corynebacterium glutamicum* and role of ADP-glucose pyrophosphorylase. Microbiology 153:1275–85.

Shimizu H, Hirasava T. 2007. Production of glutamate and glutamate-related amino acids: molecular mechanism analysis and metabolic engineering, *In* Wendisch VF (ed), Amino acid biosynthesis - pathways, regulation and metabolic engineering. Microbiology Monographs. vol 5. Springer, New York, NY. p. 2-29.

Shin JH, Kim HU, Kim DI, Lee SY. 2013. Production of bulk chemicals via novel metabolic pathways in microorganisms. Biotechnol. Adv. 31:925–35.

Shirai T, Fujimura K, Furusawa C, Nagahisa K, Shioya S, Shimizu H. 2007. Study on roles of anaplerotic pathways in glutamate overproduction *of Corynebacterium glutamicum* by metabolic flux analysis. Microb. Cell. Fact. 6:19.

Silberbach M, Schäfer M, Hüser AT, Kalinowski J, Pühler A, Krämer R, Burkovski A. 2005. Adaptation of *Corynebacterium glutamicum* to ammonium limitation: a global analysis using transcriptome and proteome techniques. Appl. Environ. Microbiol. 71:2391–402.

Snoep JL, Teixeira de Mattos MJ, Starrenburg MJ, Hugenholtz J. 1992. Isolation, characterization, and physiological role of the pyruvate dehydrogenase complex and α-acetolactate synthase of *Lactococcus lactis* subsp. *lactis* bv. diacetylactis. J. Bacteriol. 174:4838–41.

Song G, Ryu C-M. 2013. Two Volatile Organic Compounds Trigger Plant Self-Defense against a Bacterial Pathogen and a Sucking Insect in Cucumber under Open Field Conditions. Int. J. Mol. Sci. 14:9803–819.

Song H, Lee JW, Choi S, You JK, Hong WH, Lee SY. 2007. Effects of dissolved CO_2 levels on the growth of *Mannheimia succiniciproducens* and succinic acid production. Biotechnol. Bioeng. 98:1296–304.

Song Y, Matsumoto K, Yamada M, Gohda A, Brigham CJ, Sinskey AJ, Taguchi S. 2012. Engineered *Corynebacterium glutamicum* as an endotoxin-free platform strain for lactate-based polyester production. Appl. Microbiol. Biotechnol. 93:1917-25.

Stansen C, Uy D, Delaunay S, Eggeling L, Goergen J, Wendisch VF. 2005. Characterization of a *Corynebacterium glutamicum* Lactate Utilization Operon Induced during Temperature-Triggered Glutamate Production. Appl. Environ. Microbiol. 71:5920–8.

Stols L, Donnelly MI. 1997. Production of succinic acid through overexpression of NAD (+)-dependent malic enzyme in an *Escherichia coli* mutant. Appl. Environ. Microbiol. 63:2695–701.

Stormer FC. 1975. 2,3-Butanediol biosynthetic system in *Aerobacter aerogenes*. Methods Enzymol. 41:518–32.

Straathof AJJ. 2013. Transformation of Biomass into Commodity Chemicals Using Enzymes or Cells. Chem. Rev. 114:1871–908.

Sun J-A, Zhang L-Y, Rao B, Shen Y-L, Wei D-Z. 2012. Enhanced acetoin production by *Serratia marcescens* H32 with expression of a water-forming NADH oxidase. Bioresour. Technol. 119:94–8.

Syu M-J. 2001. Biological production of 2,3-butanediol. Appl. Microbiol. Biotechnol. 55:10–18.

Takeda M, Muranushi T, Inagaki S, Nakao T, Motomatsu S, Suzuki I, Koizumi J. 2011. Identification and characterization of a mycobacterial (*2R,3R*)-2,3-butanediol dehydrogenase. Biosci. Biotechnol. Biochem. 75:2384–9.

Takusagawa Y, Otagiri M, Ui S, Ohtsuki T, Mimura A, Ohkuma M, Kudo T. 2001. Purification and characterization of L-2,3-butanediol dehydrogenase of *Brevibacterium saccharolyticum* C-1012 expressed in *Escherichia coli*. Biosci. Biotechnol. Biochem. 65:1876–8.

Thakker C, Martínez I, San K-Y, Bennett GN. 2012. Succinate production in *Escherichia coli*. Biotechnol. J. 7:213–24.

Toya Y, Shimizu H. 2013. Flux analysis and metabolomics for systematic metabolic engineering of microorganisms. Biotechnol. Adv. 31:818–26.

Transparency Market Research. 2012. Butanediol (1,4 BDO & 2,3 BDO), 1,3 Butadiene And Methyl Ethyl Ketone (MEK) Market: Applications (THF, PU, PBT, SBR, ABS, NBR Etc.), Bio-Based Alternatives, Downstream Potential, Market Size And Forecast, 2010 - 2018. Transparency Market Research, Albany, NY.

Tsuge Y, Uematsu K, Yamamoto S, Suda M, Yukawa H, Inui M. 2015. Glucose consumption rate critically depends on redox state in *Corynebacterium glutamicum* under oxygen deprivation. Appl. Microbiol. Biotechnol. 99:5573-82.

Ui S, Takusagawa Y, Sato T, Ohtsuki T, Mimura A, Ohkuma M, Kudo T. 2004. Production of L-2,3-butanediol by a new pathway constructed in *Escherichia coli*. Lett. Appl. Microbiol. 39:533–7.

Usuda Y, Tujimoto N, Abe C, Asakura Y, Kimura E, Kawahara Y, Kurahashi O, Matsui H. 1996. Molecular cloning of the *Corynebacterium glutamicum* (*'Brevibacterium lactofermentum*' AJ12036) *odhA* gene encoding a novel type of 2-oxoglutarate dehydrogenase. Microbiology 142:3347–54.

Uy D, Delaunay S, Goergen J-L, Engasser J-M. 2005. Dynamics of glutamate synthesis and excretion fluxes in batch and continuous cultures of temperature-triggered *Corynebacterium glutamicum*. Bioprocess Biosyst. Eng. 27:153–62.

Vallino JJ, Stephanopoulos G. 2000. Metabolic flux distributions in *Corynebacterium glutamicum* during growth and lysine overproduction. Reprinted from Biotechnology and Bioengineering, Vol. 41, Pp 633-646 (1993). Biotechnol. Bioeng. 67:872–85.

Van der Rest ME, Lange C, Molenaar D. 1999. A heat shock following electroporation induces highly efficient transformation of *Corynebacterium glutamicum* with xenogeneic plasmid DNA. Appl. Microbiol. Biotechnol 52:541–5.

Van den Tweel, W. 2010. Sustainable succinic acid. Available at: https://www.dsm.com/content/dam/dsm/cworld/en_US/documents/oct-2010-dsm-roquette-bio-based-sustainable-succinic-acid.pdf. Last accessed 1 November 2015.

Van Haveren J, Scott EL, Sanders J. 2008. Bulk chemicals from biomass. Biofuels Bioprod. Biorefining 2:41–57.

Van Houdt R, Moons P, Hueso Buj M, Michiels CW. 2006. N-acyl-L-homoserine lactone quorum sensing controls butanediol fermentation in *Serratia plymuthica* RVH1 and *Serratia marcescens* MG1. J. Bacteriol. 188:4570–2.

Varela C, Agosin E, Baez M, Klapa M, Stephanopoulos G. 2003. Metabolic flux redistribution in *Corynebacterium glutamicum* in response to osmotic stress. Appl. Microbiol. Biotechnol. 60:547–55.

Veit A, Rittmann D, Georgi T, Youn J-W, Eikmanns BJ, Wendisch VF. 2009. Pathway identification combining metabolic flux and functional genomics analyses: acetate and propionate activation by *Corynebacterium glutamicum*. J. Biotechnol. 140:75–83.

Vemuri G, Eiteman M, Altman E. 2002. Effects of growth mode and pyruvate carboxylase on succinic acid production by metabolically engineered strains of *Escherichia coli*. Appl. Environ. Microbiol. 68:1715–27.

Vivijs B, Moons P, Aertsen A, Michiels CW. 2014. Acetoin synthesis acquisition favors *Escherichia coli* growth at low pH. Appl. Environ. Microbiol. 80:6054–61.

Voloch M, Ladisch MR, Rodwell VW, Tsao GT. 1983. Reduction of acetoin to 2,3-butanediol in *Klebsiella pneumoniae*: a new model. Biotechnol. Bioeng. 25:173–83.

Wang A, Wang Y, Jiang T, Li L, Ma C, Xu P. 2010. Production of 2,3-butanediol from corncob molasses, a waste by-product in xylitol production. Appl. Microbiol. Biotechnol. 87:965–70.

Wang A, Xu Y, Ma C, Gao C, Li L, Wang Y, Tao F, Xu P. 2012. Efficient 2,3-butanediol production from cassava powder by a crop-biomass-utilizer, *Enterobacter cloacae* subsp. *dissolvens* SDM. PLoS One 7:e40442. doi: 10.1371/journal.pone.0040442

Wang Z, Song Q, Yu M, Wang Y, Xiong B, Zhang Y, Zheng J, Ying X. 2014. Characterization of a stereospecific acetoin(diacetyl) reductase from *Rhodococcus erythropolis* WZ010 and its application for the synthesis of (*2S,3S*)-2,3-butanediol. Appl. Microbiol. Biotechnol. 98:641–50.

Wang Y, Tao F, Xu P. 2014. Glycerol dehydrogenase plays a dual role in glycerol metabolism and 2,3-butanediol formation in *Klebsiella pneumoniae*. J. Biol. Chem. 289:6080–90.

Wendisch VF, de Graaf AA, Sahm H, Eikmanns BJ. 2000. Quantitative determination of metabolic fluxes during coutilization of two carbon sources: comparative analyses with *Corynebacterium glutamicu*m during growth on acetate and/or glucose. J. Bacteriol. 182:3088-96.

Wendisch VF, Bott M, Eikmanns BJ. 2006. Metabolic engineering of *Escherichia coli* and *Corynebacterium glutamicum* for biotechnological production of organic acids and amino acids. Curr. Opin. Microbiol. 9:268–74.

Werpy T, Petersen GR. 2004. Top Value Added Chemicals from Biomass. Volume I: Results of Screening for Potential Candidates from Sugars and Synthesis Gas. U.S. Department of Energy. Oak Ridge, TN, USA.

Westerfeld WW. 1945. A colorimetric determination of paraldehyde. J. Lab. Clin. Med. 30:1076.

Wieschalka S. 2012. Engineering *Corynebacterium glutamicum* as a designer-bug for the bio-based production of chemical building blocks and biofuel. Ph.D. thesis, Ulm University. Germany.

Wieschalka S, Blombach B, Eikmanns BJ. 2012a. Engineering *Corynebacterium glutamicum* for the production of pyruvate. Appl. Microbiol. Biotechnol. 94:449–59.

Wieschalka S, Blombach B, Bott M, Eikmanns BJ. 2012b. Bio-based production of organic acids with *Corynebacterium glutamicum*. Microb. Biotechnol. 6:87-102.

Wittmann C, Heinzle E. 2001. Modeling and experimental design for metabolic flux analysis of lysine-producing Corynebacteria by mass spectrometry. Metab. Eng. 3:173–91.

Wolf A, Krämer R, Morbach S. 2003. Three pathways for trehalose metabolism in *Corynebacterium glutamicum* ATCC13032 and their significance in response to osmotic stress. Mol. Microbiol. 49:1119–34.

Xu Y, Chu H, Gao C, Tao F, Zhou Z, Li K, Li L, Ma C, Xu P. 2014. Systematic metabolic engineering of *Escherichia coli* for high-yield production of fuel bio-chemical 2,3-butanediol. Metab. Eng. 23:22–33.

Yamamoto S, Sakai M, Inui M, Yukawa H. 2011. Diversity of metabolic shift in response to oxygen deprivation in *Corynebacterium glutamicum* and its close relatives. Appl. Microbiol. Biotechnol. 90:1051–61.

Yamamoto S, Gunji W, Suzuki H, Toda H, Suda M, Jojima T, Inui M, Yukawa H. 2012. Overexpression of genes encoding glycolytic enzymes in *Corynebacterium glutamicum* enhances glucose metabolism and alanine production under oxygen deprivation conditions. Appl. Environ. Microbiol. 78:4447–57.

Yamamoto S, Suda M, Niimi S, Inui M, Yukawa H. 2013. Strain optimization for efficient isobutanol production using *Corynebacterium glutamicum* under oxygen deprivation. Biotechnol. Bioeng. 110:2938–48.

Yang T, Rao Z, Zhang X, Xu M, Xu Z, Yang S-T. 2014. Enhanced 2,3-butanediol production from biodiesel-derived glycerol by engineering of cofactor regeneration and manipulating carbon flux in *Bacillus amyloliquefaciens*. Microb. Cell. Fact. 14:122.

Yang J, Kim B, Kim H, Kweon Y, Lee S, Lee J. 2015. Industrial production of 2,3-butanediol from the engineered *Corynebacterium glutamicum*. Appl. Biochem. Biotechnol. 176:2303–13.

Yasuda K, Jojima T, Suda M, Okino S, Inui M, Yukawa H. 2007. Analyses of the acetate-producing pathways in *Corynebacterium glutamicum* under oxygen-deprived conditions. Appl. Microbiol. Biotechnol. 77:853–60.

Yu B, Sun J, Bommareddy RR, Song L, Zeng A-P. 2011. Novel (*2R,3R*)-2,3-butanediol dehydrogenase from potential industrial strain *Paenibacillus polymyxa* ATCC 12321. Appl. Environ. Microbiol. 77:4230–3.

Yu M, Huang M, Song Q, Shao J, Ying X. 2015. Characterization of a (*2R,3R*)-2,3-Butanediol Dehydrogenase from *Rhodococcus erythropolis* WZ010. Molecules 20:7156–73.

Yu N, Zhang Z, Chen P, Zhong Y, Cai X, Hu H, Yang Y, Zhang J, Li K, Ge J, Yu K, Liu X, Zhuang J. 2015. Tetramethylpyrazine (TMP), an Active Ingredient of Chinese Herb Medicine Chuanxiong, Attenuates the Degeneration of Trabecular Meshwork through SDF-1/CXCR4 Axis. PLoS One 10:e0133055. doi: 10.1371/journal.pone.0133055.

Yuzbashev T V, Yuzbasheva EY, Laptev IA, Sobolevskaya TI, Vybornaya T V, Larina AS, Gvilava IT, Antonova S V, Sineoky SP. Is it possible to produce succinic acid at a low pH? Bioeng. Bugs 2:115–9.

Zamboni N, Fendt S-M, Rühl M, Sauer U. 2009. ^{13}C-based metabolic flux analysis. Nat. Protoc. 4:878–92.

Zeikus JG, Jain MK, Elankovan P. 1999. Biotechnology of succinic acid production and markets for derived industrial products. Appl. Microbiol. Biotechnol. 51:545–52.

Zhang L, Yang Y, Sun J, Shen Y, Wei D, Zhu J, Chu J. 2010. Microbial production of 2,3-butanediol by a mutagenized strain of *Serratia marcescens* H30. Bioresour. Technol. 101:1961–7.

Zhang X, Zhang R, Yang T, Zhang J, Xu M, Li H, Xu Z, Rao Z. 2013. Mutation breeding of acetoin high producing *Bacillus subtilis* blocked in 2,3-butanediol dehydrogenase. World J. Microbiol. Biotechnol. 29:1783–9.

Zhang GL, Wang CW, Li C. 2012. Cloning, expression and characterization of *meso*-2,3-butanediol dehydrogenase from *Klebsiella pneumoniae*. Biotechnol. Lett. 34:1519–23.

Zhang L, Xu Q, Zhan S, Li Y, Lin H, Sun S, Sha L, Hu K, Guan X, Shen Y. 2014. A new NAD(H)-dependent *meso*-2,3-butanediol dehydrogenase from an industrially potential strain *Serratia marcescens* H30. Appl. Microbiol. Biotechnol. 98:1175–84.

Zhou Z, Wang C, Chen Y, Zhang K, Xu H, Cai H, Chen Z. 2014. Increasing available NADH supply during succinic acid production by *Corynebacterium glutamicum*. Biotechnol. Prog. 31:12–9.

Zhu B-F, Xu Y. 2010. A feeding strategy for tetramethylpyrazine production *by Bacillus subtilis* based on the stimulating effect of ammonium phosphate. Bioprocess Biosyst. Eng. 33:953–9.

Zhu N, Xia H, Yang J, Zhao X, Chen T. 2014. Improved succinate production in *Corynebacterium glutamicum* by engineering glyoxylate pathway and succinate export system. Biotechnol. Lett. 36:553–60.

Zuljan FA, Repizo GD, Alarcon SH, Magni C. 2014. α-Acetolactate synthase of *Lactococcus lactis* contributes to pH homeostasis in acid stress conditions. Int. J. Food Microbiol. 188:99–107.

References

Appendix I

Characterization of *Corynebacterium glutamicum* succinate producer strains by ^{13}C-NMR

Contents

Summary

Corynebacterium glutamicum is a well known industrial organism and a promising host for succinate production. The metabolism of *C. glutamicum* strains manipulated with an aim to increase succinate formation was studied using the *in vivo* ^{13}C-NMR and ^{13}C-tracer studies. Results showed that the elimination of lactate production caused a 20% increase in succinate production. Additional overproduction of pyruvate carboxylase increased the yield by an additional 15%. Acetate elimination did not further improve the yield. Analysis of pathways operating under succinate production conditions revealed low pentose phosphate pathway (6%), and succinate being produced mainly via the reductive route of the tricarboxylic acid cycle. These studies confirmed the suitability of the chosen approaches for studying the anaerobic succinate production.

Introduction

Corynebacterium glutamicum is an industrial organism used for high-scale production of L-amino acids (Shimizu and Hirasava 2007, Becker and Wittmann 2012). It is known that under oxygen limiting conditions (oxygen deprivation), this organism produces organic acids: lactic, acetic and succinic acid. In the wild-type *C. glutamicum,* succinate is a minor product of glucose metabolism. Addition of bicarbonate was shown to increase succinate production (Okino et al. 2005, Dominguez et al. 1993, Inui et al. 2004). As succinate is an important bulk chemical, several engineering strategies were applied to *C. glutamicum* with a goal of transforming it into

a host for succinate production. In one approach, lactate production was eliminated to enhance pyruvate and NADH availability for succinate formation; in addition, pyruvate carboxylase was overproduced to direct pyruvate into oxaloacetate (Okino et al. 2008a). As a result of this strategy, 1.4 mol succinate per mol glucose was produced, with acetate as the major side-product (0.3 mol per mol glucose). In another study, this strategy was upgraded by eliminating acetate production, overproducing glyceraldehyde 3-phosphate dehydrogenase, and importantly, introducing formate dehydrogenase to assure the CO_2 and NADH supply for succinate production (Litsanov et al. 2012a). A high yield of succinate (1.67 mol per mol glucose) was achieved in fermentations by this strain, using formate, bicarbonate and glucose as substrates.

The success of engineering strategies depends on thorough knowledge of the bacterial metabolism, including the information on carbon flux distribution in the network of metabolic pathways (Kiefer et al. 2004, Bartek et al. 2011). Our group applied the *in vivo* ^{13}C Nuclear Magnetic Resonance (NMR) methodology and its non-invasive characteristics to study different aspects of metabolism in non growing bacterial cells (Neves et al. 1999, Neves et al. 2002a, Carvalho et al. 2013). Using differentially labelled glucose isotopomers for the ^{13}C-tracer studies is particularly useful in discovering and quantifying pathways that are active in the cell (Schrader et al. 1993, Klapa et al. 1999). We set out to apply these two methodologies and characterize the metabolism of *C. glutamicum* strains manipulated for the production of succinate under anaerobic conditions in

the presence of CO_2, with a goal of obtaining indications for further improving succinate production.

Materials and methods

Strains and growth conditions

C. glutamicum strains used in this work are listed in the Table A1.1. All strains were grown over-night in 2L-baffled shake flasks at 30ºC and 140 RPM in modified CGXII with 4% glucose (w/v), as described in Chapter 2. *C. glutamicum* Δ*ace*Δ*pqo*Δ*C-T ilvN*Δ*ldhA*Δ*alaT*Δ*avtA* (ELB-PO1) was grown with 3% glucose (w/v), 1% potassium-acetate (w/v) and 20 mM L-alanine. Cultures (200 mL), were inoculated at an initial OD_{600} of 0.5. Precultures (25 mL), were grown for 10 h in 250mL-baffled flasks under identical conditions.

Preparation of cell suspensions

For anaerobic *in vivo* NMR experiments, different volumes of cultures in the stationary phase of growth were collected (ELB-P01: OD_{600} 20, 275 mL; other strains OD_{600} ~35, 175 mL), centrifuged (7500 rpm, 10 min, 4ºC), and washed twice (buffer: 10 mM PIPES, pH 7.0). Cells were then re-suspended in 50 mM PIPES buffer (pH 7.0); antifoaming agent (approx. 15-20 µl), D_2O (6% v/v) was added and the final volume adjusted to 50 mL. For experiments with diluted cell suspensions, 15 mL of cultures in the stationary phase of growth (ELB-P01: OD_{600} 20) were collected, and the same procedure as described above, applied. Cells were then re-suspended in 50 mM PIPES buffer (pH 7.0); antifoaming agent (approx. 15-20 µl), D_2O (6% v/v) was added and the final volume adjusted to 30 mL.

Table A1.1. Bacterial strains used in this study.

Strains	Description	Reference
C. glutamicum Δ*ldhA*	*C. glutamicum* carrying deletion of the lactate dehydrogenase	This work
C. glutamicum Δ*ldhA* (pAN6-*pyc*^{P458S})	*C. glutamicum* Δ*ldhA* with the over-expression of pyruvate carboxylase gene from *C. glutamicum* DM1727	Litsanov et al. 2012a
ELB-PO1	*C. glutamicum* with deletions of the genes coding for the E1 subunit of pyruvate dehydrogenase complex, the pyruvate:quinone oxidoreductase, lactate dehydrogenase, alanine-glutamate transaminase and alanine-valine transaminase; also carries truncated version of regulatory subunit of the acetohydroxyacid synthase	Wieschalka et al. 2012
CQPAL	*C. glutamicum* Δ*ldhA*(pAN6-*pyc*^{P458S}) with additional deletions of the pyruvate:quinone oxidoreductase, phosphotransacetylase - acetate kinase and acetyl coenzyme A (CoA):CoA transferase	Litsanov et al. 2012a

Abbreviations: *ldhA,* lactate dehydrogenase gene; *pyc*, pyruvate carboxylase.

In vivo ^{13}C-NMR experiments

Experiments were performed using the on-line system described by Neves et al. 1999. Essentially, experiments were performed as described in Chapter 2. Resting cells were kept at a constant temperature of 30ºC, and under anaerobic conditions achieved by bubbling pure CO_2. Glucose specifically labeled on carbon 1 (20 mM) was added to the cell suspension at time-point zero. The time course of glucose consumption, product formation, and changes in the pools of other metabolites was monitored *in vivo*. To calculate rates of substrate consumption, cell dry-weight was measured. Experiments were performed once. The typical variation in the *in vivo* NMR experiments is ± 10% (Chapter 2).

Analysis of metabolic fluxes in non-growing cells

Resting cells suspended in 50 mM PIPES, were kept at a constant temperature of 30ºC, and under 100% CO_2 atmosphere. The pH value was controlled at 7.0. Glucose, specifically labeled on carbon 2 (50 mM), was added to the cell suspension at time-point zero. Samples were withdrawn from the metabolizing suspension, centrifuged, and supernatants were analyzed by ^{13}C-NMR and HPLC, as described in Chapter 2. To calculate rates of substrate consumption, cell dry-weight was measured.

Results and discussion

Anaerobic glucose metabolism of the succinate producing strains measured by the *in vivo* ^{13}C-NMR

We used the *in vivo* ^{13}C-NMR methodology to estimate the effect of genetic manipulations on the production of succinate by various *C. glutamicum* strains under optimal succinate producing conditions (100% CO_2). The first step in metabolic engineering for succinate production was elimination of lactate by deleting the lactate dehydrogenase gene (Okino et al. 2008a). This step abolished the accumulation of lactate and the major products of anaerobic metabolism from the metabolism of 20 mM [1-^{13}C]glucose under 100% CO_2 conditions were succinate (24.1 mM, 1.20 mol per mol glucose) and acetate (7.4 mM, 0.37 mol per mol glucose) (Table A1.2). Further steps in engineering comprised the over-expression of pyruvate carboxylase gene from *C. glutamicum* DM1727 to enhance the flux from pyruvate towards the reductive TCA cycle; resulting strain *C. glutamicum*

Δ*ldh*(pAN6-*pyc*^{P485S}) produced 27.0 mM succinate (1.35 mol succinate per mol glucose); major side product was acetate (0.45 mol per mol glucose).

To eliminate the acetate production, strain CQPAL was constructed with additional deletions of the pyruvate:quinone oxidoreductase, phosphotransacetylase, acetate kinase and acetyl coenzyme A (CoA):CoA transferase genes in *C. glutamicum* Δ*ldh*(pAN6-*pyc*^{P485S}). CQPAL produced 25.7 mM succinate (1.28 mol succinate per mol glucose). Acetate production was decreased from 9.0 mM in Δ*ldh*(pAN6-*pyc*^{P485S} to about 1.0 mM in CQPAL. The ^{13}C-concentrations of the major and minor products of anaerobic glucose metabolism by these strains are shown in Table A1.3.

Another approach in creating a succinate producer was applied in strain ELB-PO1: similarly to the previous strains, lactate dehydrogenase gene was deleted; acetate was abolished by eliminating pyruvate:quinone oxidoreductase gene and *aceE*, enconding the catalytic subunit of the PDHC. Additionally, to prevent loss of carbon in amino acids, genes encoding alanine-glutamate transaminase and alanine-valine transaminase were inactivated; a truncated version of *ilvN* gene was used, which resulted in production of acetohydroxyacid synthase with higher K_m and lower v_{max} for pyruvate. Under fully saturated CO_2 conditions, strain ELB-PO1 produced 12.8 mM succinate, 0.5 mM lactate, and 0.2 mM acetate. Other products of the metabolism of this strain were pyruvate (11.3 mM), acetoin, α-ketoisovalerate and L-valine (Table A1.3).

Table A1.2. Products of anaerobic glucose metabolism of various *C. glutamicum* strains. The initial concentration of glucose was 20 and 50 mM for the experiments with dense and diluted cell suspensions, respectively. In dense cell suspensions (OD_{600} =100), end-products and glucose were determined online by *in vivo* NMR, while in diluted cell suspensions (OD_{600} =7.5), they were measured by ^{13}C-NMR off-line in the sample supernatants. The pH of the cell suspensions was maintained at 7.0, and anaerobic atmosphere was achieved by bubbling pure CO_2.

Strain	**Yield** (mol·mol^{-1} Glc)			**GCR** (nmol·min^{-1} mg^{-1}CDW)	**^{13}C balance**[b] (%)
	Lactate[a]	Succinate[a]	Acetate[a]		
OD_{600} = 100					
Δ*ldh*	0.0	1.20	0.37	28.8	90
Δ*ldh*(pAN6-*pyc*^{P485S})	0.0	1.35	0.45	34.7	100
CQPAL	0.0	1.28	0.05	25.5	90
ELB-PO1	0.02	0.64	0.0	18.2	74
OD_{600} = 7.5					
ELB-PO1	0.05	0.83	0.08	18.2	76

[a]Product yields were calculated assuming that [1-^{13}C]glucose was processed via the EMP pathway thus producing a labelled and an unlabelled pyruvate molecule as follows: lactate yield = [3-^{13}C]lactate×2/[1-^{13}C]glucose; acetate yield = [2-^{13}C]acetate×2/[1-^{13}C]glucose; succinate yield = ([2,3-^{13}C]succinate×2 + [1,4-^{13}C]succinate)/ [1-^{13}C]glucose; [b] ^{13}C balance is the percentage of carbon in metabolized ^{13}C-glucose that is recovered in the fermentation products. Abbreviations: Glc, glucose; GCR, glucose consumption rate.

Table A1.3. ^{13}C-labelling in the end-products derived from anaerobic metabolism of [1-^{13}C]glucose. Concentrations were determined by ^{13}C-NMR and corrected for natural abundance (1.1%). Values come from single experiments. N.d., not detected.

Metabolite	**^{13}C-Concentration** (mM)			
	Δ*ldh*	Δ*ldh*(pAN6-*pyc*^{P485S})	CQPAL	ELB-PO1
Lactate C3	n.d.	n.d.	0.05	0.24
Acetate C2	3.40	4.20	0.40	0.10
Acetate C1	0.62	0.64	n.d.	n.d.
Succ C2, C3	11.50	13.03	12.28	6.22
Succ C1, C4	1.06	0.99	1.13	0.39
Succ C1-C2	n.d.	n.d.	n.d.	0.10
Pyruvate C3	0.18	0.19	0.52	5.10
Pyruvate C3 enol	0.10	n.d.	0.37	0.31
α-KG C2	n.d.	n.d.	0.1	n.d.
α-KG C4	n.d.	n.d.	0.12	n.d.
Glycerol C1, C3	n.d.	n.d.	0.21	n.d.
Glu C4	0.27	0.24	0.61	n.d.
Glu C2	0.36	0.21	0.55	n.d.
Alanine C3	0.28	0.20	0.75	0.28
Glycogen	0.28	0.22	0.14	0.36
Acetoin	n.d.	n.d.	n.d.	0.24
α-KIV	n.d.	n.d.	n.d.	0.31
L-Valine	n.d.	n.d.	n.d.	0.20

Abbreviations: Glu, L-glutamate, Succ, succinate; α-KG, α-ketoglutarate, α-KIV, α-ketoisovalerate.

Analysis of pathways operating under anaerobic conditions in ELB-PO1

Strain ELB-PO1 is an efficient pyruvate producer under aerobic conditions (Wieschalka 2012). When atmosphere is switched to pure CO_2, this strain produced mainly succinate and pyruvate (Table A1.3, Fig. A1.1). We analyzed end-products from the metabolism of [2-^{13}C]glucose with an aim to study the underlying metabolic fluxes (Table A1.4).

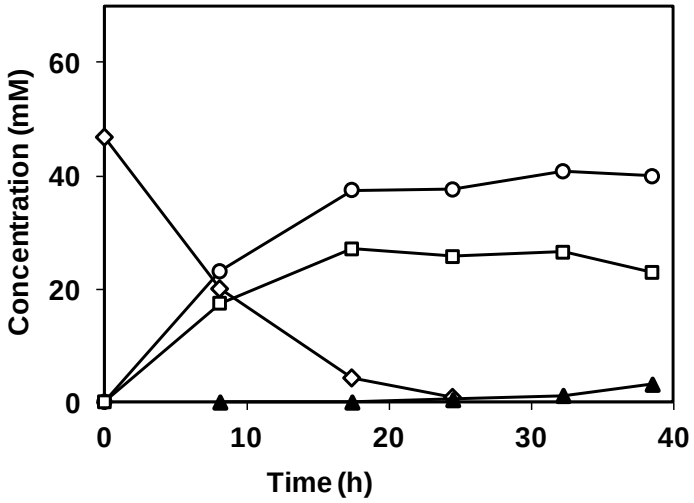

Figure A1.1. Time course of glucose consumption and product accumulation during the metabolism of 50 mM [2-^{13}C]glucose in non-growing cell suspensions of *C. glutamicum* ELB-PO1 (OD_{600} = 7.5). The experiments were carried out at 30 ºC, with pH controlled at 7.0 and bubbling 100% CO_2. Symbols: open diamonds, glucose; open circles, succinate; open squares, pyruvate; black triangles, acetate. Data shown is from a single experiment.

From the labelling in C2 and C3 of lactate or pyruvate the distribution of carbon flux between EMP and PPP can be calculated (Schrader et al. 1993, Klapa et al. 1999). The PPP in ELB-PO1 was low, with approx. 6% of glucose processed through this pathway.

The proportion between labelling in C2,C3 and C1,C4 of succinate is a measurement of the activity of the reductive TCA vs. the oxidative TCA route. In strain ELB-PO1, 3.5% of succinate was formed via the oxidative branch and/or the glyoxylate shunt, and the remaining via C3-carboxylation and reductive TCA. To produce succinate in the oxidative TCA route, some acetyl-CoA must be present. ^{13}C-labelled acetate was detected in both experiments with ELB-PO1 (dense and diluted cell suspensions). The labelling pattern indicates that it originated from ^{13}C-labelled glucose. This is a curious result, having in mind that ELB-PO1 has all acetate pathways blocked, and is auxotrophic for acetate.

Table A1.3. ^{13}C-labelling in the end-products derived from anaerobic metabolism of [2-^{13}C]glucose. Concentrations were determined by ^{13}C-NMR and corrected for natural abundance (1.1%). n.d., not detected. Values come from single experiment.

Metabolite	**^{13}C-Concentration** (mM)
Lactate C3	n.d.
Lactate C2	1.0
Lactate C1	n.d.
Succinate C2,3	19.5
Succinate C1,4	0.7
Succinate C1-2	n.d.
Acetate C2	n.d.
Acetate C1	1.6
Pyruvate C3	0.5
Pyruvate C2	13.1
Pyruvate C1	0.07
Alanine C2	0.3
Glycerol C2	0.2
DHA C2	0.4

Conclusions

In this work, the five strains designed for anaerobic succinate production from glucose were studied using *in vivo* ^{13}C-NMR and specifically labeled ^{13}C-glucose. The results indicate that the elimination of lactate production and overproduction of pyruvate carboxylase are two important steps in succinate production. *In vivo* ^{13}C-NMR and ^{13}C tracer studies are useful methodology for studying the anaerobic succinate production.

Acknowledgements and work contributions

This work was performed in the framework of project ERA-IB/BIO/0002/2008, “Bio-based production of chemical building blocks: *Corynebacterium glutamicum* as a platform for new and efficient bioprocesses”. Experiments were done in collaboration with Boris Litsanov (M. Bott lab, Forschungszentrum Jülich) and Stefan Wieschalka (B.J. Eikmanns lab, University of Ulm).

Appendix II

Stereospecificity of the lactococcal 2,3-butanediol dehydrogenases

Contents

Summary

Bacteria usually produce more than one 2,3-butanediol isomer as a result of different stereospecificities of the butanediol dehydrogenases or the existence of more than one butanediol dehydrogenase in a particular microorganism. The stereochemistry of 2,3-butanediol production is studied due to the commercial interest in producing pure stereoforms of this chemical. *Lactococcus lactis* possesses two butanediol dehydrogenase activities, which we have set out to purify and characterize. The production of recombinant proteins in *Escherichia coli* was poor, and t low activities of the two enzymes were detected in spectrophotometric measurements. Nonetheless, upon prolonged incubation of the two butanediol dehydrogenases with the racemic acetoin, 2,3-butanediol was synthesized. The first enzyme (coded by *butA*) produced mainly *meso*-2,3-butanediol (97%) and minor amounts of optically active form, confirming the *in vivo* data obtained by overproducing this enzyme in *Corynebacterium glutamicum*. The second butanediol dehydrogenase (coded by *butB*) produced minor amounts of the *meso*-2,3-butanediol, which made it difficult to draw firm conclusions about the nature of this enzyme.

Introduction

The NAD(P)-dependent alcohol dehydrogenases comprise a heterogeneous protein superfamily that catalyze the reversible oxidation of alcohols to aldehydes or ketones and can be grouped in at least three enzyme families: i) Zn-dependent medium-chain dehydrogenases/

reductases (MDR); ii) short-chain dehydrogenases/ reductases (SDR); and iii) Fe-activated alcohol dehydrogenases. Butanediol dehydrogenases (BDHs), a subgroup of this protein superfamily, are of particular interest since they are involved in the production of 2,3-butanediol (2,3-BD), which is a desirable bulk chemical. Several BDHs have been characterized so far (Table 4.1, Chapter 4). The BDHs of *Klebsiella pneumoniae*, *Serratia marescens*, and *Enterobacter cloacae* fall into to the SDR family; these enzymes introduce the new hydroxyl group in the (*S*)-configuration, thus reducing (*R*)-acetoin to *meso*-2,3-BD and (*S*)-acetoin to (*2S,3S*)-2,3-BD. *Corynebacterium glutamicum* possesses a BDH that belongs to the SDR family, but this enzyme prefers (*S*)-acetoin and (*2S,3S*)-2,3-BD over (*R*)-acetoin and *meso*-2,3-BD (Takusagawa et al. 2001). The third group comprises the BDHs of *Bacillus subtilis*, *Paenibacillus polymyxa* and *Saccharomyces cerevisiae* that belong to the MDR family, and generally catalyze the introduction of a hydroxyl group in the (*R*)-configuration; they use (*R*)-acetoin and (*S*)-acetoin to produce (*2R,3R*)-2,3-BD and *meso*-2,3-BD, respectively.

Lactococcus lactis is a natural producer of 2,3-BD, a compound which is assumed to be a part of the strategy to prevent over-acidification of the cell interior (Zuljan et al. 2014). Detailed characterization is available for the first two enzymes of the 2,3-BD biosynthetic pathway, α-acetolactate synthase (ALS) and α-acetolactate decarboxylase (ALDC) (Marlow et al. 2013, Goupil-Feuillerat et al. 1997, Snoep et al. 1992). However, the knowledge on the BDHs of *L. lactis* is limited. Partially pure preparations of

the two BDHs from *L. lactis* subsp. *lactis* D10 and more specifically, their stereochemical properties were studied (Crow 1991). Both enzymes showed activity with acetoin and diacetyl; when incubated with any of these two substrates, enzyme 1 always produced *meso*-2,3-BD, and enzyme 2 produced a mixture of *meso*- and optically active form. However, the respective genes were not assigned in this work.

Bioinformatic analysis indicates that these two activities could be coded by *butA* (llmg_1641) and *butB* (llmg_1642). Even so, some confusion exists in the literature on the properties of these two enzymes. In one study, *butB*-encoded activity (BDHB) was used in the 2,3-BD production by *E. coli*; as the resulting strain produced *meso*-2,3-BD, the authors concluded that BDHB was responsible for the *meso*-BDH activity in *L. lactis* (Nielsen et al. 2010). In another study, successfully overproduced BDHA (*butA*-encoded) caused *meso*-2,3-BD production in *L. lactis* (Gaspar et al. 2012). To clarify stereospecific properties of the two BDHs, the genes coding for *butA* and *butB* of *L. lactis* subsp. *cremoris* MG1363 were expressed int *E. coli* and the respective recombinant proteins were purified and characterized.

Materials and methods

Bacterial strains and growth conditions

Strains and plasmids used in this work are shown in Table A2.1. For the protein production, *E. coli* cultures (400 mL), harboring the gene of interest were grown in LB medium supplemented with 100 µg ampicillin per mL at 180 rpm. *E. coli* pET-19b*butA*^{LI} and *E. coli* pET-19b were grown always at

37°C to OD_{600} of 1.5, at which point protein production was induced using 1 mM Isopropyl β-D-1-thiogalactopyranoside (IPTG). Cells were collected 1 h after the induction. *E. coli* pET-19b*butB*^{LI} was grown for 3 h at 37°C (OD_{600} of 0.8), after which IPTG was added (1 mM) and protein production was continued for 16 h at 20°C.

Construction of strains and plasmids

All primers used are listed in the Table A2.1. Chromosomal DNA of *L. lactis* MG1363, isolated according to Johansen and Kibenich (1992), was used as template in PCR amplifications. To obtain expression vectors the two butanediol dehydrogenases, genes *butA*^{LI} and *butB*^{LI} were amplified from chromosomal DNA of *L. lactis* using primers butALL-FW/butALL-RE and butBLL-FW/butBLL-RE and ligated into pET-19b. Plasmid was obtained and maintained in *E. coli* BL21(DE3). Sequencing confirmation of the correctness of the insert was performed at StabVida (Lisbon).

Protein purification

Cells of *E. coli* pET19b*butA*^{LI} and *E. coli* pET19b*butA*^{LI} grown as described above, were collected, centrifuged (9,924 × *g*, 10 min, 4°C), and washed once with an appropriate buffer (Tris-HCl, 2-Amino-2-hydroxymethyl-propane-1,3-diol hydrochloride), 10 mM at pH 7.5. The resulting cell pellet was re-suspended in 4 mL of 50 mM Tris-HCl at pH 7.5; cell suspension was passed through a French press 3 times (120 MPa), and centrifuged (12,857 × *g*, 20 min, 4°C). The supernatant was applied to 5 mL-HisTrap HP column (GE Healthcare Life Sciences) and eluted according to the instruction of the manufacturer. Active fractions were then dialysed against

50 mM PIPES pH 7.0, concentrated using Amicon concentrator, and kept at 4°C.

Table 1. Bacterial strains, plasmids and primers used in this study.

Strains	Description	Reference
E. coli BL21(DE3)	Plasmid-free *E.coli* for protein expression	Stratagene
E. coli pET-19b	*E. coli* BL21(DE3) carrying pET-19b	This work
E. coli pET-19b*butA*^{LI}	*E. coli* BL21(DE3) carrying pET-19b*butA*^{LI}	This work
E. coli pET-19b*butB*^{LI}	*E. coli* BL21(DE3) carrying pET-19b*butB*^{LI}	This work
Plasmids		
pET-19b	amp^{R}, T7*lac*, N-terminal Histidine-tag with the enterokinase cutting site	Novagen
pET-19b*butA*^{LI}	pET-19b carrying *butA* gene of *L. lactis*	This work
pET-19b*butB*^{LI}	pET-19b carrying *butB* gene of *L. lactis*	This work
Primers	Sequence	Restriction site
butALL-FW	GGAATTCCATATGATGTCTAAAGTTGC	*Nde*I
butALL-RE	CGCGGATCCTTAATGAAATTGC	*BamH*I
butBLL-FW	GGAATTCCATATGATGGCTTGGTG	*Nde*I
butBLL-RE	CGCGGATCCTATAGACCTTTTCC	*BamH*I

Abbreviations: *butA*^{LI}, butanediol dehydrogenase A (BDHA) gene; *butB*^{LI}, butanediol dehydrogenase B (BDHB) gene; amp^{R}, amplicillin resistance; T7, T7 RNA polymerase promoter sequence; *lac*, lac operator sequence.

Enzymatic assays

BDH enzyme activities were assayed at 30°C in a Beckman Coulter DU 800 spectrophotometer in 50 mM MES (pH 6.2), 0.2 mM NADH and 2.5 mM acetoin (Stormer, 1975). One unit of enzyme activity is the amount of enzyme catalyzing the conversion of 1 µmol of substrate per minute under

the experimental conditions used. The protein concentration was determined using Pierce BCA Protein Assay Kit (Thermo Scientific). Specific activity was expressed as units (μmol·min^{-1}) per milligram of protein (U·mg of protein^{-1}). To measure the 2,3-BD isomer formation, a reaction mixture containing 9 mM (racemic) *R/S*-acetoin and 21 mM NADH in MES buffer (40 mM) at pH 6.2 was incubated with approximately 7.8 μg of protein for 24 h at 30°C.

NMR spectroscopy

^{1}H-NMR spectra were acquired on Bruker AVANCE II+ 800 MHz spectrometer (Bruker BioSpin GmbH) at 30ºC, using a TXI-Z H/C/N/-D probe head. Acquisition parameters: flip angle of 60º; 32K acquisition data points; repetition delay of 1.5 s, number of spectra 16.

Results and discussion

Despite huge efforts to optimize protein production, the expression levels of the two proteins remained low. This is obvious when active fractions of the two proteins are compared with control coming from *E. coli* strain carrying the empty vector (Fig. A2.1). However, the measurements in the spectrophotometer showed that the two fractions had BDH activity (approx 10 and 4.5 U·mg of protein^{-1} for BDHA and BDHB, respectively). Thus, we proceeded to test the 2,3-BD production upon incubation of these enzymes with racemic acetoin. The results of the incubation are shown in the Fig. A2.2.

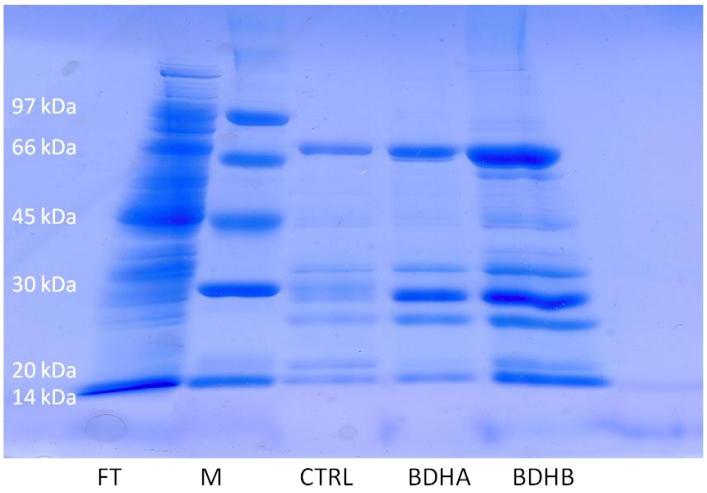

Figure A2.1 SDS-PAGE gel of different fractions eluted from the His-Trap column used for the purification of recombinant *L. lactis* butanediol dehydrogenases. The molecular masses calculated from the deduced amino acid sequences of BDHA and BDHB are 27 and 34.5 kDa, respectively. Active fractions were used for stereospecificity determinations and spectrophotometric activity measurements. Abbreviations: FT, flow-through fraction; M, marker; CTRL, proteins from the control strains; BDHA, proteins eluted in the attempted purification of BDHA; BDHB, proteins eluted in the attempted elution of BDHB.

Proteins from *E. coli* culture harboring the empty plasmid (the control culture), that were bound to the His-Trap column showed no measurable BDH activity in the spectrophotometric measurements, and 2,3-BD production in the NMR assay was not detected. BDHA (coded by llmg_1641) produced a mixture of *meso*-2,3-BD (97%) and optically active 2,3-BD (3%) after 24 h of incubation. BDHB (coded by llmg_1642) activity was extremely low, and a minor amount of *meso*-2,3-BD was detected after 24 h of incubation. This is in agreement with the results obtained in previous stereochemistry studies (Crow 1992). By amino acid similarity

analysis and size, BDHA belongs to the SDR family of alcohol dehydrogenases, and BDHB is a Zn^{2+}-dependent MDR. It is likely that BDHA introduces a hydroxyl group in an (*S*)-conformation, and prefers (*R*)-form of acetoin over the (*S*)-form. It is curious that BDHB produced *meso*-2,3-BD, since it is an MDR-type of enzyme, although this is in agreement with the results of previous *in vitro* and *in vivo* studies that involved BDHB (Crow 1992, Nielsen et al. 2010). Since very low amounts of 2,3-BD were produced, these results have to be taken with care.

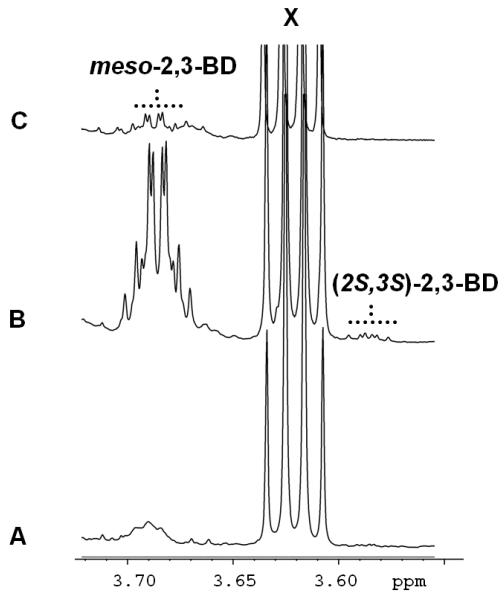

Figure A2.2 ^{1}H-NMR spectra of 2,3-BD produced in the enzymatic reaction using control proteins (**A**), BDHA (**B**), and BDHB (**C**). Reaction mixture containing 9 mM (racemic) *R/S*-acetoin and 21 mM NADH in MES buffer (40 mM) at pH 6.2 was incubated with approximately 15 µg of protein for 24 h at 30°C. Legend: *meso*-2,3-BD, *meso*-2,3-butanediol; (*2S,3S*)-2,3-BD, optically active (*2S,3S*)-2,3-butanediol; X, ethanol, common contaminant of NADH.

Conclusions

In this work, we attempt to purify and characterize two BDHs from *L. lactis*. One of the enzymes (coded by *butA* gene), identified as a SDR, produced mainly *meso*-2,3-BD and low amounts of the optically active form. From this result, and from a very high similarity between this enzyme and BDH of *K. pneumoniae* (65%), we concluded that the enzyme has preference for reducing (*R*)-form of acetoin into *meso*-2,3-BD. Further studies are necessary to confirm these results and shed more light on the stereochemical properties of the two BDHs from *L. lactis*.

References

Snoep JL, Teixeira de Mattos MJ, Starrenburg MJ, Hugenholtz J. 1992. Isolation, characterization, and physiological role of the pyruvate dehydrogenase complex and alpha-acetolactate synthase of *Lactococcus lactis* subsp. *lactis* bv. diacetylactis. J. Bacteriol. 174(14): 4838–41.

Goupil-Feuillerat N, Cocaign-Bousquet M, Godon, JJ, Ehrlich SD, Renault P. 1997. Dual role of alpha-acetolactate decarboxylase in *Lactococcus lactis* subsp. *lactis*. J. Bacteriol. 179(20):6285–93.